STUDY OF EFFECT OF GAS TURBINE AND COMPRESSOR BLADES DETERIORATION ON THE PERFORMANCE OF GAS TURBINE POWER PLANT

BY

VINOD KUMAR SINGORIA
(Enrolment Number DP/437/99)

Submitted

In partial fulfillment of the requirement of the degree of

DOCTOR OF PHILOSOPHY

To the

DEPARTMENT OF MECHANICAL ENGINEERING
DELHI COLLEGE OF ENGINEERING (NOW DTU)
UNIVERSITY OF DELHI
DELHI

SEPTEMBER 2014

CERTIFICATE

This is to certify that the thesis entitled "**STUDY OF EFFECT OF GAS TURBINE AND COMPRESSOR BLADES DETERIORATION ON THE PERFORMANCE OF GAS TURBINE POWER PLANT**" which is being submitted by **Mr. Vinod Kumar Singoria** (Enrolment Number - DP/437/99) to the Faculty of Technology, University of Delhi, Delhi, for the award of the degree of **Doctor of Philosophy** is a record of the original bonafide research work carried out by him under my guidance and supervision and has fulfilled the requirements for the submission of this thesis. The thesis, in my opinion, has attained a standard required for a Ph.D. degree of this University. The results contained in this thesis have not been submitted in part or full to any other university or institution for the award of any other degree or diploma.

Dr. Samsher
Supervisor
Professor
Mechanical Engineering Department
Delhi College of Engineering (Now DTU)
Delhi, India

Head of Department
Mechanical Engineering Department
Faculty of Technology,
University of Delhi, Delhi, India.

ACKNOWLEDGEMENTS

All praise to Almighty God, the creator and sustainer of the worlds. I wish to express my profound thanks to my supervisor Professor Samsher for his invaluable guidance, constant motivation and moral support throughout this study. It was his help and continuous encouragement in academic as well as personnel matters that has enabled this work to achieve its present form and status. It is with full humility that I desire to extend my sincere appreciation to him.

I attribute the completion of this research work to the dedicatory prayers, moral support, and love and affection of my parents and other family members. They have always been a major source of motivation and strength.

Finally, I express my sincere and hearty feelings to my wife Kusum Lata for her moral support, patience and bearing with me during the crucial moments.

Vinod Kumar Singoria

ABSTRACT

The efficiency of gas turbines used in power plants is largely dependent on their aerodynamic performance. The components like stators and rotors of the turbines and compressor are subject to abrasive and erosive wear. There are various contaminants which get deposited over the blades and produce roughnesses. The roughness magnitude both in turbines & compressors varies along the height and chord of blade and also over different stages of turbine. In actual turbines and compressors, roughness is not only found over entire surfaces of the blades but over a small portion of the surface of the blades also. The roughness is found, in the form of bands also on leading edge, middle chord and trailing edge of pressure and suction surfaces of blades of turbines and compressors.

The flow through turbines and compressors is inherently three dimensional due to the vane/blade passage geometry and other variety of reasons. The blade profile continuously changes in the span wise direction. The flow structure, along the end walls, is strongly three dimensional. This effect is tremendous in case of lower span to chord ratio. These characteristics of the flow lead to increase profile losses which in turn adversely affect the efficiency of turbomachines. The secondary flows cause to generate a non-uniform flow at exit of the blade row thereby efficiency of the blade row downstream gets further reduced. This research work in fact is an attempt to capture complex three- dimensional secondary flow vortices near end wall region along with getting results for total losses. The total losses are segregated to obtain profile & secondary loss i.e. ends losses numerically. The Computational fluid dynamics (CFD) uses numerical methods and algorithms to solve and analyze problems that involve fluid flows. The present research work is carried out using the CFD, commercial softwares, Gambit 2.4.6® and FLUENT 6.2.16®. These softwares are used for designing stage and working on it without any actual manufacturing and installation of such cascade in real working situation. The cascades of turbine and compressor are simulated to carry out study of effect of blade deterioration on various losses using three different blade profiles for turbines and one profile for compressor. Total three number blade profiles titled 6030, 5530 and 3525 as selected by Samsher [2002], from impulse and reaction turbine are chosen. Of the three profiles selected, blade profile 3525 was nearly impulse type and blade profiles titled 5530 and 6030

were of reaction type with different degree of reactions. The study is conducted for a number of cascades. There are total 13 numbers of cascades to be simulated separately for each of combinations of roughness magnitude, location of roughness and the given single blade profile for application of roughness on entire surface. In addition study of localised roughnesses of varying magnitudes is also conducted. There are 6 numbers of locations over the suction and pressure surfaces of given cascade for application of localised roughness.

The total pressure at inlet and total pressure and static pressure at exit measurement planes for numerous number of cascades are measured with the help of 'Fluent' software. These parameters are required to calculate local loss coefficients relative to nondimensional distance in the pitch wise direction along the measurement plane. The mass averaged loss coefficients is representative loss coefficient for selected pitch wise positions and calculated using the pitch wise local loss coefficients. The total loss, secondary loss and profile loss, for a cascade, are calculated on the basis of mass averaged loss coefficients for all selected span wise positions. The mass averaged loss coefficients near the end walls at both ends are higher than their values at mid span of the blade for each of cascade for all blade profiles i.e. 6030, 5530 and 3525. The local increase in mass averaged loss coefficients is observed due to the secondary flow cores near the hub and casing for all cascades.

The results with regard to the total, profile and secondary losses for BSR and PSR cascade based on mass averaged loss coefficients show that the magnitudes of total loss for these cascades for all roughness values are higher than that of the smooth cascade for all blade profiles i.e. 6030, 5530 and 3525. The total loss increases as roughness increases on the blade surfaces of each cascade for all blade profiles. The losses increase in the same order when roughness was increased from lower roughness value to high roughness value for all type of cascades. It is observed that change in respective losses with the increase in magnitude of roughness at high roughness values (such as 750 μm) are negligibly small.

The increasing of roughness on suction surface is found to be more detrimental than the same for pressure surface in terms of generation of total loss. It is found that the total loss increases as the roughness is increased on suction surfaces. The effect is combined when roughness is applied on both the surface of the blades. The

contribution of the profile loss in the total loss increases as roughness increases on the blade surfaces.

The secondary loss increases with the increase of roughness on pressure surfaces of blades of cascades. The same is decreased with the increase of roughness on suction surfaces of blades of cascades. The combined effect of increase of roughness on both the surfaces of blades is seen. The effect of roughness on secondary loss is more pronounced in blade profile 6030. The results also show that shape or geometry of the blades of the cascades significantly affect the losses.

The localised roughness and the effect of the same on losses vary from one blade profile to other blade profile. The application of localised roughness on leading edge on pressure surfaces of the cascade employing blade profile 3525 leads to more generation of total and profile losses than localised roughness on middle chord and trailing edge of same surfaces for the same cascade. On the other hand, the localised roughness on trailing edge of the pressure surfaces for blade profile 6030 and 5530 leads to more generation of total and profile losses. The application of localised roughness on blade profile 6030 and 5530 effect the phenomena of losses generation in same way. The localised roughness on various surfaces of blade profile 3525 effect the phenomenon of losses generation differently comparing with that of blade profile 6030 and 5530.

The trend of increase in total loss with the increase of surface roughness on various surfaces for compressor cascade is similar to that of turbine cascades. It is noticeable that the profile loss contributes very significantly in the total loss for all type of compressor cascades and that the roughness magnitudes do not affect secondary loss very appreciably for all type of cascades.

CONTENTS

LIST OF FIGURES

LIST OF TABLES

NOTATIONS AND ABBREVIATIONS

Nomenclature

2-D	two dimensional
3-D	three-dimensional
BSR	Both surfaces (suction & pressure sides) of all blades
CFD	Computational Fluid Dynamics
dy	elemental length in pitch wise direction.
HRSG	Heat recovery steam generator
P_{01} and P_{02}	total pressures at the inlet and outlet respectively,
P_{2s}	static pressure at outlet of the cascade,
PSR	Entire pressure surfaces of all blades
PSR 1	Pressure surface leading edge
PSR 2	Pressure surface mid-chord region
PSR 3	Pressure surface trailing edge
S	pitch distance
SSR	Entire suction surfaces of all blades
SSR 1	Suction surface leading edge region
SSR 2	Suction surface mid-chord region
SSR 3	Suction surface trailing edge end
V_a	axial velocity,

Symbols

5530, 6030, 3525g	Profiles identification number
C	Chord *(mm)*
C_p	Static pressure coefficient.

DTU	Delhi Technological University
Dy	Incremental distance in pitch-wise direction
F_i	external body force
g	gravitational acceleration
H	Total pressure measured by standard pitot tube
i	i^{th} location of the blade
k_s	Equivalent sand roughness
k_t	Turbulent thermal conductivity
L	Length/span of blade
L	Characteristic length, *(mm)*
o	Total value / Curvilinear length
P	Static pressure measured by standard pitot tube, *(Pa)*
p	static pressure
P	Static pressure at the point of interest
p_i	Static pressure at a point, i, on the blade surface, *(Pa)*
P_i	Static pressure at the point of interest
P_o	Total pressure
P_s	Static pressure,
P_{s1}	static pressure at inlet
RANS	Reynolds Mass averaged Navier Stokes
Re	Reynold number
S	Pitch, *(mm)*
S_m	Momentum source term
u_i	velocity vector of the fluid
y	Local value in pitch-wise direction

Greek symbols

ϕ	denotes a scalar quantity such as pressure, energy, species concentration
ρ	density of the fluid
μ	molecular viscosity
ζ	mass average loss coefficient,
ρ	Density of air
μ	Dynamic viscosity
τ	Mass-averaged value of loss coefficient
γ	Specific Heat Ratio for Air

Subscripts

$\frac{\partial}{\partial xi}$	divergent operator,
ρg_i	gravitational body force
δ_{ij}	Kronecker's delta
τ_{ij}	stress tensor
1	Inlet to cascade
2	Outlet of cascade
a	Axial component

CHAPTER 1
INTRODUCTION

The energy supply and demand characteristics have a great role to play in order to attain sustainable development of any modern day society. Energy is a driving force behind rapid economic growth of any country. The increasing energy demand would help foster higher economic growth. It is first requirement to accelerate the development of the energy sector to meet India's growth and electrification aspirations. In India, during the Eleventh Five Year Plan, nearly 55,000 MW of new generation capacity was created, yet there continued to be an overall energy deficit of 8.7 per cent and peak shortage of 9.0 per cent. Resources currently allocated to energy supply are not sufficient for narrowing the gap between energy needs and energy availability [Energy Statistics, 2013].

The electricity has, during the last decade, evidently replaced kerosene as the most common fuel used for lighting by rural households. Even though the pace of electrification in past few years was very high yet the overall electrification in India is still 64.5% only. The rest 35.5% of the population of India still lives without access to electricity. It is therefore the country like India needs to have more number of new coal and gas power plants. The initial capital costs of these plants among all generation plants are minimum.

India's power generation mix is considerably inclined towards coal based power generation. As per Ministry of Power, India, the total installed capacity, as on March 2012, is 199,627 MW of which the majority of share i.e 112,022 MW (56%) is coal based power plant [website 1]. It is predicted that the Indian coal sector will face

substantial shortfall in the quantum of coal production [website 2]. The same is likely to continue in future also.

Among the various energy converting devices, gas turbines are extensively used as prime movers as these also use fossil fuels. Moreover, gas turbines are also suited for Jet Propulsion. Natural gas is a clean fuel as compared to coal and can be efficiently used in power generation. Total installed capacity of Gas based power plants in India is 17,706.35 MW [Energy Statistics, 2013]. This accounts for 10% of the total installed capacity. Given limitations on the use of coal for power generation due to its environmental consequences, quality and supply constraints, the gas is likely to play an increasingly important role in India's power sector. Data of installed electricity generation capacity and capacity utilization stresses the need to improve efficiency of the technology used in electricity generation. The combined-cycle power plant is a promising mode of energy recovery and conservation in the field of electricity generation using Gas based power plants.

Efficiency of Gas based power plants is largely dependent on their aerodynamic performance. New blades of the turbines have very smooth surface finish and fine profile, but as it operate under severe conditions of temperature and pressure, with usage the blade surface deteriorates. The roughness magnitude both in turbines and compressors varies along the height and chord of blade and also over different stages of turbine. Cost of installing new capacity is much more than the capacity obtained by improving the performance of existing units. Improving the performance of existing units therefore becomes primary need. Also, there is need to find ways so that mechanism of losses generation could be identified and remedial measures may accordingly be applied to tap the losses. Available data shows that it will be desirable

to keep the existing gas power plants working efficiently as high as possible irrespective of their age. This requires a knowledge-based intervention of gas based power plant engineers in the understanding the causes of deterioration of blades and remedies thereafter.

1.1 Gas based power plant

Gas turbines are a type of internal combustion engine in which burning of an air-fuel mixture produces hot gases that spin a turbine to produce power. The process for converting the energy in a fuel into electric power involves the creation of mechanical work, which is then transformed into electric power by a generator. Gas turbines are comprised of three primary sections mounted on the same shaft: the compressor, the combustion chamber (or combustor) and the turbine. Simple cycle gas turbine plants has efficiency less than 30% on natural gas. To increase the overall efficiency of these power plants, multiple processes can be combined to recover and utilize the residual heat energy in hot exhaust gases. In attempt to recover residual heat energy in hot exhaust gases combined cycle power plants are preferred over simple cycle power plants.

The term “combined cycle” refers to the combining of multiple thermodynamic cycles to generate power. Combined cycle operation employs a heat recovery steam generator (HRSG) that captures heat from high temperature exhaust gases to produce steam, which is then supplied to a steam turbine to generate additional electric power. These power plants can achieve electrical efficiencies up to 60 percent.

The air at the ambient temperature and pressure enters the air compressor after being filtered by air filter. The temperature and pressure of the air is increased in the air

compressor. Mechanical energy of compressor is used to compress the air so that higher quantity of fuel may be added in air at lesser volume in combustion chamber. Compressed air is passed through a regenerator where high temperature combustion gases coming out of gas turbine transfer their heat to the compressed air. After gaining heat, compressed air comes to combustion chamber and fuel is added. After burning with air, chemical energy of fuel is converted into thermal energy. Combustion products temperature depends upon turbine inlet temperature which is fixed by thermal stress limit of gas turbine blade material. Combustion product temperature is controlled by making air and fuel mixture a lean mixture. The hot combustion gases enter the gas turbine where thermal energy of flue gases is converted into mechanical power of gas turbines. Gases coming out from gas turbine have large amount of thermal energy. Major part of this thermal energy is transferred to compressed air in regenerator. Gas turbines with HRSGs can be operated in either the cogeneration mode or the combined- cycle mode. In the cogeneration mode, steam produced from the HRSG is mainly used for process applications, whereas in the combined cycle mode, power is generated via a steam turbine generator.

Heat recovery steam generator (HRSG) is the link between the gas turbine and the steam turbine process, whose function is to transfer heat energy from exhaust gases to pressurized water and produces superheated steam.

In Heat Recovery Steam Generator, highly purified water flows in tubes and the hot gases passes around that and thus producing steam. The steam then rotates the steam turbine coupled with generator to produce Electricity.

These plants have low operating and maintenance costs. They also have the advantage of long-term fuel price stability, fuel flexibility and low emissions. These plants can

be located close to the power-user reducing transmission costs and increasing reliability.

1.2 Mechanisms of roughness formation

Operating conditions for Gas Turbines in India or globally are such that the components like nozzles (or stators) and rotors of these are subject to abrasive and erosive wear. This wear not only reduces the efficiency and the life of the turbine but also causes problems in operation and maintenance, which ultimately leads to economic losses. Performance deterioration in gas turbine power plant further becomes more severe due to roughening of blades of compressor. Compressor blades get roughened due to deposition of airborne particles which results from the adherence of dust or sand particles mixed with small oil droplets. The roughness magnitude both in turbines and compressors varies along the height and chord of blade and also over different stages of turbine.

Liquid and solid contamination in inlet gas can corrode, erode, and foul turbine and compressor blades, thereby reducing their efficiency and service life. For best performance of the Gas Turbine power plants, the air and fuel should be free of impurities but the natural and economic factors limit its control. The degradation effects of particle ingestion, erosion, deposition, corrosion and fouling lead to roughness, i.e. irregularities on blade surfaces of turbomachines. The roughness is resulted individually or in tandem on the blades of the turbines or compressors.

In the steam turbines, the steam flows between the blade passages of fixed and moving blades and due to the movement of the fluid, there is constant wear of the blade surfaces. Some solid and liquid particles come along with the steam and hit the

vane and rotor blade surfaces. Even particles of one to thirty microns have been known to damage exposed components of turbines. Also, there are salts dissolved in steam that get precipitated and deposited over the blades. The blade surfaces due to reasons mentioned above are adversely affected leading to increase in roughness.

Roughness results in change in blade profile. The roughness magnitude over the surface varies along the blade span as well as from initial stage to final stage. The roughness on various parts of the blades affect the performance of steam and gas turbines very significantly. Brief description on each of these three mechanisms is given below.

1.2.1 Erosion

Erosion is removal of material by cutting and ploughing by particles or local melting of material due to localized high temperature caused by particle impact. Erosion is also due to the abrasive removal of material by hard particles suspended in the gas stream.

Particles causing erosion are normally 10 microns or larger in diameter. Particles with diameters between 5 and 10 microns fall in a transition zone between fouling and erosion.

Erosion damage increases with increasing particle diameter and density, flow turning and gas velocity. Turbine and compressor manufacturers minimize erosion by increasing trailing edge thickness, installing field replaceable shields and using improved alloys.

In a particular particle-target material combination, particle size, impacting velocity, impingement angle, and metal and fluid/gas temperature affect the erosion rate and its location [Hamed and Fowler 1983]. Tabakoff [1984] observed that erosion increases

by 2.5 times when temperature increases from 26^{o}C to 649^{o}C and by 6.5 times when velocity increases from 197 m/s to 328 m/s.

For steam turbine, water drops (50-450 μm diameter) present in wet steam impinge on blades and cause erosion mainly at leading edge [Ansari, 1986]. In a two stage steam turbine, particles that initially impact the leading edge on either pressure or suction sides, again impact the pressure surface closer to the trailing edge [Tabakoff and Metwally, 1992]. Erosion increases radially towards the blade tip and increases axially from trailing to leading edge.

The resulting removal of blade material (original or deposited) generates peaks and valleys on surfaces that deepen and widen with operation. For an automotive gas turbine engine, Metwally *et. al* [1995] observed that the stator blade suffers maximum erosion at leading edge and at trailing edge near the hub, whereas for the rotor blade maximum erosion occurs mostly at the outermost radial locations. The mechanism of erosion also depends on the growth of the boundary layer over the blade surface and angle of incidence [Mann, 1999].

1.2.2 Corrosion

Corrosion is the loss of material caused by chemical reaction between machine components and contaminants which can enter the gas turbine through the gas stream, fuel system or water/steam injection system.

The presence of oxygen, carbon dioxide and wetness in steam are responsible for chemical reactions with blade surfaces for steam turbines. This phenomenon produces roughness either due to random thickening of blade profile if the oxidized material adheres to the blade surface or by random thinning if the oxidized material tears off from the blade surface. In the latter scenario, it could also contribute to erosion of

downstream stages. Corrosion depends on the electrochemical processes taking place at the boundaries of contact, usually between wet steam and the metal. Povarov and Tomarov [1985] attributed corrosion as a formation of microcells at the surface of metal consisting of anodic section where metal loses its ions and electrons and cathodic section where electrons are absorbed and, hence, the rate of corrosion is governed by overall current through the circuit. Magnetite thus formed has matching crystalline lattice parameters and adheres strongly to the blade acting as a protective layer, a process called passivation. The protective layer is disrupted due to solid particulate erosion and, thereafter, it is difficult to arrest corrosion which results in increased metal loss. The depth of erosion-corrosion is greatest in the temperature range of 150-190^{o} C due to instability of magnetite. It is less at higher temperatures due to the strong protective layer of magnetite and also at lower temperatures due to retardation of the chemical reactions. Wet steam forms a liquid film on the blade which reduces supply of oxygen to the metal and prevents formation of a passivating layer and, hence, metal loss due to erosion-corrosion caused by other factors increases with wetness. Komarov and Yurkov [1991] reported that corrosion damage occurs only on the parts operating in the phase transition zone, i.e., dry saturated to 6% wet, and no corrosion occurred on blades operating in the superheated region.

Vasilenko [1991] has reported that there is no corrosion in the pH range of 7-11, but it occurs in the range of pH<6 and also at pH >12, where fatigue strength of the blade material falls considerably.

1.2.3 Deposition

In the gas turbines, the source of deposits on hot gas path components come from the additive and ash content in fuel. The low grade liquid fuels such as the heavy blended distillates and residual fuel oil have significant ash bearing components. The contaminants can be sodium, potassium, calcium, vanadium and traces of other metals. Due to the non-availability of natural gas and distillate, user usually has no choice but to base its power generation using the residual/ crude oil.

The first problem which has to be addressed to when burning crude oil is that of the hot corrosion of turbine super-alloys due to the entrainment of certain trace metals, particularly Vanadium. The elimination of hot corrosion manifests itself in proper fuel treatment which involves the removal of these contaminants if possible, or chemical inhibition with additives.

Nonetheless vanadium exists as an oil soluble contaminant and cannot be removed by washing. The corrosive effects of vanadium are neutralized by the addition of a magnesium base compound as an inhibitor in the fuel.

Cotton and Schofield [1971] observed copper salts deposits of 1.0 mm on the nozzles of the 1st stage and 2.4 mm deposits on the 7th stage of a power plant steam turbine. On the rotor blades, deposits varied from 0.3 mm on the 1st stage to 0.5 mm on the 4th stage and 0.7 mm on the 7th stage. Water flowing in the steam path, though well treated, contains salts that are deposited on various surfaces including turbine blades. These salt deposits [David,1999]produce roughnesses and alter the blade profile causing performance deterioration and also affect the natural frequency of blading due to added mass on the blades [Stamatis, *et al.,*1999] . The sticking tendency of salts can

be controlled by mixing some additives in the working fluids which loosen up the deposits.

1.2.4 Fouling

Fouling is the adherence of particles and droplets to the surface of the Turbomachine blading. This degrades flow capacity and reduces efficiency in a short period of time. Fouling can normally be reversed by cleaning, but it often requires downtime. The deposition trajectories can be predicted for some turbine blades, the actual fouling is very much dependent on inlet gas cleanliness which varies unless it is controlled.

Nevertheless, they all recommend fine inlet filtration to prevent hard particles from entering the turbines.

1.2.5 Inlet Gas Filtration

With the current advances in filtering solid particles and coalescing aerosols from gases, the turbine inlet gas can economically be filtered to contain no more than 0.01 ppm with a particle size cut-off at 0.3µm. That absolutely eliminates erosion.

The particle filters and liquid gas coalesces do not separate corrosive vapor and gases from fuel gas. However, most of corrosive salts are dissolved and carried by liquid aerosols. Most aerosols are between 0.1 - 0.6µm and are quite removable by fine liquid/gas coalesces.

1.3 Motivation of the present study

Flow in axial turbines and compressors are extremely complex, three-dimensional and unsteady. These characteristics of the flow lead to increase losses which in turn adversely affect the efficiency of turbomachines. The fluid velocity very close to blade profile within the boundary layer changes from zero at the wall (for stationary wall) to

its free stream value. The losses so generated due to fluid flow within the boundary layer are known as profile losses.

The secondary flows are most complex flow phenomena. The secondary flows are observed mainly near the end wall. Secondary flows cause to generate a non-uniform flow at exit of the blade row thereby efficiency of the blade row downstream gets reduced. Other than profile losses, secondary losses also contribute significantly to the total loss. These flows present challenging tasks for turbine designer and researchers.

A more complete understanding of the complex three-dimensional flow, their origin and associated losses will certainly prove helpful in any attempt to make improvements in turbine performance. Primary objective of this work is numerical study of phenomena causing various losses in turbine fluid path. The experimental work conducted in past in a wind tunnel on rectilinear cascade of smooth turbine are studied. The results obtained by Samsher [2002] are used for validation of computational model for numerical study. Three -dimensional model of cascade geometry is made with the help of Gambit® 2.2.4 as preprocessor and Fluent® 6.2.16 is used as solver and post processor for flow simulation. Once the model has been validated the cascades of turbine and compressor are simulated to carry out study of effect of blade deterioration on various losses.

By determining the effect of roughness on the efficiency of the steam and gas turbines, various decisions regarding the replacement of the blades can be taken with improved certainty. Based on this information a cleaning schedule can be made and updated regularly and methods can be developed for improving surface finish. Losses occurring due to change in blade profile and thereby increment in roughness can also be ascertained.

1.4 Organization of thesis

The focus of this study is to study effect of different levels of roughnesses present over different location over the turbine and compressor blades on various losses. The study is carried out using the Computational Fluid Dynamics (CFD) commercial softwares, Gambit 2.4.6® and FLUENT 6.2.16® for creating geometry and solving the governing equations respectively. To establish sanctity of the computational work with the experimental work, the results of present work have been validated using experimental data of wind tunnel experiment on a scaled rectilinear cascade. In view to measure effects of blade deterioration on performance of turbines and compressors total three numbers "Three Dimensional Rectilinear Turbine Cascade" and "a low-speed axial flow rectilinear Compressor Cascade" are modeled respectively. The effect of blade deterioration on total, profile and secondary losses choosing the flow to be three dimensional were measured for three different blades profiles by successively employing different combinations of profiles and roughnesses on the surfaces of blades chosen for measurement.

The dissertation consists of six chapters. In the chapter 1, the topic is introduced, and in the chapter 2, a review of literature is presented. The theoretical background of Computational Fluid Dynamics (CFD) using Gambit® 2.2.4 and FLUENT 6.2.16® as preprocessor and postprocessor respectively are introduced in chapter 3. This chapter also gives computational methodology relevant for current investigation and provides basic theory on the solving governing equations of fluid motion using FLUENT 6.2.16®, various turbulence models available, computational domain, operating and boundary conditions used in current study to investigate effects of roughness in turbine cascade. Analysis of data is presented in chapter 4. The method of calculation

of energy loss coefficient using various values of pressure (total as well as static pressure) at inlet and exit is also presented in chapter 4. Chapter 5 deals with results and discussions. In chapter 6, conclusions and scope for further work are given. References are placed at the end.

CHAPTER –2
LITERATURE REVIEW

In this chapter review of published literature on related aspects is presented. This review is aimed to reveal data on work conducted in the area of Power Plant Engineering and bring out the unique contributions with regard to cause & effect of blades deterioration of turbines and compressors. The review of published literature on measurement of the losses is also included in this chapter. The relevant literature for the present study with regard to techniques and tools of Computational Fluid Dynamics (CFD) are also presented. The other relevant topics of literature review include roughness patterns, particle dynamics, fluid dynamics of flow over blades, Aerofoil Blades theory and recent works on mechanism of generation of various types of losses in turbines and compressors. The review of recent works on generation of secondary losses and reduction of the same are also out lined. The overview of literature review with regard to losses by modification of leading edge geometry and end wall fencing designs have also been presented. The overview of literature correlating experimental and computational work methods is also presented. The methods of washing of surfaces of turbines & compressors and the development trends in this field are also reviewed. Since the roughness over steam turbines blades also affect its performance in similar manner as in case of gas turbine, the relevant literatures on steam turbines are also reviewed.

The conclusions from literature review followed by scope of present study on effects of roughness on flow through turbine and compressor cascades are given at the end.

2.1 Computational Fluid Dynamics (CFD)

There are different engineering problems based on the fundamental equation of fluid mechanics which possibly may not be solved analytically. The computer-based

solution which uses CFD is available for such problems. A 'virtual prototype' of the system or device that any one wish to analyze, can be built using CFD softwares.

CFD is attractive to industry since it is more cost-effective than physical testing for complex flow simulations. The physical testing is found to be more challenging and needs a very comprehensive set of requirements. It takes a lot of engineering expertise to obtain validated solutions. CFD works with the principle to replace the continuous problem domain to a discrete domain using a grid. The discrete domain used in CFD defines a discrete value to each flow variable at every point.

CFD uses the fundamental laws of mechanics to solve the given engineering problems. The fundamental equations governing the fluid flow are Continuity equation, Second law of motion and First law of thermodynamics. This process starts with converting unsolvable governing equations (Navier-Stokes equations) to a solvable set of algebraic equations for a finite set of points within the space under consideration. According to Schlichting [1968], these equations can be solved analytically, for simple cases only. In actual practice the flows in turbomachinery are mostly three-dimensional (3-D) with various combinations such as 3-D laminar, 3-D transition and 3-D turbulent flow etc. Various other flow phenomena are also 3-D in nature such as separated flow, incompressible, subsonic, transonic, supersonic, single-phase and two-phase etc. Considering all the flow phenomena Lakshminarayana [1996] concluded that large number of flow and geometrical parameters dictates the nature of governing equations. Therefore variety of models of solution are available in the CFD such as eddy viscosity (zero equation) model, turbulent-kinetic-energy equation model (one equation), k-ε (two equations) model, Reynolds stress model, large-eddy simulations and direct simulation of turbulence [White, 1991] etc.

Asghar Alizadehdakhel et al. [2010] studied the flow and heat transfer of gas /liquid two-phase flow and the simultaneous evaporation and condensation phenomena in a thermosyphon. He compared the experimental result with the CFD simulation and found the good agreement between the two results and concluded that CFD is a useful tool to model the complex flow and heat transfer problems. It is expected that the CFD simulations must capture the different vortex structure with high precision.

2.2 Roughness pattern

The flow over the clean blades is expected to have a laminar zone. If a roughness exists on surfaces of the turbine blades then a turbulent flow is expected. The erosion, corrosion and deposition depend on various factors and hence the roughness varies from hub to tip, leading edge to trailing edge and initial stage to last stage.

Coton and Schofield [1971] observed copper salts deposits of different levels of roughness in rotor and nozzle blades. Similarly, Bolcs and Sari [1988] observed the deposits mainly on the pressure surface, and only a small number of particles stick to the suction surface. Kind et al. [1996] observed that the roughness over the suction surface is more detrimental than that over the pressure surface. Roughness over suction surface is reported to have a greater effect when the roughness band is towards the leading edge [Kind et al., 1996]. Taylor [1990] observed the roughest surfaces on the first stage blades of TF-100 and TF-39 aircraft turbines. The roughest surface for TF-100 aircraft turbine was found to be suction surface at leading edge region. The roughness thereon was measured to be 10.7 μm. On the other hand, for TF-39 aircraft turbine, the highest magnitude of roughness of 6.86 μm was found on pressure surface near mid-chord region. The roughness value at trailing edge region for TF-39 aircraft turbine was found to be 5.5 μm.

The magnitude and the statistical character of the roughness varied substantially from point to point around the blade; the blade thus does not have a single roughness value.

Bons *et al.* [2001] observed that some regions on both the suction and pressure surface are prone to specific roughness mechanism and transition between rough and smooth regions are gradual. Samsher et al. [2002], in a 210 MW steam turbine, observed that the rotor blades of initial stages of IP turbine are subjected to solid particle erosion at suction surface, and deposition over the pressure surface. The inlet steam in these turbines is superheated and the roughness can be attributed primarily to erosion and depositions. The roughnesses are predominantly in the form of bands (at mid-chord, leading edge, or trailing edge) spread all over the span. The magnitude and the statistical character of the roughness varied substantially from point to point around the blade; the blade thus does not have a single roughness value.

It can be concluded here that roughness varies substantially from point to point around the blade. Roughness caused by deposition is higher in nozzle blade compared to rotor blade, also same is more over pressure surface than over suction surface and increases towards turbine end. Typically, suction surface leading edge region and pressure surface mid-chord and trailing edge regions are the roughest.

The figure 2.1 shows how pressure and suction surfaces are affected by solid particle erosion.

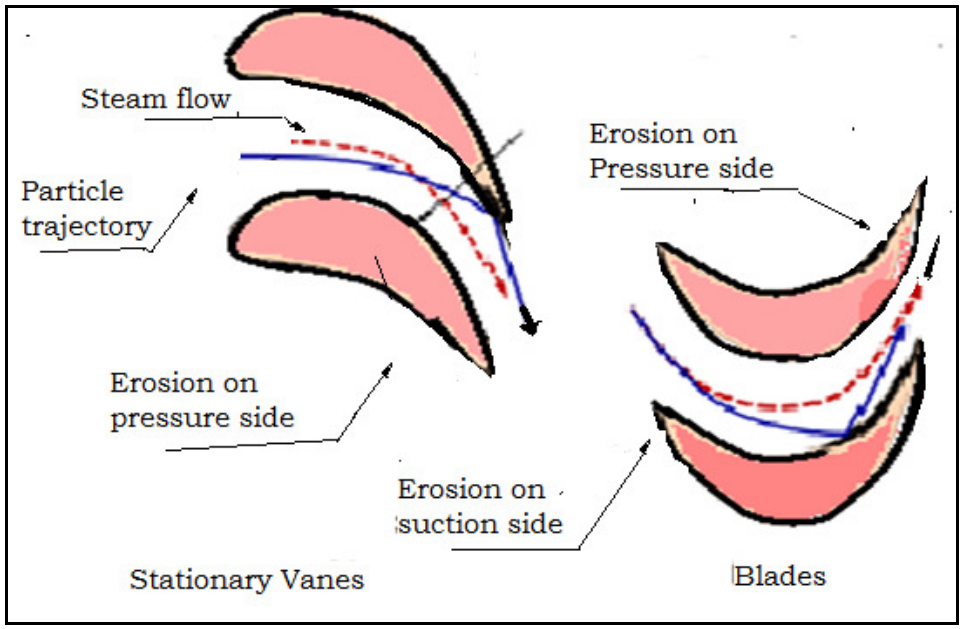

Figure 2.1: Erosion on pressure & suction side of blades

2.3 Particle dynamics

The following are few studies focusing on relative impact between particulate matter and blades. A large number of studies on particle trajectories are available; those specifically related to erosion on turbomachines flow passages are reported here.

Adverse effect of particle-laden gas flow on turbine torque, power and efficiency increases with increase in particle concentration and particle mean diameter [Tabakoff *et al.*, 1976]. As operating power plants age, the particle concentration in the steam/water increases and consequently, the performance deteriorates continuously. The local chemical environment in the steam turbines is profoundly governed by solubility and volatility of substances in the steam. The copper, sodium and iron oxides deposits degrade the surfaces of such turbines. During expansion of steam in a condensing turbine, steam partitions into liquid and the vapour phases [website *3*].

During expansion the solubility generally decreases leading to deposition of the above impurities. Such deposits may cause blockages and efficiency losses. The liquid phase is subject to concentration processes for impurities. Once the impurity is in steam, its behavior depends on solubility which determines whether the impurity remains vaporized in the steam or will precipitate out. On the other hand volatility decides where the impurity will be either in liquid phase or continue in vapour phase.

In general, the dynamics of particles through turbomachines is determined by gas-particle interaction and particle surface impacts. Using high speed photography, Hamed [1984] concluded that the hub impacts reflect the particles in the radial direction while the blade impacts reflect the particles in the circumferential direction. He found that trajectories of large particles are dominated by their surface impacts, whereas small particles are strongly influenced by the flow field. It was also observed

that the impacts for particles of the size of approximately 1000 μm, are distributed over the entire pressure surface and erosion increases towards the hub trailing edge. However, the blade erosion due to impacts by smaller particles increases with increase in impact velocity on the pressure surface from mid-chord towards the tip.

The biomass are considered to produce substitute fuels to replace natural gas for turbines since they would potentially provide CO_2 emission benefit in the case of the power plants. Moreover alternate fuels such as coal, petcoke are also used in such plants [Bons et al., 2007]. In a study on the effect of dust ingestion into a gas turbine, Batcho *et al.* [1987] observed that leading edge erosion resulted in a substantial deterioration of performance of such turbines.

To minimize erosion a coating over the blade surface is applied. Tungsten carbide and chromium carbide super D-Gun coatings not only have better erosion resistance than their D-Gun analogs, but cause little or no degradation of the fatigue properties of the blade alloys, [Walsh *et al.*, 1995]. Shanov and Tabakoff [1996] observed that with hot wall chemical vapour deposition (CVD) of TiC, erosion rate increases with the impingement angle to a maximum at 90^o. The TiC coating showed better protection on stainless steel 410 than on INCO 718.

The degradation caused by the adherence of particles on the gas turbines and compressors airfoils and annulus surfaces is conventionally defined as fouling. By being exposed to atmospheric conditions gas turbines and compressors are inevitably subjected to sources of fouling. Compressor fouling is defined as the deposition of airborne particles on to compressor blades which results from the adherence of dust or sand particles mixed with small oil droplets to compressor blade surfaces. It also results in change in blade profile and roughness over the surface that varies along the

blade span as well as from initial stage to final stage. The result is a reduction in compressor pressure ratio and an overall loss in mass flow, compressor efficiency and, therefore, overall power output. To overcome the losses so generated, the common methods of cleaning / washing the compressors include 1. Manual procedure, 2. Grit-blasting method, 3. Soak or crank (offline washing) and 4. Fired (online washing). Performance loss due to compressor fouling can be partially recovered by compressor cleaning [Friederike C. Mund et al., 2006].

2.4 Aerofoil Blades Theory

Aerofoil blade is a streamlined body having a thick, rounded leading edge and a thin trailing edge. Its maximum thickness occurs somewhere at the midpoint of the chord. The backbone line lying midway between the pressure and suction surfaces is known as the camber line. When such a blade is suitably shaped and properly oriented in the flow, the force acting on it normal to the direction is considerably larger than the force resisting its motion. The cross section of aircraft wings & the blades of various turbo machines resembles Aerofoils. The airflow across their surfaces produces an unbalanced force and the magnitude of force so produced by an aerofoil depends on:

i. Its shape, area and smoothness of its surface
ii. The speed of airflow over the aerofoil
iii. The angle at which the aerofoil meets the air

The three cases of blades orientation with respect to direction of air stream are represented in figure 2.2 a, 2.2 b and 2.2 c.

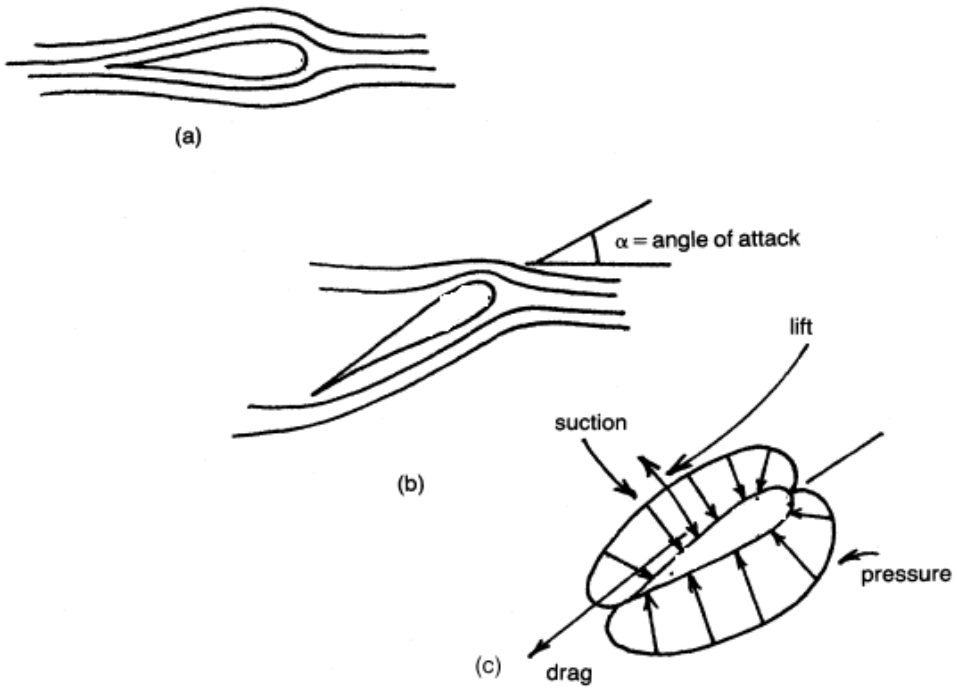

Figure 2.2 a, b & c: Flow around an aerofoil at various angle of attack

The different blade orientations with respect to directions of air stream are discussed in the following sections.

2.4.1 Blade orientation with respect to air stream: single aerofoil is oriented parallel to the air stream velocity

Air divides the body or separation at two at leading edge and joins again at the trailing edge of the body. The main stream itself suffers no permanent deflection from the presence of the aerofoil. Forces are applied to the aerofoil by the local distribution of the stream and the friction of the fluid on the surface. If the aerofoil is well designed, then flow is streamlined with no or little turbulence.

2.4.2 Blade orientation with respect to air stream: single aerofoil is oriented at an angle to the air stream velocity

In this case disturbances are created and pressure distribution along the blade, as compared to previous case, changes. The flow still remains parallel and uniform to

the blade up to certain distance. The Air undergoes a local deflection in downstream direction after some distance measuring from leading edge. The major disturbance is in suction side in the downstream direction. The pressure pushes inward on the airfoil everywhere on both the upper and lower surfaces. The force is exerted by the air as a pressure difference on the airfoil's surfaces. The flowing air reacts to the presence of the wing by reducing the pressure on the wing's upper surface and increasing the pressure on the lower surface. The lift results due to pressure difference on the lower surface and the upper surface. The phenomenon of lift can be explained on the basis of both Newton's third law of motion and Bernoulli's theorem.

Measurement of the pressure at various points on surface of aerofoil reveals the pressure distribution. Vector sum of these pressures produces some resultant force acting on the blade. This resultant force can be resolved into two components i.e. drag force and lift force. The drag force is directed opposite to the motion of the object or in the direction of the flow advancing into the object and lift force acts at right angles to the direction of drag force [website 4].

2.5 Fluid dynamics of flow over blades

The boundary layer is field of flow created around a solid body immersed in the fluid due to effect of the viscosity of flowing fluid. The boundary layer is formed when there is relative motion between a solid body and a fluid. It is formed in narrow regions adjacent to the solid surfaces if the body is of streamlined shape and if the viscosity is small. The velocity of the fluid on the passage wall is zero due to effect of the viscosity of flowing fluid. The velocity of the fluid develops fully to the free stream velocity over a short distance from the wall. The fluid flow about the body can be divided into two regions: where viscous effects are significant and the other where these are negligible. The effect of viscosity is predominant in the region of boundary

layer, causing high energy loss. The boundary layer is the slow moving layer of fluid near the solid surface. The flow outside this region is considered frictionless or potential flow. The boundary layer thickness depends upon many factors. It decreases with increase in the Reynolds number on the account of the lower viscous force compared to the inertia forces. The other factors affecting the boundary layer phenomenon are velocity of fluid flow over the surface, surface roughness, Reynolds number and curvature of the blade surface etc. Even a small roughness may cause the thin viscous inner layer to break up. This leads to increase the wall friction and heat transfer coefficient. Blade roughness effect therefore is considered to be one of the main sources of pressure loss.

2.5.1 Linear Turbines/Compressor cascade

A row of blades representing the blade ring of an actual turbo machine is called cascade. In a straight or "rectilinear cascade" the blade are arranged in a straight line. The blades can also be in an annulus, thus representing an actual blade row. This arrangement is known as an "annular cascade". Flow in a turbine blade cascade is an example of confined flow.

In the cascade, the fluid chosen for study enters at the cascade inlet, flows between the blade passages and then moves to cascade outlet while flowing between the tailboards. It is essential to design the turbine cascade in such a way so as to minimize the chances of secondary flow and losses. These losses deviates the expansion of fluid through the turbine from the isentropic process and hence reduce the work output through turbines. These losses reduce the economy of power plant as well. Tailboards of the cascade are therefore modified so as to reduce the losses. During the computational study under this research work, different orientations of tailboard are studied for achieving minimum losses condition.

2.5.2 Two dimensional flow through a Linear Turbines /Compressor cascade

The flow over the suction side of the airfoil for a low-pressure turbine is subject to a favorable pressure gradient near the leading edge, which tends to keep the boundary layer laminar, in spite of the high background turbulence level in the engine. On the contrary when the flow occurs in the direction of static pressure rise (adverse pressure gradient), the boundary layer thickens and reverses if this static pressure gradient (pressure heel) is too high. The leaving of the boundary layer from the surface and its reversal is known as separation. Flow separation occurs when the boundary layer travels far enough against an adverse pressure gradient and that the speed of the boundary layer relative to the object falls almost to zero. The fluid flow becomes detached from the surface of the object, and instead takes the forms of eddies and vortices [website 5].

The flow over the trailing section of the suction side is subject to an adverse pressure gradient. The boundary layer separates near trailing edge as it has some definite thickness. The adverse pressure gradient also tends to promote transition to turbulent flow. The separation points shift towards leading edge depending upon the extent of adverse pressure gradient [Samsher, 2002].

Transition often leads to reattachment of the boundary layer. Boundary layer separation causes a degradation of performance, particularly if the boundary layer does not reattach. The interaction between separation and transition is complex. Laminar boundary layers are more prone to separation than turbulent boundary layers, and turbulent boundary layers are more likely to reattach than laminar. The transition process is dependent on whether transition is initiated before or after the boundary layer separates. The length of the separation region is decreased as the Reynolds

number and/or the turbulence level is increased. Roughness over either of the surface will result in increase in loss, but when the roughness is applied at the separation point, if any, there will be more transverse mixing causing increase in viscous force and, hence, delaying the separation and resulting in lesser energy loss. Otherwise the roughness pushes the transition point forward causing higher losses.

The boundary layer consists of three sections that are laminar, transition and turbulent flow regions. Initially the Boundary layer is consisting of laminar flow. Thereafter the laminar flow of boundary layer destabilises and changes to turbulent flow due to changing of limiting conditions of the flow. During the course of flow the laminar flow becomes turbulent and the process is called transition.

The transition from laminar to turbulent flow depends upon many factors. The effect of roughness of the surface of the blade on this transitional effect is also very significant. The fluid flow within the boundary layer is a very complex and so is this transition process. The flow during the transition process gets detached from the surface and a reverse flow starts happening due to Boundary layer separation. In some cases the laminar flow destabilises and changes to turbulent flow.

The inviscid outer flow imposes a pressure at every point on the outer edge of the boundary layer on the blade surface and remains constant in the boundary layer perpendicular to wall [Schlichting, 1968]. Bammert and Sandstede [1980] with regard to boundary layer thickness observed that it first increased on the pressure side and reached to a maximum at approximately mid of the contour length. According to the study boundary layer become thinner just before the trailing edge and boundary layer thickness again starts increasing near the trailing edge. On the suction side, boundary layer for smooth surface is laminar up to approximately 82% of the contour length.

The boundary layer growth on the suction and the pressure sides of the blade in a real flow leads to the formation of low energy regions in exit flow field. These are distinct separate lanes of chaotic flow with considerably low fluid velocity and the pressure of vortices. These lanes are referred to as “blade wakes”. The fluid velocity raises from the wake regions to maximum in the free stream. According to Gostelow [1984] and Pope [1961] the wake sucks the fluid from the core and, hence, intensive mass transfer takes place between the wake and the core flow that results in an increase in wake width with distance from exit of the blade.

Losses due to this intensive mixing of wake and the core flow are further enhanced. The losses so generated are known as mixing losses. The two wakes on the same exit plane prior to mixing has different levels of energy. The wider wake has lower energy than thinner wake. Interaction of these two wakes results to energy loss. The core flow has the maximum energy level and energy level for a point inside the wake increases with distance from the core flow [Samsher, 2002].

The wake width and velocity defect increase with a decrease in either turbulence level or Reynolds number, Murawaski and Vafai [2000]. Coton *et al.* [2001] showed that wakes are deeper and wider and loss is increased by a factor of 10 if pitch-chord ratio is increased from 1 to 1.74 at constant Reynolds number ($1.9x10^5$). The exit flow angle is also affected by the spacing or pitch chord ratio and nature of flow. The wake flow and boundary layer separation also considerably affect the exit angle.

The Figure 2.3 shows how Boundary layer separates for a two dimensional flow through a cascade.

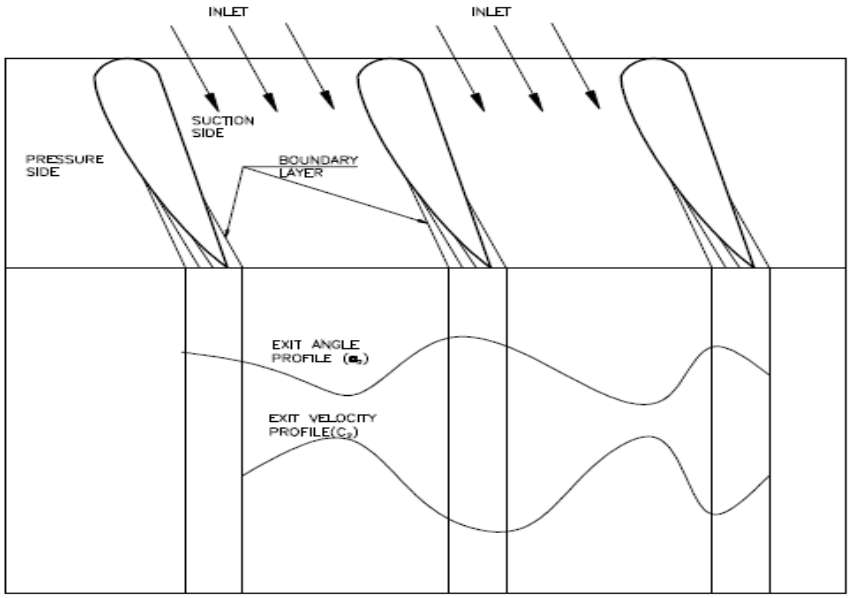

Figure 2.3: Boundary layer Separation for a Two dimensional flow through a cascade.

The point of separation depends on the geometry, roughness of the surface, nature of flow (turbulent and laminar) and Reynolds no. etc. The laminar boundary layer gets separated earlier than the turbulent. In order to reduce losses for a turbine cascade it is necessary to prevent or delay the separation of boundary layer.

The methods for controlling boundary layer separation may be summarised as under:-

i) Making arrangements for sucking away the decelerated layer

ii) Energizing boundary layer by injecting high energy fluid parallel to the surface.

iii) Separation can also be delayed by achieving earlier transition of the laminar flow into the turbulent

2.5.3 Laminar sub layer

The aerodynamics of gas turbine and compressor blades is reviewed here with regard to effect of surface roughness on boundary layer growth. Surfaces produced by a variety of processes, such as machining, honing, grinding, polishing, etc. are not

absolutely smooth. Increasing the surface finish, i.e. smaller roughness, increases the production cost substantially which is uneconomical from an overall viewpoint. The finished blade has some roughness and tolerances associated with this manufacturing trade-off. This value of surface roughness is considered as starting base value and is not treated as roughness until it influences the performance.

The turbulent boundary layer over a rough wall has recently received considerable attention from researchers. Close to the wall itself, the effects of roughness on the velocity field depend on the specific geometry of the roughness elements. It is observed that laminar sublayer is formed within a turbulent boundary layer. The sublayer is also called the viscous sublayer. This layer is very thin layer, which is formed next to the surface downstream of the laminar region and its velocity is such that the viscous forces dominate over the inertial forces. In some applications of the blade profile, the viscous drag force plays very vital role. For the very purpose of getting such application to be efficient the drag force has to be minimised. The drag force in the case of compressor cascade is very vital. The effects of surface roughness on the mean velocity are investigated for three flow regimes, namely, hydraulically smooth, transitionally rough, and fully rough. In case the main body of the flow ignore the roughness of surface if it is smaller than laminar sublayer. The flow is then assumed to be passing through hydraulically smooth surface. The flow is defined as hydraulically rough in case roughness elements are larger than the laminar sublayer. The hydraulically rough surfaces perturb the flow passing over to them. The admissible value of surface peaks which can be treated as hydraulically smooth (K_{adm}) depends on the Reynolds number and a characteristic length (L) as per the following criteria, Schlichting [1968]:

$$\frac{K_{adm}}{L} \leq \frac{100}{R_e}$$

Figure 2.4 shows a 2D view of the formation of boundary layer and laminar sublayer within the boundary layer during the flow over the blades of a rectilinear cascade.

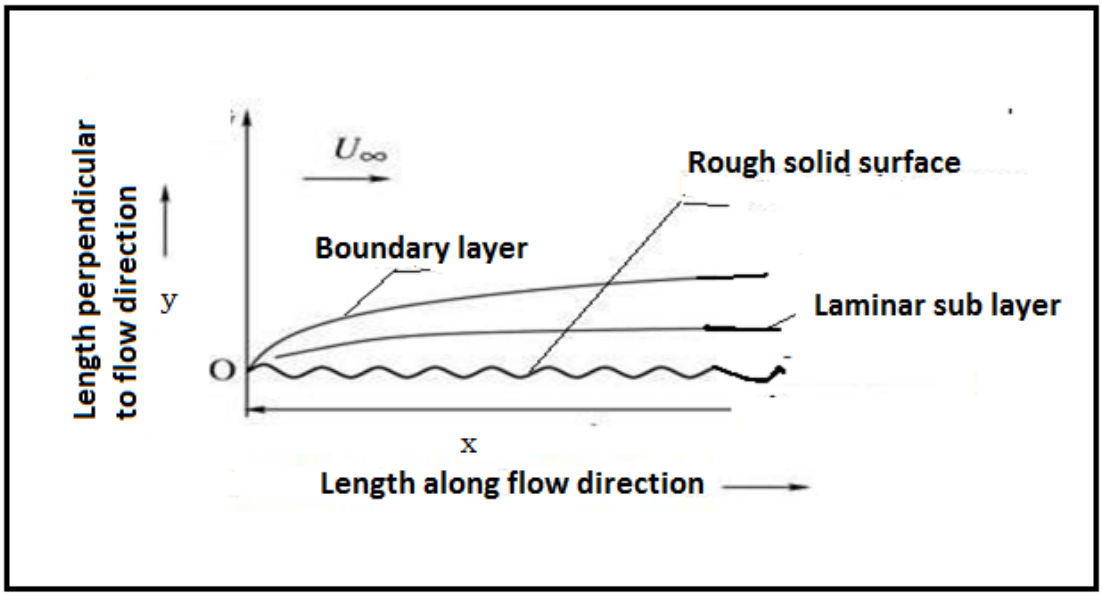

Figure 2.4: Formation of boundary layer and laminar sublayer within the turbulent boundary layer

At high Reynolds number, the flow undergoes a change from laminar to turbulent motion characterized by strong mixing of fluid in a direction normal to the flow. This motion results in increased momentum transfer in a transverse direction. For a flat plate zero pressure gradient, at Reynolds numbers less than $2x10^5$ the flow is laminar and for more than $6x10^5$ the flow is turbulent, called critical Reynolds number. If pressure gradient is positive, the value of critical Reynolds number decreases, and if pressure gradient is negative it increases [Schlischting, 1968]. In turbine blades pressure gradient is positive at leading edge of the pressure surface and trailing edge part of the suction surface. However, the results of the CFD of turbine cascade showed that excess of the roughness do not increase the loss predominantly over the moderately smooth surfaces. However, the loss increases more rapidly with the increase of roughness at the smaller values of roughness.

In the compressors, the contribution of adverse pressure gradient to the overall losses is more, as compared to that of surface roughness. In case of compressor Cascades the

flow through the passages between two consecutive blades sections occurs in the direction of static pressure rise (adverse pressure gradient). This is why the boundary layer thickens in such cases. The laminar boundary layer formed initially at upstream of a blade profile gets separated due to dropping of surface pressure as it marches downstream from the leading edge to trailing edge. There could be a zone of an adverse pressure gradient depending on the turning on the surface of the blade. Thus, the boundary layer could grow rapidly or even separate in such a region.The laminar boundary layer formed initially at upstream has more chances of separation as it moves downstream on the Suction surface of blade. The boundary layer for the turbine flows is lesser prone to separate as the fluid flow in the direction of pressure drop. Because of the generally falling pressure in turbine flow passages, much more turning in a given blade row is possible without danger of flow separation than in an axial compressor blade row. In turbine the leading edge is thicker than a compressor.

The compressors differ in this regard as fluid undergoes a pressure rise in the compressor. The chances of separation of boundary layer in case of Compressor is more because adverse pressure gradient retard the fluid in the Boundary layer & ultimately brings the fluid in to rest thereby the outer layer of stagnant fluid separates from this fluid.

2.6 Energy Losses in Turbines and Compressors

The viscous diffusion in the flow through turbine cascade decreases integrated flux of total pressure through the cascade. Since this decrease in total pressure flux is related to the amount of kinetic and potential energy loss in the cascade, hence, this pressure flux is termed as ‘total pressure loss’ or simply ‘loss’.

Losses of various kinds, adversely affects the efficiency of turbines and compressors. Researchers in the power plant area are hankering for maximum use of available

energy. Minimizing losses by getting best aerodynamic performance is a very important step in this direction. Optimizing blades conditions i.e. Length, Aerodynamic Section, Shape, Aerofoil thickness and last but not least the surface smoothness would be inevitable for a better aerodynamic performance.

The two major losses encountered in the cascade are termed as 'profile loss' and 'end loss' or secondary loss.

2. 6 .1 Profile loss

The profile loss is the loss due to boundary layer on the blade surface and trailing edge thickness. An increase in Reynolds number and roughness at separation point delays the laminar separation. This will result in less loss. But if flow does not show any symptoms of separation then increase in Reynolds number or roughness over blade surfaces moves transition points ahead and boundary layer becomes turbulent early causing increase in loss. Coton *et al.* [2001] showed that loss increases by a factor of 10 when pitch chord ratio is increased from 1 to 1.74 at constant Reynolds number of $1.9x10^5$. Horlock [1966] showed how the components of energy losses for flow through turbine blade cases are affected with incidence angles. The losses are minimum when the incidence angle of the inlet airflow is within the range of 0 to 15°. The profile and secondary losses both increase when the incidence angle exceeds 15°.

2.6.2 End wall or secondary losses

The term secondary flows refers to the three- dimensional vortical flow structures that develop in blade passages due to high turning of the flow and non-uniform inlet total pressure profiles.

2.6.3 Tip clearance loss

This loss occurs due to clearance between moving blade and the casing. Due to the static pressure difference, the flow leaks from the pressure side towards the suction side of the turbine or compressor blade.

2.7 Mechanism of generation of Secondary Losses

The aerodynamics of the flow in a turbine stage (stator/rotor) is a complex issue and always been a subject of research. The flow through a cascade is inherently three dimensional and usually viscous. Due to the blade profile the flow becomes unstable and also subjected to separation. Both of these phenomenon leads to development of vortices and these vortices are the source of cross or circulatory flow which is termed as secondary flow. The primary flow usually matches very closely the flow pattern predicted using simple analytical techniques and assuming the fluid is inviscid and is usually governed by basic principles of physics. However, in real flow situations, there are regions in the flow field where the flow is significantly different in both speed and direction to what is predicted for an inviscid fluid using simple analytical techniques. The flow in these regions is the secondary flow. These regions are usually in the vicinity of the end walls.

Following are three main flow patterns which are potential sources of losses in turbomachinery:

(i) The passage vortex, which is generated by the interaction of the pressure gradient and the boundary layers near the solid walls.

(ii) The horseshoe vortex, which is generated by the interaction of the boundary layers on the end walls with a leading edge when the flow is curved by blades.

This vortex starts at the leading edge near the end walls and develops in the inter-blade passage.

(iii) The wake, which is the lower velocity flow generated behind a blade.

The formation of vortex in a turbine system largely affects the secondary loss. The incoming boundary layer separates upstream of the leading edge, forming a horseshoe vortex. This vortex is consisted of two legs. The leg formed at the pressure side and suction side of the blade are called pressure vortex and suction vortex respectively. The legs so formed differ from each other. The suction side leg is affected mainly by curvature of the suction surface. Whereas the pressure side leg is affected by curvature and pressure difference between pressure side and suction side of adjacent blade of the corresponding flow channel. The pressure side vortex leg is usually increases towards the exit of the cascade. The formation of a suction and pressure side leg and passage vortex in a wind tunnel experiment is shown in figure 2.5.

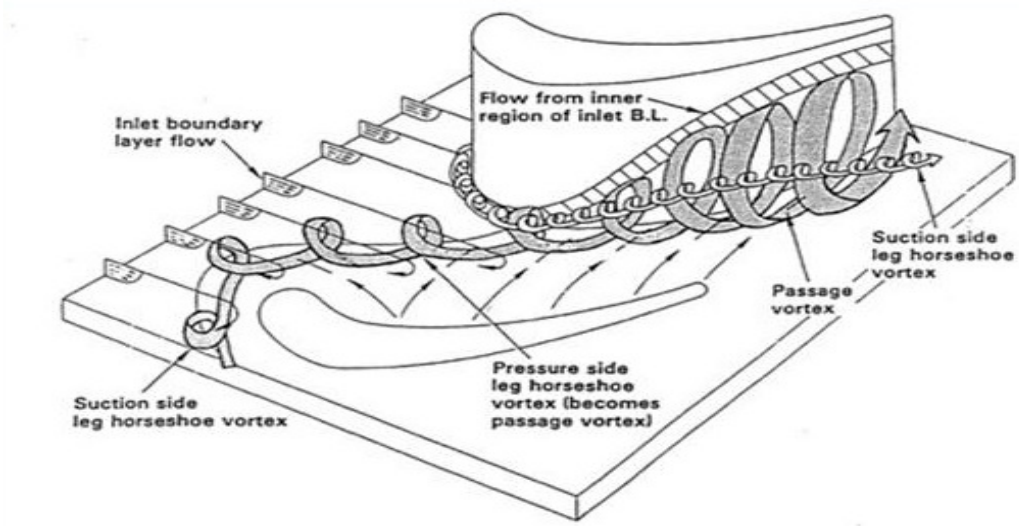

Figure 2.5: Vortex formation due to separation of incoming boundary layer at leading edge of the blade of cascade

Langston et al. [1977] was among the first to study the evolution of secondary flows using hot wire and flow visualization techniques to qualitatively assess flow patterns at boundary layer, near the end wall region of a cascade. According to Langston, the incoming inlet boundary layer splits into two streams, one moves towards the pressure surface and other towards suction surface. Adverse pressure gradient is resulted in 3-D flow separation and horseshoe vortex formation. Passage vortex is formed due to boundary layer and pressure gradient across the blade passage and rotates in anticlockwise direction. Cross flow is observed at end wall, because of the blade to blade pressure gradient. Suction surface leg rotates in opposite direction of pressure surface leg and consequently termed as counter vortex. The pressure surface leg of horseshoe vortex merges and strengthens the passage vortex. Later, different experiments were performed by Marchal et al. [1977], Sieverding et al., [1983], Wang et al. [1997] and Sharma et al. [1987] which complied with the conclusions of Langston et al. [1977]. Wang et al. [1997] concluded that pressure side vortex moves towards the suction side and merge with passage vortex at approximately one fourth of the distance from the leading edge.

The physics of the underlying flow regime of a curved passage flow is governed by the interaction of the pressure gradient linked to the curvature of the main flow with the non-uniform flow (for instance due to boundary layers on solid walls). The flow, moving slower in the boundary layers, is pushed from the pressure side to the suction side, leading to an overturning in the end-wall regions. This gives rise to stream-wise vorticity generating an end-wall vortex in the curved passage (as illustrated in figure 2.6).

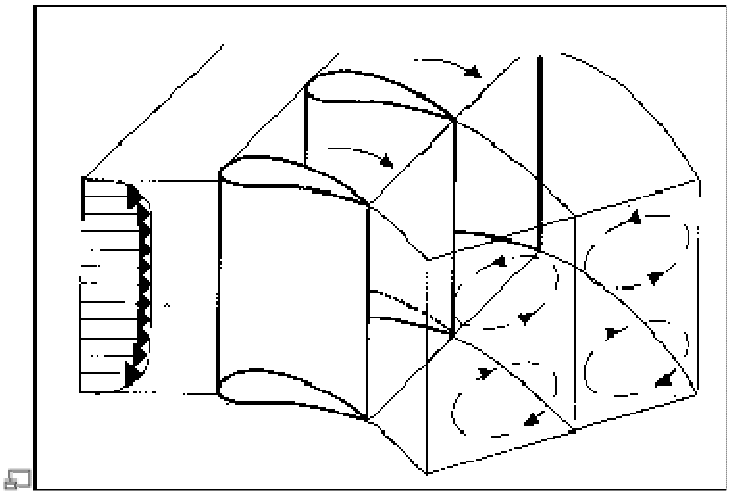

Figure 2.6. Stream-wise vorticity generation in the curved passage [Japikse, D. and Baines, N.C., 1997]

It should be pointed out that the basic mechanics of this secondary flow generation is inviscid. Furthermore, due to the presence of a rounded leading edge, horseshoe vortices are also generated, which merge with the passage vortices.

The correct representation of this flow regime is of importance because:

(i) It induces extra losses

(ii) It leads to significant 3D separation on the blade suction side

(iii) It induces a non-uniform heat transfer on the blade and end-wall surfaces and has a strong influence on the blade film cooling

(iv) It affects the blade lifetime because of enhanced thermal and mechanical stresses

(v) It has an influence on the turbine stage work output

(vi) It has an impact on downstream blade row efficiency due to an enhanced non-uniformity of the exit flow

This flow regime is influenced by numerous factors such as the blade shape, the pitch-chord ratio, the aspect ratio, the Mach number, and the inlet boundary layer thickness. Owing to its importance in turbomachinery design and to its interaction with other secondary motions, an excessive amount of work has been done on this flow regime.

There are two main designs for leading edge geometry: the fillet and the bulb for reducing secondary flow loss. Young J. Moon et al. [2000] analyzed the effect of end wall fencing for reducing the secondary flow using k-ξ turbulence model. They also justified the optimized positioning of the endwall fencing for reducing the secondary flow losses, because the end wall fencing prevents the merging of pressure side horse shoe vortex with the passage vortex and hence total pressure loss decreases.

Arun K. Saha et al. [2008] analyzed the turbulent flow through a three dimensional non-axisymmetric blade passage and observed that endwall contouring reduces the pitch wise pressure gradient near the endwall which reduces the chances of flow separation. SonodaToyotaka et al. [2009] used axis-symmetrical end wall contouring method for reducing the secondary losses in high pressure turbine having low aspect ratio. They investigated the effect of three types of end wall contouring: 1) only hub contour, 2) only tip contour and 3) hub and tip contour and observed that hub contouring, the tip contouring and the hub and tip contouring all reduce the mass averaged overall loss by 4%, 5%, and 10%, respectively, as compared to the base line.

Brear et al. in [2010] strived to reduce the pressure surface separation by modifying the leading edge geometry. They observed that increasing the blade thickness at the pressure surface decrease the strength of secondary flow by increasing the momentum near the wall. Shih et al. [2003] observed effects of leading-edge airfoil fillet on the flow in a turbine. The increased size of the stagnation zones on the endwalls about the

airfoil's leading edge lowers the flow speed and velocity gradients there, which in turn reduces turbulence production. G. I. Mahmood et al. [2007] studied the secondary flow structure in a blade passage with and without leading edge fillet and observed that the size and strength of the passage vortex become smaller with the fillets. T. Korakianitis et al. [2010] has proposed a direct design method based on specifying blade surface-curvature distributions so as to minimize the chances of flow separation. Qi Lei et al. [2011] analyzed the effect of leading edge modification on the secondary loss. They used vortex generator for introducing counter rotating vortex which oppose the passage vortex and hence reduce the secondary flow losses.

Much work has been done to understand the occurrence and modeling of secondary flow and end loss phenomenon. Moreover researchers had tried to reduce the secondary loss in any cascade in order to get higher aerodynamic efficiency of the power plant. It is a well-established fact that roughness over the blade surface increases the profile loss and corresponding total loss for a given cascade. But effect of roughness on the secondary flow and corresponding losses has not been studied much. In this thesis results of computational study of flow through Three Dimensional Rectilinear Turbine and Compressor Cascade in general and secondary loss and its dependence on roughness of the blades of the Cascades in particular is presented.

Denton[1993] carried out a study on end losses and found that end wall loss is the most difficult loss component to understand & predict, as virtually all prediction methods are still based on correlations of empirical data, often with very little underlying physics. Yaras and Sjolander [1992] showed the schematic breakdown of losses in the end region excluding profile losses. According to him the profile loss is dominant in the mid span of the blade and end losses are very significant near the end wall. The end losses at the end walls include tip leakage flows and gap losses.

Schematic breakdown of losses in the end region, excluding profile loss are shown in figure 2.7.

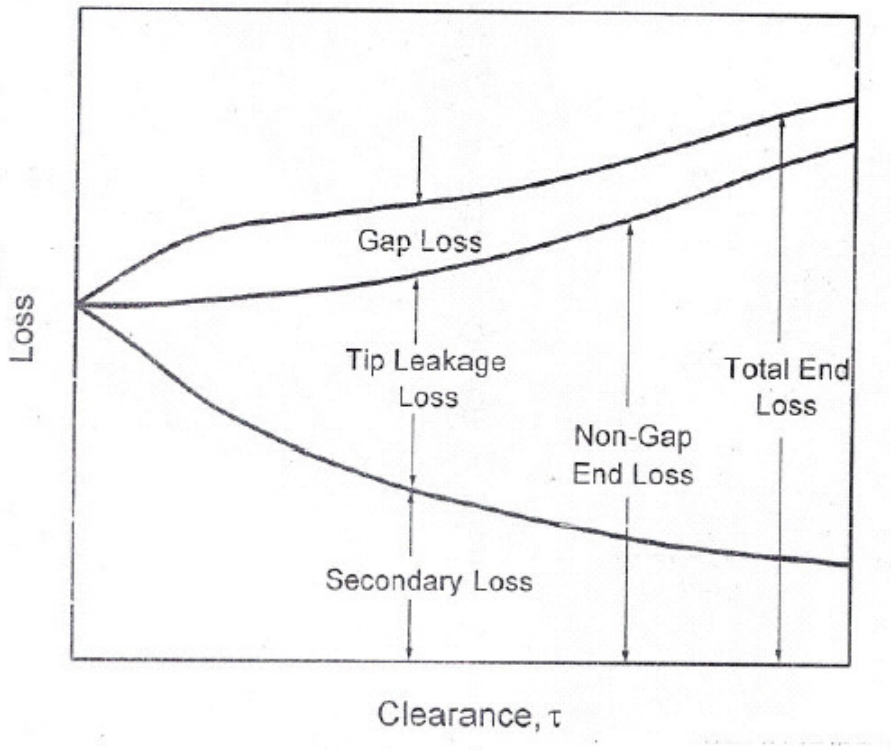

Figure 2.7: Schematic breakdown of losses in the end region, excluding profile loss [Yaras and Sjolander, 1992]

Prediction of end loss becomes more difficult due to interaction with tip leakage losses. Most of the prediction methods of end losses are still based on empirical data both in initial and detailed design phase of turbomachines due to its being greatly complicated.

2.8 Conclusions from literature review and gaps in the literature

It is reviewed that roughness varies substantially from point to point around the blades. It is also clear from the literature review that Several researcher has made attempt to characterize roughness, actually encountered over the gas turbines. It has been reviewed that only a few publications report work with the localized roughness,

whereas in real situations, the roughness is different for suction and pressure surface, and varies along chord and height [Taylor [1990], Cotton and Schofield [1971], Bammert and Sandstede [1972], and Bolcs and Sari [1988]]. The results of Forster [1966-67] indicate that roughness over 30% of the suction surface and 50% of the pressure surface from the leading edge does not lead to any increase in losses. The review shows that pressure surfaces of blades of a turbine cascade get eroded for a larger range of angle of incidence of the inlet airflow and that roughness on suction surfaces is more detrimental.

Thus, there is a need to find the effect of localized roughness on various surfaces numerically. In addition to that, there is very scare database with regard to the secondary loss for very complex three-dimensional flow through turbine and compressor cascade. This research work, in fact, is an attempt to study the complex three-dimensional secondary flow vortices near end wall region using FLUENT® 6.2.16 along with getting results for total losses. The total losses are segregated to obtain profile & secondary loss i.e. ends losses numerically.

In view of the findings reported in the previous sections, the argentines this PhD work is to:

(i) To determine the effect of roughness on secondary flow loss and profile loss by applying roughness over the entire blade, and over suction and pressure surfaces separately for three different blade profiles on turbine cascades separately.

(ii) To determine the effect on secondary flow loss and profile loss when localised roughness is applied over three different regions (width one-third of surface length) at leading edge, mid chord and trailing edge for three different blade profiles separately for impulse and reaction turbines.

(iii) To determine the effect on secondary flow loss and profile loss when roughness is applied over the entire blade and over suction and pressure surfaces separately for the compressor cascade.

The methodology/procedure to meet the objectives defined here, has been discussed in the next chapters.

CHAPTER –3
METHODOLOGY

The losses are generated as the fluid flows through blades passages in the turbines and compressors. The roughness on blade surfaces affects these losses greatly. The present computational study is targeted to get results of effect of roughness on blade surfaces on losses. This research work is carried out using the Computational Fluid Dynamics (CFD) commercial softwares i.e. Gambit 2.4.6® and Fluent 6.2.16® for creating geometry and solving the governing equations respectively. A number of geometries of three dimensional rectilinear turbines and compressor cascades are created specifying boundary zones and allocating boundary types to the surfaces so created. The geometries are meshed suitably with the help of the Gambit. Thereafter geometries so created are subjected to be post processed with the help of Fluent .

In this chapter the brief of above CFD softwares, an overview of computational methodology relevant for current investigation and over view of basic theory on the solving governing equations of fluid motion is presented. The topics relevant to CFD software FLUENT 6.2.16®, such as turbulence models available, computational domain, operating & boundary conditions used in current study to investigate effects of roughness for turbine and compressor cascades are also discussed. Method of finding various values of pressure (total as well as static pressure) at inlet & exit of the respective cascade, using the Fluent software, is also discussed. Methods of calculation of energy loss coefficient at various selected pitchwise positions at the exit measurement plane, chosen at 15% and 30% of chord length, after blade outlet, for turbines and compressor cascades respectively are also presented. The Local Loss Coefficients for various pitch wise positions are calculated using the relation proposed by Dejc and Trojanovskij (1973). The Local Loss Coefficients at a given pitchwise

position is calculated using values of pressure (total as well as static pressure) at inlet & exit measurement plane**.** Local Loss Coefficient for a span wise position is arithmetic mean of all the Local Loss Coefficients for various pitch wise positions. The Local Loss Coefficient does not take the mass and velocity of the flow into account. It is therefore assumed that Mass Averaged Loss Coefficients would be appropriate choice for finding losses. Therefore in view to getting the results to be more reliable and practically relevant Mass Averaged Loss Coefficients are calculated using local loss coefficients. The Mass Averaged Loss Coefficients are evaluated taking mass flow rate through various pitch wise positions into consideration. The Mass Averaged Loss Coefficient for a given span position is evaluated from bottom end wall till complete blade height for each cascade of turbines and compressor aiming to quantify losses at the end walls and mid span**.** The coefficients are computed along the complete blade span starting from end-wall surface at zero mm to other end-wall surface both in case of turbine and compressor cascades. Final calculated Mass Averaged Loss Coefficients for all the span locations are expressed in percentage of total energy of incoming air. Initially for all the turbine and compressor cascades both surfaces of all the blades are kept as smooth and various losses are measured. Thereafter various magnitudes of roughnesses are applied, one by one, on the surfaces of the blade of above cascades. Various losses are measured for each of such arrangements. The magnitudes of losses for smooth and other cascades are compared and tabulated.

In view to achieve targeted objectives, it is imperative to adopt a proper methodology. This chapter mainly describes methodology adopted for meeting the objectives of the work. Inter alia objectives of the work should primarily be specified to adopt a proper methodology.

First and foremost, it is required that user ought to have a thorough understanding of the CFD softwares so as to know their specialties, uses and functions. Moreover user need to make himself acquainted with the tools available for efficient use of softwares. It needs a lot of practice and in fact is a painstaking task. The brief regarding to the softwares used i.e. Fluent and Gambit, is mentioned in the following paragraph:

The Fluent software solve the fundamental nonlinear differential equations (mentioned below) that describe fluid flow (Navier-Stokes and allied equations), for predefined geometries and boundary conditions.

i. Conservation of momentum (Navier-Stokes equation)

$$\frac{\partial}{\partial t}(\rho u_i) + \frac{\partial}{\partial x_j}(\rho u_i u_j) = -\frac{\partial p}{\partial x_j} + \frac{\partial \tau_{ij}}{\partial x_j} + \rho g_i + F_i \qquad (3.1)$$

ii. Conservation of energy (Energy Equation)

$$\frac{\partial}{\partial t}(\rho E) + \frac{\partial}{\partial x_i}(u_i(\rho E + p)) = \frac{\partial}{\partial x_i}\left(k_{eff}\frac{\partial T}{\partial x_i} - \sum_{j} h_j j_j v + u_j(\tau_{ij})_{eff}\right) + S_h \qquad (3.2)$$

iii. Conservation of mass (Continuity equation)

$$\frac{\partial \rho}{\partial t} + \frac{\partial}{\partial x_i}(\rho u_i) = S_m \qquad (3.3)$$

Fluent converts unsolvable governing equations (Navier-Stokes equations) to a solvable set of algebraic equations for a finite set of points within the space under consideration. Fluent uses iteration technique for finding detailed information with respect to velocity, pressure, temperature, and chemical species etc. Typical blade cascade geometries models of all cascades are made using Gambit as preprocessor. Virtual prototype is prepared allocating proper boundary conditions representing the

actual flow behavior. Thereafter the computational software Fluent is used as solver & post processor for flow simulation.

In turbomachinery flow is affected by rotation, three- dimensionality, curvature, separation, free stream turbulence, compressibility, large scale unsteadiness, heat transfer and other effects. Fluid flows of practical relevance are mostly turbulent. Turbulence models approximate these transport processes in terms of mean flow field by empirical formulations. Therefore, in view to obtain a better result, turbulence modeling is chosen due to its being realistic. Turbulence models modify the original unsteady Navier Stokes equations by introduction of mass averaged fluctuating components to produce Reynolds Mass averaged Navier Stokes (RANS) equations. The most widely used models for turbomachinery application is the κ-ε model [Shih et al., 2003]. In this model, the turbulent kinetic energy (κ) and the energy dissipation rate (ε) are considered as the properties, which govern the turbulent flow phenomena. The Realizable κ-ε turbulence model of Shih et al. [2003] has been selected for solutions of present research work. This model is expected to provide more accurate results since it contains additional terms in the transport equations for κ and ε that are more suitable for stagnation flows and flows with high streamline curvature.

3.1 Selection of roughness, location of roughness and profiles for turbine Cascades

The selection of roughness and its location is based on the roughness pattern mentioned in the literature and studies carried out by Samsher [2002] on the roughness actually encountered on the blades of turbines operating at a number of power plants in India. To study the effect of blade profiles on losses, Samsher [2002]

selected three profiles from an operating 100 MW steam turbine - 1st HP stage, last LP stage 30% height and last LP stage 50% height. Of the three profiles, the profile from 1st stage of the 100 MW steam turbine is nearly impulse and remaining two profiles i.e. from last LP stage 30% height and last LP stage 50% height are reaction profiles. These profiles are also present at different heights of blades in the IP and LP turbine as well. All the total three number blade profiles titled 6030, 5530 and 3525 are chosen for the present study. The titles are informative with regard to their shape. It is clear from the titles that the degrees of reaction of these blade profiles differ from each other very significantly. Different numbers in the title of the profile indicate that each profile has different inlet air angle and outlet air angle. Consequently the reaction also changes from one profile to another profile. Moreover these blades profile are chosen from wide range of blade positions of actual turbine i.e. from hub to tip. The reaction of given blade profile changes from one stage to another stage and from hub to tip of a given blade. It is clarified that section of the blade close to the hub are nearly impulse and that close to the tip are of high reaction. The degree of reaction, typically designated to a stage, is the average value of reaction considering full heights of both the stationary and rotor blades. Thus results of these three profiles would be applicable to a large portion of the blading. Of the three selected profiles one (3525) is nearly impulse type & remaining two (5530 and 6030) are of reaction type with different degree of reaction. The degree of reaction for the blade profiles 5530, 6030 & 3525 is about 65 %, 55 % and 10 % respectively. The figure 3.1 shows the profiles 6030, 5530 and 3525.

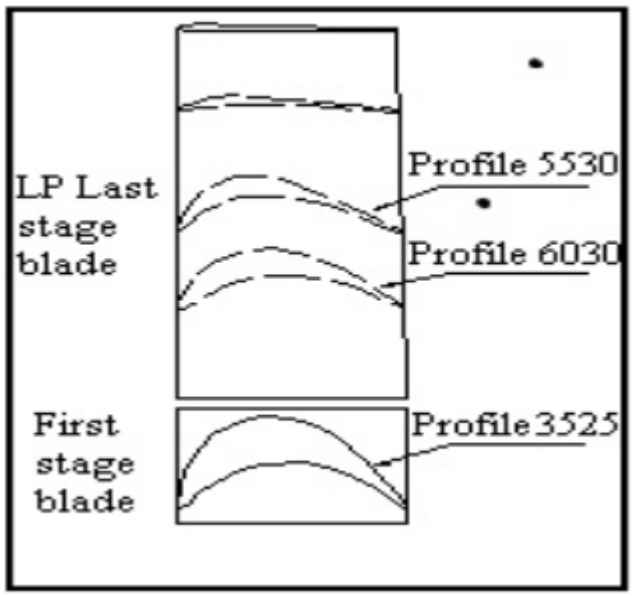

Figure 3.1 : Blade profiles from various positions of blades of First stage (3525) and last stage blades (6030 & 5530) of an operating 100 MW steam turbine as selected by Samsher [2002]

Table 3.1 shows various parameters of profiles as selected by Samsher [2002] for the test.

Table 3.1: Parameters of profiles as selected by Samsher [2002] for the experiment

Parameters	Cascade of blade profile		
	Profile 3225	Profile 6030	Profile 5530
Chord (mm), c	50	50	50
Pitch (mm), S	29	22	24
Pitch chord ratio, S/c	0.58	0.44	0.48
Height (mm), l	95	95	95
Aspect Ratio, l/c	1.9	1.9	1.9
No of blades	6	6	6
Inlet flow angle, (degrees)	40	65	52
Stagger angle (degrees)	80	70	72

Four equivalent roughnesses of 250, 500, 750 &1000 µm were selected to generalize the present study for a wide range of roughnesses. The roughnesses of 250, 500, 750 &1000 µm are applied on suction and pressure surfaces individually as well as on both the surfaces together.

Samsher [2002] observed distinct bands of roughness over the in-service blades. These roughness bands are replicated by applying fixed-width roughness over the entire blade height (span) at different locations. Each of roughness bands are simulated individually. These cascades are simulated such that the pressure and suction surface are divided into three zones each, as front one-third at the leading edge, middle one-third (adjacent to the front zone, i.e beginning one-third of chord from the leading edge), and a third up to the trailing edge. Similarly roughness on entire surfaces of the blades of turbines and compressor cascades are applied to see the effect of roughness over entire surfaces. For this purpose roughnesses of varying magnitudes 250, 500, 750 &1000 µm are applied over entire blade (each of blades of cascades) i.e. suction surfaces (SSR) and pressure surfaces and the entire pressure surfaces and entire suction surfaces together (BSR), one at a time for the case of turbine cascades. The figure 3.2 show experimental setup and figure 3.3 show grid display with regard to computational studies. Both the figures give a comparison between methodology of experimental vis a vis computational studies.

Figure 3.2: Experimental setup of Samsher[2002]

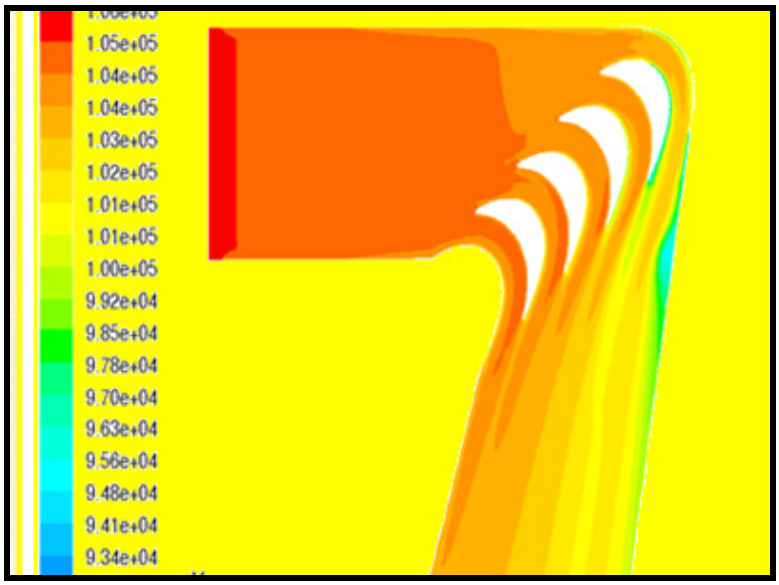

Figure 3.3: Grid display for pressure loss measurement for computational studies

3.2 Summary of locations of roughness for turbine Cascades

Broadly the roughness on all blades of a given cascade is applied either on entire surface or in localised way. Following is summary of locations of roughness application for finding Energy loss coefficients for turbine Cascades:

1. Entire blade

   (i) both suction and pressure surfaces

   (ii) Only suction surface

   (iii)Only pressure surface

2. Localised roughness

   (i) Suction surface leading edge region (SSR 1)

   (ii) Suction surface mid-chord region (SSR 2)

   (iii)Suction surface trailing edge end (SSR 3)

   (iv)Pressure surface leading edge (PSR 1)

   (v) Pressure surface mid-chord region (PSR 2)

   (vi)Pressure surface trailing edge (PSR 3)

3.3 Selection of roughness, location of roughness and profile for compressor cascade

An actual blade of compressor operating at a gas power plant is chosen for study of the compressor cascade. A section of the blade for the study was chosen for the purpose. The vertex data (x and y coordinates of the blade profile) of the blade section are obtained using a profilometer of the Delhi Technological University (DTU), Delhi, India. The profile obtained by joining various coordinates so generated is shown by the figure 3.4.

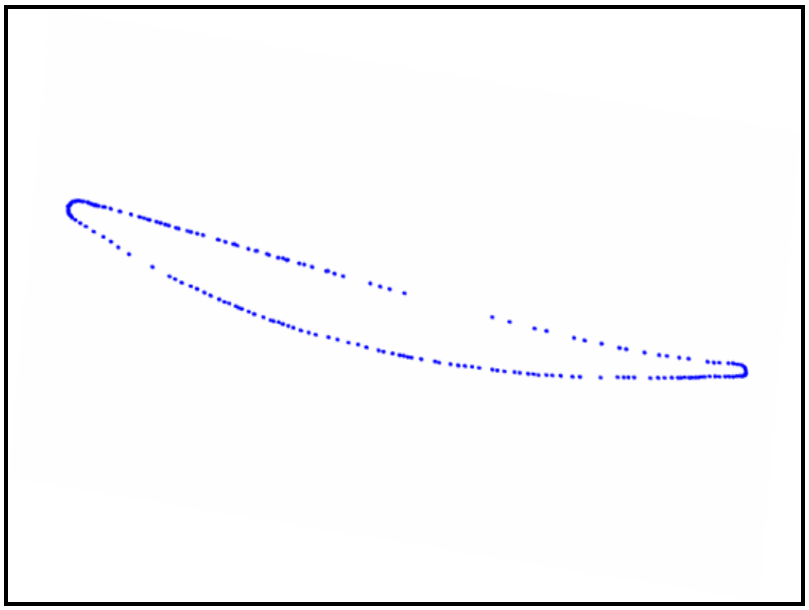

Figure 3.4: Blade profile for compressor cascade created by joining vertex data of section of an actual blade, obtained with the help of profilometer

The vertex data are used to create two dimensional model of the profile, with the help of Gambit. The 2-D model so created is then converted into 3-D by sweeping the faces by respective blades heights.

Cascades are simulated with varying roughness magnitudes of 250, 500 & 750 μm, one at a time for measuring the effects of blade deterioration on performance of compressor. For this purpose, roughnesses of above magnitudes, one at a time, are applied over entire blade (each of blades of cascades) i.e. suction surfaces (SSR) and pressure surfaces and the entire pressure surfaces and entire suction surfaces together (BSR) for cascades and employing compressor blade profile as discussed above.

3.4 Summary of locations of roughness for compressor cascade

Roughness has been applied in one-way only i.e. on entire surface of all blades of a given cascade. Following is summary of locations of roughness application for finding Energy loss coefficients for compressor cascades:

(i) both suction and pressure surfaces

(ii) Only suction surface

(iii) Only pressure surface

The loss coefficient for a given pitchwise and span wise position, similar to the case of turbines, is calculated using respective values of pressure (total as well as static pressure) at inlet & exit of the compressor cascade. The measurement plane is chosen at 30% of the chord length downstream to the compressor cascade outlet as per setup of Seung Chul Back et.al [2010]. Local loss coefficient for each corresponding pitch wise position is calculated using the relation proposed by Dejc and Trojanovskij (1973) and then these coefficients are used to evaluate mass averaged loss coefficient for various span position from bottom end wall till complete blade height for a particular span location.

Various losses i.e. total, profile and secondary losses similar to the case of turbines are measured over the entire blade, and over suction and pressure surfaces separately by successively employing roughnesses over each of them or combinations thereof. The various magnitudes of roughnesses of 250, 500 & 750 μm are selected over the blades of Compressor Cascade for a purpose of generalizing the present study for a wide range of roughness simulations.

3.5 Description of 3-D geometry modeling

Accuracy of computational model is dependent on accurate choice of boundary conditions and assumptions of the analysis. Grid quality, density and quality of representation of actual geometry are the second issue that determines the accuracy of a computational simulation. Grid quality depends on orthogonality, low aspect ratio and low stretching ratio of mesh cells. Sufficient grid density is achieved when further

grid refinement does not change the results; i.e. when a grid independent solution is achieved. Accurate geometry representation is important, as computer simulation will only predict flow for the idealised model.

The present CFD simulations are relying upon pressure correction based finite volume solver i.e. Fluent. This CFD software is especially applicable to three dimensional end wall flows because it allows for solution adaptive grids based on flow. For purpose of studying the three dimensional end wall losses, first 2-D models are created for each of turbines and compressor cascade. In order to make models to represent the actual flow these are converted into 3-D by sweeping the faces by respective blade heights. The figure 3.5 and figure 3.6 show 2-D and 3-D model respectively of a rectilinear turbine cascade.

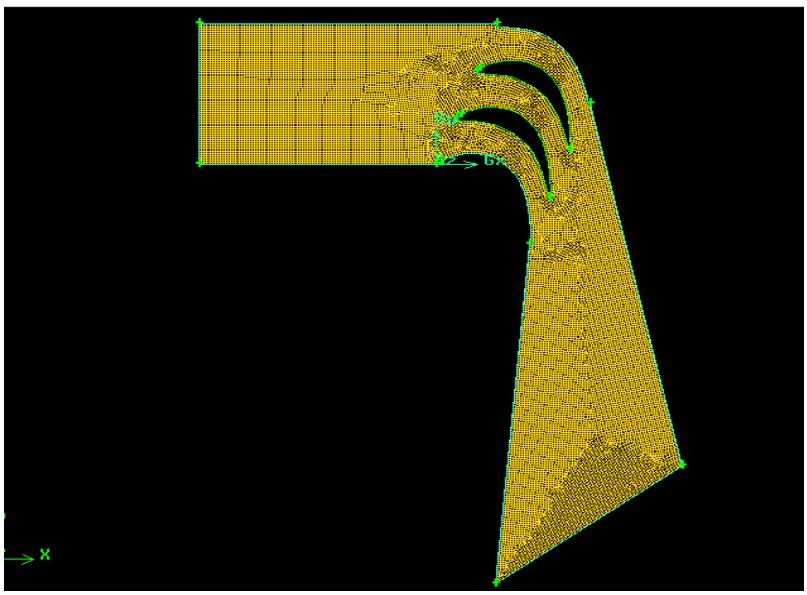

Figure 3.5: Two dimensional meshed model of turbine cascade

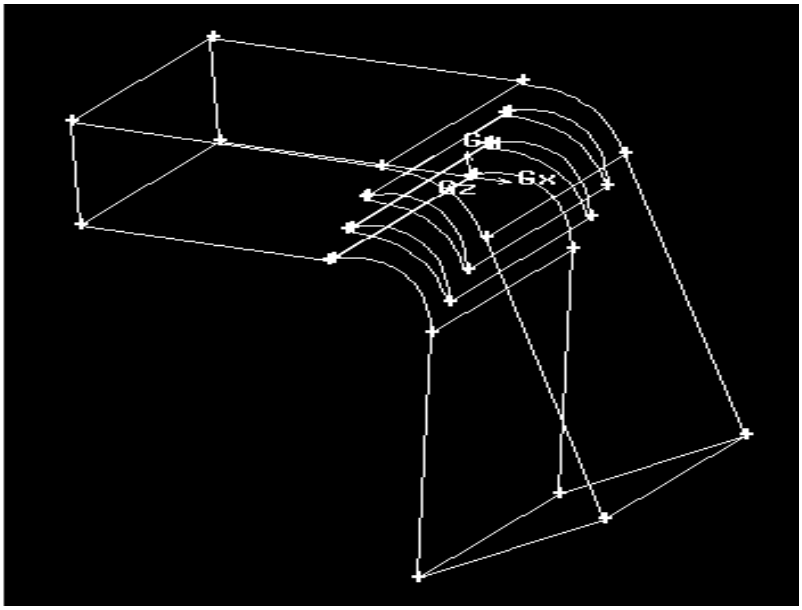

Figure 3.6: Three dimensional model of turbine cascade by sweeping the faces of 2-D model by respective blades heights

3.6 Modeling of turbines and compressor cascades

Geometry creation and meshing is the most important part for any study using CFD as it has tremendous influence on the solution. Therefore, great care has to be taken in choosing appropriate mesh and mesh size.

Initially two dimensional models for each of blade profiles are created, with the help of vertex data (x and y coordinates of all the blade profiles) in Gambit® 2.2.4 and dimensions of the models were kept same from inlet measurement plane to exit of tunnel as per experimental set ups of Samsher [2002] and Seung Chul Back et.al [2010] for rectilinear turbines and compressor cascades respectively. Three dimensional models of the profiles each for turbines and compressor cascades is designed with the help of Gambit and the dimensions of the models were kept similar to the above experimental setups. Flow is assumed to be symmetric about the mid span plane.

However, in order to optimize on computing power/processor capacity, rectilinear cascades with three flow channels using four test blades are constructed choosing stagger angle, chord, pitch, and inlet fluid flow angle and inlet and outlet section for fluid (air) to flow appropriately. The actual experimental setup had five flow channels using six-blades [Samsher, 2002] for turbine cascades. Similarly for the compressor cascades the stagger angle, chord, pitch, inlet fluid flow angle are kept as per experimental data of Seung Chul Back et.al [2010] for rectilinear compressor cascades. Atmospheric temperature is assumed to be constant at 27 °C. Pressure outlet value at exit had been assigned as zero gauge pressure, as exit had been directly exposed to atmosphere for all of the turbines and compressors cascades.

Static and total pressure at inlet of cascades and total and static pressure at 15 % of chord downstream of the cascade outlet were measured in case of turbine cascades. However, for the compressor cascade same parameters at inlet and outlet of the cascade are measured at 30 % of chord downstream of the cascade. The distances of measurement planes downstream of the cascade are kept as per experimental data of Samsher [2002] and Seung Chul Back et.al [2010] for rectilinear turbines and compressor cascades respectively. The distances of measurement planes for turbines & compressor cascades are kept different because the respective experimental setups used different distances of respective measurement planes. Using of different distances of respective measurement planes may be attributed to difference in geometries of blades and other parameters of cascades used for experimental setups in case of turbines & compressor.

Results of this computational study are compared with values of percentage loss coefficients measured along the pitch by Samsher [2002]. The results of present study

and experiment are found to be in agreement. After validation, all the models are taken for investigation of effect of roughness on the total and secondary flow losses.

3.6.1 Modeling of three different cascades for impulse and reaction turbines

Three dimensional models of all the profiles for turbine blades so selected are created, one by one, with the help of Gambit2.4.6® and the dimensions of the models were kept same as the experimental setup of Samsher [2002]. After creating the volume or each of the cascade, meshing of the same is done. Various boundary zones are created from various faces & boundary types are assigned to each of them. Flow is assumed to be symmetric about the mid span plane.

The parameters selected during the experimental study of the wind tunnel conducted by Samsher [2002] are used for construction of geometries of the cascades. Chord of all the blades are 50 mm and height is 95 mm. Horizontal distance between inlet and the cascade is 165mm and distance between cascade and outlet is 500mm. The shape and specifications of one turbine blade cascade model is shown in figure 3.8.

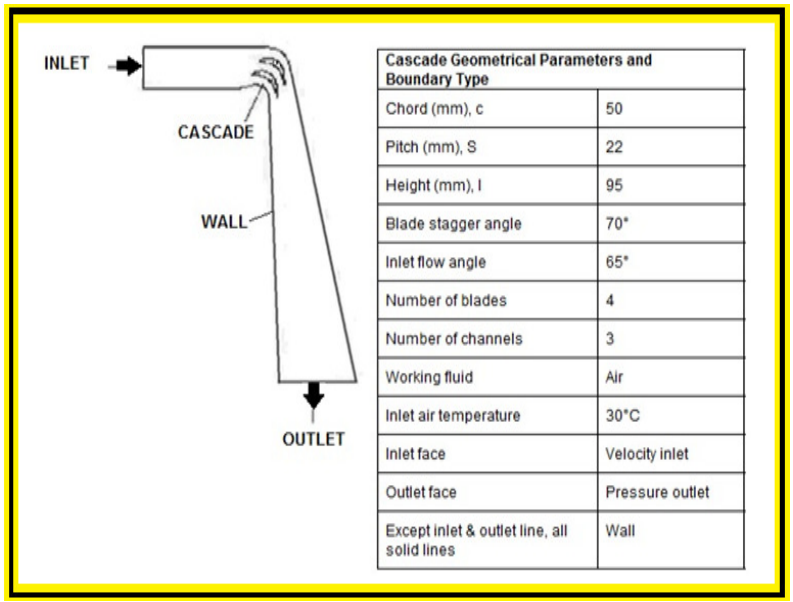

Cascade Geometrical Parameters and Boundary Type	
Chord (mm), c	50
Pitch (mm), S	22
Height (mm), l	95
Blade stagger angle	70°
Inlet flow angle	65°
Number of blades	4
Number of channels	3
Working fluid	Air
Inlet air temperature	30°C
Inlet face	Velocity inlet
Outlet face	Pressure outlet
Except inlet & outlet line, all solid lines	Wall

Figure 3.7: Shape and specifications of turbine blade cascade model

3.6.2 Modeling of compressor cascade

A model of four blades compressor Cascade is created using Gambit for geometry creation. The blades of compressor cascade have chord length of 37 mm and arranged linearly at a pitch of 0.84 times of the chord length. The span of the blades is 37.5 mm. Air with an inlet velocity of 30 m/s is passed through the cascade. The cascade is open to atmosphere at the exit. Three dimensional model of the compressor cascade employing the blade profile, similar to the case of turbines cascades, is created. The dimensions of the models were kept same as setup of Seung Chul Back et.al [2010]. After creating the volume which is subjected to fluid flow meshing of the same is done. Similar to the turbine cascades, for the compressor cascade also, various boundary zones are created from various faces & boundary types are assigned to each of them. Flow is assumed to be symmetric about the mid span plane in the case of compressor cascade also. A Schematic diagram of compressor cascade model for the present study is shown in figure 3 .9.

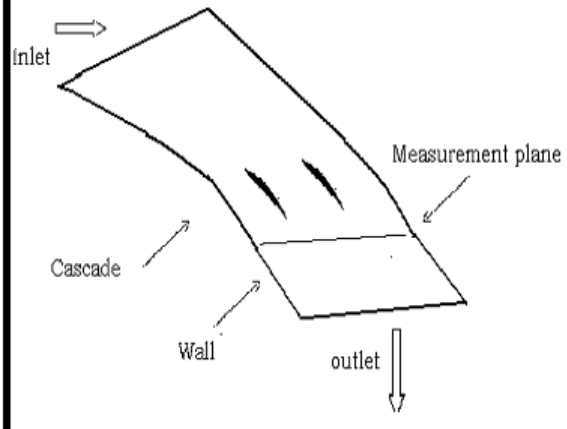

CASCADE GEOMETRY PARAMETERS	
Aspect ratio (c/h)	0.987
Chord length, c	37 units
Pitch of the cascade (s)	31.09 units
Solidity(c/s)	1.19
Inlet velocity	30 m/s
Reynolds No.	8.161×10^{3}
Viscous model used	k-epsilon
Software used	Gambit and Fluent
Type of analysis	3D

Figure 3.8: Shape and specifications of compressor blade cascade model

In order to classify the surface roughness over the blades of the cascade the equivalent sand grain roughness is converted into non-dimensional roughness characteristic value by finding ratio between equivalent sand grain roughness and the chord length. The table 3.2 shows dimensionless equivalent roughness for sand grain roughnesses of 250, 500 & 750 µm.

Table 3.2: Roughness characteristics of test blades

S/N	**Sand grain roughness (k_s) in µm**	**Dimensionless Equivalent roughness ($\frac{k_s}{c}$)**
1	250	0.0067
2	500	0.0135
3	750	0.0202

Based on the equivalent sand grain roughness (k_s) values, the roughness Reynolds number (k^+) has also been calculated, and the range of roughness Reynolds numbers for each type of blade of cascade is found using the correlation (Seung Chul Back et.al, 2010)

$$k^+ = \mathrm{Re}_c \frac{k_s}{c}\sqrt{\frac{c^f}{2}}$$

where

$$c^f = [2.87+1.58\log\frac{c}{K_s}]^{-2.5} \;\&$$

$$\mathrm{Re}_c = \frac{30\times 0.037}{0.000136} = 8161.765$$

The table 3.3 shows that roughness regime based on roughness Reynolds Number k^+ for each of roughnesses of 250, 500 & 750 µm is fully rough. The roughness Reynolds numbers as shown in table 3.3 reveal that the present roughness study **is** therefore, constrained in the fully rough region.

Table 3.3: Determination of Roughness regime based on roughness Reynolds Number k^+ for test blades (Seung Chul Back et.al, 2010)

Reynold number of flow ($\mathrm{Re_c}$) ($\frac{Vl}{\nu}$)	**Dimensionless Equivalent roughness** ($\frac{k_s}{c}$)	c^f	**roughness Reynolds numbers** k^+	**Roughness regime**
8161.765	0.007	6.299	389.133	Fully rough
8161.765	0.014	5.823	705.516	
8161.765	0.020	5.545	995.455	

Results for span wise loss coefficients were obtained for three-dimensional compressor cascade. The roughness Reynolds numbers are found based on the equivalent sand grain roughness (k_s), as shown in table 3.2 and 3.3 reveal that the present roughness study is therefore, constrained in the fully rough region.

3.7 Grid generation & Meshing

Meshes are classified broadly into two types viz., structured and unstructured. Structured meshing is easy to handle as far as discretisation, linearisation and solving is concerned. Typical structured meshes for blades include H-grid, O-grid, C-grid and combinations thereof. The structured mesh is used for geometry creation for all cascades, each for turbines and compressors, throughout the present study. Meshing of turbomachinery fluid domain involves mainly meshing of the blade passages. A typical meshing of the blade passages near leading edge of the blade is shown in figure 3.10.

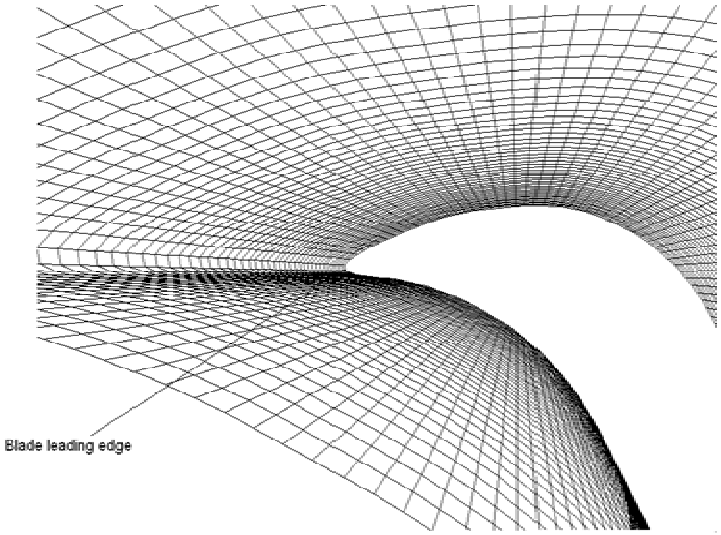

Figure 3.9: A 3-D typical meshing of the blade passages near leading edge of the blade

Accuracy of a solution and its cost in terms of necessary computer hardware and calculation time are dependent on grid quality. Grid quality for good solutions depends upon grid density, skewness and adjacent cell length/volume ratios. Hence every care has been taken to generate good quality grid without increasing computational cells inordinately. Separate boundary zones are created from various faces & boundary types are assigned as shown in the table 3.4.

Table 3.4: Boundary zones created from various faces and assigning of boundary types to them

S/no	**Boundary zone**	**Boundary type**
1.	Inlet faces	Velocity inlet
2.	Outlet faces	Pressure outlet
3.	Suction surfaces No 1, 2, 3 & 4	Walls
4.	Pressure surfaces No 1, 2, 3 & 4	Walls
5.	Bottom end wall & Top end wall	Walls

Meshes generated for each of the cascades are exported to FLUENT. Continuity, energy and momentum equations are solved in a segregated way. Segregated solvers are used where momentum equations are first solved using an “initial pressure”, and an equation for pressure correction is generated a large number of iterations are typically required until a solution by postprocessor based on “initial pressure” is obtained.

3.8 Boundary and operating conditions

3.8.1 Boundary conditions at inlet & outlet

Accuracy of computation of results is largely dependent upon Boundary conditions for the CFD solver i.e. Fluent. The manner in which boundary conditions are imposed also influences convergence properties of solution. Boundary conditions are therefore required to be specified accurately to capture the physics of the flow. Boundary conditions specify flow and thermal variables on boundaries of the physical model.

Velocity inlet & pressure outlet boundary conditions are used for present computations. Boundary conditions used for inlet plane are inlet velocity and for exit plane are exit static pressure.

The blade surfaces are assigned as wall and rest of bounded edges also, wall boundary conditions are prescribed.

3.8.2 Operating conditions

Operating pressure affects the solution in different ways for different flow regimes. In a low Mach number compressible flow the overall pressure drop is small compared to the absolute static pressure, and can be significantly affected by rounding off numerically. To avoid the problem of rounding off error, the operating pressure is

added with the gauge pressure. The relation between the operating pressure, gauge pressure and absolute pressure is expressed as in equation 3.4.

$$P_{abs} = p_{op} + p_{gauge} \qquad (3.4)$$

3.9 Total number of roughness studies per profile

In view to measure effects of blade deterioration on performance of turbine and compressor, roughness is applied over three different regions (width one-third of surface length) at leading edge, mid-chord and trailing edge, and also over the entire blade, and over suction and pressure surfaces separately and by successively employing different combinations of profiles and roughnesses.

Roughness may be applied on the surfaces of blade profile of the cascade geometry in various ways. The roughness for a selected surface is allocated once the cascade geometry created using Gambit is exported as "*.Msh" file into CFD solver Fluent so as to find the effect of the applied roughness on chosen surface. The "*.Msh" file once processed using CFD solver Fluent is saved as "Cas" file. The various surfaces are allocated roughness during the processing of "Cas" file. During the processing of "Cas" file using the CFD solver Fluent selection of model, allocating operating conditions and roughness on the surface are completed. After the processing of "Cas" file by inputting various conditions as above "Cas" file is saved as Cas & Data file. The Cas & Data file is the final document and can be accessed using CFD solver Fluent. This file is the processed file, which can subsequently be used for getting results with regard to parameters of the flow after iteration such as static pressure, total pressure, viscosity etc.

As the results obtained from computation are matching with experimental works, this model would be used to calculate various types of losses at higher Mach numbers which are actually encountered in modern utility turbines.

3.10 Geometry Creation to Post Processing: A Glance

The summary of various steps of simulation of the flow through turbines and compressor cascades for measuring the effect of roughness on losses are summarized to have a quick glance. The following are the steps for completing two major work i.e. Geometry Creation and Post Processing.

(i) cascade geometry is created using the necessary inputs of the experimental setup

(ii) Separate boundary zones are created from various faces & boundary types are assigned.

(iii) mesh is generated.

(iv) File extension "*.Msh" file is exported into CFD solver Fluent so as to find the effect of the applied roughness on chosen surface

(v) the post processor solves, continuity, energy and momentum equations in a segregated way

(vi) computational and viscosity model is selected

(vii) operating and boundary conditions are allocated

(viii) wall momentum thickness (roughness magnitude) is quantified

(ix) A large number of iterations are required for converged solution

(x) The residuals of continuity, velocity components, energy, turbulent kinetic energy and kinetic energy dissipation are continuously monitored.

(xi) converged solution is achieved

(xii) post processing using the fluent software is started

CHAPTER –4
ANALYSIS OF DATA

The uses of gas turbines are not only for generating electricity but also for aircraft propulsion. The researchers in the field of gas turbines, in order to save the invaluable fossil fuel, have been striving hard for improved performance, reliability, and efficiency of gas turbines. The improvement in the efficiency of gas turbines is of lot of importance. The present work is targeted to find effect of roughness on losses and to conclude as to how the surface roughness on blades of the turbomachines impacts their efficiency.

This chapter gives an overview of the relevant procedures for data analysis and calculation of results with regard to this dissertation. First of all, an analysis is made with regard to various types of cascades. In this chapter, a brief introduction of measurement of parameters using experimental and computational methods for the flow through turbomachines cascades is also presented. The computational methods specially those which have been used to find as to how effect of roughness on blades of the turbomachines impact their efficiency are discussed with greater impetus.

Subsequent to introduction of methods for parametric studies of flow through turbomachines cascades, an insight of all the quantities and terms which appear frequently in this dissertation is given. The brief of terms and quantities such as laminar or turbulent flow, stream line flow, total pressure, static pressure, dynamic pressure and stagnation pressure etc. are presented. The brief of other relevant nondimensional quantities like static pressure coefficient, local energy loss coefficient and mass averaged energy loss coefficient are also given. The relation between Local loss coefficient (ζ_y) and mass averaged loss coefficient (ζ) as proposed by Yahya

[2002] is also introduced. Data with regard to calculation of local loss coefficient and mass average value of loss coefficient, their interpretation in terms of energy lost during the flow through a given cascade and segregation of total loss into profile and secondary loss, all are analysed.

The number of cascades modeled for this research work comes out to be large due to which the quantum of the data required to be handled happens to be very large. The data with regard to measurement of effect of blade deterioration on losses for flow through these cascades is discussed. Interalia, an insight of quantum of the data required to be handled is also given.

The factors specially those which are directly linked to losses generation for the flow through turbomachines are analyzed. An analysis is also presented with regard to factors which bring change in magnitudes of losses for the flow through turbomachines cascades. The present research work targets to conclude as to how various factors affect the magnitudes of losses for the flow through turbomachines cascades. For the purpose of measurement of effect of roughness on losses, following factors are identified for this research work:

(i) Surfaces chosen for application of roughness

(ii) Magnitude of the roughness applied onsurfaces chosen as (i) above

The dependence of above factors on losses generation for the flow through turbomachines cascades is presented in this chapter. The roughnesses of different magnitudes are applied, in localized and non localized way, one by one, on suction and pressure surfaces individually as well as on both the surfaces together. Thus, each roughness is applied into 9 ways. The details about surfaces on blades of cascades

used for application of roughness, in localized and non localized way, are also given subsequently.

4.1 Losses measurement methods: Experiments versus CFD techniques

The testing and measurement of parameters for flow through turbomachines are generally carried out using following two methods:

(i) Experiments

(ii) Computational method using CFD techniques

The experimental methods need high subsonic conditions at the time of performance where Mach number and Reynolds number are maintained similar to the actual turbine conditions. These laboratory tests not only allow detailed flow field measurements but also give the experimenter the possibility to investigate the effect of several parameters separately. The advantages of experimental testing are accurate and reliable results. However, there are lots of practical complexities in performing flow field measurements for a turbine or compressor at operating conditions experimentally.

Another way of measurement of parameters for flow through turbomachines is computational method using CFD techniques. The results obtained using experimental methods are supposed to be accurate and reliable. Therefore, prior to taking up any research work based on computational simulation, results of such tests conducted earlier are studied. The results of wind tunnel experiments as obtained by previous researchers are reviewed in chapter 2 of this dissertation. Understanding the physics that governs the flow and the associated turbine cascade, effect of blade surface roughness on profile loss and exit angle over rectilinear steam turbine cascade was measured by Samsher

[2002], through wind tunnel experiments. The results of turbine cascade obtained through this computational study are also validated with results of wind tunnel experiments as obtained by Samsher [2002] using experimental methods. The results obtained through this computational study are found to be in agreement with those obtained by Samsher [2002], experimentally for a smooth turbine cascade. Having got the results of computational study validated with those obtained through experiments as above, the results for remaining cascades for the present study including that of compressor are found.

In fact computational simulation, using CFD techniques, is another way available for obtaining results of measurements of various parameters pertaining to turbines or compressors. CFD techniques are used extensively for the design and analysis of turbomachinery components. A lot of work has been done in order to understand flow physics of turbomachines using CFD techniques. The advantages of computational simulation are speed, reduced cost, more data, and rapid design modifications. Through the use of advanced and accurate computer simulations, much of the preliminary experimental testing may be eliminated, in some cases. The CFD softwares are also proven to be easy to investigate the effect of several parameters separately related to turbomachinery. In nutshell, it can easily be said that CFD is an extremely valuable tool for turbomachinery design and other measurements. In this research work also, complex three dimensional (3-D) flows through various turbomachine cascades using computational simulation are modeled for measurement of desired parameters. Two dimensional (2-D) steady flows are the base upon which many unsteady flows visualization systems are developed. Each 3-D geometry is basically a modification over 2-D geometry.

This dissertation is an effort to present the results of measuring effect of deterioration of blades of turbines and compressors on losses, obtained through computational study of three dimensional turbines and compressors cascades. CFD commercial softwares Fluent and Gambit are used to model turbine and compressor cascades for this work. It is needless to mention that this project work, contrary to experimental work, is accomplished without any actual manufacturing and installation of cascade in real working situation. The distinctive features of the current computational study include specifying boundary zones to the faces of geometries, allocating boundary types to the surfaces so created, meshing and analyzing all turbine and compressor cascades. The steps of computational methodology for this have already been described in detail in chapter 3.

The following two types of cascades are used for study of various phenomena of flow through turbomachines:

(i) Annular cascades

(ii) Linear cascades.

There are various issues worth considering as far as selection out of two types of cascades is concerned. The annular cascades are closer to real life conditions. Therefore an alternate simple and cost effective method to analyze turbine or compressor blades is by the use of a linear cascade. Using a linear cascade user can, not only reduce the number of blades but the testing can also be done at smaller mass flow rates [Hesham M. El-Batsh, 2012]. In linear cascades, the static pressure changes along the blade passage producing pressure gradient from the blade pressure side to the blade suction side. This gradient induces secondary flow which is symmetrical along blade midspan in linear cascades whereas in actual turbines, the cascades are annular with pressure gradient along blade passage from the pressure side to the

suction side and a pressure gradient along blade span caused by the curvature of the endwalls at the hub and at the casing. The annular cascades are not used widely being complex and expensive.

4.2 Basic terminologies used

In this section, the terms which are frequently used in this dissertation and their application relevant to the present work are explained. This section deals with the terminologies such as Streamline or Laminar flow, Turbulent flow, Total pressure, Static Pressure, Dynamic Pressure and Stagnation pressure etc.

4.2.1 Streamline or laminar flow

Streamlines are commonly used to visualize particle paths in steady flows. A streamline at any instant can be defined as an imaginary curve or line in the flow field so that the tangent to the curve at any point represents the direction of the instantaneous velocity at that point. The flow of a fluid is said to be streamline if every particle of the fluid follows exactly the path of its preceding particle and has the same velocity as that of its preceding particle when crossing a fixed point of reference. Since there is no normal component of the velocity along the path, mass cannot cross a streamline. The mass contained between any two streamlines remains the same throughout the flow field.

Properties of streamline or laminar flow

(i) Because the fluid is moving in the same direction as the streamlines, fluid can not cross a streamline.

(ii) Streamlines cannot cross each other. If they were to cross this would indicate two different velocities at the same point. This is not physically possible.

(iii) Any particles of fluid starting on one streamline will stay on that same streamline throughout the fluid.

4.2.2 Streamtube flow

The passage of fluid flow is called streamtube if neighboring streamlines are imagined to form a bundle through which the fluid flows.

Properties of Streamtube:

(i) The streamtube is bounded on all sides by streamlines.

(ii) Fluid velocity does not exist across a streamline, no fluid may enter or leave a streamtube except through its ends.

(iii) The entire flow in a flow field may be imagined to be composed of flows through streamtubes arranged in some arbitrary positions.

The streamlines around an aerofoil show velocity and pressure. An important feature of streamlines is that adjacent pairs of streamlines behave like the walls of a flexible tube. When the flow accelerates, decrease in static pressure is resulted, which causes the streamtubes to contract, and the streamlines move closer together. The distance between streamlines is thus an indication of relative velocity and static pressure. Streamtubes passing over the various edges either contract or expand. In view of above, it can be concluded that the streamtubes when contract indicate an accelerating flow and pressure decrease. In contrary to it the streamtubes when expand indicate a decelerating flow and pressure increase.

4.2.3 Turbulent flow

The flow of a fluid is said to be turbulent or disorderly, if its velocity is greater than its critical velocity. Critical velocity of a fluid is that velocity up to which the fluid flow is streamlined and above which its flow becomes turbulent. When the velocity of

a fluid exceeds the critical velocity, the paths and velocities of the fluid particles begin to change continuously and haphazardly. The flow loses all its orderliness and is called turbulent flow.

4.2.4 Total pressure

According to kinetic theory of gases, molecules of fluid are very small relative to the distance between molecules. The molecules within a fluid are in constant random motion and collide with each other and with the walls of the container of the fluid. The motion of the molecules gives the molecules a linear momentum and the fluid pressure is a measure of this momentum. If a gas is at rest, all of the motion of the molecules is random. As the gas molecules collide the molecules impart momentum to the walls, producing a force perpendicular to the wall. The sum of the forces of all the molecules acting per unit area of the wall is defined to be the pressure. The temperature of a gas is a measure of the mean kinetic energy of the gas.

Bernoulli's Theorem deals with conservation of energy for incompressible and frictionless steady flow. According to this theorem, the total energy of the flow in a conduit is constant at various cross sections though energy transformations from one form to another take place.

In many fluid flow situations of interest, changes in elevation are insignificant and can be ignored. With this simplification, the equation 4.1 is a form of Bernoulli's equation for incompressible flows:

$$P + \tfrac{1}{2}\rho v^2 = P_0 \qquad (4.1)$$

Where:

P - Static pressure at the point of interest

$\tfrac{1}{2}\rho v^2$ -dynamic pressure

v - velocity of flow field

ρ - density of air

P_0 - total pressure which is constant along any streamline

There are so many applications of Bernoulli's Theorem of which Venturimeter is one. This theorem could be understood with the example of Venturimeter. The Venturimeter provides a means of demonstrating Bernoulli's Theorem. In the case of Venturimeter, a streamline of fluid is accelerated up to the throat of a Venturimeter. In other words, static pressure drops as the fluid approaches throat of a Venturimeter. The decrease in static pressure is equal to increase in dynamic pressure.

The Streamline flow over low speed airfoil could also be understood with the help of Bernoulli's Theorem. Bernoulli's Theorem is applicable if flowing fluid is incompressible. Bernoulli's equation then reduces to a simple relation between velocity and static pressure if changes in elevation are insignificant. Since the velocity varies along the streamline, Bernoulli's equation can be used to compute the change in pressure. The static pressure integrated along the entire surface of the airfoil gives the total aerodynamic force on the foil. Pressure is highest at the stagnation point (where it equals static plus dynamic pressure). Here airflow comes to a stop and the streamlines split on either side to follow either the suction or pressure surface. The low pressure generated by the acceleration of the flow over the leading edge creates a suction that draws the airflow forward from the stagnation point to trailing edge.

Streamline is the path, a massless particle traces under the instantaneous velocities of a given vector field. Thus the pressure and velocity of particle which is moving in the direction of motion of the fluid flow along a streamline is determined on the basis of Bernoulli's Theorem. The flow will witness acceleration or deceleration in direction and corresponding pressure change on the basis of this theorem. Suppose direction of

a particle moving along a flow through a passage is chosen to be in the direction of x-axis and that the particle has a finite size in the same direction. Difference of pressure between two ends of the same particle in the direction of x-axis will exist if the particle is accelerating or decelerating as the case may be. The change in magnitude of static pressure (increase or decrease) in x direction would be determined on the basis of Bernoulli's theorem. In case the pressure drops in the *x*-direction, the particle experiences a positive net force in the same direction. According to Newton's second law, this force causes acceleration and the particle's velocity increases as it moves along the streamline. Conversely, if the pressure increases in the direction of the flow, the particle decelerates. This means that if the pressure drops along a streamline, the velocity increases and vice versa [web site 6].

4.2.5 Static Pressure

As the gas molecules collide the molecules impart momentum to the walls, producing a force perpendicular to the wall. The pressure of a gas is then a measure of the average linear momentum of the moving molecules of a gas. The pressure has two components, one is the average linear momentum of the ordered motion of the gas and another is average linear momentum of random motion of the molecules. This random motion of the molecules produces a pressure called the static pressure. In other words, the pressure measured relative to the moving fluid is called the static pressure. Static pressure is referred to as the actual pressure of the fluid, which is associated not with its motion but with its state.

The variation of static pressure along the blade chord is shown in figure 4.1. This figure also shows the variation of static pressure separately on pressure surface and suction surface of given blades.

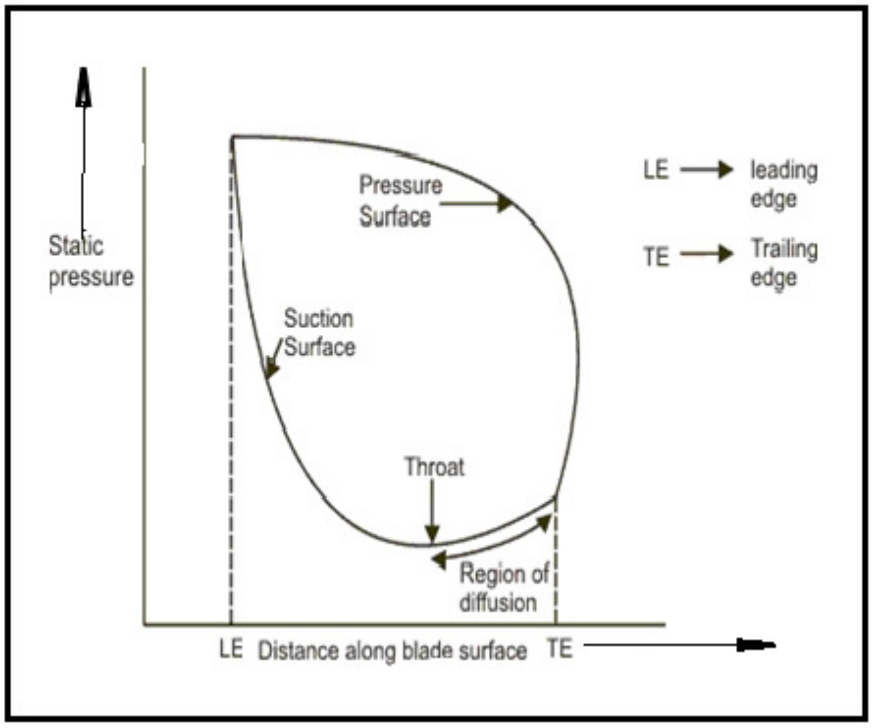

Figure 4.1: Variation of static pressure relative to blade chord in cascades

4.2.6 Dynamic Pressure

Dynamic pressure is defined as average linear momentum of the molecules of the gas which are in ordered motion. From a conservation of energy and momentum, the static pressure plus the dynamic pressure is equal to the total pressure in a flow. According to the Bernoulli's theorem any dynamic pressure increase must be equal to the static pressure decrease and vice versa. The conversion of pressure energy into kinetic energy and vice versa could simply be understood on the basis of Bernoulli's Theorem. This can further be explained by an example of large pressure vessel containing a gas. The gas filled in large pressure vessel has a certain static pressure and no velocity. The gas container has a small opening so as to make the gas free, as the need be. The gas is allowed to move through the opening. As the gas moves through the opening, it accelerates, releasing the stored energy of static pressure to push and accelerate the gas. This momentum is measure of dynamic pressure of the

gas. This pressure is due entirely to the motion of the flow and depends upon the velocity and the density of the fluid.

4.2.7 Stagnation pressure

At a stagnation point the fluid velocity is zero and all kinetic energy is converted into pressure energy. Stagnation pressure is equal to the sum of the free-stream dynamic pressure and free-stream static pressure.

If a symmetrically shaped object is placed in a moving airstream, like the leading edge of an aerofoil, the airstream at the leading edge of the aerofoil would stagnate and the relative flow velocity at this point would be zero. The airstream dynamic pressure will be converted into an increase in static pressure at the stagnation point. Thereafter the airflow will divide on the surface of the aerofoil and local velocity will increase from zero at stagnation point to some maximum value on both the surfaces.

To measure stagnation pressure airstream is brought to a complete stop in a tiny boundary on the nose of the Pitot tube. The tube measures total pressure and in this case stagnation pressure happens to be equal to the sum of the static plus dynamic pressure i.e. total pressure. If Pitot tube is moved in an airstream in the direction of flow, with the same velocity that of airstream then pressure measured by the tube would be equal to static pressure [web site 7].

4.3 Nondimensional quantities

The dimensional analysis technique help identify the variables involved and group them into nondimensional quantities much lesser in number than variable themselves. In the performance tests nondimensional quantities are varied instead of the large number of parameters forming the quantities.

Consider a blade of aerofoil cross-section which is placed horizontally in a streamline flow in such a way that every particle of the fluid passing through the blade is not disturbing the existing streamline flow. Alternatively, it can be stated that the particles

of the fluid passing through the blade follow exactly the path of respective preceding particles and each one of them have the same velocity as that of their respective preceding particles when crossing a fixed point of reference everywhere on the blade surface.

The aerodynamic performance of airfoil sections can be studied most easily by reference to the distribution of pressure over the airfoil. This distribution is usually expressed in terms of the pressure coefficient. The pressure coefficient is a non dimensional quantity which describes the relative pressures throughout a flow field in fluid dynamics. The pressure coefficient is used in aerodynamics and hydrodynamics. Every point in a fluid flow field has its own unique pressure coefficient.

The variation of static pressure coefficient is measured all-around of a chosen aerofoil cross-section of the blade. The blade is lying horizontally in such as a way that upper and lower surfaces of the blade are working as suction and pressure surface respectively. The figure 4.2 depicts both suction and pressure surfaces of a blade.

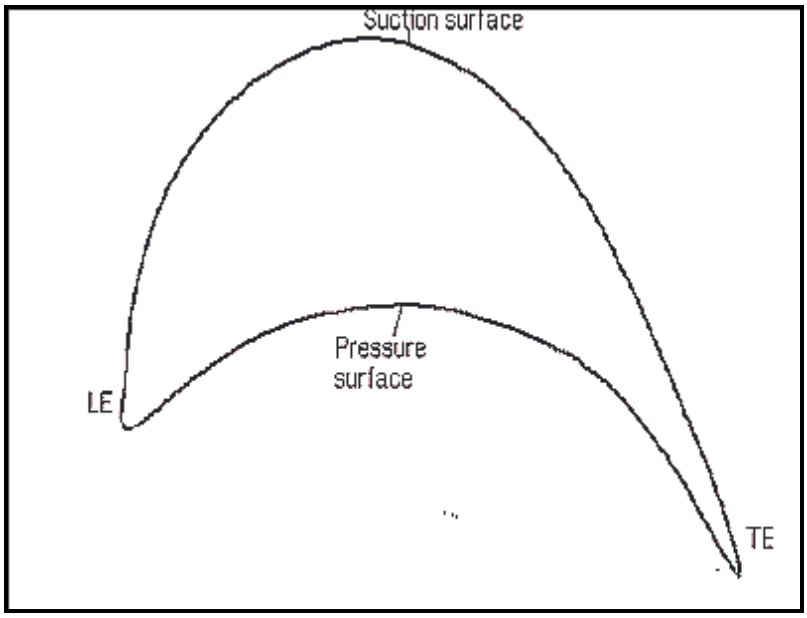

Figure 4.2: Suction and pressure surface for a horizontally placed blade

4.3.1 Static pressure coefficient (C_p)

The static pressure coefficient (C_p) is the difference between local static pressure and free stream static pressure, nondimensionalized by the free stream dynamic pressure. The static pressure coefficient at a location on the blade surface is given by the following relation:

$$C_p = \frac{P_i - P_{s1}}{\frac{1}{2} \rho \ v_1^2}$$

Where:

P_i - Static pressure at the point of interest

P_{s1} - static pressure at inlet

v_1 - velocity at inlet

ρ - density of air

As in an incompressible subsonic flow:

$$\rho = \rho_0 = \text{constant}$$

Therefore for incompressible subsonic flows the following are true:

if $v = 0$ where v is velocity at the point of interest

$\Rightarrow$ $C_p = 1$

and when $v = v_1$

$\Rightarrow$ $C_p = 0$

Following are two cases with regard to magnitudes of C_p being zero or one for an incompressible subsonic flow:

I. When $C_p = 0$

When the value of the static pressure coefficient (C_p) equals to 0 then the pressure at the point of interest is the same as the free stream pressure.

II. When $C_p = 1$

When the value of the static pressure coefficient (C_p) equals to 1 then the pressure at the point of interest is stagnation pressure and the point is a stagnation point.

4.3.2 Variation of Static pressure coefficient (C_p) downstream on pressure surface and suction surface of the blade

Consider that a blade is lying horizontally as shown in figure 4.2. The upper and lower surfaces of the blade are working as suction and pressure surface respectively , based on assumption that fluid flows from leading edge to trailing edge. The variation of magnitude of C_p along the blade chord is shown in figure 4.3 [Abbott et al., 1949]. The plot between C_p and non dimensional distance along the chord length, x/c (C_p versus x/c) is shown in this figure. This figure also shows the variation of magnitude of C_p separately on pressure surface and suction surface of given blade. As shown in this figure, the magnitude of C_p at the stagnation point near the leading is 1.0. The top and downward portion of the graph as shown in this figure are depicting plot for suction and pressure surface of blade as shown in figure 4.3 respectively.

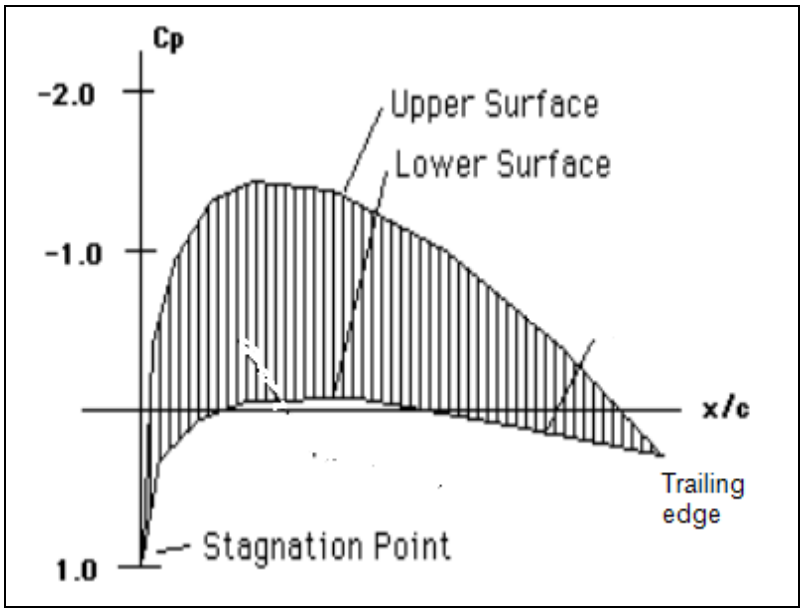

Figure 4.3: variation of magnitude of C_p separately on pressure and suction surface for a horizontally placed blade [web site 8]

4.3.3 Local energy loss coefficient and mass averaged energy loss coefficient

Local energy loss coefficients at various pitch wise positions, for a particular span position (specifically for present work being 3D-modeling) are calculated, on the basis of results of computational work. The total pressures at inlet and total pressures and static pressures at outlet at various pitch positions are measured using CFD softwares. Using the various pressure values so obtained, local energy loss coefficients, ζ_y, are calculated using the following relation proposed by Dejc and Trojanovskij (1973) as shown in equation 4.2.

$$\zeta_y = \left(\frac{P_{s2}}{P_{01}}\right)^{\left(\frac{k-1}{k}\right)} \frac{1-\left[1-\left(\frac{P_{01}-P_{02}}{P_{01}-P_{s2}}\right)\left(1-\frac{P_{s2}}{P_{01}}\right)\right]^{\left(\frac{k-1}{k}\right)}}{\left(1-\left(\frac{P_{s2}}{P_{01}}\right)^{\left(\frac{k-1}{k}\right)}\right)\left[1-\left(\frac{P_{01}-P_{02}}{P_{01}-P_{s2}}\right)\left(1-\frac{P_{s2}}{P_{01}}\right)\right]^{\left(\frac{k-1}{k}\right)}} \qquad (4.2)$$

Where,

P_{2s} is static pressure at outlet of the cascade,

P_{01} and P_{02} are the total pressures at the inlet and outlet respectively,

γ is the ratio of specific heats for air

The calculations for local energy loss coefficients, ζ_y, are made using the Microsoft office Excel software. In order to calculate the values of ζ_y, for each of extremely large number of pitch wise positions, suitable divisions of the formula, as shown in equation 4.2 are made. In fact, the formula for calculating the values of ζ_y is quite large such that making a single program in Microsoft office, Excel software would not be appropriate. Therefore, to avoid a large number of variables in a single program, the variables shown in various brackets in the formula are grouped and calculated separately. Each such

calculation is made in different columns. Therefore, 25 numbers of various columns are included in the Excel sheet so as to yield value of ζ_y for each pitch wise position at a particular span position. The calculation of local loss coefficients for all pitchwise positions, for each span position along the blade height, is made on a separate Excel sheet. The Table 4.1 shows extract of Excel sheet prepared using Microsoft office Excel software for calculating local loss coefficients in the pitch wise direction for various positions for a typical turbine cascade. The Excel sheet showing programming, in full, cannot be reproduced in this dissertation being too large. The programming in Excel sheet needs a very large number of columns (and rows also) and may not fit in single A4 sheet so as to reproduce in this dissertation. Therefore, instead of the original, the table 4.1 represents a suitably modified Excel sheet with lesser number of columns. This table shows only important columns of the original Excel sheet. The local loss coefficients for all pitchwise positions, 74 in numbers in all, are shown in column marked "T" in table 4.1.

Table 4.1: Local energy loss coefficients at various pitch wise positions and mass averaged loss coefficients

((xy/Key/label "OUTLET") X coordinates of pitch positions	((xy, y=1, "INLET") X coordinates of pitch positions	Total pressure inlet(tot pr inlet)	Static pressure outlet (st pr ra)	Total pressure outlet (tot pr ra1)	Average Total pressure inlet(pinav)	Average absolute Total pressure inlet(Pinav)	Absolute Static pressure outlet (Pst)	Absolute Total pressure outlet (Pout)	Local Loss Coefficient	velocity of the flow at various pitch positions	Product of multiplication of velocity with respective local loss coefficient
		(in pascal)									
A	B	C	D	E	F	G	H	I	T	X	Y=T*X
0.01	0.01	8057.69	-29306.90	-3211.12	7943.80	109268.80	72018.10	98113.88	0.25	208.55	51.51
0.01	0.01	8058.21	-28520.50	-1726.94	7943.80	109268.80	72804.50	99598.06	0.22	211.32	46.09
0.01	0.01	8054.81	-27754.00	297.80	7943.80	109268.80	73571.00	101622.80	0.18	216.22	37.85
0.01	0.01	8050.47	-26995.80	2460.23	7943.80	109268.80	74329.20	103785.23	0.13	221.57	28.21
0.01	0.01	8045.99	-26258.40	3210.00	7943.80	109268.80	75066.60	104535.00	0.11	221.62	24.92
0.01	0.01	8041.36	-25576.80	3856.19	7943.80	109268.80	75748.20	105181.19	0.10	221.48	21.98
0.01	0.01	8036.58	-24895.30	3827.27	7943.80	109268.80	76429.70	105152.27	0.10	218.79	22.45
0.01	0.01	8031.69	-24189.30	3849.20	7943.80	109268.80	77135.70	105174.20	0.10	216.17	22.67
0.01	0.01	8026.67	-23482.60	3638.80	7943.80	109268.80	77842.40	104963.80	0.11	212.61	24.14
0.00	0.01	8021.48	-22929.50	3471.09	7943.80	109268.80	78395.50	104796.09	0.12	209.76	25.32
0.00	0.01	8016.27	-22408.90	3275.53	7943.80	109268.80	78916.10	104600.53	0.13	206.90	26.66
0.00	0.02	8011.12	-21923.00	2957.61	7943.80	109268.80	79402.00	104282.61	0.14	203.64	28.64

0.00	0.02	8006.01	-21610.50	2744.75	7943.80	109268.80	79714.50	104069.75	0.15	201.47	29.97
0.00	0.02	8000.95	-21336.90	2291.21	7943.80	109268.80	79988.10	103616.21	0.16	198.44	32.55
0.00	0.02	7995.97	-21058.70	1643.05	7943.80	109268.80	80266.30	102968.05	0.19	194.52	36.13
0.00	0.02	7991.12	-20829.50	658.65	7943.80	109268.80	80495.50	101983.65	0.22	189.24	41.29
0.00	0.02	7986.40	-20630.30	-460.89	7943.80	109268.80	80694.70	100864.11	0.26	183.35	46.88
0.00	0.02	7981.80	-20382.10	-1467.12	7943.80	109268.80	80942.90	99857.88	0.29	177.55	51.70
0.00	0.02	7977.31	-20111.00	-2224.33	7943.80	109268.80	81214.00	99100.67	0.32	172.66	55.23
-0.01	0.02	7972.85	-19856.80	-3082.37	7943.80	109268.80	81468.20	98242.63	0.35	167.20	58.96
-0.01	0.02	7968.49	-19600.90	-3224.97	7943.80	109268.80	81724.10	98100.03	0.36	165.21	59.73
-0.01	0.02	7963.97	-19322.70	-3122.84	7943.80	109268.80	82002.30	98202.16	0.36	164.32	59.55
-0.01	0.03	7958.37	-19052.80	-2649.71	7943.80	109268.80	82272.20	98675.29	0.35	165.34	57.88
-0.01	0.03	7956.78	-18728.00	-1369.87	7943.80	109268.80	82597.00	99955.13	0.31	170.09	52.68
-0.01	0.03	7954.12	-18371.40	-239.24	7943.80	109268.80	82953.60	101085.76	0.27	173.84	47.73
-0.01	0.03	7950.18	-18041.00	651.69	7943.80	109268.80	83284.00	101976.69	0.25	176.51	43.60
-0.01	0.03	7944.88	-17781.00	1673.00	7943.80	109268.80	83544.00	102998.00	0.21	180.06	38.47
-0.01	0.03	7940.14	-17464.10	2732.68	7943.80	109268.80	83860.90	104057.68	0.18	183.47	32.84
-0.01	0.03	7935.52	-17126.60	3651.42	7943.80	109268.80	84198.40	104976.42	0.15	186.09	27.72
-0.02	0.03	7930.90	-16812.50	4312.70	7943.80	109268.80	84512.50	105637.70	0.13	187.64	23.90

-0.02	0.03	7926.02	-16589.50	4661.03	7943.80	109268.80	84735.50	105986.03	0.12	188.20	21.86
-0.02	0.03	7920.88	-16406.50	4870.60	7943.80	109268.80	84918.50	106195.60	0.11	188.31	20.63
-0.02	0.03	7915.84	-16247.80	5010.04	7943.80	109268.80	85077.20	106335.04	0.11	188.23	19.82
-0.02	0.04	7911.11	-16130.20	5088.33	7943.80	109268.80	85194.80	106413.33	0.10	188.05	19.38
-0.02	0.04	7905.72	-16063.70	5021.34	7943.80	109268.80	85261.30	106346.34	0.11	187.46	19.84
-0.02	0.04	7898.77	-16073.50	4739.70	7943.80	109268.80	85251.50	106064.70	0.12	186.25	21.64
-0.02	0.04	7893.27	-16082.60	4452.50	7943.80	109268.80	85242.40	105777.50	0.13	185.00	23.45
-0.02	0.04	7890.68	-16007.10	3910.06	7943.80	109268.80	85317.90	105235.06	0.15	182.20	26.87
-0.02	0.04	7890.27	-15965.10	3317.20	7943.80	109268.80	85359.90	104642.20	0.17	179.27	30.50
-0.03	0.04	7889.52	-15908.90	2710.96	7943.80	109268.80	85416.10	104035.96	0.19	176.16	34.12
-0.03	0.04	7885.06	-15826.50	2077.35	7943.80	109268.80	85498.50	103402.35	0.22	172.74	37.81
-0.03	0.04	7880.41	-15731.20	1448.81	7943.80	109268.80	85593.80	102773.81	0.24	169.21	41.36
-0.03	0.04	7879.15	-15629.10	1012.63	7943.80	109268.80	85695.90	102337.63	0.26	166.54	43.78
-0.03	0.04	7876.85	-15515.20	777.14	7943.80	109268.80	85809.80	102102.14	0.27	164.78	45.11
-0.03	0.05	7873.58	-15380.40	565.81	7943.80	109268.80	85944.60	101890.81	0.28	163.02	46.32
-0.03	0.05	7870.42	-15233.90	752.97	7943.80	109268.80	86091.10	102077.97	0.28	163.23	45.48
-0.03	0.05	7867.42	-15081.50	1161.81	7943.80	109268.80	86243.50	102486.81	0.26	164.54	43.46
-0.03	0.05	7864.62	-14909.90	1517.43	7943.80	109268.80	86415.10	102842.43	0.25	165.47	41.69

-0.03	0.05	7862.09	-14666.60	2177.32	7943.80	109268.80	86658.40	103502.32	0.23	167.55	38.19
-0.04	0.05	7859.91	-14382.20	2770.11	7943.80	109268.80	86942.80	104095.11	0.21	169.08	34.97
-0.04	0.05	7858.08	-14045.60	3280.87	7943.80	109268.80	87279.40	104605.87	0.19	169.93	32.13
-0.04	0.05	7856.60	-13690.30	3813.54	7943.80	109268.80	87634.70	105138.54	0.17	170.80	29.06
-0.04	0.05	7855.47	-13354.30	4215.99	7943.80	109268.80	87970.70	105540.99	0.16	171.13	26.69
-0.04	0.05	7854.75	-13036.30	4517.79	7943.80	109268.80	88288.70	105842.79	0.15	171.05	24.90
-0.04	0.06	7854.57	-12729.20	4622.86	7943.80	109268.80	88595.80	105947.86	0.14	170.06	24.39
-0.04	na	na	-12403.10	4950.78	7943.80	109268.80	88921.90	106275.78	0.13	170.07	22.34
-0.04	na	na	-12086.30	5200.57	7943.80	109268.80	89238.70	106525.57	0.12	169.74	20.78
-0.04	na	na	-11785.50	5330.20	7943.80	109268.80	89539.50	106655.20	0.12	168.90	20.02
-0.04	na	na	-11497.90	5362.70	7943.80	109268.80	89827.10	106687.70	0.12	167.63	19.95
-0.05	na	na	-11218.90	5389.75	7943.80	109268.80	90106.10	106714.75	0.12	166.38	19.92
-0.05	na	na	-10947.50	5414.34	7943.80	109268.80	90377.50	106739.34	0.12	165.14	19.89
-0.05	na	na	-10683.60	5423.25	7943.80	109268.80	90641.40	106748.25	0.12	163.84	19.98
-0.05	na	na	-10420.30	5316.89	7943.80	109268.80	90904.70	106641.89	0.13	161.95	20.93
-0.05	na	na	-10165.30	5212.65	7943.80	109268.80	91159.70	106537.65	0.14	160.09	21.87
-0.05	na	na	-9918.16	5112.38	7943.80	109268.80	91406.84	106437.38	0.14	158.27	22.78
-0.05	na	na	-9671.03	4955.04	7943.80	109268.80	91653.97	106280.04	0.15	156.13	24.11

-0.05	na	na	-9422.13	4729.24	7943.80	109268.80	91902.87	106054.24	0.17	153.58	25.96
-0.05	na	na	-9180.56	4509.80	7943.80	109268.80	92144.44	105834.80	0.18	151.05	27.74
-0.05	na	na	-8946.04	4296.48	7943.80	109268.80	92378.96	105621.48	0.20	148.56	29.47
-0.06	na	na	-8697.06	3694.92	7943.80	109268.80	92627.94	105019.92	0.24	143.71	33.88
-0.06	na	na	-8451.48	3023.79	7943.80	109268.80	92873.52	104348.79	0.28	138.29	38.54
-0.06	na	na	-8214.19	2375.83	7943.80	109268.80	93110.81	103700.83	0.32	132.85	42.76
-0.06	na	na	-7986.42	1771.15	7943.80	109268.80	93338.58	103096.15	0.36	127.53	46.39
										9603.33	1825.32

The Local loss coefficients are highlighted in column marked "T" of this table. The simplified program for calculating the values of ζ_y is shown in the cell at intersection of topmost row and column marked T of the same table:

$$\zeta_y = 1-[1-\{(Pinav-Pout)/(Pinav-Pst)\}*(1-Pst/Pinav)]^{.286}$$

Where:

y –span position i.e. non dimensional distance in span wise direction

Pinav- Average of all values of absolute total pressure at various positions in the pitch wise direction at inlet

Pout- Absolute total pressure at a particular position in the pitch wise direction at outlet

Pst-Absolute static pressure at a particular position in the pitch wise direction at outlet

4.3.3.1 Graphical representation of pitch wise variation of Local loss coefficients

Various graphs showing variation of local loss coefficients are plotted with respect to the nondimensional distance along the pitch wise direction, at various span positions. The figure 4.4 shows pitch wise variation of local loss coefficients for SSR 250 turbine cascades at non dimensional span of 0.02. Whereas the figure 4.5 and 4.6 show pitch wise variation of local loss coefficients at non dimensional distance of 0.16 on blade span for BSR 250 and BSR 500 turbine cascades respectively.

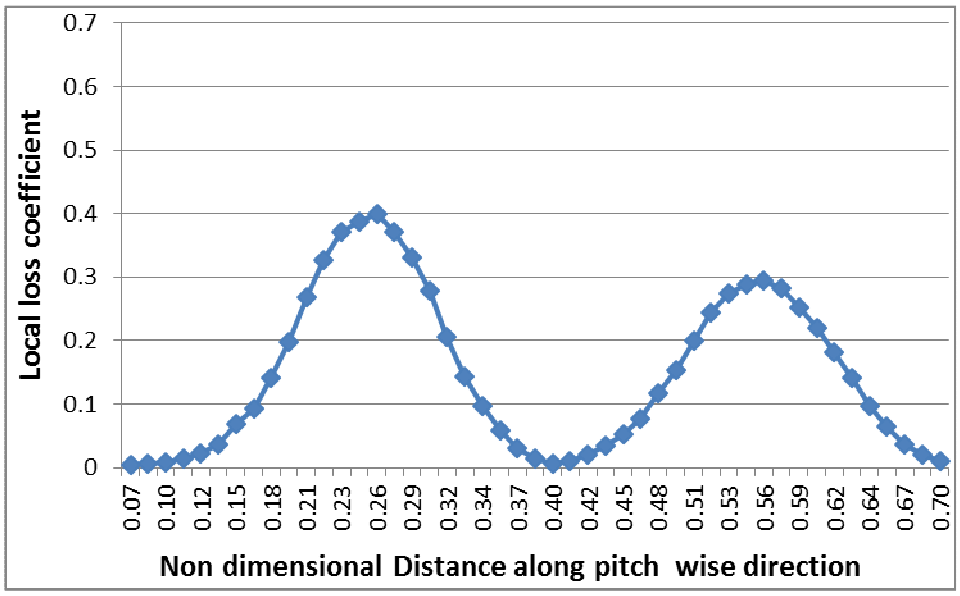

Figure 4.4: Graphs depicting pitch wise variation of Local loss coefficients for Non dimensional distance of 0.02 for SSR 250 turbine cascades

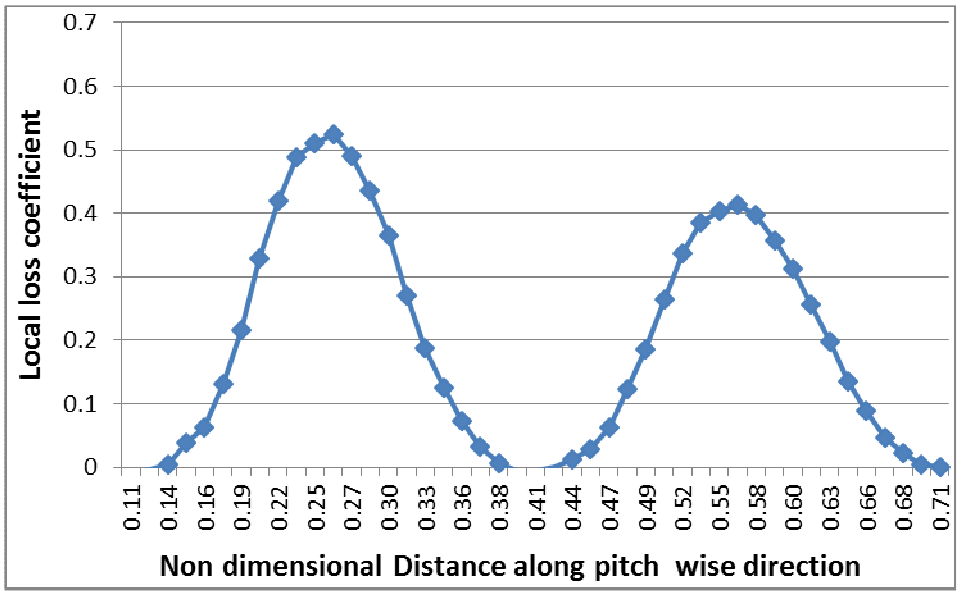

Figure 4.5: Graphs depicting pitch wise variation of Local loss coefficients for Non dimensional distance of 0.16 for *BSR 250* turbine cascades

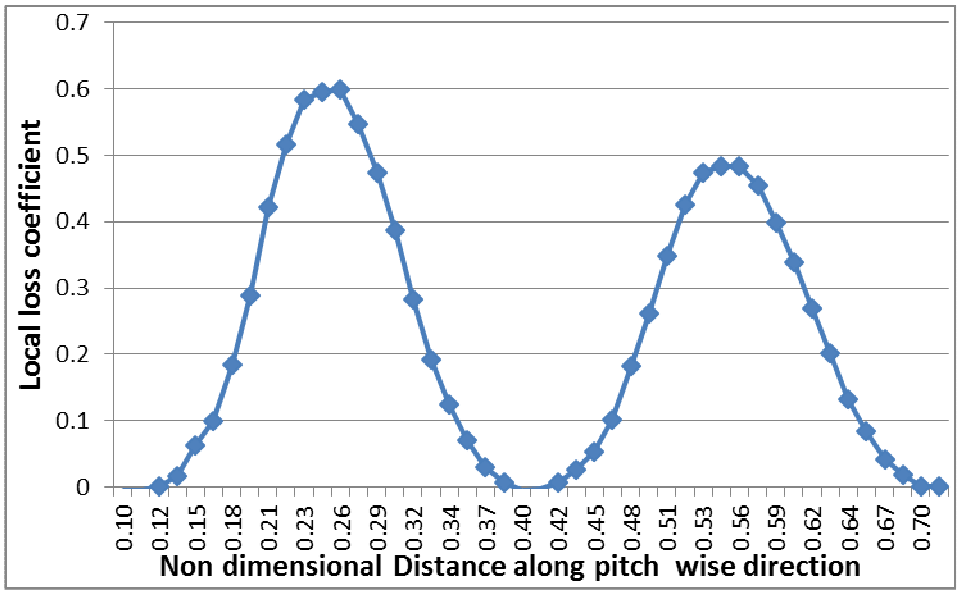

Figure 4.6: Graphs depicting pitch wise variation of Local loss coefficients for Non dimensional distance of 0.16 for BSR 500 turbine cascades

4.3.3.2 Relation between local energy loss coefficient (ζ_y)and mass averaged loss coefficient (ζ)

The mass averaged value of loss coefficient, a single value of energy loss coefficient representing all pitch wise loss coefficients, at a particular span position, is calculated using the relation from, Yahya (2002) as shown in equation 4.3.

$$\zeta = \frac{\int_0^s \zeta_y \, \rho \, V_a \, dy}{\int_0^s \rho \, V_a \, dy} \tag{4.3}$$

Where:

ζ is the mass average loss coefficient,

V_a is the axial velocity,

ρ is the density of air,

S is the pitch distance

dy is the elemental length in pitch wise direction.

Researchers i.e. Denton and Dawes [1999], Michael, *et al.* [2002] and Rodrick [1998] used mixed-out average in their study which is axial independent. According to another study the mass averaged energy loss coefficient is independent of axial location of averaging plane ignoring the mixing loses occur downstream. The loss due to gradual mixing in axial direction goes on increasing [Samsher, 2002]. According to this study the profile loss at cascade exit is same whether it is taken at exit or far away from the cascade exit, only the width of the wake widens and the loss at peak of the wake goes on reducing due to mixing of the wake with the potential flow. Michael, *et al.,*[2002], on influence of axial stator-rotor gap on unsteady losses, as a result of computation study carried out by him, using Fluent solver, observed that the loses in the rotor is higher than in stator. It is so because rotor experiences not only the frictional and potential flow effects, but also the wake from stator.

4.3.3.3 Mathematical representation of Mass averaged loss coefficient

Mass averaged loss coefficient takes the velocity of flow into account whereas local loss coefficient does not. In order to find the former, velocity of the flow at the exit measurement plane is required to find out mass of flow passing through the exit plane. Similarly the local loss coefficients as per column marked " T " of table 4.1 would be required. Therefore first of all an expression for the velocity would be required to find.

4.3.3.4 Expression for finding of velocity of the flow at the exit measurement plane

When changes in elevation are insignificant and can be ignored, the following is simplified form of Bernoulli's equation for incompressible flows. The notations used have their usual meaning.

$$P + \tfrac{1}{2}\rho v^2 = P_0$$

$$\Rightarrow \quad \tfrac{1}{2}\rho v^2 = P_0 - p$$

$$\Rightarrow \quad v^2 = \frac{2(P_0 - p)}{\rho}$$

$$\Rightarrow \quad v = \sqrt{\frac{2(P_0 - p)}{\rho}}$$

Therefore

$$v = \sqrt{\frac{2(P_0 - p)}{\rho}} \tag{4.4}$$

It is clear from the expression that velocity of flow can be found using equation 4.4, if static pressure p and total pressure p_0 is known**.** The velocity of the flow at various pitch positions as obtained as per column marked "A" in table 4.1 are multiplied with respective local loss coefficients and the summations of all such values are placed in numerator and the value so obtained is divided by summations of velocities of the flow at various pitch positions. The quotient is termed as Mass averaged loss coefficient. The calculations are made using the Microsoft office Excel software.

Mathematically, the equation 4.3 for finding Mass averaged loss coefficient reduces to equation 4.5 as under:

$$\xi = \frac{\sum \rho AV\zeta}{\sum \rho AV} \tag{4.5}$$

4.3.3.5 Procedure for calculation of mass averaged loss coefficients

Based on above formula, calculations are carried out in Excel worksheets for evaluation of local loss coefficient for each pitch wise position using values of total and static

pressure taken for same pitch wise positions at measurement plane at inlet and outlet of each of the cascades. The local loss coefficients so obtained, are used to evaluate integrated mass averaged loss coefficient for all selected span locations. Span positions near end walls are more prone to secondary flows and losses associated therewith.

The span positions where mass averaged loss coefficient for turbines and compressors differ from each other because the geometries created for them are different as the dimensions of the models were kept same from inlet measurement plane to exit of tunnel as per experimental set ups of Samsher [2002] and Seung Chul Back et.al [2010] for rectilinear turbines and compressor cascades respectively.

For each of span position a Mass averaged loss coefficient is calculated on the basis of the local loss coefficients for all the pitch wise positions on the basis of formula already mentioned in equation 4.2. The mass averaged loss coefficient, represent all local loss coefficients for various pitch positions {except few local loss coefficients (column marked T in table 4.1) for the half pitch at both the ends are not considered}. Therefore, it can be said that this coefficient, in fact, replaces many number of local loss coefficients. The mass averaged loss coefficient representing all these different local loss coefficients is calculated using Microsoft office Excel software in the same Excel sheet in which local loss coefficients are calculated. The last two columns are included over and above the required number of columns in the Excel sheet prepared for calculating local loss coefficients as shown in table 4.1. These columns are required for programming and calculating following:

(i) Velocity of flow at the outlet measurement plane of cascade

(ii) Multiplication of the velocity of flow obtained in (i) and corresponding respective local loss coefficient.

The table 4.1 shows extract of Excel sheet prepared using Microsoft office Excel software for calculating local loss coefficients and subsequently the mass averaged loss coefficients in the pitch wise direction for various positions for a typical turbine cascade. The programming in Excel sheet needs a very large number of columns (and rows also). The measurement process for mass averaged loss coefficient each for turbines and compressor cascades is presented, one by one, as under.

4.3.3.6 Measurement of mass averaged loss coefficient for Three Dimensional Rectilinear Turbine Cascades

It is worthwhile to mention here that to obtain mass averaged loss coefficients, pitch wise Local loss coefficients are first computed. There is a requirement of calculation of local loss coefficients at each selected span positions. Once Local loss coefficients are found for each span position, Mass averaged loss coefficients were computed starting from end-wall surface at zero mm to other end-wall surface at 95 mm height, along the complete blade. In order to visualize the flow near the end wall, the measurements near the endwalls are taken at small distances and secondary losses were computed. For first 10 mm height from bottom end wall, measuring points are 2 mm apart from each other. Thereafter, it was computed at every 5 mm interval till 85 mm blade height. Finally for the last 10 mm height it was again computed at every 2 mm interval in case of all turbine cascades. The span locations showing intervals between two consecutive span locations for cascades for a turbine are given in table 4.2. This table also shows nondimensional distance for all cascades employing various blades profiles in case of all turbines.

Table 4.2: Non dimensional distance on blade span for turbine cascades

S.N	Distance from bottom wall (mm) (a)	Non Dimensional Distance (b)= (a)/ 95	S.N.	Distance from bottom wall (mm) (a)	Non Dimensional Distance (b)= (a)/ 95
1	0	0	14	50	0.53
2	2	0.02	15	55	0.58
3	4	0.04	16	60	0.63
4	6	0.06	17	65	0.68
5	8	0.08	18	70	0.74
6	10	0.11	19	75	0.79
7	15	0.16	20	80	0.84
8	20	0.21	21	90	0.95
9	25	0.26	22	87	0.92
10	30	0.32	23	89	0.94
11	35	0.37	24	91	0.96
12	40	0.42	25	93	0.98
13	45	0.47	26	95	1

4.3.3.7 Measurement of mass averaged loss coefficient for Three Dimensional Rectilinear compressor Cascade

As far as all compressor cascades are concerned, pitch wise Local loss coefficients, similar to turbine cascades, are first computed. Once Local loss coefficients are found for each span position, Mass averaged loss coefficients were computed starting from end-wall surface at zero mm to other end-wall surface at 37.5 mm height. In order to visualize the flow near the end wall, the measurements near the end-walls for compressor Cascade also were taken at small distances and secondary losses were computed. For first 1.5 mm height from bottom end wall, measuring points are 0.5 mm apart from each other. Thereafter, it was computed at every 2 mm interval till

15.5 mm blade height. Thereafter the loss coefficient for mid span height at 18.75 mm is computed. The computations for the loss coefficient are similarly repeated for upper half section of the blade till the top end wall at height of 37.5mm. The Table 4.3 shows the various span positions at which Local loss coefficients were found for compressor cascade. This table also shows nondimensional distance for all cascades for compressor.

Table 4.3: Non dimensional distance on blade span for compressor cascade (One No.)

S.N	Distance from bottom wall (mm) (a)	Non Dimensional Distance (b)= (a)/ 37.5	S.N.	Distance from bottom wall (mm) (a)	Non Dimensional Distance (b)= (a)/ 37.5
1	0	0.00	**14**	22	0.59
2	0.5	0.01	**15**	24	0.64
3	1	0.03	**16**	26	0.69
4	1.5	0.04	**17**	28	0.75
5	3.5	0.09	**18**	30	0.80
6	5.5	0.15	**19**	32	0.85
7	7.5	0.20	**20**	34	0.91
8	9.5	0.25	**21**	36	0.96
9	11.5	0.31	**22**	36.5	0.97
10	13.5	0.36	**23**	37	0.99
11	15.5	0.41	**24**	37.5	1.00
12	18.75	0.50			

It is clear from the tables 4.2 and 4.3 showing span positions and Non dimensional distance on blade span that more numbers of the span positions near the end walls are selected, comparing to midspan positions so as to study secondary flows and losses associated therewith, more accurately.

4.3.3.8 Mass averaged loss coefficient neglecting effect of side walls of cascade

The linear turbine or compressor cascades introduce the aspect of flow periodicity by arranging a number of blades of constant cross-sections separated by a constant pitch. In current research work, the geometry creation is first and foremost step of modeling of cascade. In order to achieve maximum efficiency and aerodynamic losses generated to be least, the cascade blades are arranged at optimum incidence angle. The tail boards are also set at optimum angle so as to get uniform distribution of the flow to all blades. In fact, many attempts, in case of all the cascades are made before a final geometry is selected.

In the present case, all the turbine and compressor cascades for which modeling is supposed to be accomplished, have faces for inlet and outlet, equally spaced blades with suitable geometry and profile, all walls etc. In order to study effect of bottom end wall and top end wall, the effect of other remaining two side walls should be ignored. Therefore, to ignore effect of these walls, local loss coefficients (column marked T in table 4.1) for the half pitch at both the ends and respective velocities (column marked X in table 4.1) for pitch positions are not considered for calculating mass averaged loss coefficient. In fact, remaining pitch locations are only considered for calculating mass averaged loss coefficient. It is clear from the table 4.1 that the minimum loss position is determined in the pitch wise direction. There is a provision of selecting either pitch wise X or Y coordinates. The Fluent software, during post-processing, selects pitch wise positions either in the form of X or Y coordinates. Thus, the pressure values are the function of these X or Y coordinates. However, the user has privilege to select either X or Y coordinates relative to which the pressure values are to be measured. Fluent post processor has the capability to plot the graph between pitch wise positions (either X or Y coordinates) and respective values of total as well as static

pressure at inlet and outlet of the cascade. There is also the provision of preparation of file of the measured values of pressure so that data recorded therein could be further analysed. This option is called “write to file”. The measured values of pressure are obtained in a file which can later be converted into the Microsoft Excel file. The measured values of pressure as a result of the CFD work are very important as these can be recorded in the form of graph or table format.

The variation of total pressure relative to the pitch wise direction at the exit measurement plane is continuous. The variation is in form of series such that minima and maxima are placed one after another. It could be understood that minima refers to maximum loss condition and vice versa.

The pitch wise position for minimum loss condition is to be determined first so as to get the value of mass averaged loss coefficient through calculation process as already mentioned in the preceding paragraphs. The corresponding rows (one each at both ends) in the table 4.1 related to the minimum loss condition are highlighted. The local loss coefficients between these two minimum loss conditions are used for calculating the mass averaged loss coefficient. The figure 4.4 and 4.5 and 4.6 depict pitch wise variation of Local loss coefficients for turbine cascades. In order to study effect of bottom end wall and top end wall only the effect of remaining two walls are ignored throughout this research work. It is clear from the graphs as shown in figures 4.4, 4.5 and 4.6 showing variation of local loss coefficient relative to nondimensional distance in the pitch wise direction that each graph starts and ends from zero value of local loss coefficient. It is also clear from figures 4.4, 4.5 and 4.6 that the magnitudes of local loss coefficients for three cascades are different as three cascades have different magnitudes of roughness on blades.

4.3.3.9 Calculation of Mass averaged loss coefficient on excel sheet

It is needless to say that there is requirement to refer table 4.1 for explaining the procedure of calculation of Mass averaged loss coefficient on excel sheet. It can be observed from this table that the CFD softwares, Fluent and Gambit yielded 74 positions in the direction of Y-axis (or X coordinates, as the case may be, depending upon selection by user). The necessary provision for the measurement planes, in the geometry, is made at the time of geometry creation using Gambit software so that during post processing the same could be made functional. Having created the measurement planes in the form of either lines or rakes, static pressure at outlet of the cascade and the total pressures at measurement planes at the inlet and outlet of the cascade for all 74 positions are obtained.

The column marked C, D and E as marked in 2nd topmost row of table 4.1 are showing total pressure at inlet and static pressure and total pressure at exit of cascade at respective measurement planes at various pitch positions. The column marked F, G, H and I as marked in 2nd topmost row of table 4.1are showing average inlet pressure, absolute total pressure at inlet (by adding 101325 Pascal to value of average inlet pressure, being gauge pressure values as given in column marked F), static pressure and total pressure at exit of cascade (by adding 101325 Pascal to value of static pressure and total pressure at exit of cascade being gauge pressure values as given in column marked D and E). The values as given in column marked T, are local loss coefficients at various pitch positions as shown in column marked A in the table 4.1.

The values as given in column marked X and Y, represents the velocity of the flow at various pitch positions as per column marked ”A” and multiplication of respective local loss coefficients (column marked T in table 4.1) and velocities as given in

column marked X, respectively. The intersection of last row and column marked X and Y yield the integrated values of all the respective values of column marked X and Y. The integrated value in column marked Y is divided with integrated value in column marked X to get mass averaged loss coefficient representing all the values in column marked T in table 4.1. Taking the values from respective cells from the table 4.1, mass averaged loss coefficient is calculated as under:

Mass averaged loss coefficient = The integrated value in column marked Y / integrated value in column marked X

=1825.316/9603.334=0.190

4.3.3.10 Graphical representation of variation of mass averaged loss coefficient relative to nondimensional distance along span of the blades

The patterns of variation of local loss coefficients relative to the nondimensional distance in pitch wise direction at the end walls are very significantly different than that of midspan for both of turbine and compressor cascades. It is obvious from the results with reference to local loss coefficients that the magnitudes of mass averaged loss coefficients near the end walls at both ends are higher than their values at mid span of the blade. The variation of mass averaged loss coefficient relative to nondimensional distance along span of the blades is found to be symmetric about the mid span.

The mass averaged loss coefficients are found to be highest at span positions near to the end walls. The graphs for each roughness simulation are found to be similar for both of turbine and compressor cascades. All of the patterns of variation as above for both of turbine and compressor cascades are following similar trends.

The mass averaged loss coefficient at the bottom end wall and top end wall are of greater magnitude as compared to the values of same at midspan. This phenomenon can be understood in a better way with the help of figure 4.7 and figure 4.8. The figure 4.7 shows that pressure surfaces and suction surfaces of two adjacent blades for a set of two blades of the cascade form a flow channel for the flowing fluid. Another figure 4.8 shows that pressure difference exists between these two surfaces (the horizontal lines with arrowheads show the direction of force due to difference of pressure). This figure also shows as to how vortices are formed at bottom end wall and top end wall for each such flow channels. The vortices so formed are the main cause of secondary losses.

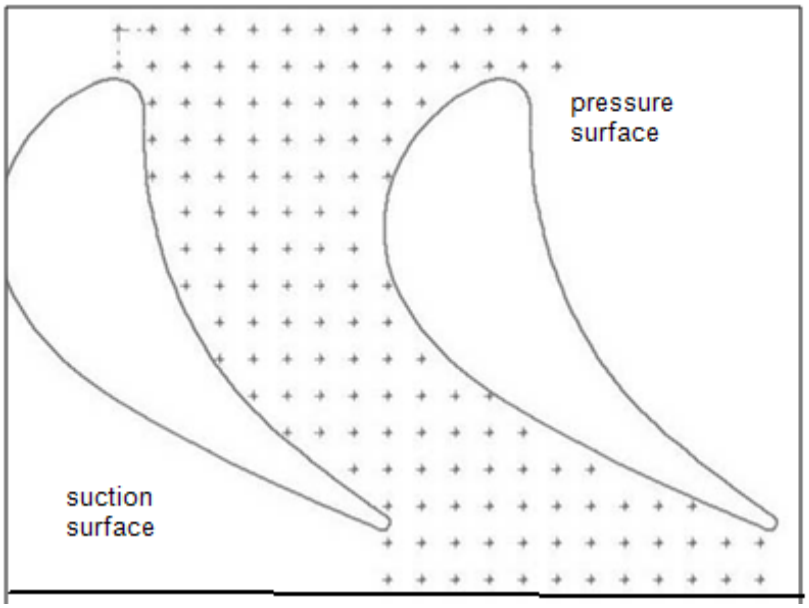

Figure 4.7: Flow through flow channel formed between pressure surfaces and suction surfaces of two adjacent blades of cascade

Secondary losses are largely influenced by roughness on surfaces of the blades for given flow channel. The pressure surface and suction surface and behave differently and leads to different magnitudes of losses. The turbine and compressor cascades which are modeled under this research work configure such flow channels. The

modeled cascades in the present study are having four blades per cascade leading to three flow channels. The study of one flow channel is sufficient to understand the flow phenomenon for all the remaining channels so formed**.**

The incoming boundary layer flow approaches to the flow channel and reaches to leading-edge of the blades for a given flow channel at both the end walls. The pressure at the boundary layer goes on reducing as the flow moves down stream along the flow channel. The fluid which is in contact to the end walls moves from pressure surface of one blade to suction surface of adjacent blade of flow channel. The movement of fluid due to this pressure difference forms vortices at bottom end wall and top end wall. The vortices so formed have direction of rotation as shown in figure 4.8. The direction of rotation is decided by the pressure difference as discussed above. This figure is self-explanatory in this regard. The direction of rotation is from pressure surface to the suction surface at both the end walls. The direction of rotation of vortices so formed at both the end walls as denoted by circles is shown in figure 4.8.

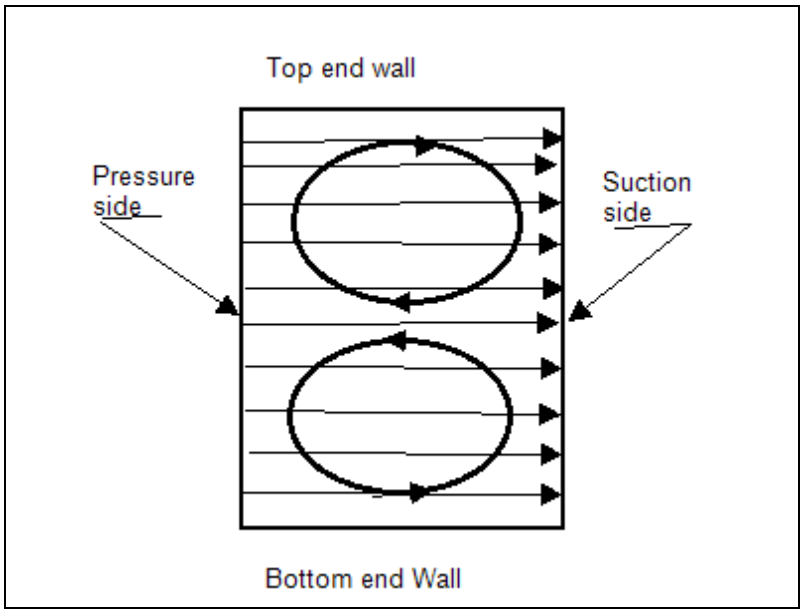

Figure 4.8: Direction of rotation of vortices formed for flow through flow channel formed between pressure surfaces and suction surfaces of two adjacent blades of cascade

One typical graph between various values of mass averaged loss coefficient at different span positions and nondimensional distance along span of the blades is shown in figure 4.9.

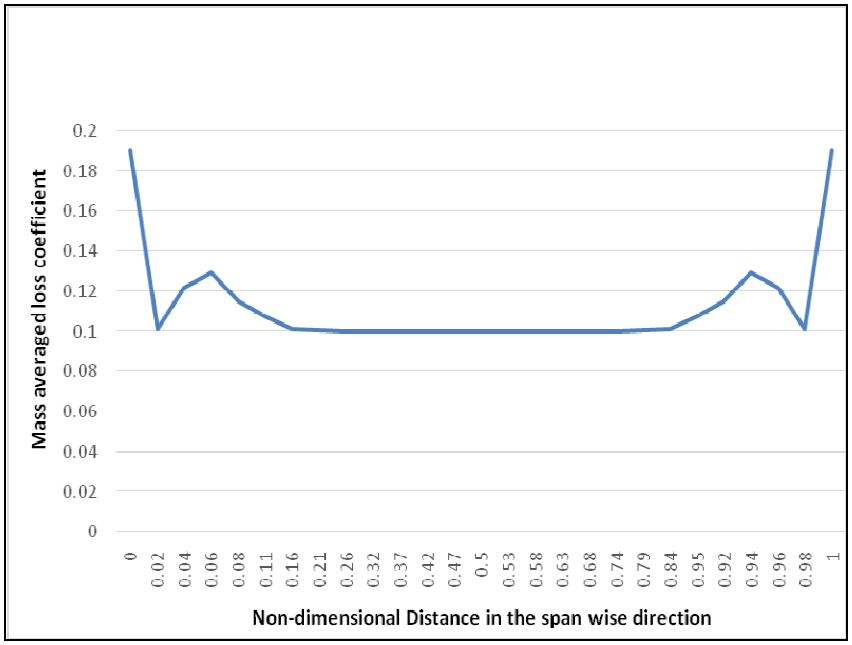

Figure 4.9: Variation of mass averaged energy loss coefficients along nondimensional blade span for smooth turbine cascade

In this chapter, all the patterns of variation of local loss coefficient in the pitch wise direction are analysed. It is clear from the graph is shown in figure 4.9 that bumps are seen in the patterns of variation of mass averaged loss coefficients relative to nondimensional distance along spanwise direction obtained near end wall regions, for all turbine cascades. However bumps are not seen in such patterns for compressor cascade. The reason for the same can be attributed to phenomenon of pressure drop in the turbines and a pressure rise in the compressors. The pressure drop in the turbine is sufficient to keep the boundary layer generally well behaved. The boundary layer in compressors is more prone to separate because of an adverse pressure gradient. However same can be avoided in turbines. Flow passages in a given blade row in

turbine without danger of flow separation than in an axial compressor blade row because of falling pressure in the direction of the flow. Alternatively it can be said that the loss is reduced in an accelerating flow and increased in a decelerating flow; this effect is difficult to quantify due to involvement of large number of variables.

Mass Averaged Loss Coefficient is evaluated from bottom end wall till complete blade height for various span positions, for each cascade of turbines and compressor. Results for each of such variation will be presented in detail and discussed appropriately in the subsequent chapter.

4.4 Effect of roughness on blade surface on losses

The location and roughness level on blades of turbomachines varies from stage to stage as the pressure varies within the region of flow of working substance through various stages. Pressure varies with in the same stage also depending on loads. According to previous study carried out by Samsher [2002], roughness over the blades was found to be on entire surface. Roughness was observed in bands also (localized regions). The preferred parameters which researchers mostly measure are magnitude of losses generation, exit angle of flow at exit of the stages of various turbomachines, effect of changing of the shape or other geometry of the blades on the exit flow and effect of increasing Reynolds number of the flow etc. Due to scarcity of fossil fuels and in order to minimize losses for flow through turbine and compressor cascades, measurement of losses generation making changes in blade geometry including shape, size, pitch chord ratio, and orientation of blades in cascade is amongst very popular choices of researchers of the field of power plants. The researchers thereby optimize cascade geometry. The losses are measured to be different for the cascades which are separately and successively simulated for measuring effect of roughness on losses choosing surface of the application of

roughness differently. Similarly the losses are measured to be different for two cascades which simulated choosing different roughness magnitude.

Therefore magnitudes of losses generated due to effect of roughness on the blades of the cascade depend on selection of surface for roughness application and magnitude of roughness thereon. Discussion on the dependence of change in magnitudes of losses so generated during the flow through turbine and compressor cascades, on above factors is presented, one by one, as under:

4.4.1 Effect of roughness: when surfaces chosen for application of roughness are different

As discussed earlier in the chapter 3, there are nine different ways of application of roughness for a single cascade. The methods of application of roughness are broadly of two types as under:

(i) Non-localised application

(ii) Localised application

The two types of methods of application of roughness are further classified into 9 ways collectively. The term non-localized refers to full surface application of roughness. The following three ways for non-localised application of roughness are:

(i) full blade (including combinations of both surfaces)

(ii) suction surface only

(iii) pressure surface only

Further, there are six ways for localized method of application of roughness. The localized roughness here means that instead of full surface, roughness is applied in

bands, which replicate the actual roughness patterns in the real operating turbines. Thus, six numbers of equally wide surfaces (one-third of total blade surface on either side of the blades) available for applications of roughness, in localized ways are following:

(i) leading edge

(ii) centre of the blades

(iii) trailing edge

Different combinations of profiles and equivalent roughnesses of varying magnitudes of 250, 500, 750 and1000 μm are applied successively on various turbine and compressor cascades. The roughnesses of above magnitudes are applied, one by one, on suction and pressure surfaces individually as well as on both the surfaces together, in localized way also, as above.

The losses are measured to be different when one type of surface is chosen out of pressure surfaces and suction surface, at a time, for roughness simulation the loss magnitudes are found to be different than the instance when remaining surface is chosen. The different magnitudes of losses are observed mainly because the boundary layer on both the surfaces behaves differently. This phenomenon is largely influenced by magnitude of roughness, curvature of the blade surface, trailing edge thickness and last but not the least shape of the blade.

4.4.2 Effect of roughness: when roughness magnitude is different

For pursuing research objectives under this work, local and mass averaged Loss Coefficients at the appropriately chosen measurement plane at exit of the turbine and compressor cascades are measured by successively employing different combinations

of profiles and roughnesses of varying magnitudes of 250, 500, 750 and1000 μm on various turbine and compressor cascades. The losses are measured to be different for two cascades which are separately and successively simulated choosing different roughness magnitude. The different magnitudes of losses are observed mainly because loss generation is largely influenced by phenomena of growth of boundary layer over the blade surfaces. This phenomenon, as mentioned in the previous paragraph, is largely affected by magnitude of roughness over the blade surfaces.

The magnitude of total loss increases with the increase in magnitude of roughness. However, the magnitude of secondary loss may decrease with the increase in magnitude of roughness when the suction surface is chosen for application of roughness. The cause and effect of selection of surface for roughness application and magnitude of roughness on the blades of cascades and formation of bumps in the pattern of variation of mass averaged loss coefficient relative to nondimensional distance in the span wise direction near end wall regions for turbine cascades will be discussed in detail in the subsequent chapter namely results and discussions. The flow through cascades is studied both for turbine and compressor cascades. The local loss coefficient varied differently for turbine and compressor cascades. The analysis on proportion of profile loss in total loss is also to be made in the subsequent chapter. Proportion of profile loss in total loss is measured to be higher for the compressor than for turbine cascades. The grid displays showing static pressure, total pressure and velocity vector etc. are used to explain areas prominent for profile and secondary flows losses in the next chapter.

4.5 Quantum of Data

This section describes quantum of data with regard to analysis of CFD work carried out for achieving research objectives. It will not be out of place to mention that the primary objectives are to measure effect of various magnitudes of roughnesses on secondary flow loss and profile loss for the flow through turbomachines cascades. The effect of roughness on losses generation depends upon following:

(i) Surfaces chosen for application of roughness

(ii) Magnitude of the roughness applied

Therefore effect of roughness on losses generation is measured by applying roughness over the entire blade, and over suction and pressure surfaces separately for three different profiles on turbine cascades separately. The same is measured for localized roughnesses also for turbine cascades. The effect of roughness on losses generation is also measured for the compressor cascade similar to turbine cascades. The difference lies in the number of blade profiles and surfaces chosen for roughness application. The magnitudes of roughness application also differ in case of compressor cascades. The compressor cascades are simulated applying non-localised roughness on three locations for a single compressor blade profile. On the other hand, there are nine locations for each of three different blade profiles for turbines, for the purpose.

In order to get targeted result of this work, the measurement is carried out using CFD for following:

(i) Static pressure at exit of each of cascades

(ii) Total pressure at both the inlet and exit of each of cascades for the 3D flow simulation in present work.

The Local loss coefficient at a given pitchwise position is calculated using values of pressure (total as well as static pressure) at inlet and exit measurement plane using the relation as mentioned in the preceding section of this chapter. For a complex 3D flow simulation, the quantum of calculations of local loss coefficients for various pitchwise positions are commonly large. The disk requirement for storing the flow data would also proportionately increase. Obtaining solutions of this magnitude is a challenge with current disk storage technologies. In order to get the in sight of quantum of data for this Study, the above points need further elaboration.

The first step include creation of geometry of all cascades using the necessary inputs of the experimental setup. For each of the applicable each of turbines and compressor cascade, primarily 2-D models are created. In order to analyse the flow through cascades specially targeting to measurement of three dimensional end wall losses, 3-D modeling would be required. Therefore the 2-D model so created are converted into 3-D model by sweeping each of them. All other work, include creation of separate boundary zones and allocation of boundary types to various faces of 3-D geometry for each of cascade . Thereafter mesh is generated for each. Here the grid selection is very important. The grid are of various types, therefore each type is to be studied for achieving converged solution. The work is accomplished using Gambit software. The files so created are saved in the system to a predefined path with the extension '*.dbs'. The geometries are created using different grid types. Grid quality and density determines the accuracy of a computational simulation. The grid independent solution is achieved as and when there is no scope for further grid refinement. The geometry is exported as '*.Msh' file'. The '*.Msh' file is exported into CFD solver Fluent for processing. The computational and viscosity model are selected from the options under the fluent software. Thereafter operating and boundary conditions are

applied. The next step is to quantify wall momentum thickness (roughness magnitude) successively in a segregated way, in localised and non-localised way over the blades of cascades so modeled. The next step for obtaining converged solution is to solve the flow governing equations in segregated way. Therefore large numbers of iterations are required to obtain a converged solution. The residuals of continuity, velocity components, energy, turbulent kinetic energy and kinetic energy dissipation are continuously monitored. Continuous monitoring of residuals is important. The solution is supposed to be completed when the solution is converged or further iterations do not affect the results. Thereafter Excel worksheets for all combinations of cascades and roughnesses are prepared for calculating Local loss coefficient and mass averaged loss coefficients using results of "pressure" are obtained. These coefficients are calculated using a separate sheet for each combination of following:

(i) profile of blade

(ii) surface selected for roughness application and

(iii) magnitude of roughness separately for turbine and compressor cascades.

For meeting the objectives of this research work, modeling of the cascades, equivalent to number of combinations is required to be executed. In fact, an activity such as finding of local loss coefficient at a given pitch wise position is repeated several times. The local loss coefficients thus calculated are further used to get the values of mass averaged loss coefficients. The process of finding of mass averaged loss coefficients is also repeated many times. The calculations however have been lesser laborious due to using of Microsoft office excel software.

The summary of quantum of data giving approximate *number of* Excel worksheets prepared for measurement of effect of roughness on losses for turbine and compressor

cascades are presented as under so as to be able to know as to how much work for calculating local loss coefficients along pitch wise direction at various selected span positions would be required using Microsoft office excel software. Alternatively, following point wise summary of quantum of data give an insight for volume of work handled under this research work:

(i) Total 27 and 24 number of Excel worksheets are used for each of turbines and compressor cascades respectively for calculations for a single application of roughness only. The results with regard to locals loss coefficients and Mass averaged loss coefficients, for span positions starting from end-wall surface at zero mm to other end-wall surface at 95 and 37.5 mm height respectively for turbine and compressor are recorded there in.

(ii) There are approximate 243 number of Excel worksheets are used in case of turbine cascades including application of a single roughness on nine locations for a single turbine blade profile. Whereas approximate 72 excel sheets are prepared, in all, for single roughness application on three locations for a single compressor blade profile.

(iii) There are approximate 729 (243 X 3) excel sheets prepared, in all, for roughness application on nine locations for turbines for all the three turbine blade profiles. Thus, approximate 729 and 72 excel sheets prepared, in all, for all roughness application for the three blade profiles for turbines and a single blade profile for compressor respectively

(iv) Thus, approximate 801 excel sheets are prepared, in all, for all roughness applications combining the three blade profiles for turbines and a single blade profile for compressor. One set of location consists of total pressure at inlet

measurement plane and total and static pressure, both, at outlet measurement plane of the cascade. Pitch wise position for both measurement planes is same for finding the above referred pressure values. Thus for a pitch wise position three pressure values are required. The number of pitch wise positions is arbitrarily chosen by user.

(v) Each such Excel sheet has the record of values of static and total pressure of 74 (or more as the number of pitch wise positions are arbitrarily chosen by user) locations at inlet and outlet of the cascade in the pitch wise directions. Thus, for each pitch wise position, three pressure values are required. The number of pitch wise positions is arbitrarily chosen by user. Thus, a single Excel sheet is comprising of 202 (74 x3) or more pressure values.

(vi) Therefore, total number of pressure values recorded under 801 Excel sheets would be approximately 161802 (801 x 202) for all four blade profiles. Over and above the number of Excel sheets, another 700 Excel sheets are prepared for recording various types of losses, their comparisons and graphs etc.

4.6 Interpretation of loss coefficients for the flow through a given cascade

As discussed in the previous sections, following are two types of loss coefficients:

(i) local loss coefficient

(ii) mass averaged loss coefficient

The details with regard to loss coefficients are presented in previous sections. The term loss coefficient is a nondimensional quantity. It can be understood by a ratio of total energy lost during flow through the cascade to the total energy available at the inlet of the cascade. It is obvious that both the energy values have same units. Therefore, the

ratio of these two quantities may be termed as a nondimensional quantity i.e. loss coefficient. In this section the interpretation of loss coefficient in terms of lost and incoming energy will be made.

In order to compute effect on total, profile and secondary losses for particular magnitude of roughness over entire blade height for the given cascade, the flow area of the section of the cascade and representing height for each of Mass averaged total loss coefficient in span wise direction are taken into consideration. The following paragraph explains various terms such as 'representing height' and 'double integration of loss coefficient over pitch and span wise direction' etc.

The local loss coefficient takes into account the pressure values (static as well as total) at inlet and outlet as per relation proposed by Dejc and Trojanovskij (1973) as shown in equation 4.2. On the other hand, the mass averaged loss coefficients take the aforesaid local loss coefficients and velocities at various pitchwise positions into account. Moreover, this loss coefficient is calculated using values of local loss coefficients, calculation process in respect of which is clear from the table 4.1. Thus it can be said that mass averaged loss coefficient does not only represent one position in pitch wise direction but represents complete distance in the pitch wise direction i.e width of wind tunnel (which is being represented by a cascade in the present research study). Therefore, it may be treated to have been obtained by integration of loss coefficient in the pitch wise direction (the local loss coefficients and velocities for half pitch positions at both ends in pitch wise direction of cascade are not included for calculation of this coefficient). In present case manual procedure may be said to have been adopted in place of actual mathematical integration. Mass averaged Loss coefficient would therefore represent an imaginary pitch line only unless it represents a height of blades too. Therefore, to obtain total loss for the complete cross-section of

the cascade (representing volume of unit length in the direction of flow), it would be desirable to integrate the variation of Mass averaged Loss coefficients (treating them as a variable) with respect to the infinitesimal displacement also (in present case infinitesimal displacement is in the span was direction i.e. height of blades). Thus mass averaged loss coefficients would be said to have been integrated in span as well as pitchwise direction. Inter alia, it can be said that the mass averaged loss coefficients, obtained as results of CFD work under this research project, are sufficiently representative and reliable.

The figure 4.10 shows a wind tunnel used for losses measurement for flow through turbomachine cascades. The wind tunnel has a flow channel at inlet and outlet separated by section where cascades of blades are arranged.The figure 4.10 shows that its structure includes a plurality of blades arranged in series. A number of blades of given shape and size at the required pitch and stagger angle are assembled in a cascade. The flow channel of wind tunnel at inlet and outlet are having rectangular cross section.The height and width of rectangular cross section of turbine cascades which are modeled in this research work are 95 mm and 41mm respectively.

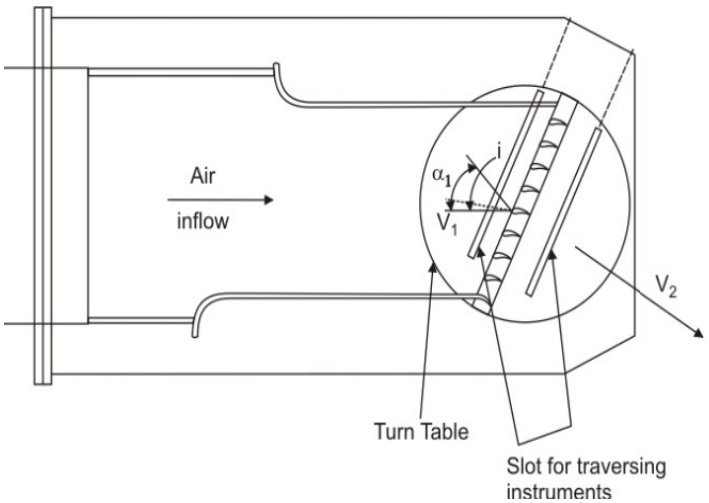

Figure 4.10: Wind tunnel for losses measurement for flow through turbomachine cascades

The Microsoft office excel software is used for calculation of magnitude of total loss . The table 4.4 shows procedure for calculating the total loss as a percentage of incoming total energy. The total loss for various smooth cascades is compared with losses for all those cascades surfaces of which are roughened with roughness of different magnitudes. Thus comparative studies of such cascades with smooth cascades are made in current research work.

Table 4.4: Calculation of the total loss as a percentage of incoming total energy

	Mass averaged loss coefficient in span wise direction	Representing hieght	Distance from Bottom end wall (in mm)	Non dimensional distance in span wise direction	Mass averaged loss coefficient x representing hieght	Total width of cross section of cascade	Mass averaged loss coefficient x representing hieght x Total width of cross section of cascade
	A	B	C	D	E	F	G
1	0.1901	1	0	0	0.1901	41	7.7929
2	0.1014	2	2	0.02	0.2028	41	8.3151
3	0.1220	2	4	0.04	0.2440	41	10.0039
4	0.1293	2	6	0.06	0.2586	41	10.6031
5	0.1147	2	8	0.08	0.2295	41	9.4091
6	0.1073	2	10	0.11	0.2146	41	8.8000
7	0.1011	6.5	15	0.16	0.6574	41	26.9524
8	0.1004	5	20	0.21	0.5020	41	20.5823
	0.1002	5	25	0.26	0.5012	41	20.5474
10	0.1002	5	30	0.32	0.5009	41	20.5363
11	0.1002	5	35	0.37	0.5008	41	20.5311
12	0.1001	5	40	0.42	0.5007	41	20.5280

13	0.1001	4.5	45	0.47	0.4506	41	18.4739
14	0.1001	0.5	47.5	0.5	0.0501	41	2.0526
15	0.1001	4.5	50	0.53	0.4506	41	18.4739
16	0.1001	5	55	0.58	0.5007	41	20.5280
17	0.1002	5	60	0.63	0.5008	41	20.5311
18	0.1002	5	65	0.68	0.5009	41	20.5363
19	0.1002	5	70	0.74	0.5012	41	20.5474
20	0.1004	5	75	0.79	0.5020	41	20.5823
21	0.1011	6.5	80	0.84	0.6574	41	26.9524
22	0.1073	2	90	0.95	0.2146	41	8.8000
23	0.1147	2	87	0.92	0.2295	41	9.4091
24	0.1293	2	89	0.94	0.2586	41	10.6031
25	0.1220	2	91	0.96	0.2440	41	10.0039
26	0.1014	2	93	0.98	0.2028	41	8.3151
27	0.1901	1	95	1	0.1901	41	7.7929
	Summation of all mass averaged loss coefficient x representing heights x 41						408.2036298

The table 4.4 shows as to how mass averaged loss coefficients are placed in a column and column adjacent to it is used for placing the representing height for each mass averaged loss coefficients. It is clear from the values shown for representing heights that the same are less for mass averaged loss coefficients pertaining to end walls. This is so because the intervals chosen at end walls are small due to which respective representing heights are also small. The representing heights (represented on vertical axis i.e. "Y" axis) for two consecutive mass averaged loss coefficients may be considered to have formed two parallel sides of a trapezium and the line joining two magnitude of loss coefficients along the graph showing variation these loss coefficients represent the one of nonparallel side. The fourth nonparallel side is formed by the horizontal vertical axis i.e. "X" axis representing nondimensional distance in the span wise direction. The sum of areas of all the trapeziums equals to total losses at the time of exit of the flow through cascade. Assuming a unit length in the flow direction a cuboid is considered to have been formed at the cross section of wind tunnel at the position of measurement plane at inlet of the cascade. The energy of total incoming air of this volume is compared with energy at the exit of cascade at the cross section of wind tunnel at the position of another measurement plane. It is clear from foregoing paragraph that the mass averaged loss coefficient are double integrated in the pitch wise direction and in span wise direction as well. The pitch wise integration can be understood in terms of finding of mass averaged loss coefficients themselves. Whereas the multiplication of different mass averaged loss coefficients with the representing heights (as per column E of table 4.4) can be understood as integration in span wise direction.

The numerical values in the cell at intersection of last row and last column of table 4.4 represents the lost area (or area of all trapeziums as mentioned above).

The losses are measured in terms of percentage of total energy at the measurement plane at inlet of the cascade. The losses as percentage of total energy at inlet are illustrated with the help of numerical values shown in table 4.4. The column A of table 4.4 shows mass averaged loss coefficient obtained in the span wise direction. The representing heights are shown in column B against each mass averaged loss coefficient. The column C of table 4.4 shows distance of the corresponding positions in the span wise direction starting from bottom end wall in respect of all mass averaged loss coefficients. The corresponding non dimensional distances in span wise direction starting from bottom end wall are shown in column D. The column E of table 4.4 shows products of multiplication of mass averaged loss coefficients and respective representing heights. The column F and G of this table show width of cross section of cascade and multiplication of the values shown in column E and total width of cross section of cascade respectively. The values in column G thus equal the product of mass averaged loss coefficient, representing height and total width of cross section of cascade. Alternatively, the sum of all values in column H equal to integration of local loss coefficients in pitchwise direction as well as span wise direction. If a unit length is considered in the direction of the flow through the cascade, the sum of all values in column G of table 4.4 shows total energy loss of 408.2036 (unit) out of total energy at inlet of 3895 (unit), for the volume occupied by the unit length in the flow direction. The figure 3895 is the product of multiplication of 95 and 41. The 95 mm and 41mm are the height and width of cross section of the given cascade respectively. Thus, the unit length in the direction of the flow and multiplied by cross-sectional area of the cascade gives figure of 3895. If the unit of the energy is chosen to be in Joule, incoming energy at inlet of cascade for the volume occupied by a unit length in the flow direction would be 3895 Joule. Whereas area of

all trapeziums as mentioned above, comes out to be 408.2036 which represents the lost area. If a unit length in the direction of the flow through the cascade is considered for the lost area also, lost energy during flow through cascade for the same volume that of incoming energy, would be 408.2036 Joule. The total loss as a percentage of total incoming energy (shown in fraction) is shown in table 4.5.

Table 4.5: Calculation of total loss as percentage of total incoming energy

Summation of all products of mass averaged loss coefficients x total area x 41	**total area of cross section of cascade 41 X 95**	**ratio of Summation of all products of mass averaged loss coefficient x representing heights x 41 to the total energy at inlet of cascade**	**Profile loss (Midspan value of all mass averaged loss coefficients in column A of Table 4.4)**	**Secondary loss**	**percentage of secondary loss in total loss**
A	B	C= A/B	D	E= C-D	F=E*100/C
408.204	3895	0.1048	0.1001	0.0047	4.48651

The ratio of both numeric values of 408.2036 and 3895 can be presented as a fraction, as per column C of the table 4.5. The column C of this table shows the fraction representing total loss as percentage of total incoming energy. Whereas the column E of this table shows the absolute value of secondary loss as a fraction. This table shows as to how percentage of secondary loss with the help of numerical values given in column A of table 4.4 could be found. Thus losses are measured in terms of percentage of total energy (or as a fraction as mentioned in table 4.5) at the measurement plane at inlet of the cascade. Thus total losses due to flow through intermediately placed cascade section could be measured. It is customary to convert the fractions into percentage by multiplying the same by 100.

4.7 Segregation of total loss into profile and secondary loss

The phenomenon of secondary flow is observed only near the end wall. In the mid span of the blade, profile loss is dominant. Secondary loss at the end walls includes loss from the boundary wall on the end wall wetted surface, loss due to flow separation and diffusion of passage secondary vortex. Energy loss coefficients represent total energy loss while fluid flow is taking place along the cascade from inlet to outlet. Energy loss coefficient at mid span where flow is 2- dimensional represents profile loss, whereas near the walls, it represents total loss i.e. profile loss plus secondary flow loss. To segregate secondary loss at the end wall, profile loss at the mid span is subtracted from the total loss.

The total (combined) losses in all blade cascade are estimated by the energy loss coefficient ζ, which is essentially the sum of profile loss coefficient and end loss coefficient as given by Kostyuk and Frolov[1988] in equation 4.6.

$$\zeta_{total} = \zeta_{profile} + \zeta_{end} \qquad (4.6)$$

The mass averaged loss coefficient calculated at blade mid span, where the flow is two-dimensional and influence of end wall effect is not present, constitutes profile losses. Thus, end loss or secondary loss coefficient along blade height is calculated as the difference between the total loss (the fraction shown in column C of table 4.5) and profile energy loss coefficients in a cascade. The secondary loss is expressed in terms of percentage of total loss. It is calculated based on the total loss coefficient and mass averaged loss coefficient measured at middle of span of blades. The method of calculation of total loss coefficient as ratio of summation of all numerical values shown in column G of table 4.4 and total cross-sectional area of the cascade is expressed in table of 4.5. The table 4.5 also shows as to how percentage of secondary

loss in total loss can be found. The column E of table 4.5 shows absolute value of secondary loss as a fraction. The column F of table 4.5, however, shows the secondary loss expressed in terms of percentage of total loss. The column F of table 4.5 depicts the method of converting the absolute value of secondary loss (as shown in column E) of table 4.5 into percentage of secondary loss in total loss.

The chapter Analysis of Data is used to introduce the methods, formulae etc. used in next chapter namely results and discussion of this dissertation.

CHAPTER 5
RESULTS AND DISCUSSIONS

The computational study of numerous numbers of configurations representing roughness magnitude-location combination, for each profile, along with smooth blade profile is carried out both for turbine and compressor cascades. This study includes simulation of the flow through turbomachines cascades for measuring effect of roughness on losses generation. In this chapter, detailed numerical results of the computational study, conducted as above, are presented.

The parameters for the present study are total and static pressure and local loss coefficient. The results of study of variation of all relative to the nondimensional pitch distance, at measurement planes, downstream of trailing edges for turbine cascades and compressor cascades are presented. For all the three turbine profiles titled 6030, 5530 and 3525 as selected by Samsher [2002], computational study on, 39 configurations, in all, representing roughness magnitude-location combination are carried out. Of the three profiles selected, one was nearly impulse type & remaining two were of reaction type with different degree of reaction. The results with regard to cascades representing all such combinations are presented. The pictorial presentation of various cascades configurations are showcased in previous chapters also, including the figures, obtained as a result of grid displays using the Fluent and Gambit software, during the process of simulation of flow through turbomachines. The few other pictorial presentations for flow visualisations on the end-wall surfaces demonstrating the influence of the different cascade configurations are showcased herein.

In this chapter, the total and static pressure distribution over the entire computational domain is shown for various cascades. The pressure values at various positions are

obtained with the help of FLUENT software. The variation of total pressure and static pressure value relative to nondimensional distance in the pitch wise direction is also discussed. The spanwise distributions of the pitchwise local loss coefficients are presented for different cascades. The results with regard to mass averaged loss coefficient for each of selected span wise positions are also presented. Variation of mass averaged loss coefficient relative to nondimensional distance in span wise direction is shown graphically also and analysis thereof is presented for various cascades. The mass averaged loss coefficient is calculated by double integration of local loss coefficients for all pitch positions all along the span positions. The method of finding the total loss with the help of mass averaged loss coefficient is also discussed. The method of segregation of losses using the mass averaged loss coefficient is discussed. Thus, the measurement of effect of increase of roughness on the turbomachines blades is carried out. An analysis is made striving to get results with regard to total loss, profile loss and secondary loss for various cascades for each of cascades.

First of all, process of simulation of flow through turbomachines cascades is discussed in the context of measurement of total as well as static pressure in detail, in section 5.1. The pictorial presentations of various stages of measurement processes using various software are introduced, in this section, so as to give glimpses of activities under the softwares. The profile wise results are discussed in detail in this chapter. The effect of roughness on profile 6030 is discussed in section 5.2 followed by profile 5530 in section 5.3 and thereafter profile 3525 in section 5.4 of this chapter. Thereafter the results obtained for magnitude of losses for application of localized roughnesses and comressor cascade is presented subsequently in section 5.5 and 5.6 respectively. The variation of loss coefficients for turbine and compressor cascades in the pitch wise direction for various cascades are presented graphically in various

sections of this chapter. The variation of mass averaged loss coefficients in the span wise direction for various cascades are also presented graphically therein. The results with regard to secondary losses are discussed conclusively for all the profiles for turbines. Similarly secondary losses for compressor cascade are also discussed. The relative performance evaluation across the profiles and implications of these findings in the context of efficiency of turbine power plant are also presented.

5.1 process of simulation of flow through turbomachines cascades

The process of simulation include various activities, using the Gambit software, right from geometric creation, boundary type allocation, meshing of the geometry and exporting the geometry after meshing for postprocessing using the Fluent software. First of all, the results of turbine cascade obtained through this computational study are validated with results of wind tunnel experiments as obtained by Samsher [2002] using experimental methods. For the present study, each cascade both for turbine and compressor has three flow channels using four test blades. The actual experimental setup had five flow channels using six-blades [Samsher, 2002] for turbine cascades. Had computing power/processor capacity not been of any consideration any number of blades could be chosen for present the study also.

5.1.1 Validation of total loss computed from 3-D simulation with experimental data along blade span

Computational results of pitch wise local loss coefficients for smooth turbine cascade are compared with experimental data of same profile and shown in figure 5.1. There is good agreement between trend of computational results & experimental data. Aim of validation is to show that present numerical model used for simulation is reliable and can be used for further analysis & parametric studies.

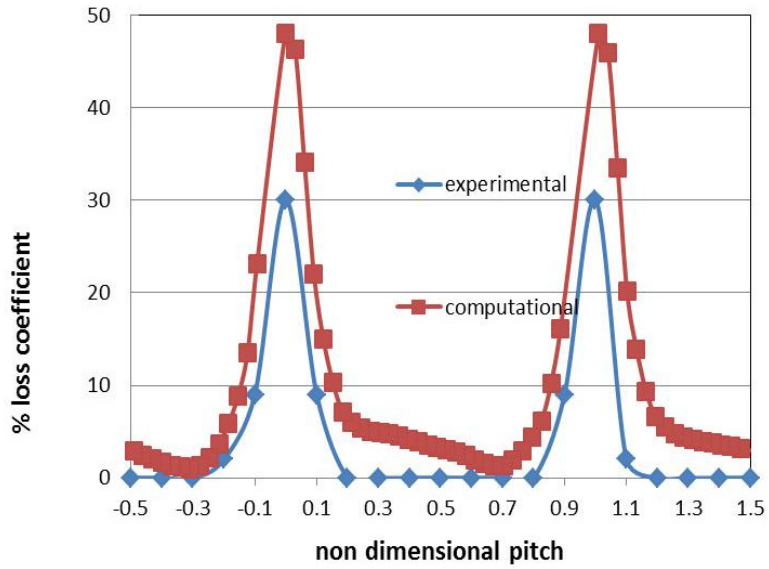

Figure 5.1: Comparison of simulation results with experimental data on mass averaged loss coefficient along blade height

5.1.2 Allocation of boundary types to various faces and surfaces of the geometries of cascades

It would be desirable to know as to how total pressure varies within entire computation domain. Therefore some input fluid velocity at the inlet of the cascade is required to be selected so that total pressure or other variables at various locations in the flow field could be determined. For the present study, the fluid velocity at the inlet of the each of turbine cascade is chosen to be 104 m/s. For this purpose, the face at inlet of the cascade, through which the air is supposed to flow is assumed to be velocity inlet. Similarly the face at outlet of the cascade, through which the air is supposed to pass through is assumed to be pressure outlet. The boundary type, surfaces of blades are allocated to, is “wall”. The process of assigning boundary types to faces etc., under GAMBIT software, using Zone command, is required to be completed at the time of geometry creation. The various processes are depicted with pictorial presentations as shown in subsequent section.

5.1.3 Various Pictorial presentations

The CFD software GAMBIT displays various stages of geometry creation. Similarly, another CFD software FLUENT, used in this study, is useful for visualisation of various flow phenomena in the flow field. The Fluent, under display section, shows pressure and velocity contours which are very useful for visualizing various flow phenomena. The Fluent software allows users to view display related to velocity, pressure etc. In this section, all such important displays, obtained during process of measurement of various parameters using Gambit &Fluent, are introduced.

The figure 5.2 shows a display obtained during creation of geometry of turbine cascade using Gambit software. During this process boundary types are allocated using Zone command.

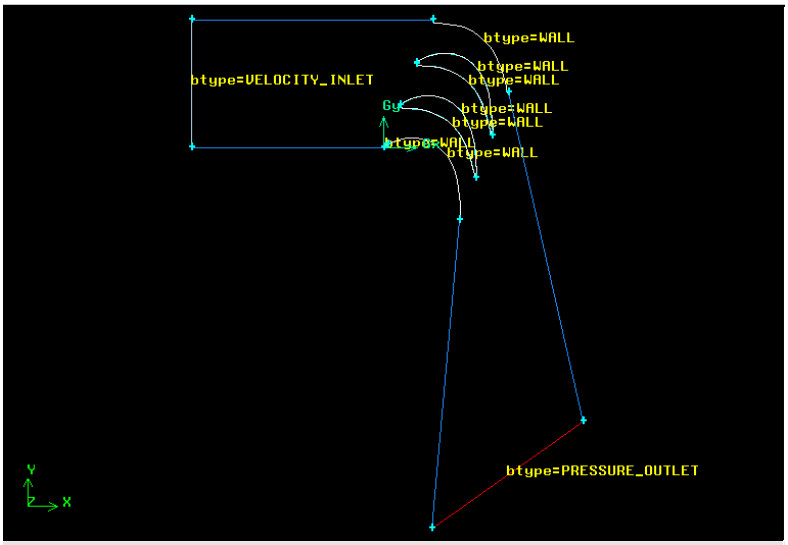

Figure 5.2: Grid display showing allocation of boundary types using Zone command

The purpose of assigning boundary type is to ascertain 'wall effect' of the blades so that the post processor i.e. Fluent software could process the same. The wall so modeled are allocated roughness during processing by the Fluent software. The models of rectilinear cascades representing the actual flow through blade passages of

turbine stages are made with a layer of roughness over the smooth blades, which is equivalent to the roughness generated by the deposits on the actual turbine. The roughness is applied to various similar locations of all blades of the cascade. Similar location here means the surfaces which have same geometry, curvature and air angle etc. The pressure and suction surfaces of all blades form a group of similar surfaces individually. The roughness is applied to such surfaces separately and individually. Alternatively it can be said that the roughness is separately applied over each pressure surface of all the blades at a time. Similarly, roughness maybe applied on all the suction surfaces of all the blades at a time. Summarising above it can be stated that the roughness of 250, 500, 750 & 1000 μm (for turbine cascades) and roughness of 250, 500, 750 μm (for compressor cascades) is applied separately over:

(i) Entire pressure surfaces of all blades (PSR)

(ii) Entire suction surfaces of all blades (SSR)

(iii)Both surfaces (suction & pressure sides) of all blades (BSR)

The BSR, SSR and PSR are the abbreviated names of cascades. The roughness magnitude is used as suffix to describe a given cascade specifying roughness thereon. For example if roughness of 500 μm, is applied on all blades of a cascade, choosing both surfaces together for application of roughness then abbreviated name of the cascade would be BSR 500. Similarly PSR500 and SSR500 are the abbreviated names of cascades when surface(s) chosen for application of roughness on blades surfaces of the cascade are separately pressure surfaces and suction surfaces respectively. In this dissertation, the abbreviated names of cascades are frequently used.

All the results for BSR, SSR, PSR cascades are compared, one by one, separately with losses associated with smooth blade cascades. The roughness values are successively

increased and losses associated with smooth blade cascades are again compared with those obtained for cascade, blades of which are roughened. Each result is separately discussed in the context of increase or decrease of loss with the increase in roughness from the reference level i.e. respective cascade with smooth blade. In various sections of this chapter, the profile wise results are discussed one by one, as mentioned above. The results for the smooth blades are first of all presented in the context of comparing the same with results of respective cascade with rough surfaces in each section.

All the results for BSR, SSR, PSR cascades are compared with that of this reference level i.e. respective cascade with smooth blade. The effect of roughness on profile and secondary loss due to application of roughness on different surfaces and changing magnitude of roughness are discussed. The results for roughness on the surfaces, in localized way, on various cascades are presented next. The roughness is first applied on suction surface at leading edge region, at mid-chord and at last at trailing edge region. The similar work is carried out by applying roughness on remaining surfaces i.e. pressure surfaces. Similar practice is also repeated by applying roughness on both surfaces together, at a time. The effects of roughness locations and its magnitude are then discussed for each combination as above. The analysis for Total, profile and secondary loss is separately discussed in each section.

Fluent need input of roughness value in the column of wall momentum thickness as a prerequisite for running the geometry with the proper boundary type allocation, meshing of the geometry and creating a file with the extension '*.msh'. The Fluent software 'writes' magnitudes of pressures at the outlet measurement plane at various pitch locations so as the measured values can later be opened using Microsoft Excel file.

After proper meshing and testing, this model is exported to Fluent and the parameters as discussed above are measured at the measuring plane. The figure 5.3 shows measurement planes at inlet and exit of a turbine cascade. Another figure 5.4 shows a meshed geometry of turbine cascade.

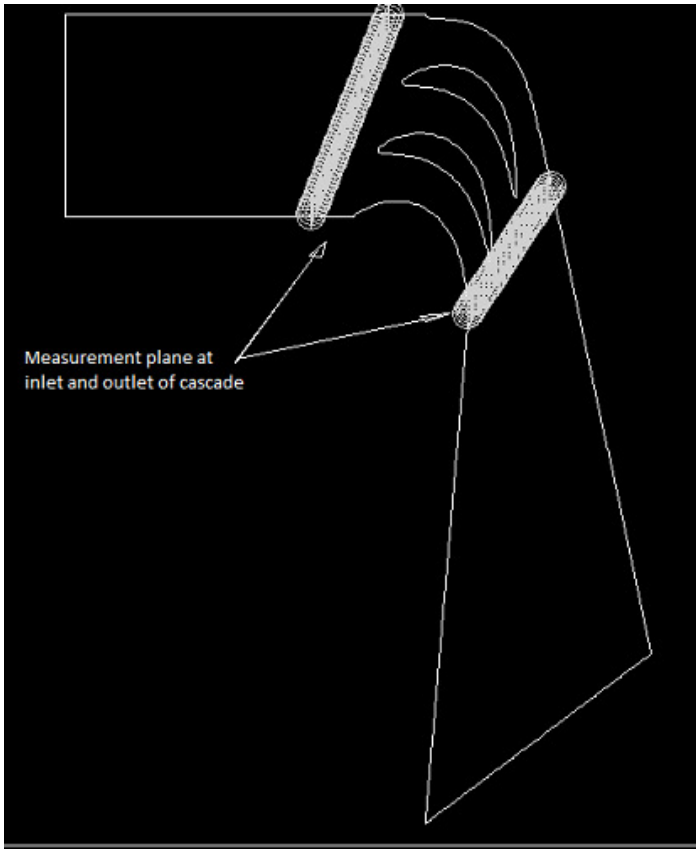

Figure 5.3: A grid display showing measurement planes at inlet and exit of a turbine cascade

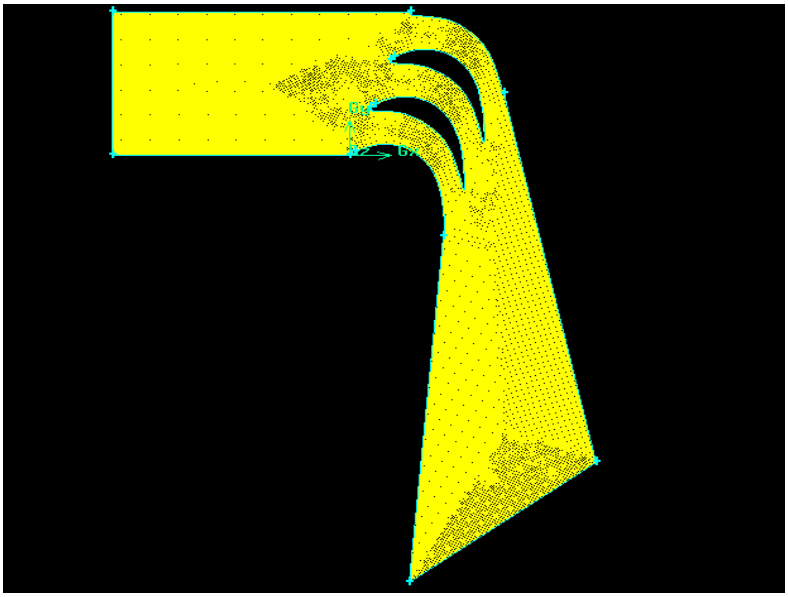

Figure 5.4: A grid display showing meshed geometry of turbine cascade

The measured values of pressure as a result of the CFD work are very important as these can be recorded in the form of graph or table format and analysed for results. The Fluent software also displays the pressure distribution for complete flow domain. The total pressure distribution over the entire computational domain is shown in figure 5.5.

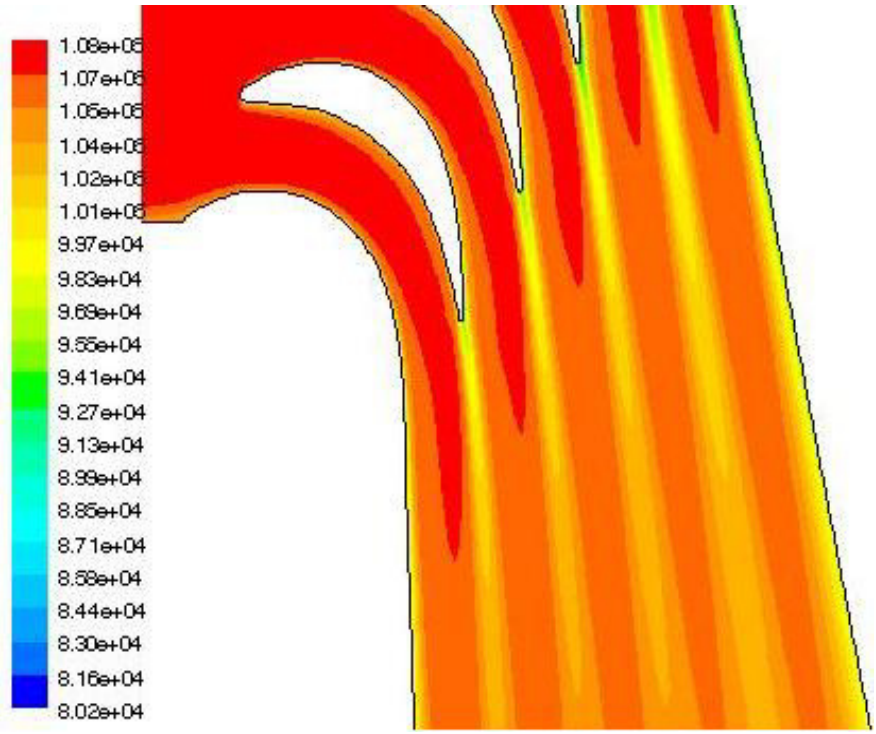

Figure 5.5: Grid display (exaggerated in order to show intermixing of the core flow and the wake) showing the total pressure distribution at downstream of the trailing edge of a blade of a cascade

It is clear from figure 5.5 that total pressure remains constant before the high pressure fluid enters the cascade section and that the total pressure reduces due to expansion of fluid over the cascade section and at the exit of the cascade the wakes are formed, where the total pressure drops significantly. The same phenomenon is presented in the figure 5.6 also. It is clear from the figure 5.5 and figure 5.6 that the pressure drop is very less in the core flow region.

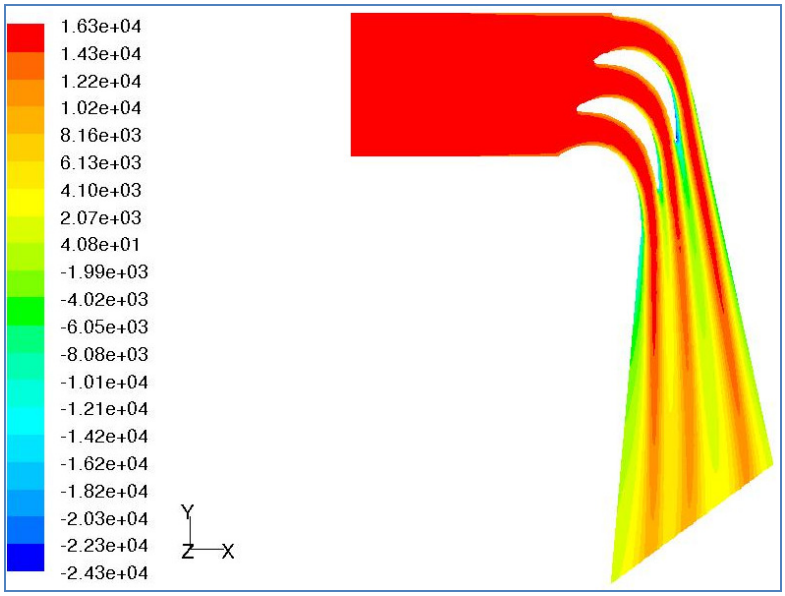

Figure 5.6: Total pressure distributions in wake region at mid span of BSR cascade having Roughness of 500 µm.

At significant distance from the trailing edge, the total pressure drops due to the intermixing of the core flow and the wake. The figure 5.7 shows velocity contours at trailing edge exit showing formation of trailing edge exit vortex and areas of flow reversal.

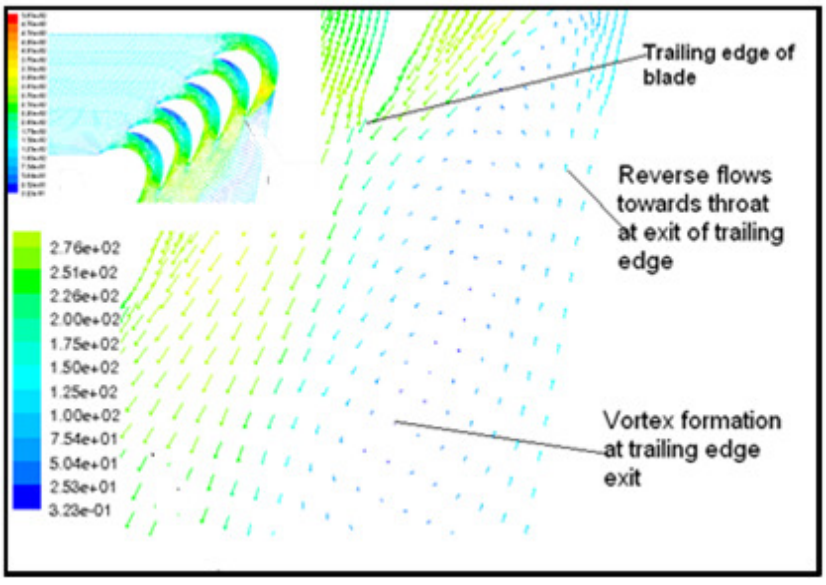

Figure 5.7: Velocity contours at trailing edge exit showing separation of flow

In the present research work, the local loss coefficients are measure of the pitch wise loss that will be presented subsequently in this chapter. According to a study [Samsher, 2002], width of the wake depends on the pressure drop in the cascade section. According to him, higher is the pressure drop, larger is the width of the wake.

5.1.4 Velocity Vectors

A typical cascade velocity vectors over the computation domain are shown in Figure 5.8. It is shown in the figure 5.8 that the fluid moves with constant velocity up to the inlet section of the cascade.

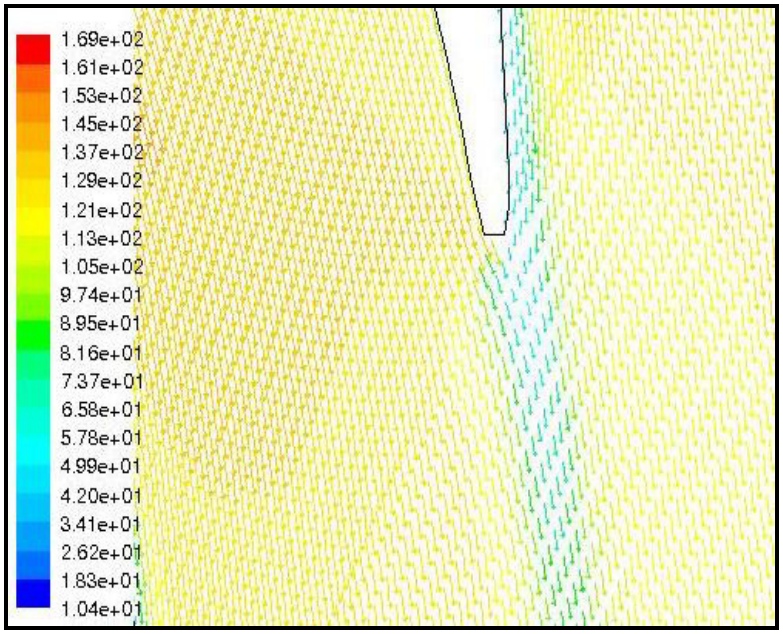

Figure 5.8: Velocity vectors for the flow of fluid afterwards the mixing of the core flow and the flow in the wake region

The velocity reaches its highest value when the fluid passes through the throat section of the cascade. The velocity reduces afterwards when the core flow and the flow in the wake region mix. The flow further reduces in the diverging portion of the model before finally escaping in to the atmosphere. It is observed from figures 5.7 and 5.8 that there is a flow separation on the suction side at the trailing edge.

5.1.5 Local loss coefficients: a measure of effect of roughness

In order to measure the effect of increasing roughness and application of same roughness at different locations (surfaces of blades of cascades so modeled), the local loss coefficients are calculated by using pressure values at various positions at inlet and exit measurement planes, obtained as per process described above.

5.1.6 Non-dimensionalising the losses with total loss of smooth cascade

The reason for non-dimensionalising the loss for given cascade with total loss in smooth blade cascade is to measure effect of roughness comparing the same with respective value of loss for smooth cascade. This effect of roughness would be measured by finding difference between the particular type of loss for a cascade, for a selected magnitude of roughness and the respective value of loss for smooth cascade. The results of computational study show that the total energy loss is increased with application of roughness for both of turbine and compressor cascades in spite of absolute change in profile & secondary losses separately. When the absolute change in profile & secondary losses are non-dimensionalised with total loss with the same roughness the same is not truly reflected in the percentage change in profile & secondary losses separately. This is so because the total energy loss is also increased with application of roughness therefore profile & secondary losses are not truly reflected in the percentage change when the absolute changes in these losses are considered. In these circumstances, a base value is required to be fixed with reference to which a change in magnitude of losses as a result of increase of roughness on various surfaces and application of roughness on different locations could be found. Therefore, for the present study, secondary losses in total energy loss are non-dimensionalised with the total loss of cascade employing smooth blades. By increase

of percentage change, it can easily be concluded as to which location is more prone to show effect of roughness. Inter alia it can also be concluded as to how magnitude of roughness affects the losses generated. The Table 5.1 depicts how secondary losses are nondimensionalised with total loss of the smooth cascade. The values of height & width are chosen to be 95 & 41mm respectively for calculation of various types of losses in the table 5.1.

Table 5.1 Process of nondimensionalising secondary losses with total loss of the respective smooth cascade

Σmass averaged loss coefficients × representing heights	**Total cross-sectional area of the cascade**	**Total loss as a fraction**	**Profile loss as a fraction**	**Secondary loss as a fraction**	**Secondary loss as nondimensionalised with total loss of the smooth cascade**
410.26	3895.00	0.11	0.10	0.01	4.94

It is clear that the numerical value in table 5.1 may be multiplied by 100 to convert the fraction to find the percentage of various types of losses i.e. total loss and profile loss.

Several cascades representing all unique combinations of profile, roughness value and location are modeled. In order to meet objectives of this research work, striving for measurement of flow parameters for each cascade is inevitable. The measurement of flow parameters such as the total pressure and static pressure at measurement planes at inlet & exit of cascades are needed for achieving objectives of this research work.

5.1.7 Variation of total pressure and local loss coefficients relative to nondimensional distance along pitch wise direction

The shapes of graphs, for various span positions, representing variation of total pressure and local loss coefficients relative to nondimensional distance along pitch wise direction, are similar in many respects for all cascades. The distance between two consecutive blades for a given cascade is a pitch distance. The pressure surface of one blade and suction surface of its adjacent blade form a flow channel for a set of

two blades of the cascade. This arrangement repeats many times depending upon number of blades employed for the given cascade. The local loss coefficients as well as magnitudes of total pressure, both, at a given span position, repeat for each pitch distance. The both parameters may not exactly repeat their magnitude for each corresponding pitch location but the same would be approximately equal. It is observed that the patterns of variation of local loss coefficients and magnitudes of total pressure are images of each other (the pattern of local loss coefficients would be reversed up-down relative to that of total pressure and vice versa). The local loss coefficients would be reversed up-down relative to that of total pressure and vice versa.

5.1.8 Nondimensional distance in the pitch and span wise direction

The variation of these parameters for a large number of cascades is measured for which the nondimensional distance is required to be specified first. This distance is measured from one end to other end of the measurement plane in the pitch wise direction. The intermediary distances are non-dimensionalized by the total distance between one end to other end of the measurement plane. Similarly, the positions on blade height i.e. span of the blades are also non-dimensionalized by dividing the distance between bottom end wall and the position of interest by respective blade height.

5.1.9 Comparative study of variation of magnitude of pressure and local loss coefficients in the pitch wise direction

The analysis of variation of local loss coefficients and magnitudes of total pressure is very useful for studying the effect of roughness on blade surfaces of a turbomachines cascade. The variation for these parameters gives a lot of information with regard to insight of the flow through the cascade under investigation. Thus the variation of magnitude of pressure and local loss coefficients in the pitch wise direction is

required to be studied all along the span of the blades. A few of graphs showing variation of magnitude of pressure relative to the nondimensional distance in the pitch wise direction for BSR turbine cascade for the roughness magnitude of 750 µm are presented in figures 5. 9, 5.10, 5.11and 5.12 for various span positions.

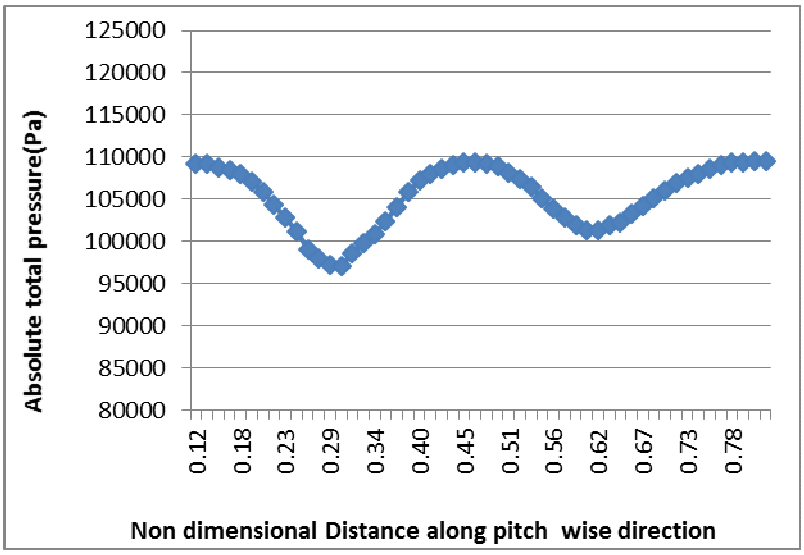

Figure 5.9: Variation of magnitude of absolute total pressure relative to the pitch wise direction, for the span position of 0 mm (at the lowest position of the blades i.e. at bottom wall)

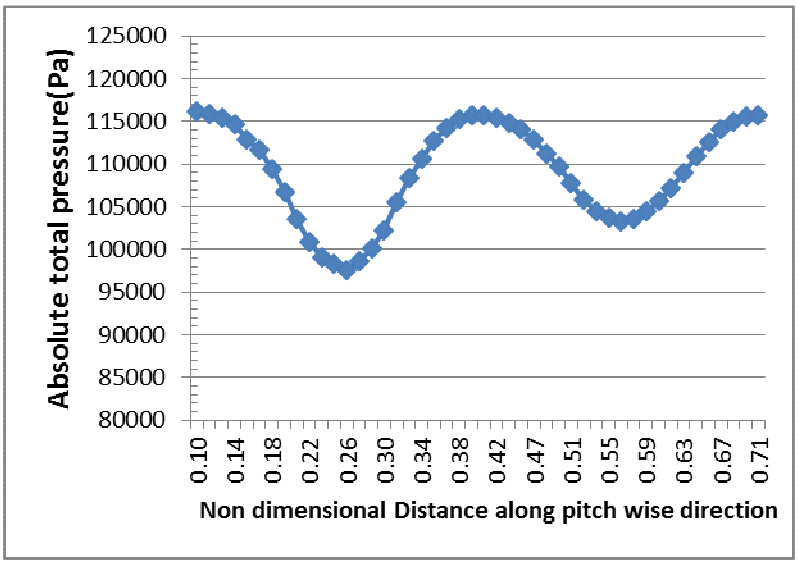

Figure 5.10: Variation of magnitude of absolute total pressure relative to the pitch wise direction, for the span position of 2mm from bottom wall

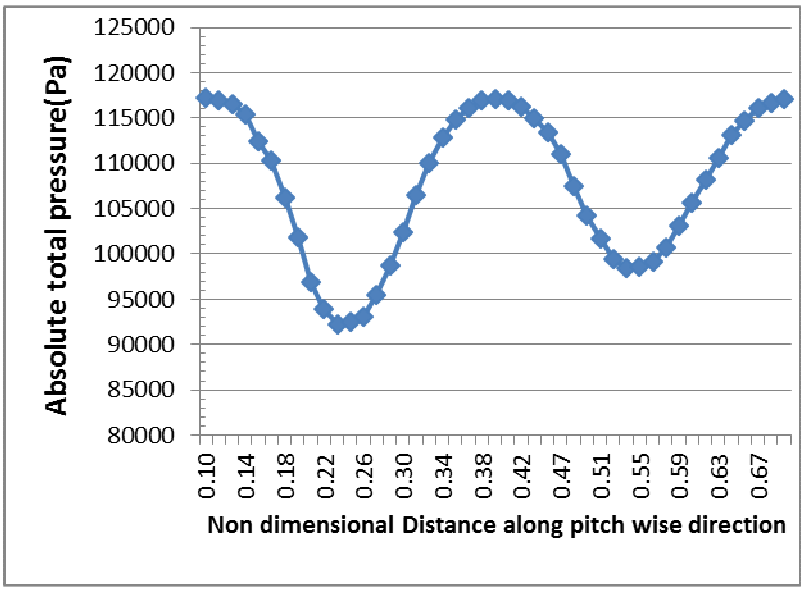

Figure 5.11: Variation of magnitude of absolute total pressure relative to the pitch wise direction, for the span position of 8mm from bottom wall

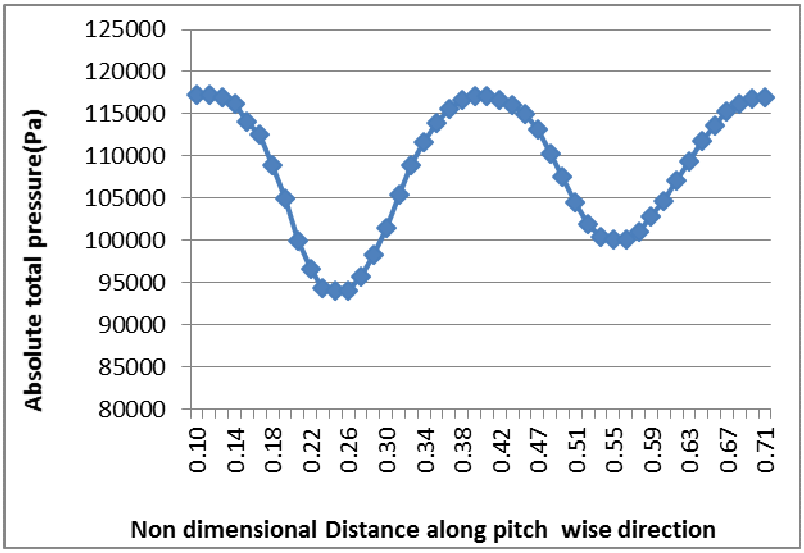

Figure 5.12: Variation of magnitude of absolute total pressure relative to the pitch wise direction, for the midspan position (47.5 mm from bottom wall)

Similarly pitch-wise variation of local profile loss coefficients for each of cascade is measured for all cascades. The figures 5.13, 5.14, 5.15 and 5.16 are showing graphs depicting pitch-wise variation of Local Loss Coefficients at various span wise positions, for BSR turbine cascade on the blade surfaces of which the roughness of magnitude of 750 µm are applied.

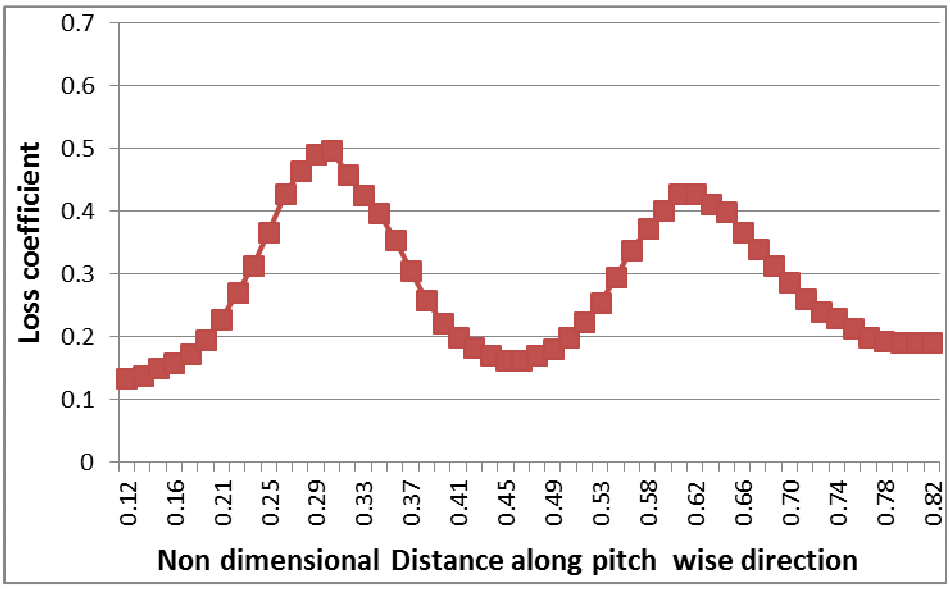

Figure 5.13: Variation of Local Loss Coefficients relative to the nondimensional distance in pitch wise direction, for the span position of 0 mm (at the lowest position of the blades i.e. at bottom wall)

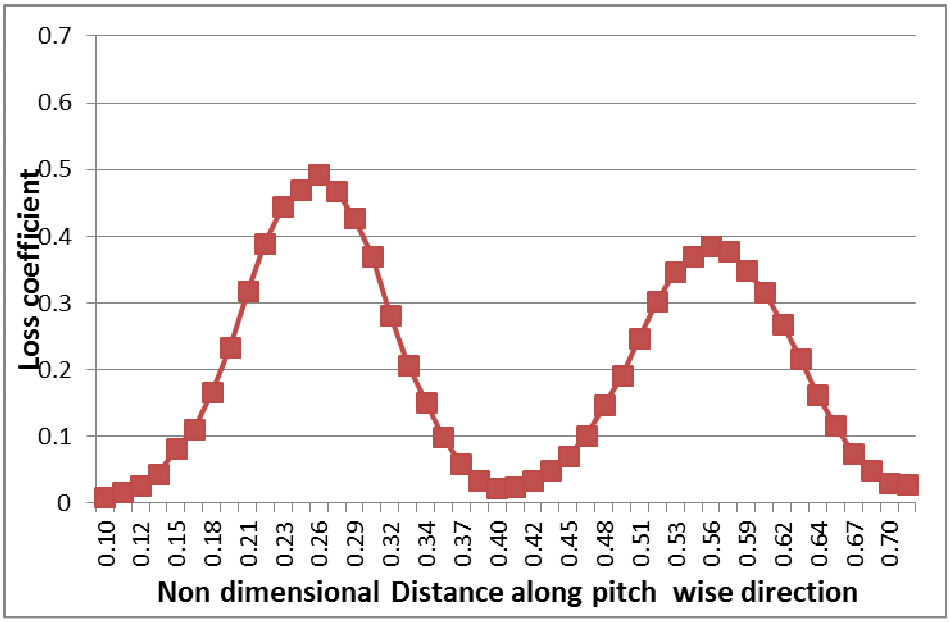

Figure 5.14: Variation of Local Loss Coefficients relative to the nondimensional distance in pitch wise direction, for the span position of 2mm from bottom wall

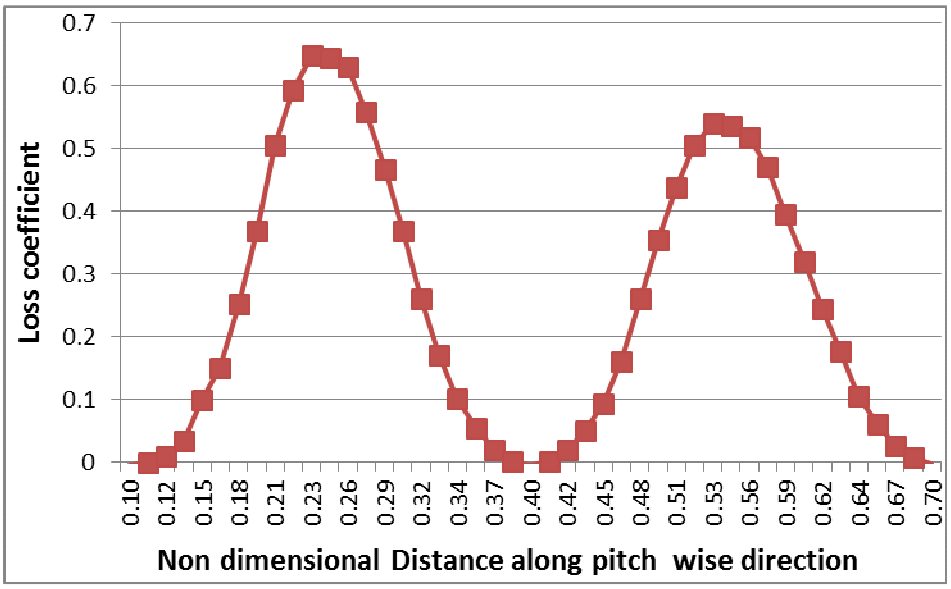

Figure 5.15: Variation of Local Loss Coefficients relative to the nondimensional distance in pitch wise direction, for the span position of 8mm from bottom wall

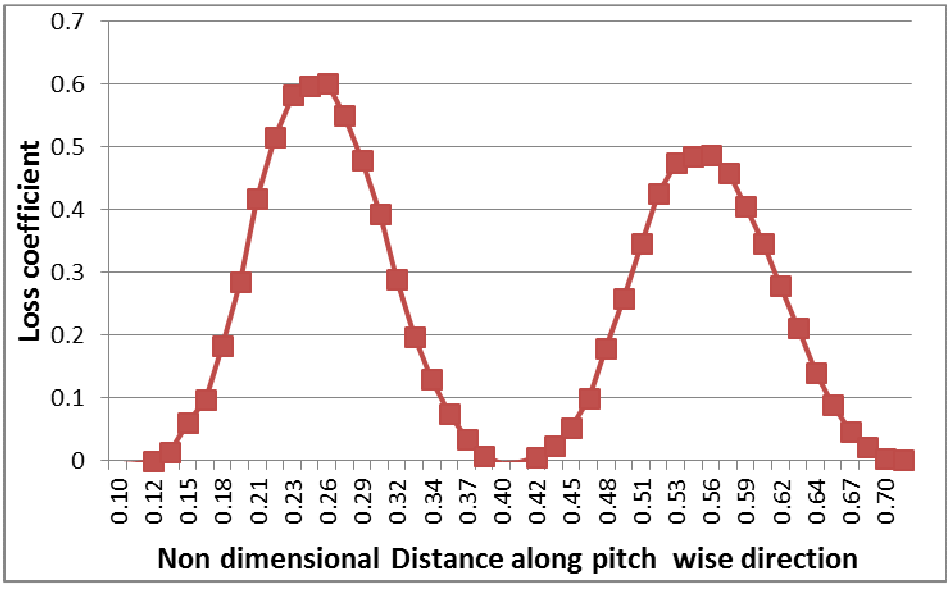

Figure 5.16: Variation of Local Loss Coefficients relative to the nondimensional distance in pitch wise direction, for the midspan position (47.5 mm from bottom wall)

However for calculating mass averaged loss coefficients the effect of vertical side walls for all cascades are ignored. Thus, the mass averaged loss coefficient, represent all local loss coefficients for various pitch positions excluding few local loss coefficients for the half pitch at both the ends. The figures 5.17, 5.18, 5.19 and 5.20 show graphs depicting pitch-wise variation of Local Loss Coefficients at various span

wise positions, ignoring effects of side walls (few local loss coefficients for the half pitch at both the ends are not taken into account while calculating mass averaged loss coefficient), for BSR turbine cascade on the blade surfaces of which the roughness of magnitude of 750 µm are applied.

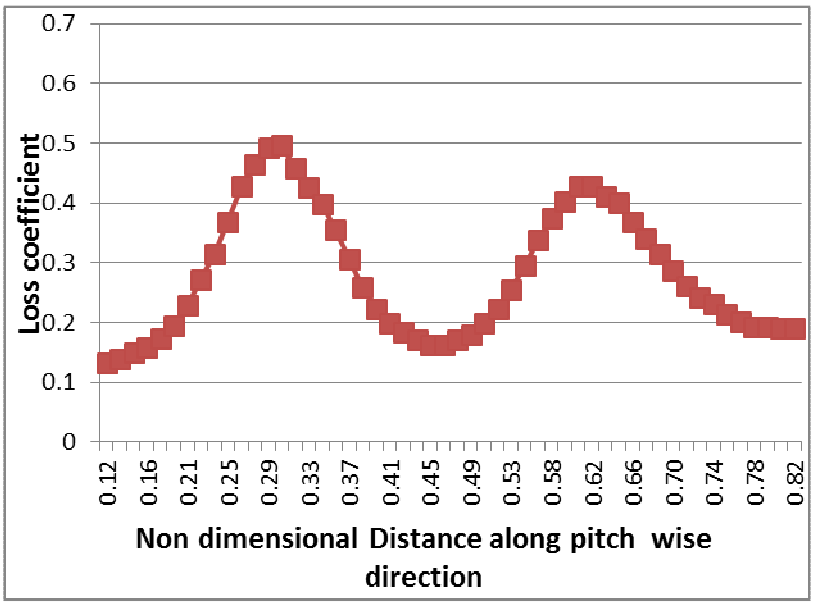

Figure 5.17: Variation of Local Loss Coefficients relative to the nondimensional distance in pitch wise direction, for the span position of 0 mm (at the lowest position of the blades i.e. at bottom wall)

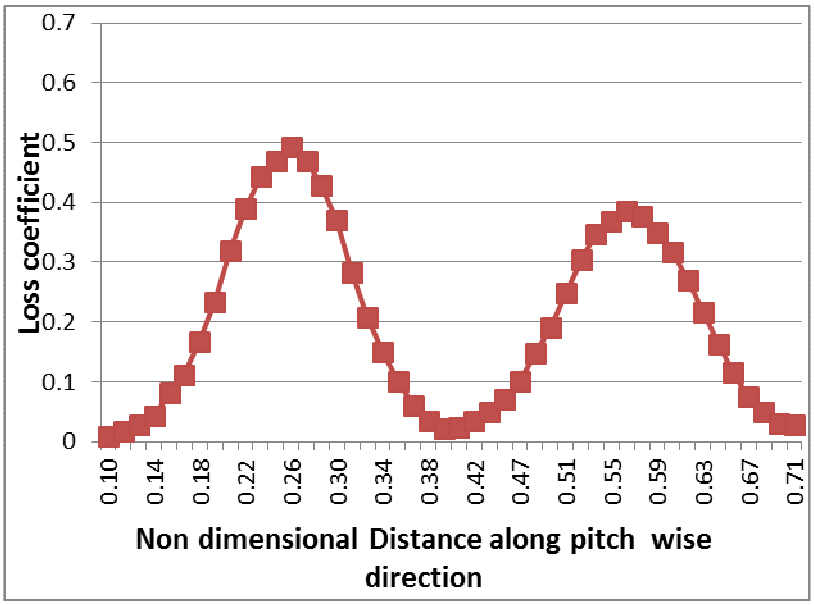

Figure 5.18: Variation of Local Loss Coefficients relative to the nondimensional distance in pitch wise direction, for the span position of 2mm from bottom wall.

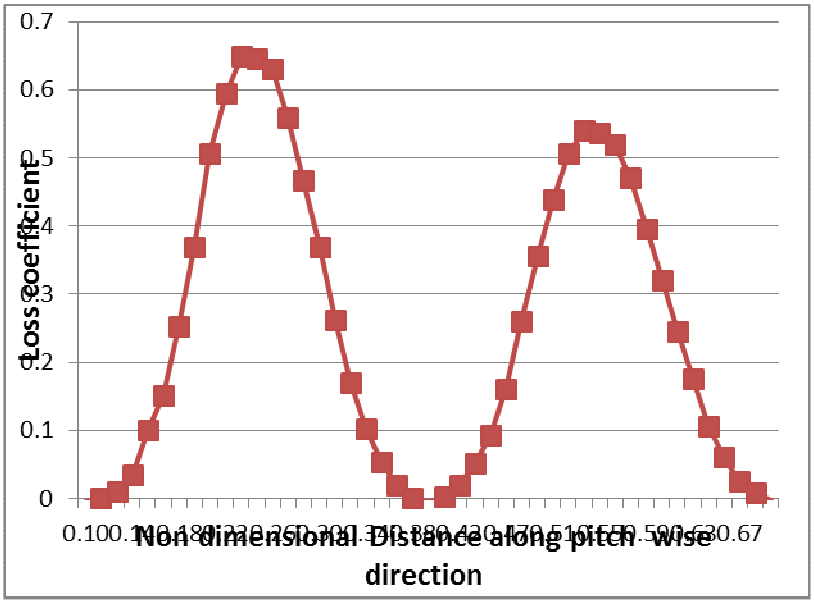

Figure 5.19: Variation of Local Loss Coefficients relative to the nondimensional distance in pitch wise direction, for the span position of 8mm from bottom wall.

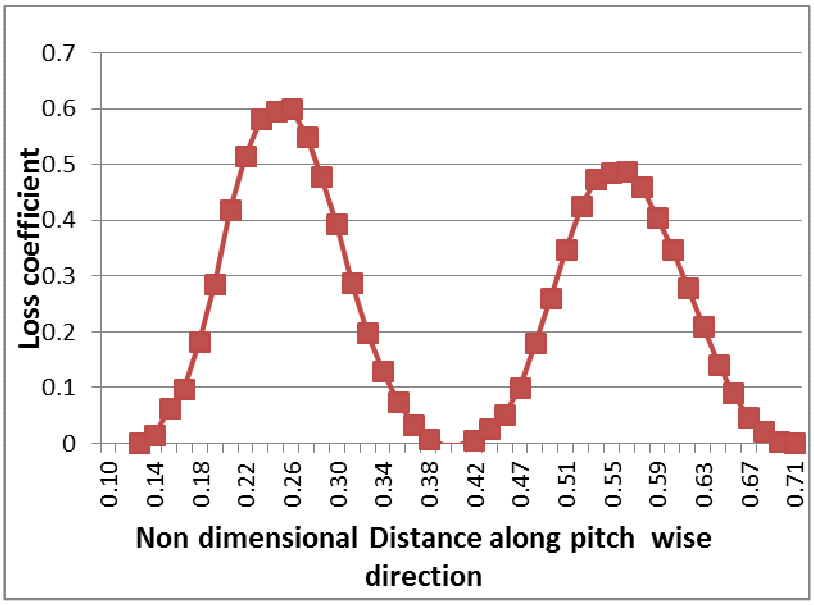

Figure 5.20: Variation of Local Loss Coefficients relative to the nondimensional distance in pitch wise direction, for the midspan position (47.5 mm from bottom wall)

The shapes of graphs showing variation of local loss coefficient or total pressure in pitch wise direction for all cascades resemble to be same. Hence, graphs showing variation of local loss coefficients in pitch wise direction for all cascades, are not

shown to avoid repetitiveness. Therefore, only a few of variation of local loss coefficients and magnitudes of total pressure are presented in this section. The variation of magnitude of pressure and local loss coefficients in the pitch wise direction for the cascades are presented in two ways i.e. either ignoring or not ignoring effects of side walls. However, variations of magnitude of pressure and local loss coefficients ignoring effects of side walls are only to be presented or discussed in this dissertation.

5.1.10 Total Number of cascades representing combinations of location of roughness and blade profile

The results of the investigations carried out with all the three profiles 5530, 6030 and 3525 for turbine cascades are presented and discussed in this chapter. The figure 5.21 shows indicative shapes of all the profiles used for geometry creation of turbine cascade and modeling thereafter. The figure 5.21 shows that the leading and trailing edge thicknesses camber angles etc. for the profiles are different from each other.

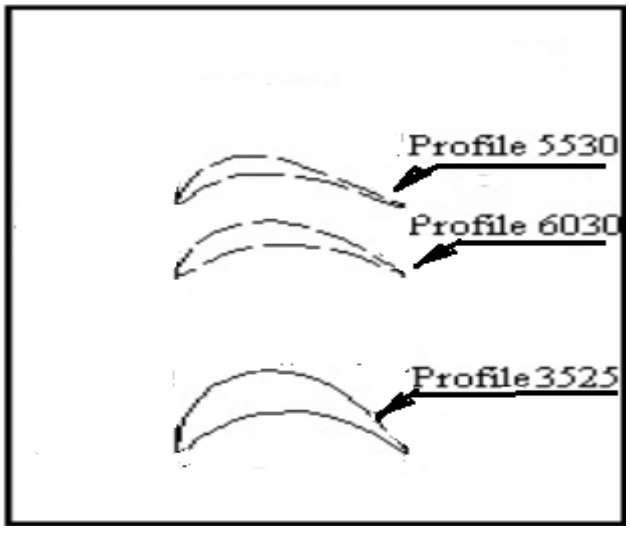

Figure 5.21: Indicative shapes of 3 Nos. blade profiles used for geometry creation of turbine cascades

It is obvious that the results for the different profiles would certainly be different as the various parameters of cascade and factors affecting shape of blades i.e. the curvature of the surfaces, camber angle, trailing edge thickness, pitch and chord ratio, span and chord ratio, leading edge geometry, convergence of inter blade channels formed by profiles, curvilinear lengths of suction and pressure surfaces of profile and many more other factors of a given blade profile affect losses to be generated. In order to distinguish the loss mechanism for each such profile, numerous number of cascades are simulated using the blade profile. The three profiles differ in the curvilinear length of suction and pressure surfaces, besides the degree of convergence of inter blade channels formed by them. The thickness in the chord wise direction also differ for each of blade profiles. The flow turning capacities of blades profiles also differ largely from each other.

The effect of blade deterioration (due to roughness) on performance of turbines is studied in two ways. The first is by changing of location for application of roughness and second by increasing roughness on the same surface. The number of cascades required to be simulated depends on whether entire surface (s) of various blades of the cascade are chosen for application of roughness. Another method of application of roughness is localised roughness. The following are the list of cascades simulated for each of combinations of location of roughness and one blade profile, out of three blade profiles for turbines applying roughness on entire surface. The following list does not cover the cascades required to be simulated applying localised roughness:

1. smooth blade cascade
2. blade employing roughness of 250 μm
    i. SSR 250
    ii. PSR 250
    iii. BSR 250

3. blades employing roughness of 500 µm
    i. SSR 500
    ii. PSR 500
    iii. BSR 500
4. blade employing roughness of 750 µm
    i. SSR 750
    ii. PSR 750
    iii. BSR 750
5. blade employing roughness of 1000 µm
    i. SSR 1000
    ii. PSR 1000
    iii. BSR 1000

Thus, total 13 cascades are simulated separately for each of combinations of roughness magnitude, location of roughness and the given single blade profile. Therefore total number of cascades for all three blade profiles 37 cascades would be required to be simulated excluding those using localised application of roughness for turbines. The total number of cascades required to be simulated for compressor, for one blade profile, would be 10. For each such simulation the variation of pressure and local loss coefficients relative to nondimensional distance along pitch wise direction are measured for each span position from bottom end wall to top end wall**.** The number of span positions from bottom end wall to top end wall are 27 and 21 for turbine and compressor cascades respectively.

5.1.11 Segregation of total losses into profile losses and secondary losses

According to the relation proposed by Kostyuk and Frolov **[1988]** (as mentioned in the equation 4.6, chapter 4) **,** the total (combined) losses in all blade cascade are estimated by the mass averaged loss coefficient ζ, which is essentially the sum of profile loss coefficient & end loss coefficient. The mass averaged loss coefficient as obtained are the measure of total loss. The unit height along the vertical axis of each graph showing variation of mass averaged loss coefficients for various cascades relative to the nondimensional distance in the direction of blade span is assumed to be equal to total energy of incoming air from inlet of the cascade. Thus total area below the line drawn parallel to horizontal axis (abscissa) from the point representing unit height on vertical axis of each such graph is assumed to be equal to the area analogous to the total energy available at the inlet of the given cascade. The area below the graph is equal to the area analogous to the total energy lost during the flow through the given cascade. The table 4.4 of chapter 4 shows as to how mass averaged loss coefficient are double integrated in the Pitch Wise Direction and in Span Wise Direction. The area analogous to the total energy lost can be understood to be equivalent to the value obtained by double integration of all local loss coefficients in pitch wise direction and span wise direction. The area and energy analogy can be best understood with the help of figure 5.22. The area analogous to the total energy lost can be understood to be equal sum of all the areas of trapeziums as shown in figure 5.22. The section 4.7 of chapter 4 may be referred for the detailed procedure of "double integration of all local loss coefficients".

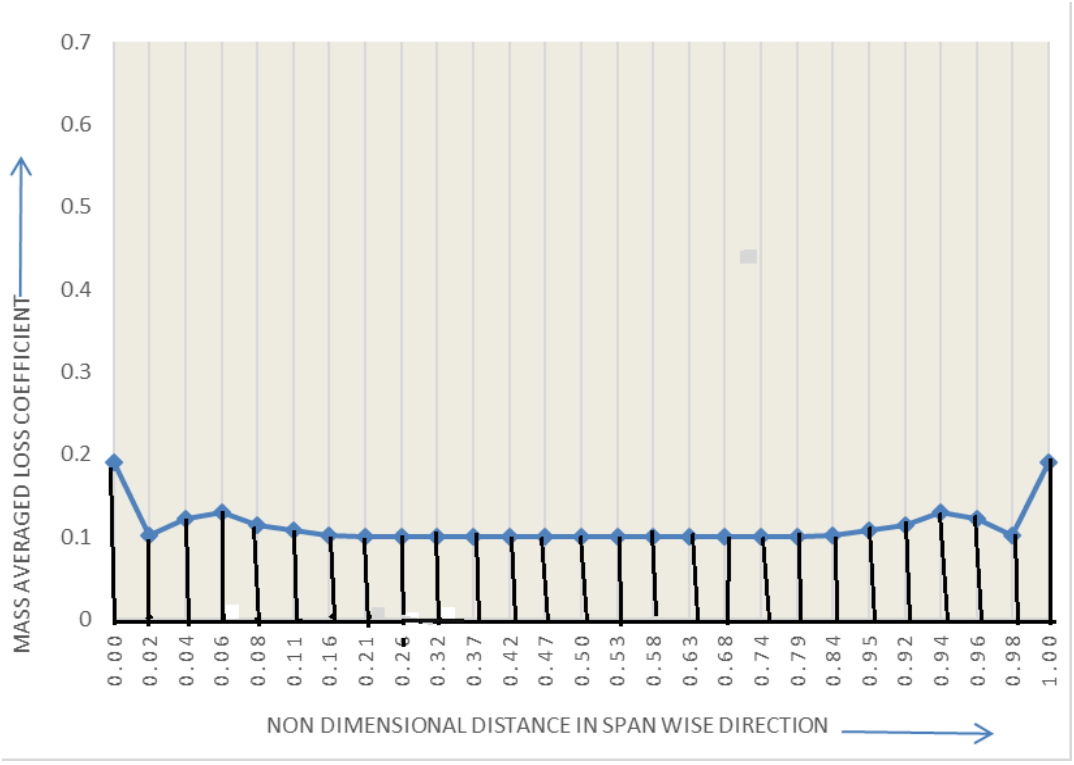

Figure 5.22: Relation between sum of areas of trapeziums and total loss for a cascade

Mass averaged Loss coefficient calculated at blade mid span, where the flow is two-dimensional & influence of end wall effect is not present, constitutes profile losses. The value of mass averaged loss coefficient so calculated at blade mid span would be termed as profile loss coefficient. Thus, end loss or secondary loss coefficient along blade height is calculated as the difference between the total and profile loss coefficients in a cascade.

There are two components of total loss i.e. profile loss and secondary loss. The magnitude of profile loss and secondary loss may differ for different for two different cascades as result of the effect of changing of roughness magnitude or geometry of the blades. The losses mentioned in this dissertation are expressed in percentage loss. The total loss has been expressed as percentage of total energy of the air. Similarly profile loss is also expressed as percentage of total energy of the air. The secondary flow loss are expressed as percentage of total loss. The total (combined) losses in all

blade cascade are estimated by the mass averaged loss coefficient, which is essentially the sum of profile loss coefficient & end loss coefficient. The absolute value of percentage of secondary loss in total energy is found by subtracting percentage values of total energy loss & Profile loss in total energy. This absolute value is very less. Therefore, a term called, percentage of secondary loss in total loss is used in this dissertation. The term percentage of secondary loss as non-dimensionalised with the total loss in case of smooth blades will be used more frequently in this dissertation.

The section 4.8 of chapter 4 may be referred for description with regard to method of determining the profile and secondary loss coefficient from the available mass averaged loss coefficients. The same section may be referred for description with regard to method of segregation of total loss into profile and secondary loss (as a percentage of total incoming energy or as percentage of total loss nondimensionalising with total loss of the smooth cascade for same blade profile, as the case may).

This research work, include the simulation of flow through cascades choosing all the blade profiles for turbine and compressor separately. The subsequent section includes results for cascade, employing 6030 blade Profile.

5.2 Measurement of magnitude of losses for Turbine Cascades employing blade profiles 6030

The degree of reaction of this profile is about 55 %. The convergence of inter blade channels formed by this profile would be more as compared to the blade profile 3525, which is of lesser degree of reaction. The curvilinear lengths of suction and pressure surfaces of this profile are 55 mm & 66 mm.

Therefore patterns of variation of magnitudes of total pressure are not shown in graphical form in case of each of cascades to avoid repetitiveness. Similarly all graphs showing variation of local loss coefficients are also not shown in graphical form to avoid repetitiveness. However a few of such graphs are already shown in figures 5.13, 5.14, 5.15 and 5.16 so as to differentiate various results of cascades which employ different blade profile, having been applied with predetermined roughness, location of roughness and magnitude of roughness. First of all, the smooth blade cascade, employing 6030 blade Profile, is discussed in this section.

5.2.1 Smooth Blade for Profile 6030

The variations of various parameters for three dimensional turbine cascade employing smooth blades profile 6030 are discussed in the following paragraphs. There are numerous number of span positions for all the cascades inclusively. In order to analyse the flow and losses generation mechanisms, variation of two parameters i.e. local loss coefficients and total pressure are inevitably required.

It is not possible to present graphs for each of span wise positions, for all the cascades. Therefore, a few of graphs showing variation of local loss coefficients and total pressure are shown in this dissertation in view to present quantitative differences and similarities between them. In fact, neither any two graphs chosen from all of the cascades are similar in all respects nor their magnitude of losses are same.

5.2.2 Variation of local loss coefficients along pitch wise direction for the smooth cascade

The figures 5.23 show the results for local loss coefficients for the cascades employing blade profile 6030 and no roughness is applied over any of the surface the cascades. In other words the cascade is employing smooth blade profile 6030.

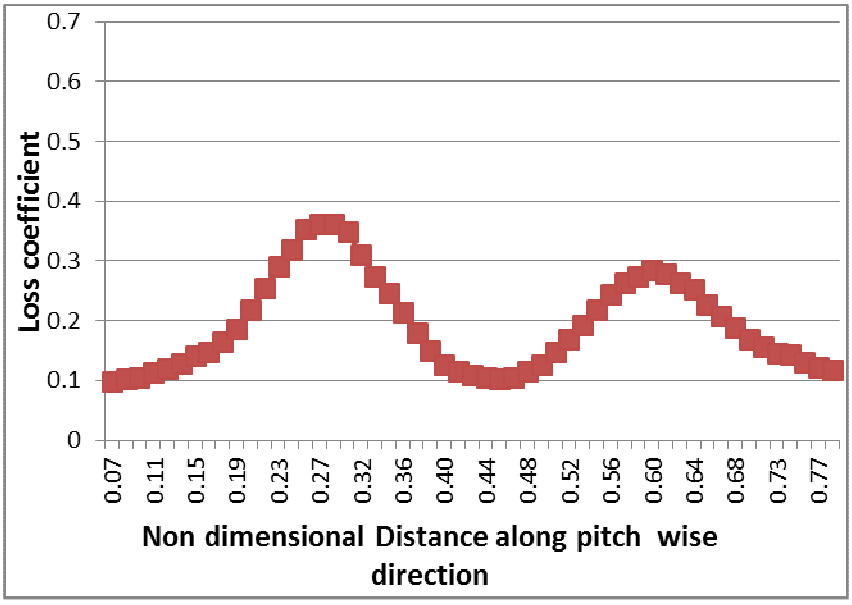

Figure 5.23: Variation of Local Loss Coefficients for smooth cascade employing blade profile 6030 relative to the nondimensional distance in pitch wise direction, for the nondimensional span position of zero

The figure 5.23 shows the variation in local loss coefficient for a smooth cascade employing blade profile 6030 for nondimensional span position of zero (the result is representing the bottom end wall) and it shows that the distribution of local loss coefficients over pitch wise distance is in such a way that loss seems to be at minimum among all other cascades, presented in previous sections (refer figures 5.13, 5.14, 5.15 and 5.16). The local loss coefficients for the smooth cascade, employing blade profile 6030 have lesser magnitude such that the peak value of local loss coefficients reaches only up to approximate 37% (figure 5.23). Whereas the peak value of local loss coefficients for BSR cascades (figure 5.13, 5.14, 5.15 and 5.16) reaches even up to 90%.

Another Figure 5.24 for cascade employing same blade profile for nondimensional span position of 0.5 (representing the middle of span of blades), shows the variation of local loss coefficient over pitch wise distance and it shows that the peaks of local loss coefficients is even lower than those for the span position of zero. Similarly

lowest values of local loss coefficients are also lower than those for the nondimensional span position of zero. The lowest values of loss coefficients at outlet of measurement plane at exit of flow channels formed by various blades are approximately zero for nondimensional span position of 0.5.

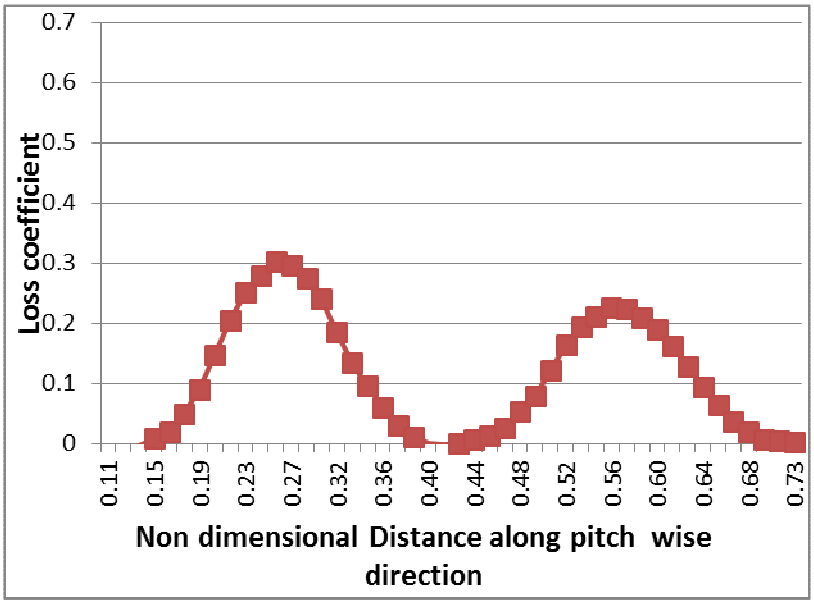

Figure 5.24: Variation of Local Loss Coefficients for smooth cascade employing blade profile 6030 relative to the nondimensional distance in pitch wise direction, for the midspan position (47.5 mm from bottom wall)

It can easily be concluded with the help of figures that there is large variation in the values of local loss coefficients for two different span positions of a given cascade. It can also be concluded that there exists a unique pattern for each span position which is never repeated for other span position. Two graphs representing variation of local loss coefficients at two nearby span positions for a given cascade seem to be same but they are also not equal in all respects. It can be stated very clearly that the magnitude of loss coefficients for two nearby span positions, at various pitch positions will be different for the cascade representing the actual flow. Although the difference would be very minimal. The variation in the values of local loss coefficients for any other

two span positions chosen randomly from all of the span positions from each of different cascades may be large.

5.2.3 Results with regard to effect of roughness on the loss for cascades employing blade profile 6030 with roughness application on entire surfaces

The result with regard to smooth blade cascade for profile 6030 is already discussed in preceding paragraphs. The remaining 12 numbers cascades employing the same blade profile i.e. 6030 are discussed, one by one, in this section in order to differentiate results of each of following cascades from remaining cascades, employing different magnitude of roughness or location of roughness application. Some representative graphs, for two span positions i.e. 0.0 (at the lowest position of the blades i.e. at bottom wall) and 0.5 (for the midspan position) are discussed for each of 12 cases. It is needless to mention that other span positions are not represented by graphs in order to avoid repetitiveness.

5.2.3.1 Variation of local loss coefficients along pitch wise direction for SSR 250 cascade

The cascade of which suction surfaces of all the blades are applied roughness of 250 μm is named as SSR 250 cascade. The graphs, for two span positions i.e. 0.0 and 0.5, showing variation of local loss coefficients relative to nondimensional distance in the pitch wise direction for SSR 250 cascade are shown in figures 5.25 and 5.26.

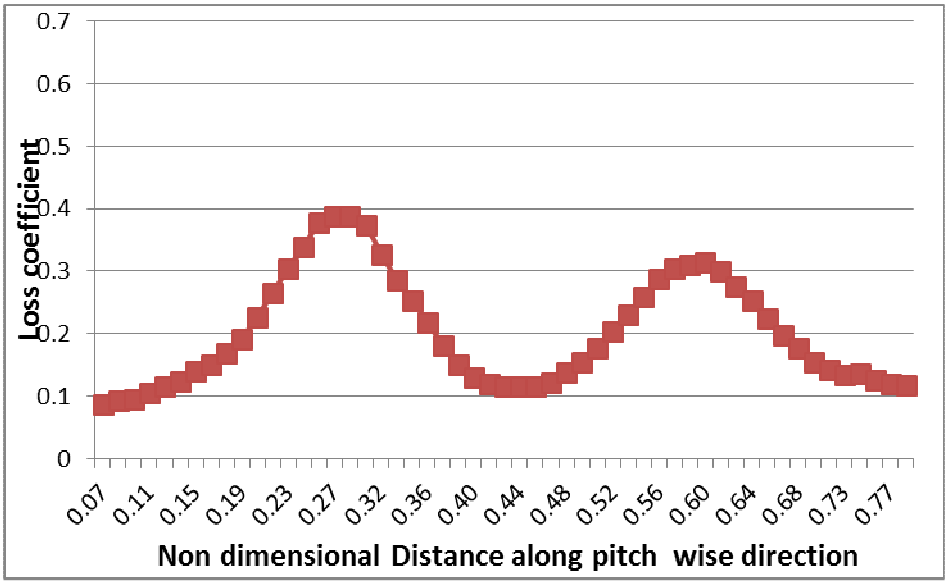

Figure 5.25: Variation of Local Loss Coefficients for SSR 250 cascade employing blade profile 6030 relative to the nondimensional distance in pitch wise direction, for the nondimensional span position of zero

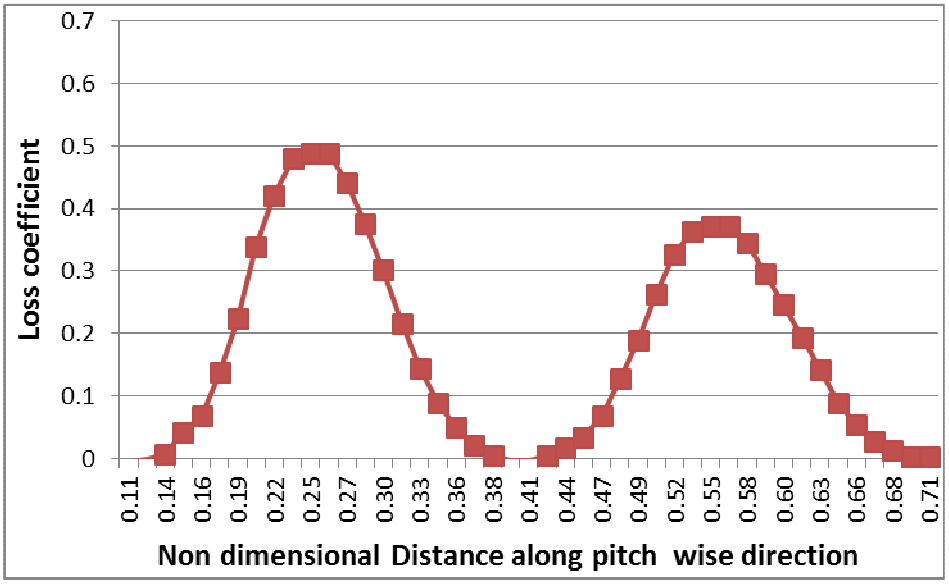

Figure 5.26: Variation of Local Loss Coefficients for SSR 250 cascade, employing blade profile 6030, relative to the nondimensional distance in pitch wise direction, for the midspan position (47.5 mm from bottom wall)

5.2.3.2 Variation of local loss coefficients along pitch wise direction for PSR 250:

The cascade of which pressure surfaces of all the blades are applied roughness of 250 µm is named as PSR 250 cascade. The graphs for two span positions i.e. 0.0 and 0.5, showing variation of local loss coefficients relative to nondimensional distance in the pitch wise direction for PSR 250 cascade are shown in figures 5.27 and 5.28

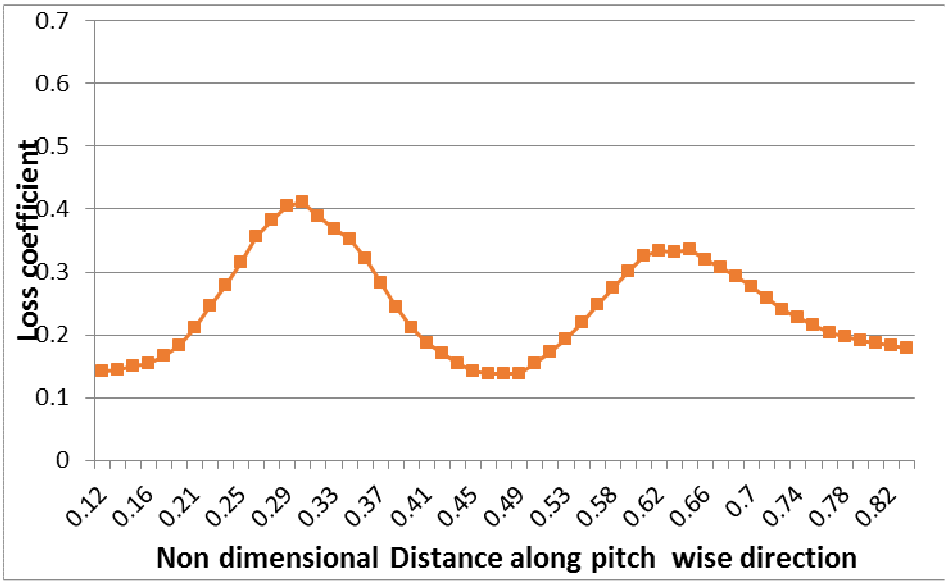

Figure 5.27: Variation of Local Loss Coefficients for PSR 250 cascade employing blade profile 6030 relative to the nondimensional distance in pitch wise direction, for the nondimensional span position of zero

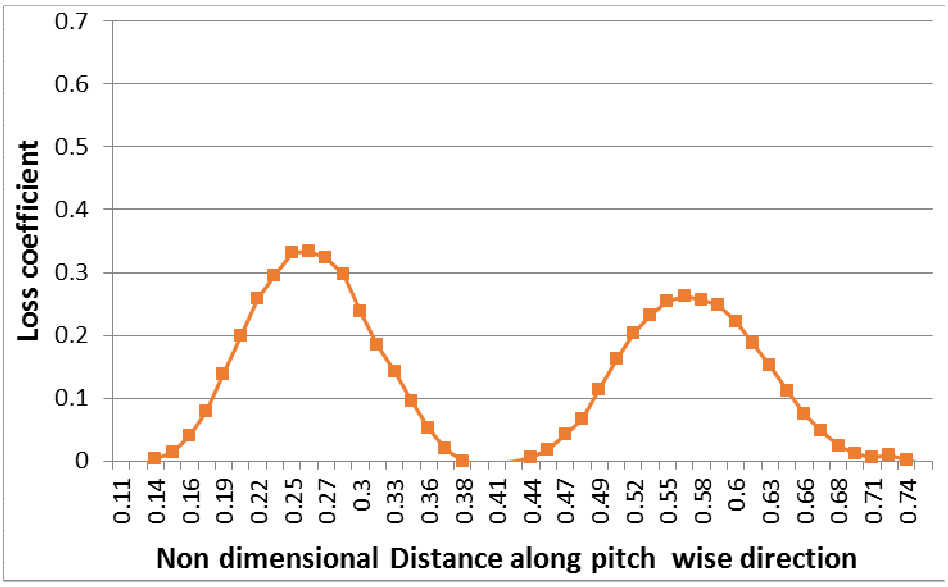

Figure 5.28: Variation of Local Loss Coefficients for PSR 250 cascade employing blade profile 6030 relative to the nondimensional distance in pitch wise direction, for the mid span position

5.2.3.3 Variation of local loss coefficients along pitch wise direction for BSR 250:

The cascade of which both surfaces of all the blades are applied roughness of 250 µm is named as BSR 250 cascade. The graphs for two span positions i.e. 0.0 and 0.5, showing variation of local loss coefficients relative to nondimensional distance in the pitch wise direction for BSR 250 cascade are shown in figures 5.29 and 5.30

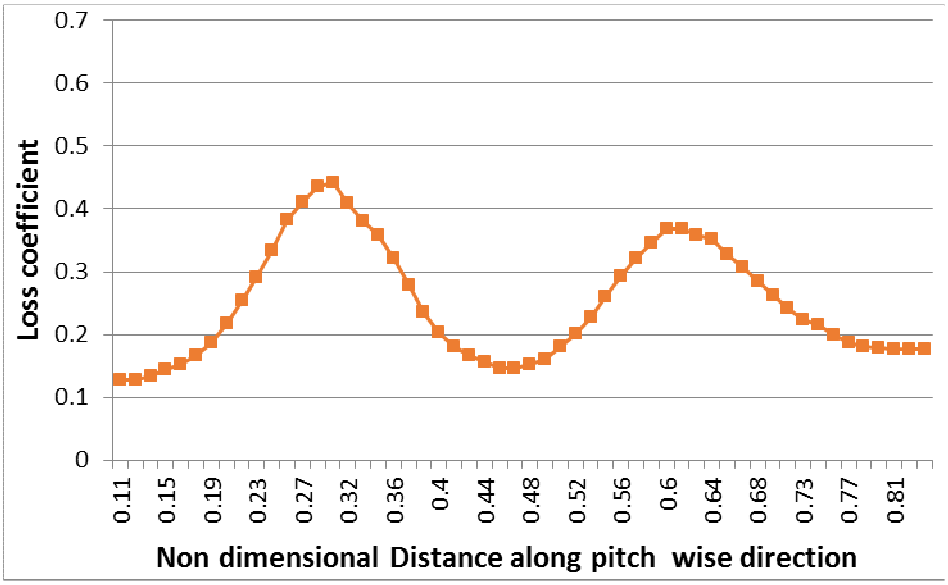

Figure 5.29: Variation of Local Loss Coefficients for BSR 250 cascade, relative to the nondimensional distance in pitch wise direction, for the span position of 0 mm (at the lowest position of the blades i.e. at bottom wall)

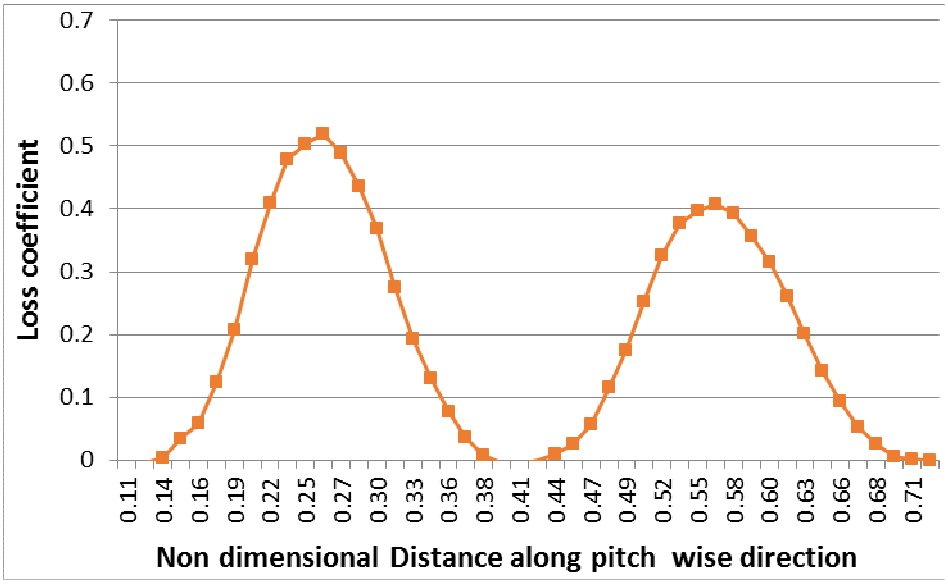

Figure 5.30: Variation of Local Loss Coefficients for BSR 250 cascade, relative to the nondimensional distance in pitch wise direction, for the mid span position (47.5 mm from bottom wall)

5.2.3.4 Variation of local loss coefficients along pitch wise direction for SSR 500:

The cascade of which, suction surfaces of all the blades are applied roughness of 500 µm is named as SSR 500 cascade. The graphs for two span positions i.e. 0.0 and 0.5, showing variation of local loss coefficients relative to nondimensional distance in the pitch wise direction for SSR 500 cascade are shown in figures 5.31and 5.32

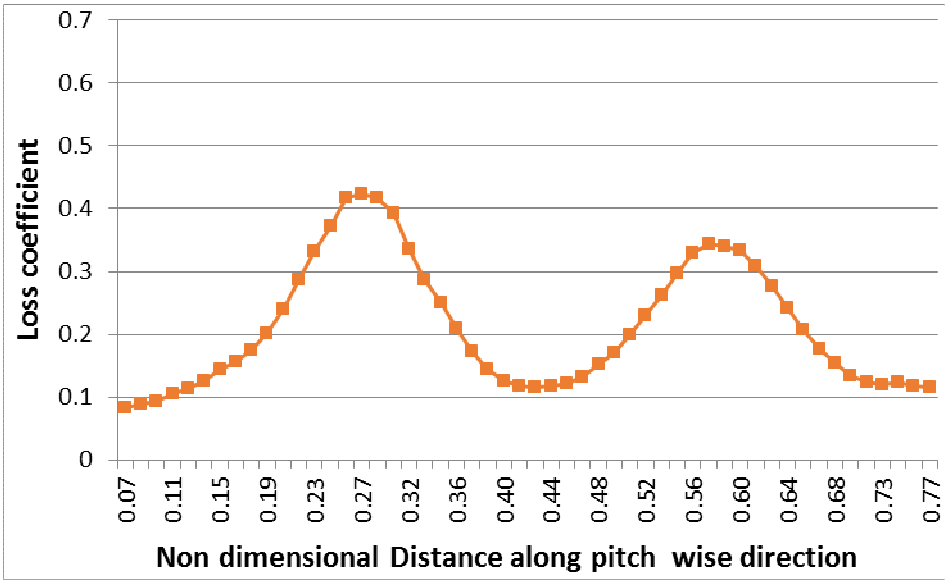

Figure 5.31: Variation of Local Loss Coefficients for SSR 500 cascade, relative to the nondimensional distance in pitch wise direction, for the span position of 0 mm (at the lowest position of the blades i.e. at bottom wall)

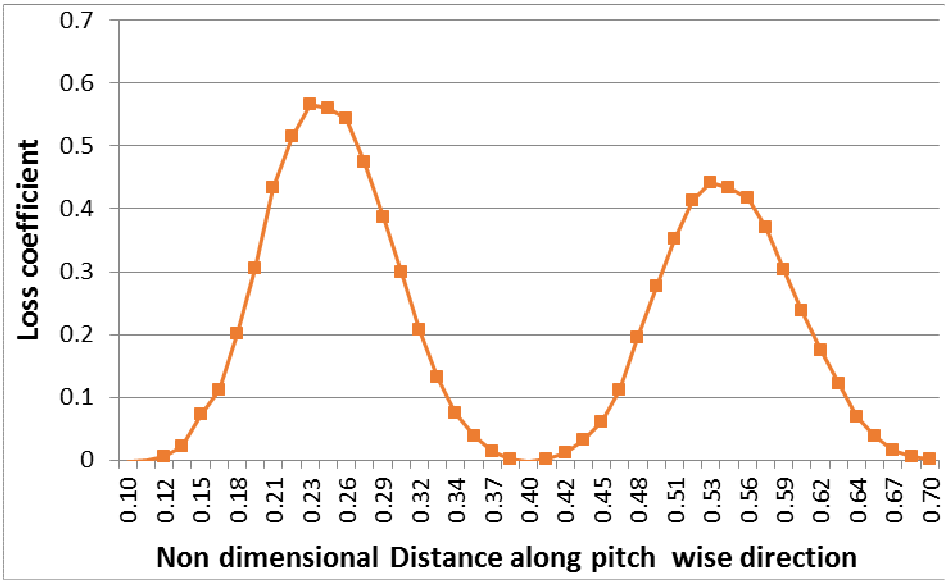

Figure 5.32: Variation of Local Loss Coefficients for SSR 500 cascade, relative to the nondimensional distance in pitch wise direction, for the mid span position (47.5 mm from bottom wall)

5.2.3.5 Variation of local loss coefficients along pitch wise direction for PSR 500:

The cascade of which pressure surfaces of all the blades are applied roughness of 500 µm is named as PSR 500 cascade. The graphs for two span positions i.e. 0.0 and 0.5, showing variation of local loss coefficients relative to nondimensional distance in the pitch wise direction for PSR 500 cascade are shown in figures 5.33and 5.34

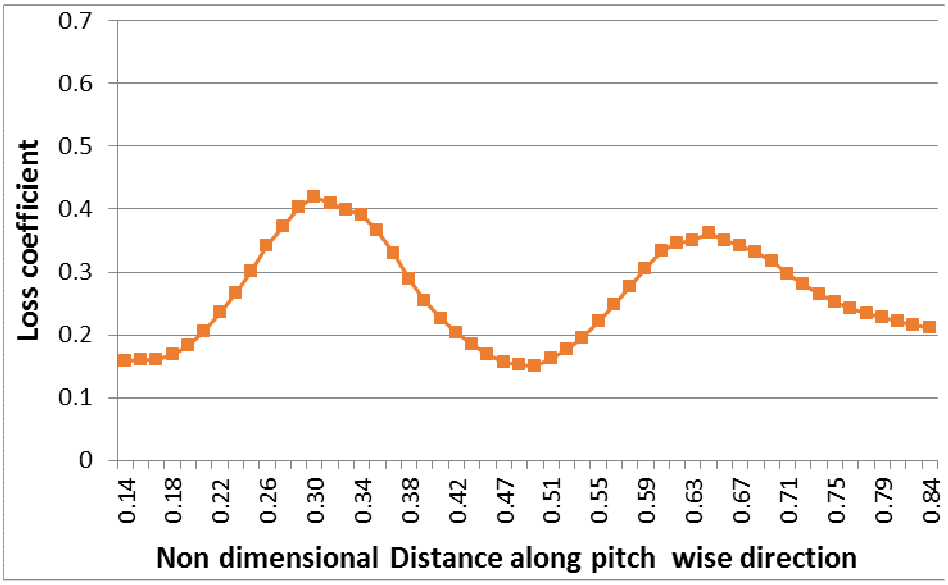

Figure 5.33: Variation of Local Loss Coefficients for PSR 500 cascade employing blade profile 6030 relative to the nondimensional distance in pitch wise direction, for the nondimensional span position of zero

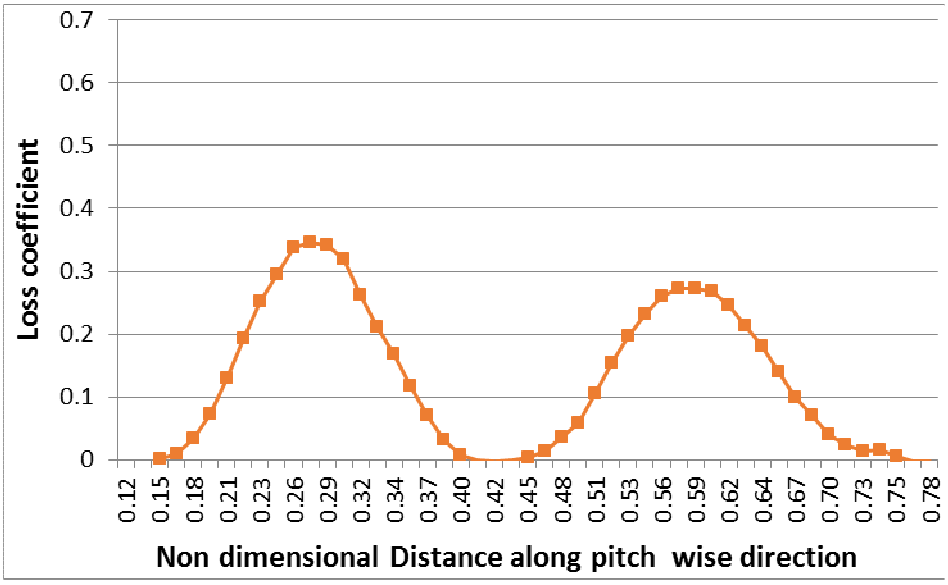

Figure 5.34: Variation of Local Loss Coefficients for PSR 500 cascade, employing blade profile 6030, relative to the nondimensional distance in pitch wise direction, for the midspan position (47.5 mm from bottom wall)

5.2.3.6 Variation of local loss coefficients along pitch wise direction for BSR 500:

In case of BSR 500 cascade, both surfaces of all the blades of the cascade are applied roughness of roughness of 500 µm. The graphs for two span positions i.e. 0.0 and 0.5, showing variation of local loss coefficients relative to nondimensional distance in the pitch wise direction for BSR 500 cascade are shown in figures 5.35 and 5.36.

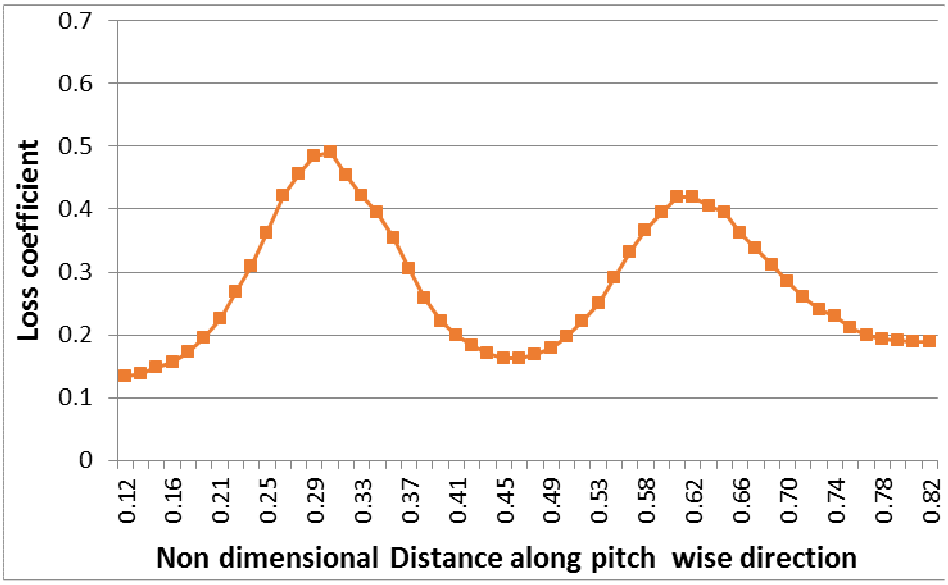

Figure 5.35: Variation of Local Loss Coefficients for BSR 500 cascade, relative to the nondimensional distance in pitch wise direction, for the span position of 0 mm (at the lowest position of the blades i.e. at bottom wall)

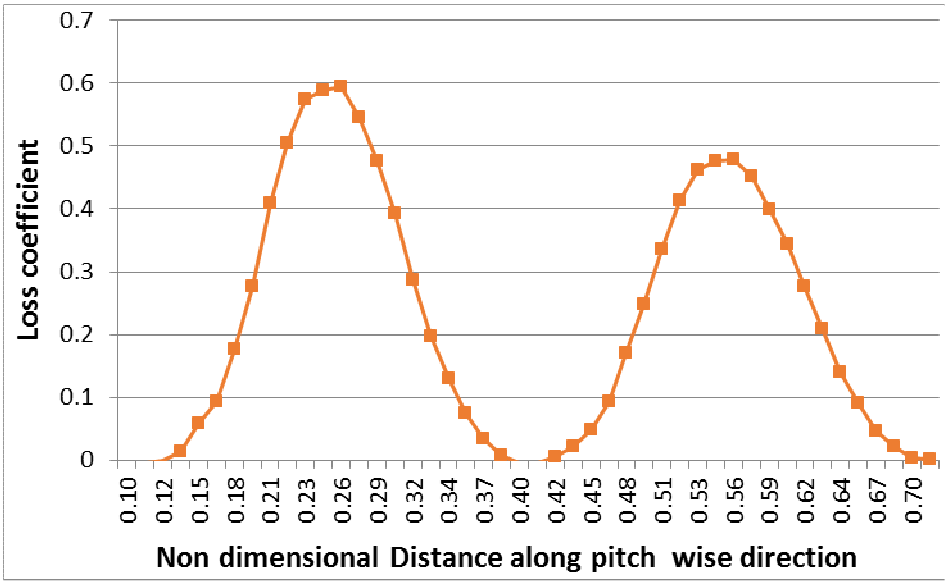

Figure 5.36: Variation of Local Loss Coefficients for BSR 500 cascade, relative to the nondimensional distance in pitch wise direction, for the mid span position (47.5 mm from bottom wall)

5.2.3.7 Variation of local loss coefficients along pitch wise direction for SSR 750:

In case of SSR 750 cascade, all the suction surfaces of all the blades of the cascade are applied roughness of roughness of 750 µm. The graphs for two span positions i.e. 0.0 and 0.5, showing variation of local loss coefficients relative to nondimensional distance in the pitch wise direction for SSR 750 cascade are shown in figures 5.37 and 5.38.

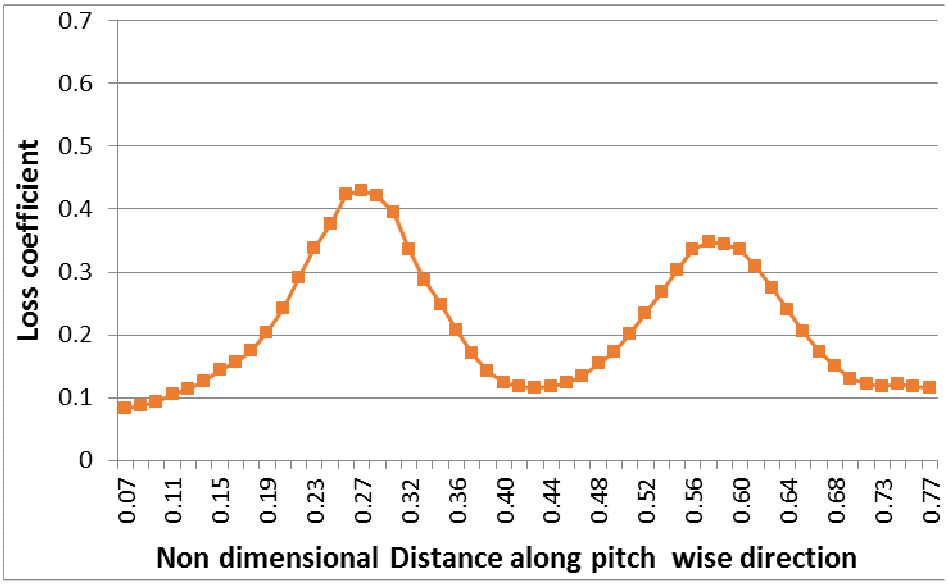

Figure 5.37: Variation of Local Loss Coefficients for SSR 750 cascade employing blade profile 6030 relative to the nondimensional distance in pitch wise direction, for the nondimensional span position of zero

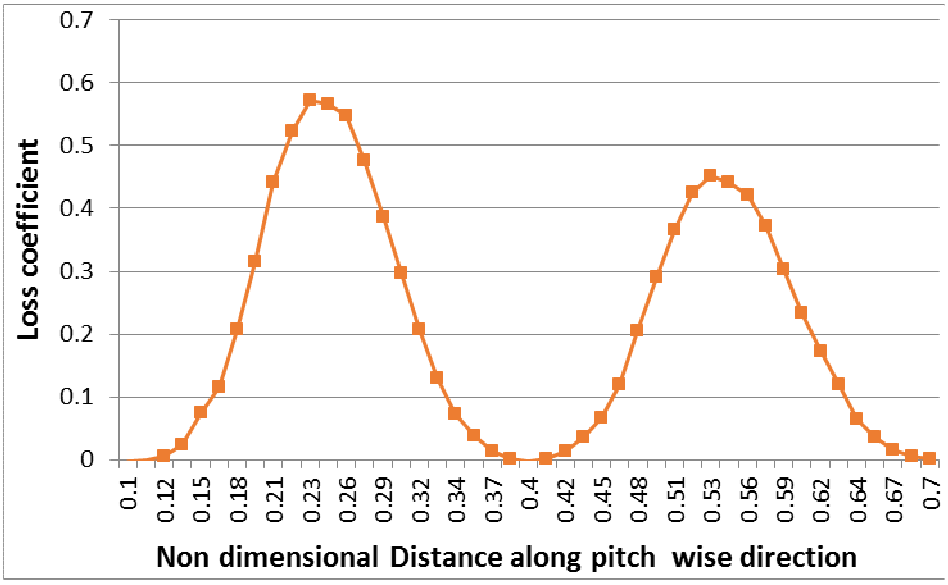

Figure 5.38: Variation of Local Loss Coefficients for SSR 750 cascade, employing blade profile 6030, relative to the nondimensional distance in pitch wise direction, for the midspan position (47.5 mm from bottom wall)

5.2.3.8 Variation of local loss coefficients along pitch wise direction for PSR 750:

In case of PSR 750 cascade, each of pressure surfaces of all the blades of the cascade are applied roughness of roughness of 750 µm. The graphs for two span positions i.e. 0.0 and 0.5, showing variation of local loss coefficients relative to nondimensional distance in the pitch wise direction for PSR 750 cascade are shown in figures 5.39 and 5.40.

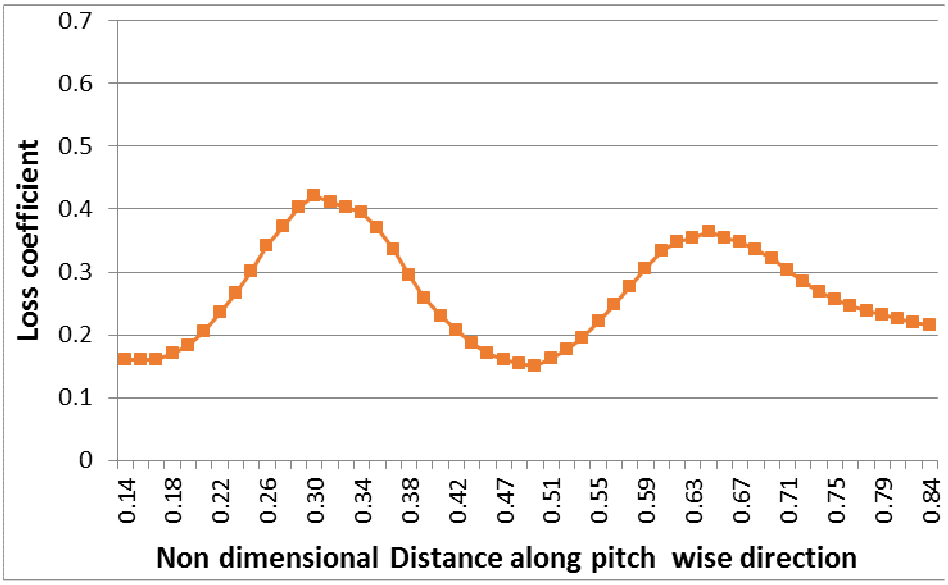

Figure 5.39: Variation of Local Loss Coefficients for PSR 750 cascade employing blade profile 6030 relative to the nondimensional distance in pitch wise direction, for the nondimensional span position of zero

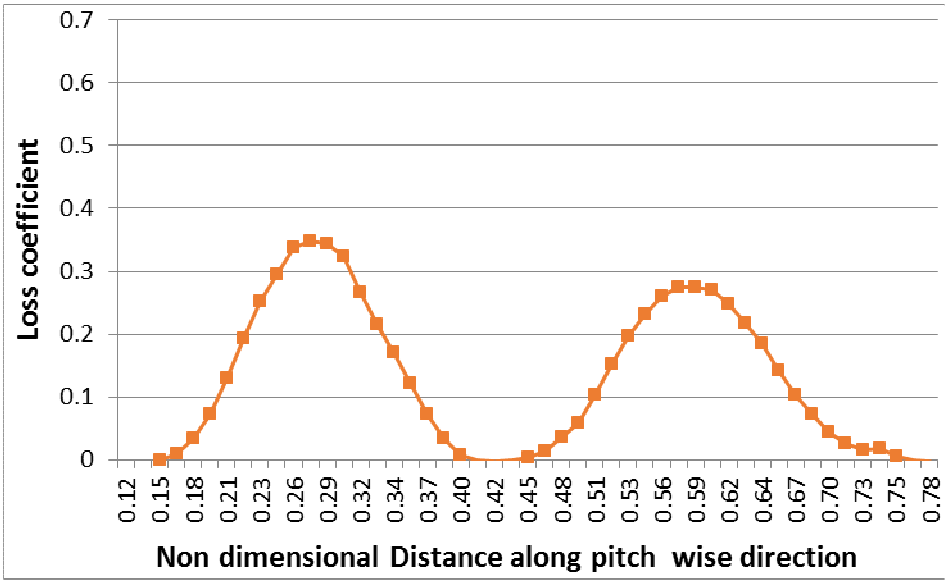

Figure 5.40: Variation of Local Loss Coefficients for PSR 750 cascade, employing blade profile 6030, relative to the nondimensional distance in pitch wise direction, for the midspan position (47.5 mm from bottom wall)

5.2.3.9 Variation of local loss coefficients along pitch wise direction for BSR 750:

The cascade of which both surfaces of all the blades are applied roughness of 250 µm is named as **BSR 750** cascade. The graphs for two span positions i.e. 0.0 and 0.5, showing variation of local loss coefficients relative to nondimensional distance in the pitch wise direction for BSR 750 cascade are shown in figures 5.41 and 5.42.

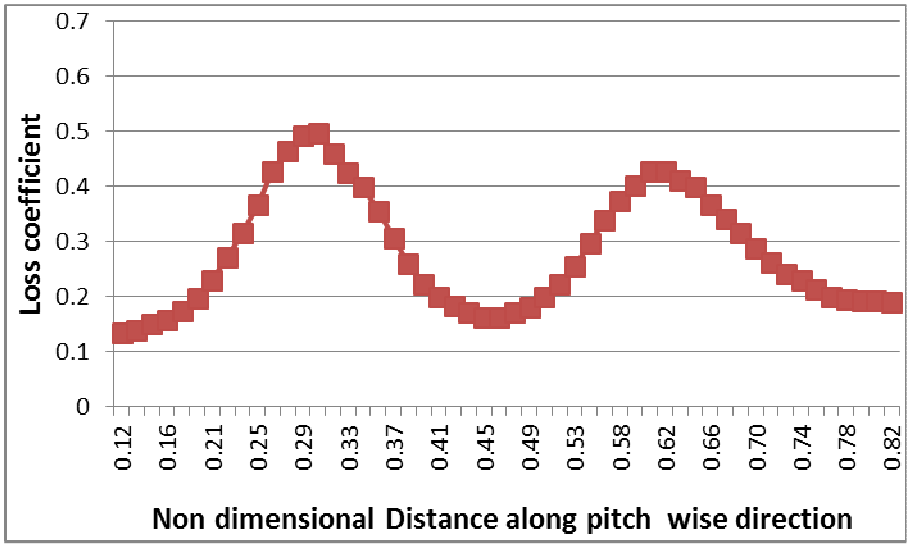

Figure 5.41: Variation of Local Loss Coefficients for BSR 750 cascade, relative to the nondimensional distance in pitch wise direction, for the span position of 0 mm (at the lowest position of the blades i.e. at bottom wall)

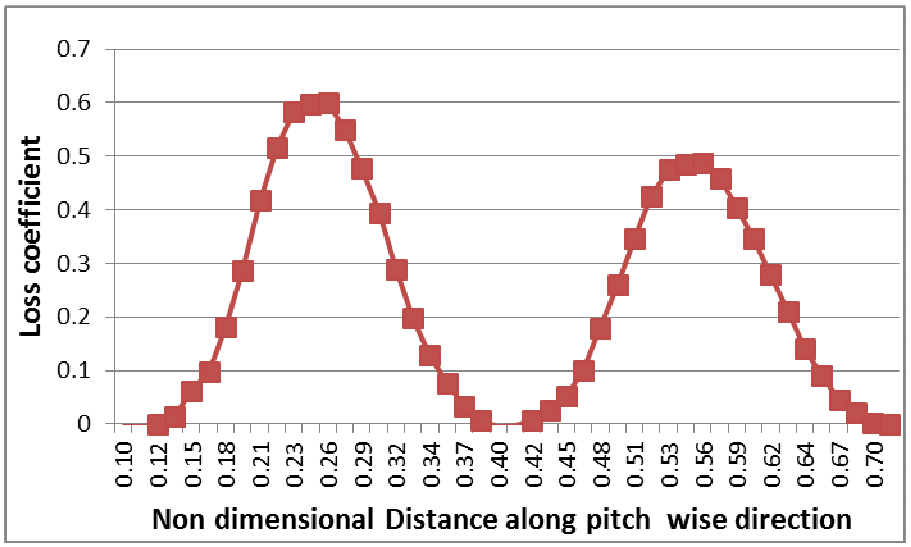

Figure 5.42: Variation of Local Loss Coefficients for BSR 750 cascade, relative to the nondimensional distance in pitch wise direction, for the midspan position (47.5 mm from bottom wall)

5.2.3.10 Variation of local loss coefficients along pitch wise direction for SSR 1000:

In this type of cascade roughness of 1000 µm is applied on suction surfaces of all the blades of the cascade. The graphs for two span positions i.e. 0.0 and 0.5, showing variation of local loss coefficients relative to nondimensional distance in the pitch wise direction for SSR 1000 cascade are shown in figures 5.43 and 5.44.

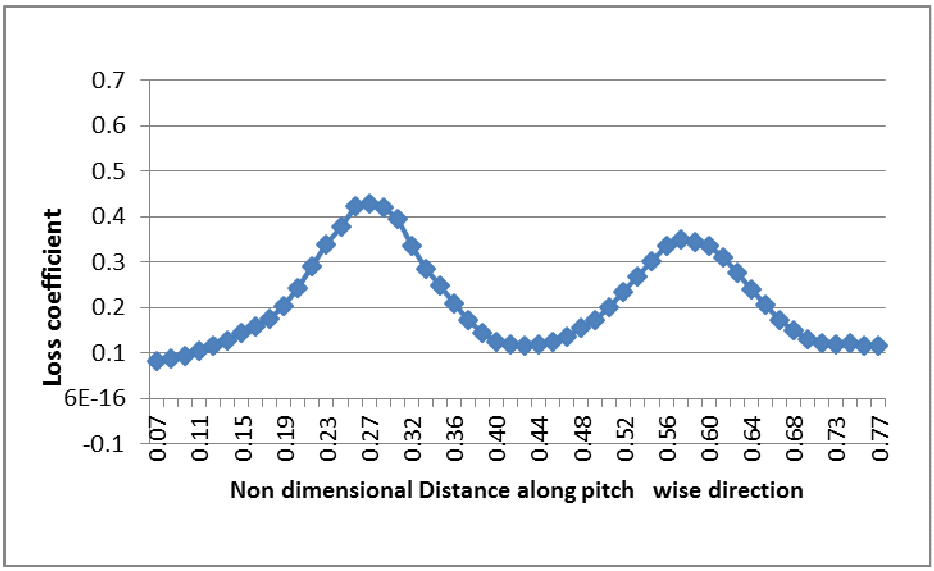

Figure 5.43: Variation of Local Loss Coefficients for SSR 1000 cascade, relative to the nondimensional distance in pitch wise direction, for the span position of 0 mm (at the lowest position of the blades i.e. at bottom wall)

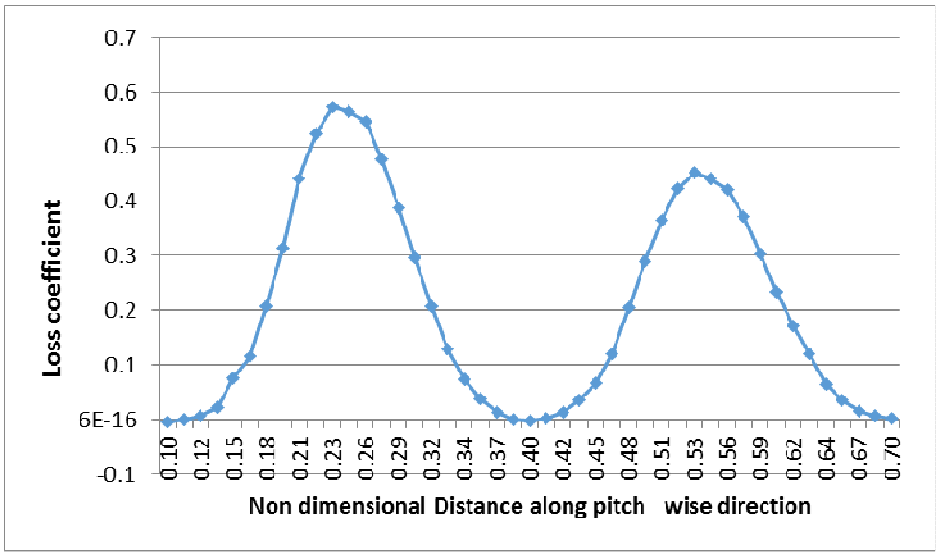

Figure 5.44: Variation of Local Loss Coefficients for SSR 1000 cascade, relative to the nondimensional distance in pitch wise direction, for the midspan position (47.5 mm from bottom wall)

5.2.3.11 Variation of local loss coefficients along pitch wise direction for PSR 1000:

In this type of cascade, pressure surfaces of all the blades of the cascade are applied roughness of 1000 µm. The graphs for two span positions i.e. 0.0 and 0.5, showing variation of local loss coefficients relative to nondimensional distance in the pitch wise direction for PSR 1000 cascade are shown in figures 5.45 and 5.46.

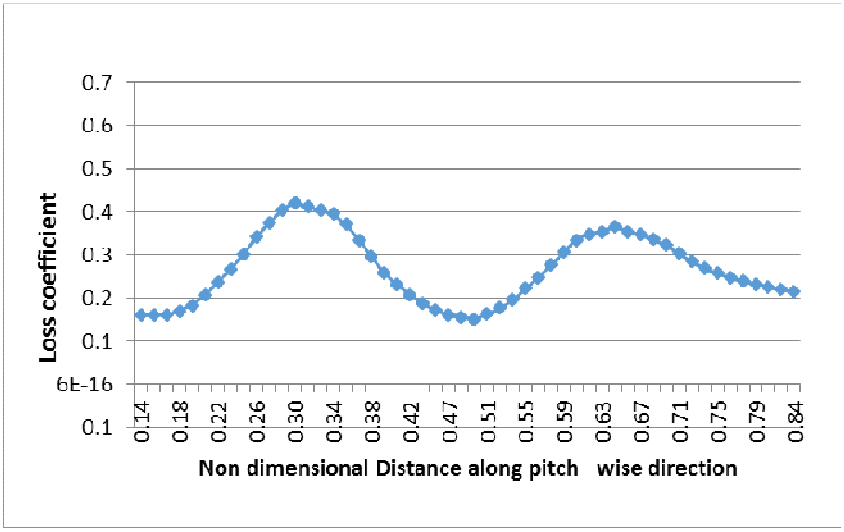

Figure 5.45: Variation of Local Loss Coefficients for PSR 1000 cascade employing blade profile 6030 relative to the nondimensional distance in pitch wise direction, for the nondimensional span position of zero

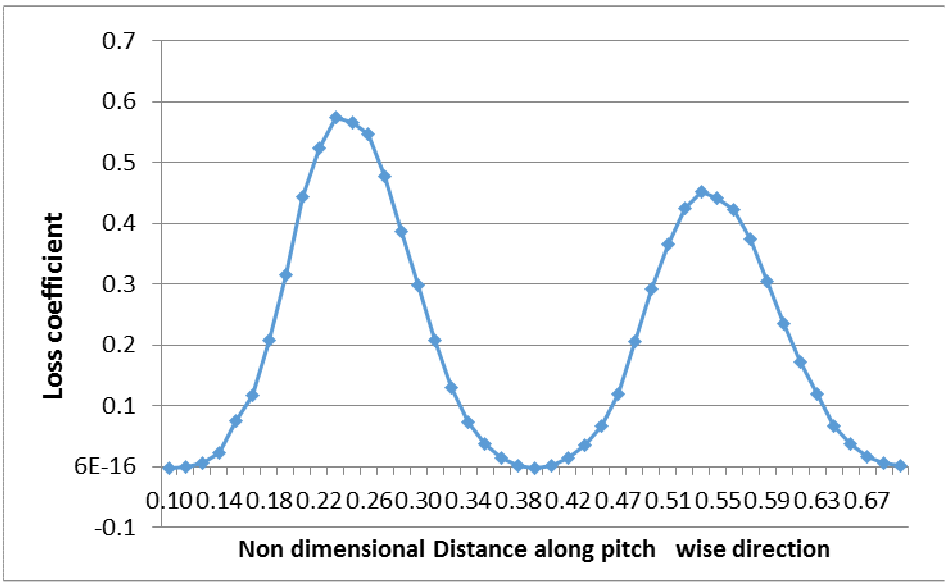

Figure 5.46: Variation of Local Loss Coefficients for PSR 1000 cascade, employing blade profile 6030, relative to the nondimensional distance in pitch wise direction, for the midspan position (47.5 mm from bottom wall)

5.2.3.12 Variation of local loss coefficients along pitch wise direction for BSR 1000:

The cascade of which both surfaces of all the blades are applied roughness of 1000 µm is termed as BSR 1000 cascade. The graphs for two span positions i.e. 0.0 and 0.5, showing variation of local loss coefficients relative to nondimensional distance in the pitch wise direction for BSR 1000 cascade are shown in figures 5.47 and 5.48.

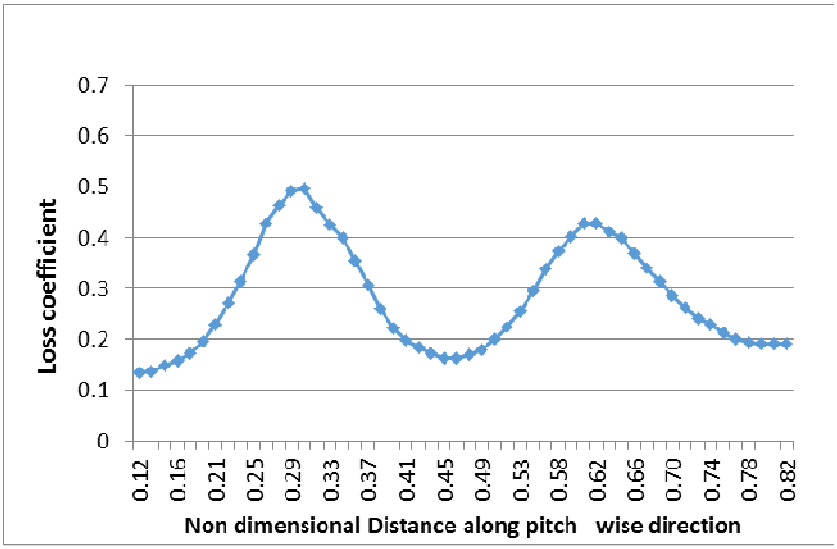

Figure 5.47: Variation of Local Loss Coefficients for BSR 1000 cascade, relative to the nondimensional distance in pitch wise direction, for the span position of 0 mm (at the lowest position of the blades i.e. at bottom wall)

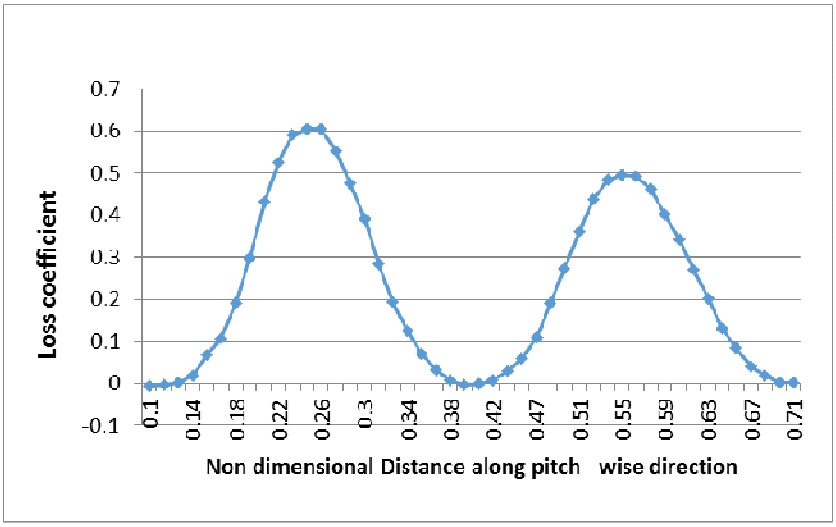

Figure 5.48: Variation of Local Loss Coefficients for BSR 1000 cascade, relative to the nondimensional distance in pitch wise direction, for the midspan position (47.5 mm from bottom wall)

5.2.4 Effect of roughness on distance between two consecutive lowest energy points

The distance between two consecutive lowest energy points for a given cascade is affected by roughness on the blades. During the process of simulation of flow through turbomachines cascades, Local Loss Coefficients relative to the nondimensional distance in pitch wise direction, for various blade span positions are measured for various cascades. The nondimensional distances in pitch wise direction for significant positions are also noted during the measurement of Local Loss Coefficients. The lowest energy points for the flowing fluid through the given cascade, are the points of highest loss coefficients for a flow channel which pressure surface and suction surface of two adjacent blades form for a set of two blades. The lowest energy points fall into the wakes formed downstream of the two adjacent blades. This distance has been measured for a cascades employing blade profile 6030. The figure 5.49 shows lowest energy point 1 & point 2 for a cascade.

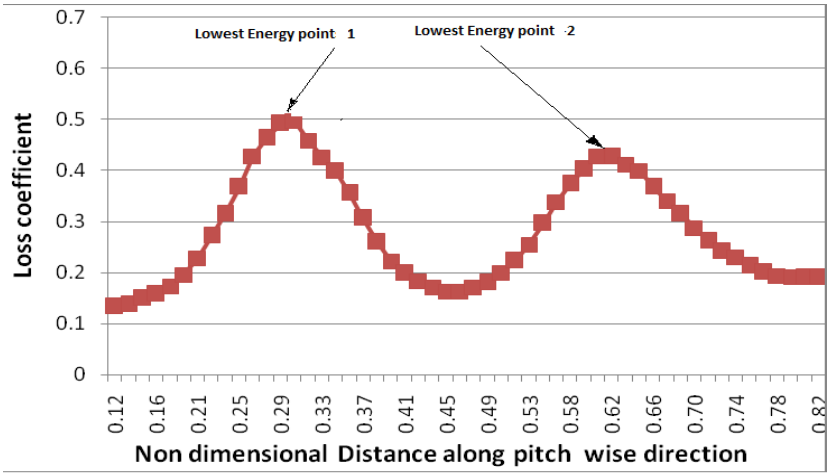

Figure 5.49: Two consecutive energy points on the graph showing variation of Local Loss Coefficients relative to the nondimensional distance in pitch wise direction

The roughness affects the positions of the lowest energy point 1 & point 2 for a cascade and the distance between them. It is evident from measured values of these points as shown in table 5.2.

Table 5.2: Non dimensional distances of positions of the lowest energy point 1 & point 2 for various cascade and the distance between the same

Type of cascade (roughness magnitude)	span position	Non-dimensional distance in pitch wise direction		
		lowest energy point 1	lowest energy point 2	Distance between lowest energy point 1 & point 2
Smooth Blade				
Smooth	0	0.29	0.6	0.31
	47.5	0.27	0.56	0.29
Pressure surface rough				
250	0	0.3	0.63	0.33
	47.5	0.27	0.58	0.31
500	0	0.32	0.66	0.34
	47.5	0.27	0.59	0.32
750	0	0.3	0.66	0.36
	47.5	0.29	0.6	0.31
1000	0	0.3	0.64	0.34
	47.5	0.3	0.64	0.34
Suction surface rough				
250	0	0.25	0.55	0.3
	47.5	0.25	0.55	0.3
500	0	0.27	0.58	0.31
	47.5	0.23	0.53	0.3
750	0	0.27	0.58	0.31
	47.5	0.23	0.53	0.3
1000	0	0.27	0.58	0.31
	47.5	0.23	0.53	0.3
both surface rough				
250	0	0.3	0.62	0.32
	47.5	0.3	0.62	0.32
500	0	0.3	0.62	0.32
	47.5	0.26	0.56	0.3
750	0	0.3	0.6	0.3
	47.5	0.25	0.55	0.3
1000	0	0.3	0.6	0.3
	47.5	0.25	0.55	0.3

The measured values represent the nondimensional distance on the pitch wise direction for a given cascade. It is observed that as the roughness increases, the distance between lowest energy point 1 & point 2 increases as compared to that of the smooth blade cascade. The wake is wider for a cascade on blades of which roughness of various magnitudes are applied as compared to smooth blade values. The wake widens with increasing roughness. The nondimensional distance of lowest energy point inside the wake shifts towards the suction surface as the roughness increases as compared with the reference location of the same point with sooth blades. These variations related to the smooth blade can be attributed to increase in boundary layer thickness over both the suction and pressure surfaces, increase in trailing edge thickness caused by application of roughness and shifting of rear stagnation point towards the suction surface. It can be expected that the boundary layer on the rough suction surface would be thicker than that on the smooth pressure surface. Hence, flow over the pressure surface will shift the rear stagnation point towards the suction surface and the wake too shifts towards the suction surface. The boundary layer phenomena also affects the magnitude of the pressure coefficients over both the surfaces of two adjacent blades of a flow channel. The magnitude of the pressure coefficients decreases due to the accelerated flow in the confined passage due to a growing boundary layer. The greater decrease in pressure coefficient over the suction surface indicates a thicker boundary layer compared to the pressure surface.

5.2.5 Effect of increasing roughness or changing location for application of roughness for cascades employing blade Profile 6030

In the preceding section, local loss coefficients for each of cascade for various positions, in the pitch wise direction, are presented graphically for blade profile 6030. The table 4.1 of previous chapter shows method of calculation of local loss

coefficients for all pitchwise positions (74 or more number, in all). The calculated values of local loss coefficients are shown in column marked “T” in table 4.1 for a typical turbine cascade.

The parameter namely mass averaged loss coefficients is calculated taking the aforesaid local loss coefficients and velocities at various pitchwise positions into account. The 2 Nos. cells formed at intersection of last row and last 2 Nos. columns marked X and Y of table 4.1, show the summation of all the respective values of column marked X and Y. The integrated value in column marked Y (1825.316) is divided with integrated value in column marked X (9603.334) to get mass averaged loss coefficient (0.190), as mentioned in previous chapter. Thus, for measurement of magnitude of losses, “mass averaged loss coefficients” would be sufficiently representative and reliable.

5.2.6 Summary of results with regard to magnitude of pitch wise local loss coefficients for various nondimensional span position

It can be concluded that magnitude of local loss coefficients for mid span position of each of cascade are lower than those for the nondimensional span position of 0 mm (at the lowest position of the blades i.e. at bottom endwall). The lowest values of loss coefficients for mid span position of each of cascade at outlet of various blades are approximately zero. Similarly, the lowest magnitudes of loss coefficients at outlet of various blades for nondimensional span position of zero for each of cascade, unlike to the case of midspan position, are more than zero. Therefore, it can be said with regard to lowest magnitudes of local loss coefficients at outlet of various blades for nondimensional span position of zero that there is an effect of end wall and in no case magnitudes of local loss coefficients are zero. The magnitudes of local loss

coefficients lowest magnitudes of local loss coefficients at outlet of various blades for mid span position are nearly zero because end wall effect are absent at that position.

5.2.7 Mass averaged loss coefficient for cascades employing blade profile 6030

The mass averaged loss coefficient at a given location is a measure of total losses. Therefore the term total loss coefficient is also used in place of mass averaged loss coefficient. The terms i.e. Mass averaged loss coefficient and total loss coefficient are is synonymous to each other and will be used interchangeably in this dissertation. The value of this coefficient is a fraction which shows as to how much amount the energy of the incoming air has been lost during the course of flow through the cascades.

One set of local loss coefficients for various selected pitch wise positions yields result with regard to mass averaged loss coefficient for a single span position of a given cascade. The pattern of variation of local loss coefficient, relative to pitch wise distance are similar in shape (table 4.1). Moreover, the pattern of variation of mass averaged loss coefficient for a cascade is similar to other remaining cascades. Therefore, the numerical values of mass averaged loss coefficient for all the span positions is not presented in this dissertation to avoid repetitiveness.

The table 5.3 shows results with regard to mass averaged loss coefficients for all BSR cascades employing blade profile 6030 for all roughness values of 250, 500, 750 &1000 µm.

Table 5.3 : Results with regard to mass averaged loss coefficients (or total loss coefficients) for all BSR cascades employing blade profile 6030 for all roughness values of 250, 500, 750 &1000 µm

S/no.	Type of cascade and roughness magnitude					distance from bottom end wall in mm	Nondimensional distance in the span wise direction
	SMOOTH	BSR250	BSR500	BSR750	BSR1000		
	Mass averaged loss coefficient/ Total loss coefficient						
1	0.190	0.244	0.270	0.273	0.273	0	0.00
2	0.101	0.151	0.180	0.183	0.183	2	0.02
3	0.122	0.189	0.207	0.210	0.210	4	0.04
4	0.129	0.195	0.218	0.221	0.221	6	0.06
5	0.115	0.178	0.207	0.210	0.210	8	0.08
6	0.107	0.176	0.201	0.204	0.204	10	0.11
7	0.101	0.172	0.191	0.194	0.194	15	0.16
8	0.100	0.166	0.190	0.193	0.193	20	0.21
9	0.100	0.166	0.190	0.193	0.193	25	0.26
10	0.100	0.166	0.189	0.193	0.193	30	0.32
11	0.100	0.166	0.189	0.193	0.193	35	0.37
12	0.100	0.166	0.190	0.193	0.193	40	0.42
13	0.100	0.166	0.190	0.193	0.193	45	0.47
14	0.100	0.166	0.190	0.193	0.193	47.5	0.50
15	0.100	0.166	0.190	0.193	0.193	50	0.53
16	0.100	0.166	0.190	0.193	0.193	55	0.58
17	0.100	0.166	0.189	0.193	0.193	60	0.63
18	0.100	0.166	0.189	0.193	0.193	65	0.68
19	0.100	0.166	0.190	0.193	0.193	70	0.74
20	0.100	0.166	0.190	0.193	0.193	75	0.79
21	0.101	0.172	0.191	0.194	0.194	80	0.84
22	0.107	0.176	0.201	0.204	0.204	90	0.95
23	0.115	0.178	0.207	0.210	0.210	87	0.92
24	0.129	0.195	0.218	0.221	0.221	89	0.94
25	0.122	0.189	0.207	0.210	0.210	91	0.96
26	0.101	0.151	0.180	0.183	0.183	93	0.98
27	0.190	0.244	0.270	0.273	0.273	95	1.00

It is clear from the table 5.3 that results are obtained using values of mass averaged loss coefficient for all 27 numbers of the span positions along the blade span for a given cascade of turbine. The mass averaged loss coefficients are calculated for all span positions using Microsoft Excel office software. The variation of mass averaged loss coefficients, relative to span wise distance are similar (table 5.3). Therefore only a few of results showing pattern of variation of mass averaged loss coefficients are presented to avoid repetitiveness.

The variation of mass averaged loss coefficient for each of smooth cascade, BSR250, BSR500, BSR750 and BSR1000 turbine cascades employing blade profile 6030 relative to the nondimensional distance in the direction of blade span are separately shown in figures 5.50, 5.51, 5.52 and 5.53 respectively. Each graph represent variation of 27 Nos. mass averaged loss coefficient over 27 span positions for a single cascade.

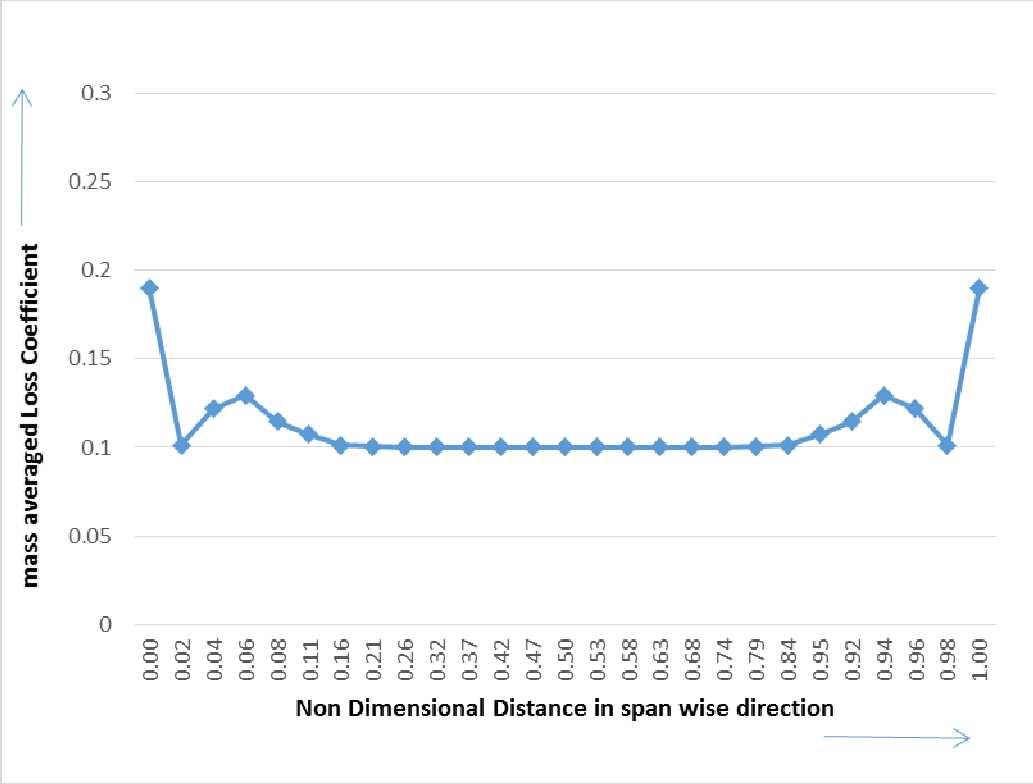

Figure 5.50: Variation of mass averaged loss coefficients, for smooth turbine cascade employing blade profile 6030, relative to the nondimensional distance in the direction of blade span

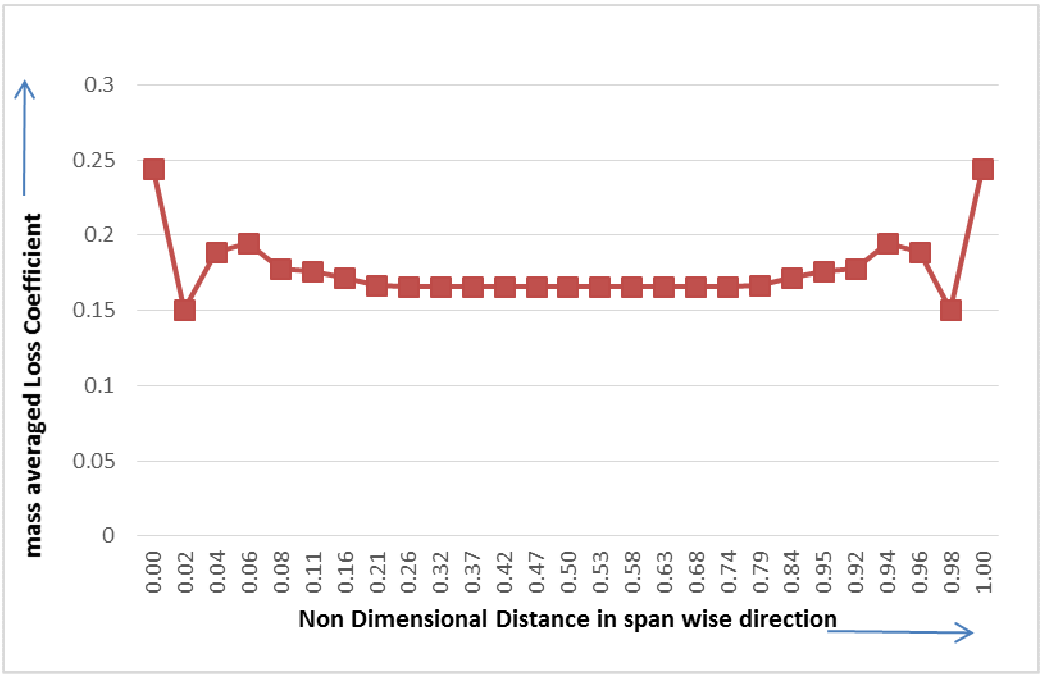

Figure 5.51: Variation of mass averaged loss coefficients, for BSR 250 turbine cascade employing blade profile 6030, relative to the nondimensional distance in the direction of blade span

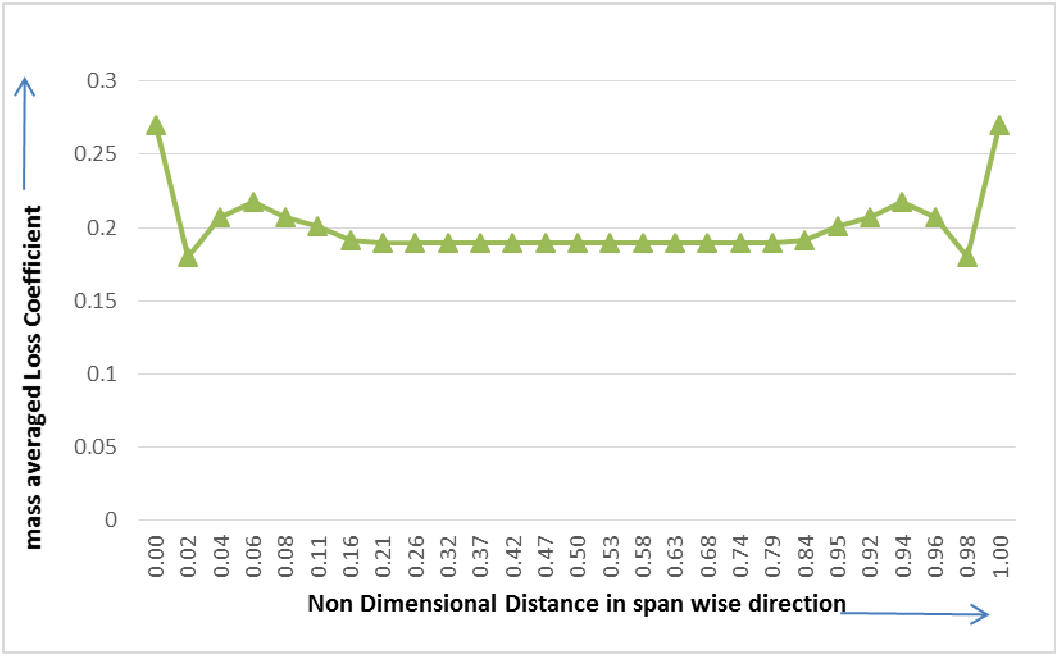

Figure 5.52: Variation of mass averaged loss coefficients, for BSR 500 turbine cascade employing blade profile 6030, relative to the nondimensional distance in the direction of blade span

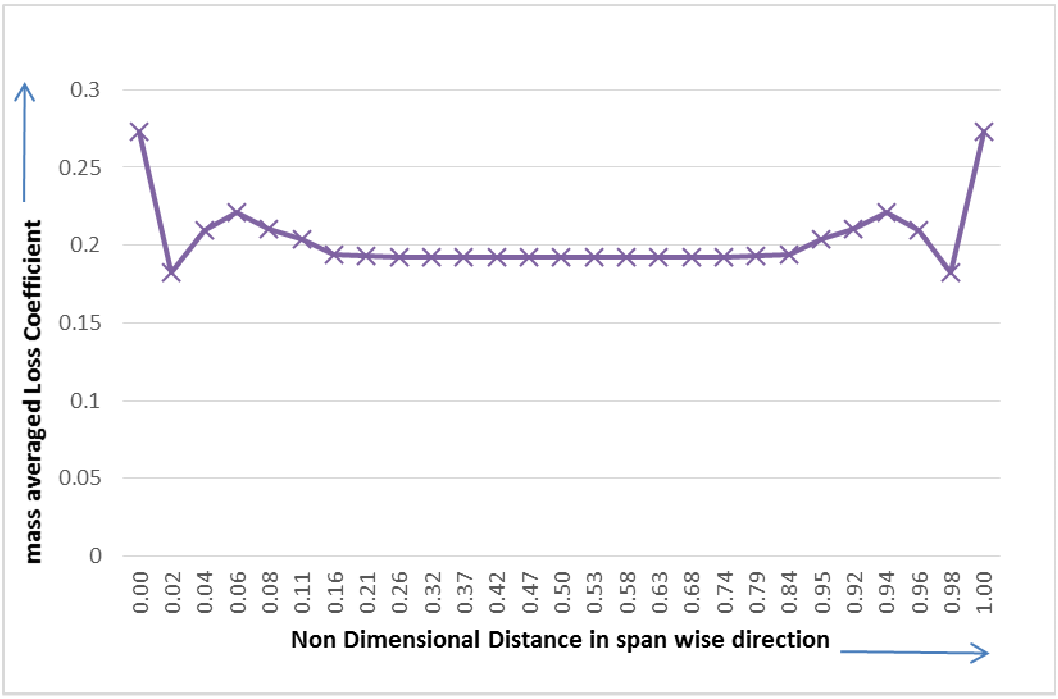

Figure 5.53: Variation of mass averaged loss coefficients, for BSR 750 turbine cascade employing blade profile 6030, relative to the nondimensional distance in the direction of blade span

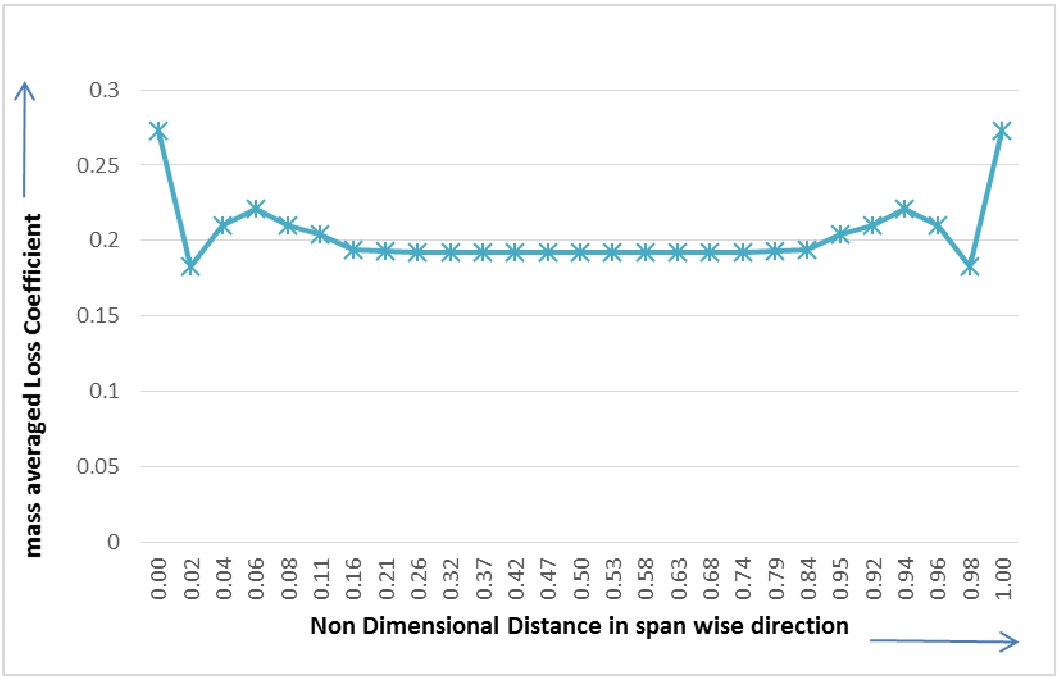

Figure 5.54: Variation of mass averaged loss coefficients, for BSR 1000 turbine cascade employing blade profile 6030, relative to the nondimensional distance in the direction of blade span.

The variation of mass averaged loss coefficients for all BSR cascades, including the smooth cascade, employing blade profile 6030 are separately shown in figures 5.50, 5.51, 5.52, 5.53 and 5.54. Each of the graph showing this variation, in isolation, may not be as useful for quantitative comparison of total loss and profile loss as the combined graph might be. Therefore, in order to make quantitative comparison regarding total loss and profile loss generated due to increasing roughness between all cascades for all 4 roughness values are superimposed in figure 5.55, 5.56 and 5.57. The combined graphs show variation of mass averaged loss coefficients for all cascades applying each of roughness on same surface employing blade profile 6030. Subsequently, combined graphs showing variation of mass averaged loss coefficients changing the location for application of same magnitude of roughness will be presented in order to present effect of changing location (surfaces) for application of roughness for blade profile 6030.

5.2.8 Effect of increasing the roughness on same surface (s) for blade profile 6030

In order to make quantitative comparison of effect of increasing the roughness, in terms of total loss and profile loss generated, due to increasing roughness, the combined graph is presented between various types of cascades. First of all, in order to depict effect of increasing roughness on both surfaces of all blades of the cascade, at a time, a superimposed graph for 4 numbers of BSR cascades employing blade profile 6030, including the smooth cascade, is presented in figure 5.55.

.

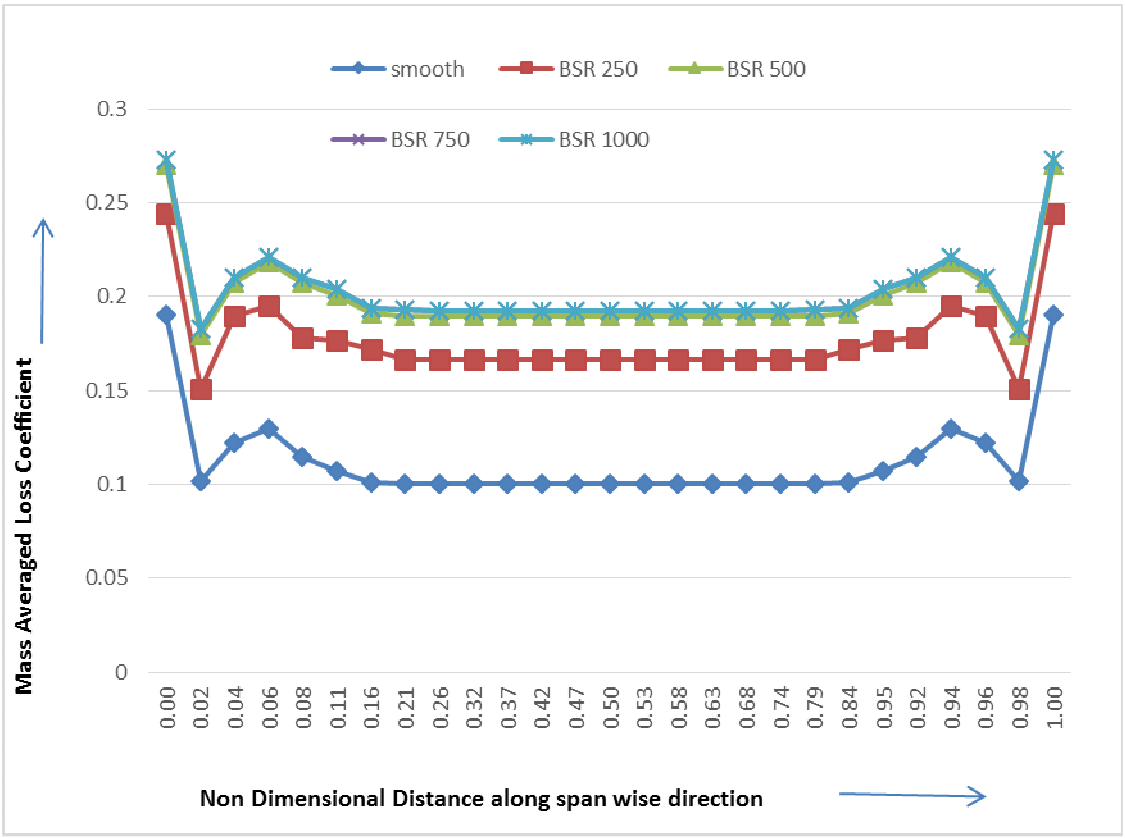

Figure 5.55: Superimposed results for mass averaged loss coefficient with regard to cascades BSR 250, BSR 500, BSR 750 and BSR 1000, including the smooth cascade (the loss coefficient axis has been formatted to exaggerate the variation)

The variation of mass averaged loss coefficient for a given turbine cascades employing blade profile 6030, individually for PSR turbine cascades i.e. PSR250, PSR500, PSR750 and PSR1000, and SSR turbine cascades i.e. SSR250, SSR500, SSR750 and SSR1000 are also plotted relative to the nondimensional distance in the direction of blade span (figures 5.56 and 5.57). However, in order to avoid repetitiveness combined graphs in figures 5.56 and 5.57, for PSR and SSR turbine cascades only, are included in this section, respectively.

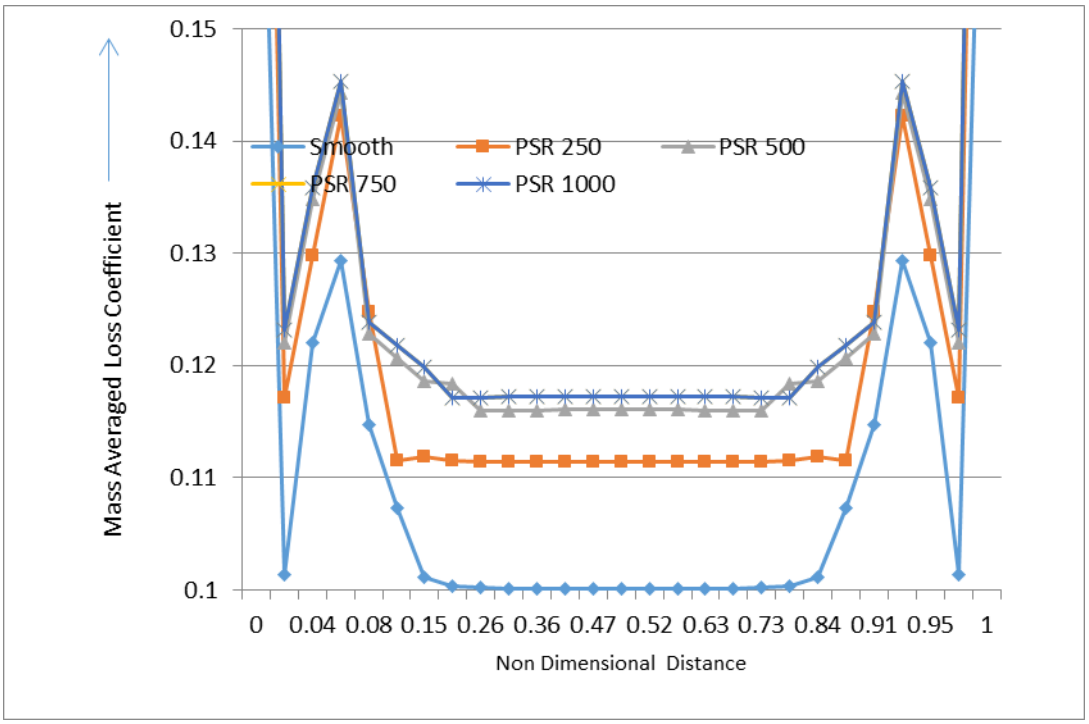

Figure 5.56: Superimposed results for mass averaged loss coefficient with regard to PSR 250, PSR 500, PSR 750 and PSR 1000 turbine cascades, including the smooth cascade (the loss coefficient axis has been formatted to exaggerate the variation)

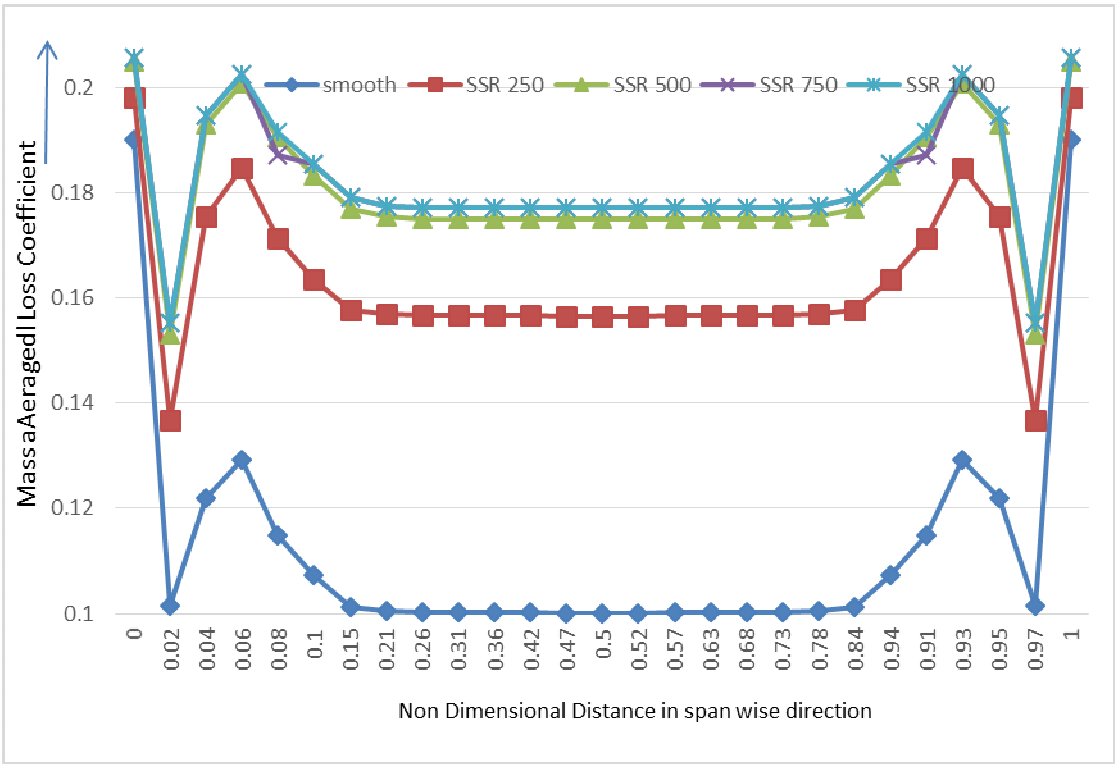

Figure 5.57: Superimposed results for mass averaged loss coefficient with regard to SSR 250, SSR 500, SSR 750 and SSR 1000 turbine cascades, including the smooth cascade (the loss coefficient axis has been formatted to exaggerate the variation)

The combined plots in the figure 5.56 and 5.57 clarify as to how total energy loss coefficients for PSR250, PSR500, PSR750 and PSR1000 and SSR 250, SSR 500, SSR 750 and SSR 1000 cascades are higher than that of smooth cascade. The values of mass averaged loss coefficient for roughnesses i.e. 750 and 1000 µm are almost same. Therefore the loss coefficient axis has been formatted to exaggerate the variation as the graphs for roughnesses i.e. 750 and 1000 µm overlap as shown in figure 5.56 and 5.57. Had the plots not been shown exaggerating along the vertical axis the combined plot wouldn't be able to separately show trend for variation with regard to roughnesses i.e. 750 and 1000 µm.

In general, the trends of variation of local loss coefficients and mass averaged loss coefficient for all cascades of roughness values 250, 500, 750 &1000 µm are found to be similar in shape (pattern) to that of smooth blades for profile 6030 except changes in magnitude of loss. The figures 5.55 and 5.56 show that the total and profile losses for BSR and PSR cascade, increase with increasing roughness respectively. Also, the magnitudes of total loss for all BSR and PSR cascades for all roughness values are higher than that of the smooth cascade. Comparison of loss coefficients in all such cascades reveals that the loss coefficient is high at hub and casing due to the endwall boundary layers. The local increase in loss coefficient is observed due to the secondary flow cores near the hub and casing. The presence of humps at hub and casing occur because of the formation of vortex cores that leads to high-value, mass averaged loss coefficient. It is clear that the mass averaged loss coefficients near the end walls at both ends are higher than their values at mid span of the blade.

The results for SSR 250, SSR 500, SSR 750 & SSR 1000 reveal that the loss coefficient is high at hub and casing due to the endwall boundary layers. The increase in loss coefficient is observed due to the secondary flow cores near the hub and

casing. The presence of humps at hub and casing occur because of the formation of vortex cores that leads to increase in local energy loss coefficient. The losses increase in the same order when roughness was increased from 250 to 500, 500 to 750 & 750 to 1000 µm for all type of cascades. The trend of increase in losses is insignificant with the increase in magnitude of roughness (beyond 500µm) for all types of i.e. SSR PSR & BSR cascades of roughness values 250, 500, 750 &1000 µm.

5.2.9 Effect of changing location (surfaces) for application of roughness for blade profile 6030

The roughness of 250 µm, is applied on surface(s) chosen for application of same on similar blades surfaces of cascade employing blade profile 6030 in following ways.

(i) on pressure surfaces only

(ii) on suction surfaces only

(iii) on pressure surfaces and suction surfaces together

The figure 5.58 depicts a combined graph showing variation of mass averaged loss coefficients for various cascades choosing the roughness of 250 µm to be applied separately over similar type of surfaces of the cascades employing blade profile 6030, one by one.

The figure 5.58 thus shows combined graph showing variation of mass averaged loss coefficients for cascades such as PSR 250, SSR 250 & BSR 250 cascades and also the smooth cascade (in view to make quantitative comparison with PSR 250, SSR 250 & BSR 250 cascades).

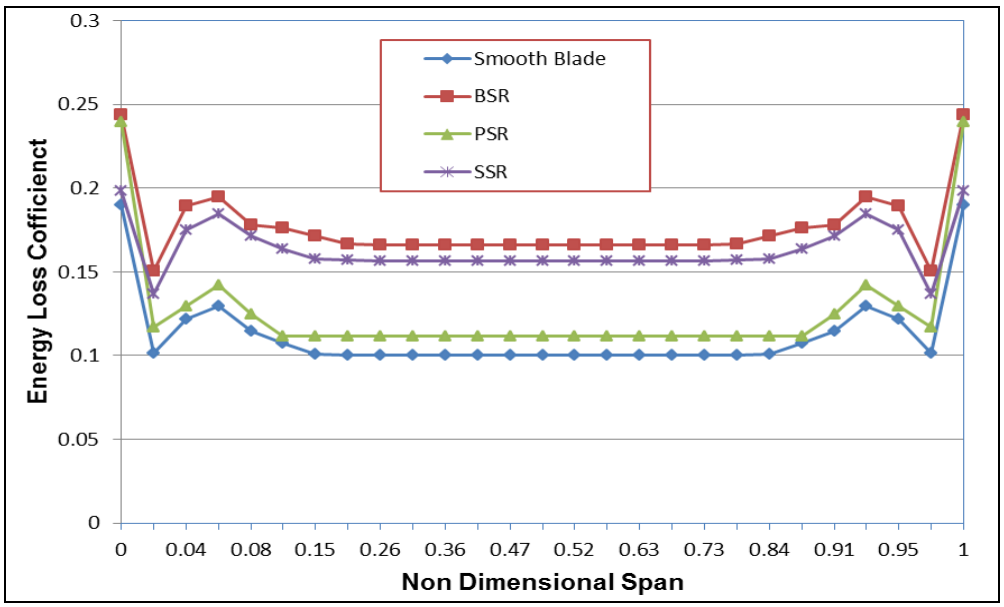

Figure 5.58: Variation of total energy loss coefficients with respect to Non-Dimensional Distance from bottom to top endwall for smooth, PSR 250, SSR 250 & BSR 250 turbine cascades

Another figure 5.59 depicts a combined graph showing variation of loss coefficients for various cascades when roughness of 500 is applied over the entire blade and over suction and pressure surfaces individually and on both the surfaces together in non localized way such as PSR 500, SSR 500 & BSR 500 cascades and smooth cascade.

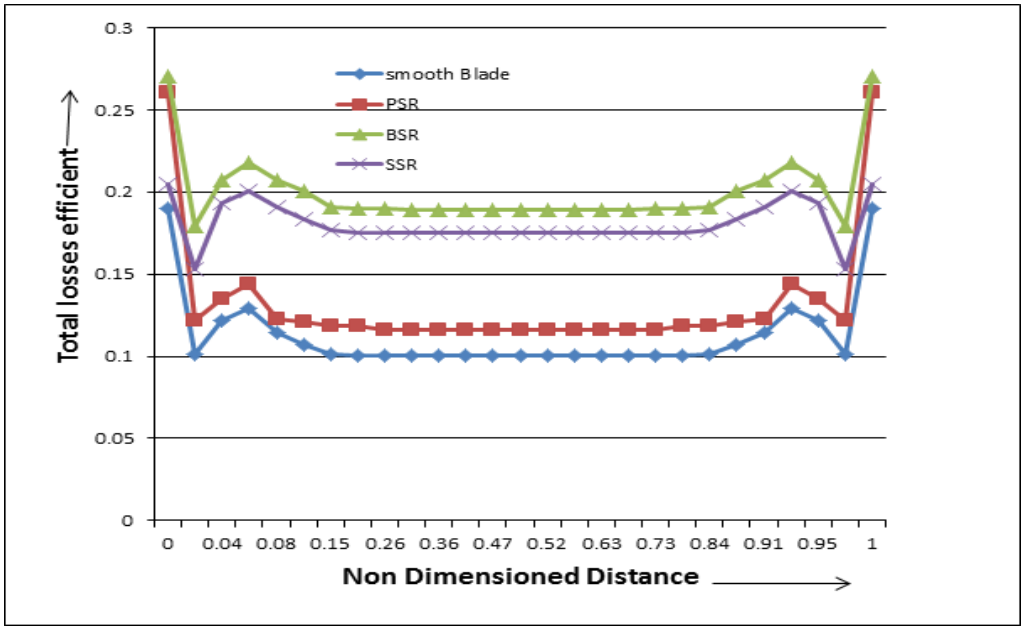

Figure 5.59: Variation of total energy loss coefficients with respect to Non-Dimensional Distance from bottom to top endwall for smooth, PSR 500, SSR 500 & BSR 500 turbine cascades

The combined plots as shown in figures 5.58 and 5.59 depict as to how total energy loss coefficients for cascades PSR 250, SSR 250 & BSR 250 are higher than that of smooth cascade.

It is clear from the combined graphs that same roughness is significantly detrimental with regard to total & profile losses when applied over suction surface, whereas it increases marginally compared to the smooth blade value when roughness is applied over pressure surface. The combined effect of roughness over pressure and suction surface is seen when the case of roughness over both the surfaces is applied together.

5.2.10 Percentage of increase in the losses due to effect of roughness for a given cascade vis-a-vis losses for smooth cascade employing blade profile 6030

The total energy loss, profile loss and secondary loss of all type of cascades is separately compared with that of smooth cascade and percentage increase in each case is found and presented in this section. It is worthwhile to mention that the comparison of any one type of loss for given cascade with the similar type of loss of respective smooth cascade is made without considering as to what are the magnitudes of remaining type of losses of the given cascade.

The percentage increase of losses i.e. Total Energy Loss, Profile Loss and Secondary Loss with the increase in roughness of the blades comparing with that of respective smooth cascade is found separately for all PSR, SSR & BSR cascades for different levels of roughnesses.

The each of total loss, profile loss and secondary loss for all PSR, SSR & BSR and smooth cascades, for all of roughness values, are tabulated. There is a separate table for each of PSR, SSR & BSR cascades. First of all, the percentage increase of total

loss for each of PSR 250, PSR 500, PSR 750 and PSR 1000 cascades with respect to the total loss for smooth blades cascade is presented in following section.

5.2.11 Effect of roughness on total loss for Turbine Cascades employing blade profile 6030

The tables 5.4, 5.5 & 5.6 show percentage increase of total loss with respect to the total loss for smooth blades cascade, as the base or reference (basis points as 0), separately for PSR, SSR & BSR cascades respectively for different levels of roughnesses.

Table 5.4: Effect of roughness on percentage increase in total losses for all PSR cascades comparing with smooth cascade

Type of PSR cascade paired with smooth cascade for comparison of total losses				
Percentage increase in total losses of the PSR cascade comparing with smooth cascade	**PSR 250**	**PSR 500**	**PSR 750**	**PSR 1000**
	11.14	16.19	17.08	17.08

Table 5.5: Effect of roughness on percentage increase in total losses for all SSR cascades comparing with smooth cascade

TYPE OF SSR cascade paired with smooth cascade for comparison of total losses				
Percentage increase in total losses of the SSR cascade comparing with smooth cascade	SSR 250	SSR 500	SSR 750	SSR 1000
	51.63	68.83	70.54	70.55

Table 5.6 : Effect of roughness on percentage increase in total losses for all BSR cascades comparing with smooth cascade

TYPE OF BSR cascade paired with smooth cascade for comparison of total losses				
Percentage increase in total losses of the BSR cascade comparing with smooth cascade	**BSR 250**	**BSR 500**	**BSR 750**	**BSR 1000**
	62.35	84.33	87.19	87.19

Similarly in order to present a pictorial comparison of effect of increasing the roughness on profile losses with that of smooth cascade, at a time, a combined graph for all 12 numbers of cascades employing blade profile 6030 is presented in figure 5.60.

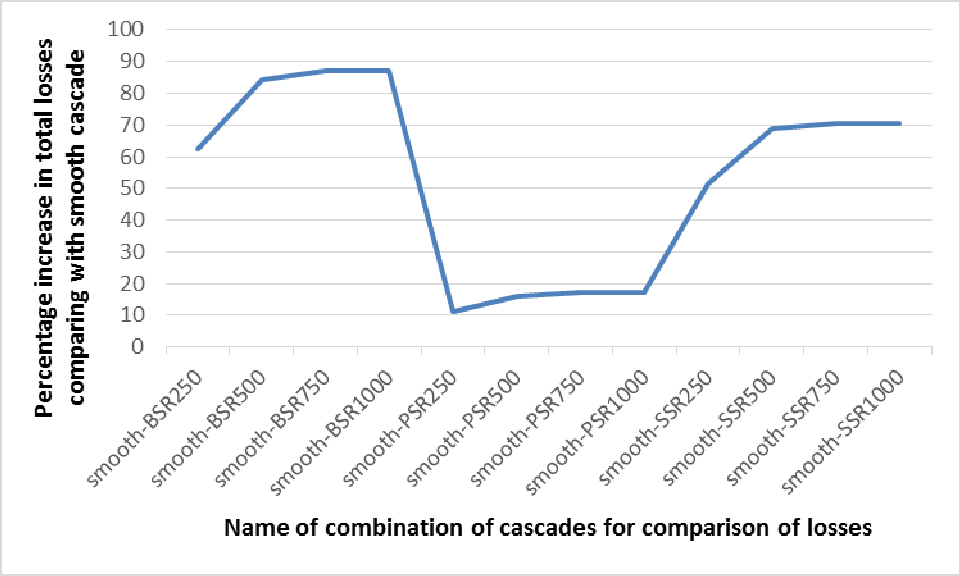

Figure 5.60 : Comparison of effect of increasing the roughness on total losses for all cascades with that of smooth cascade employing blade profile 6030, at a time

5.2.12 Effect of roughness on profile losses for Turbine Cascades employing blade profile 6030

The mid span values of loss coefficients for various cascades, such as smooth, PSR 250, SSR 250 & BSR 250 cascades as shown in combined graph in figure 5.58 reveals that the profile losses for PSR 250, SSR 250 & BSR 250 are higher than that of smooth cascade. It is also observed that profile loss is lowest for smooth blade and for BSR cascade it is maximum followed by SSR and PSR.

The mid span values of loss coefficients measured for SSR 250, SSR 500, SSR 750 & SSR 1000 cascades are depicted in figure 5.8. The similar trend that of SSR cascades is found for all PSR & BSR cascades of roughness values 250, 500, 750 & 1000 μm.

The percentage increase in the Profile Loss with the increase in roughness of the blades comparing that with smooth cascade is found for PSR, SSR & BSR cascades for different levels of roughness. The tables 5.8, 5.9 and 5.10 show percentage increase of profile losses for PSR, SSR & BSR cascades comparing with profile loss for respective smooth blades cascade respectively. The profile loss for smooth blade is assumed as reference.

Table 5.7 : Effect of roughness on percentage increase in profile losses for all PSR cascades comparing with smooth cascade

TYPE OF PSR cascade paired with smooth cascade for comparison of profile losses				
Percentage increase in profile losses of the PSR cascade comparing with smooth cascade	**PSR 250**	**PSR 500**	**PSR 750**	**PSR 1000**
	11.26	15.91	17.11	17.11

Table 5.8 : Effect of roughness on percentage increase in profile losses for all SSR cascades comparing with smooth cascade

TYPE OF BSR cascade paired with smooth cascade for comparison of profile losses				
Percentage increase in profile losses of the BSR cascade comparing with smooth cascade	**BSR 250**	**BSR 500**	**BSR 750**	**BSR 1000**
	65.88	89.26	92.28	92.28

Table 5.9 : Effect of roughness on percentage increase in profile losses for all BSR cascades comparing with smooth cascade

TYPE OF SSR cascade paired with smooth cascade for comparison of profile losses				
Percentage increase in profile losses of the SSR cascade comparing with smooth cascade	**SSR 250**	**SSR 500**	**SSR 750**	**SSR 1000**
	56.37	74.71	76.79	76.79

Similar to the case of total loss, the figure 5. 61 shows a combined graph for all 12 numbers of cascades employing blade profile 6030 in order to present comparison of effect of application of roughness of varying magnitudes on profile losses with that of smooth cascade, at a time.

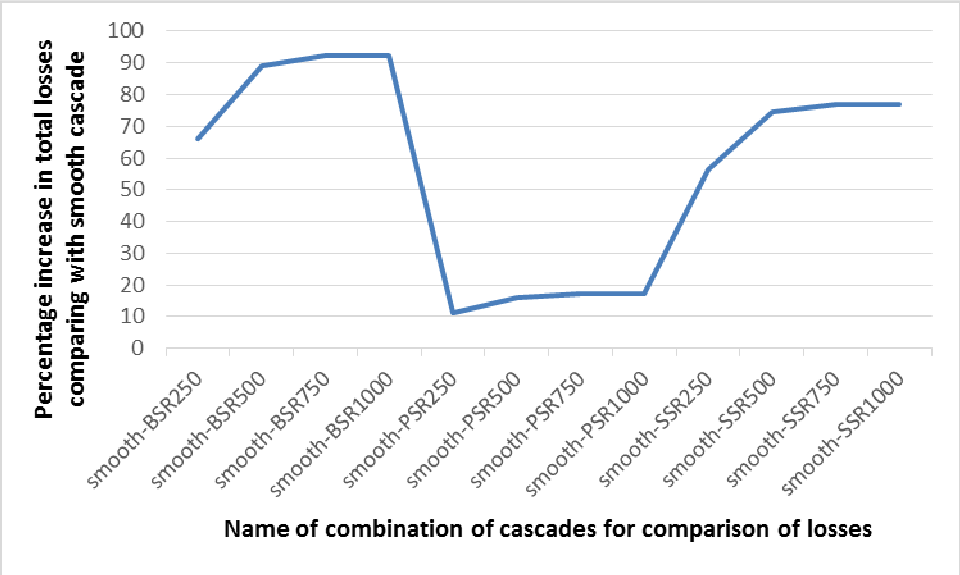

Figure 5.61 : Comparison of effect of increasing the roughness on profile losses for all cascades with that of smooth cascade employing blade profile 6030, at a time

It is observed from table 5. 4 to 5.11 and figures 5.60 and 5.61 that the same roughness is significantly detrimental with regard to total & profile losses when applied over suction surface followed by pressure surface. The combined graphs shown in figures 5.60 and 5.61 depict that the combined effect of roughness over pressure and suction surface is seen when the case of roughness over both the surfaces is applied together.

5.2.13 Effect of roughness on Secondary loss for Turbine Cascades employing blade profile 6030

Similar to total and profile losses presentation, the percentage of increase in the Secondary Loss with the increase in roughness of the blades comparing that with smooth cascade is found for SSR, PSR & BSR cascades for different levels of roughness. Similarly the magnitude of losses for all cascades are tabulated also to be able to compare them with the magnitude of losses for smooth blades cascade. The tables 5.12, 5.13 and 5.14 show numerical values of percentage increase of secondary

losses separately for PSR, SSR & BSR cascades for different levels of roughness comparing with smooth blades cascade respectively. The value for secondary loss for smooth blade cascade is assumed as reference (basis points as 0).

Table 5.10: Effect of roughness on percentage increase in secondary losses for all PSR cascades comparing with smooth cascade

Type of PSR cascade paired with smooth cascade for comparison of secondary losses				
Percentage increase in secondary losses of the PSR cascade comparing with smooth cascade	**PSR 250**	**PSR 500**	**PSR 750**	**PSR 1000**
	2.15	-4.46	0.53	0.53

Table 5.11: Effect of roughness on percentage increase in secondary losses for all SSR cascades comparing with smooth cascade

TYPE OF SSR cascade paired with smooth cascade for comparison of secondary losses				
Percentage increase in secondary losses of the SSR cascade comparing with smooth cascade	**SSR 250**	**SSR 500**	**SSR 750**	**SSR 1000**
	151.82	203.32	239.57	238.54

Table 5.12: Effect of roughness on percentage increase in secondary losses for all BSR cascades comparing with smooth cascade

TYPE OF BSR cascade paired with smooth cascade for comparison of secondary losses				
Percentage increase in secondary losses of the BSR cascade comparing with smooth cascade	**BSR 250**	**BSR 500**	**BSR 750**	**BSR 1000**
	71.77	106.36	110.08	110.09

In pursuit of comparing effect of increasing the roughness, a combined graph for all 12 numbers of cascades employing blade profile 6030 is presented with regard to

making comparison of effect of increasing the roughness on secondary losses with that of smooth cascade, at a time, in figure 5.62.

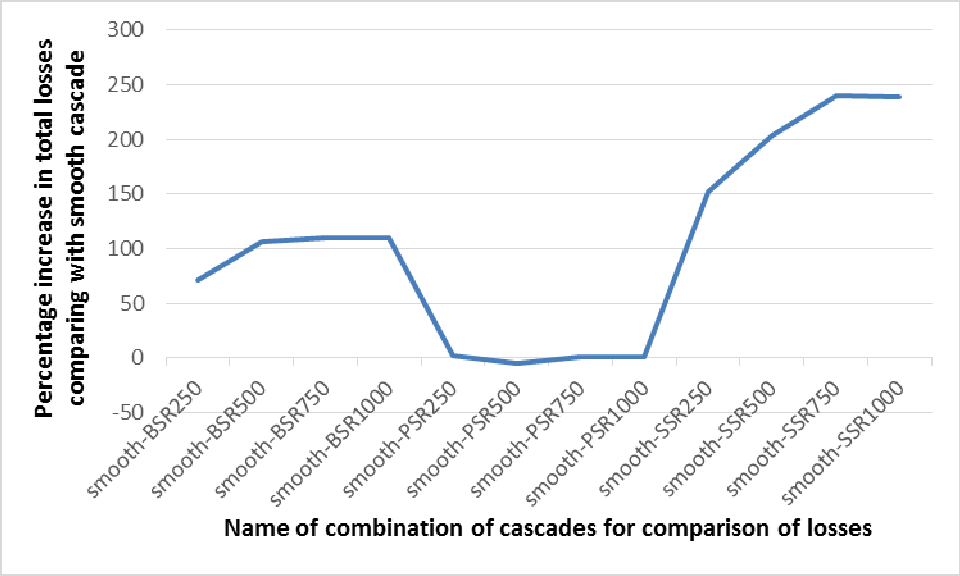

Figure 5.62: Comparison of effect of increasing the roughness on secondary losses for all cascades with that of smooth cascade employing blade profile 6030, at a time

The effect of different levels of roughnesses (250, 500, 750 &1000 μm) over various surfaces of blades separately on total, profile and secondary loss are summarized in preceding paragraphs without nondimensionalising the same with total loss of the cascade. Similarly various type of loss or not shown non-dimensionalising the same with total loss in smooth blade cascade. In preceding paragraphs, percentage of increase of Total Energy Loss, Profile Loss and Secondary Loss over and above respective losses for the smooth cascade are separately discussed.

In order to interrelate the total, profile and secondary loss for all the cascades, the magnitudes of same are discussed inclusively in succeeding paragraphs. The respective losses are shown non-dimensionalising the same appropriately.

5.2.14 Summary of Total Energy Loss, Profile Loss and Secondary Loss for smooth, SSR, PSR & BSR cascades for different levels of roughness for turbine cascades employing blade profile 6030

The Table 5.16 may be referred for summary of total, profile and secondary loss all the cascades. This table 5.16 gives an overview regarding effect of different levels of roughnesses (250, 500, 750 &1000 μm) over various surfaces of blades on the total, profile and secondary loss. The secondary losses for all cascades are shown non-dimensionalising the same with total loss in smooth blade cascade.

Table 5.13 : Summary of Total Energy Loss, Profile Loss and Secondary Loss for smooth, SSR, PSR & BSR cascades for turbine cascades employing blade profile 6030.

Type of cascade	Roughness levels	Total Loss in percentage of total energy	Profile Loss in percentage of total energy	Percentage of Profile Loss in total loss of the same cascade	Percentage of Profile Loss in Total Loss of smooth blade cascade	Absolute value of percentage Sec. Loss	Percentage of Sec. Loss in Total Loss of the same cascade	Sec. Loss Non-dimensionalising with Total Loss of smooth blade cascade
Smooth	--------	10.53	10.01	95.06	95.06	0.52	4.94	4.94
PSR	**250**	11.71	11.14	95.17	105.77	0.57	4.83	5.37
	500	12.24	11.61	94.83	110.19	0.63	5.17	6.00
	750	12.33	11.73	95.09	111.33	0.61	4.91	5.75
	1000	12.33	11.73	95.09	111.33	0.61	4.91	5.75
SSR	**250**	15.97	15.66	98.04	148.65	0.31	1.96	2.97
	500	17.78	17.49	98.37	166.08	0.29	1.63	2.75
	750	17.96	17.70	98.55	168.06	0.26	1.45	2.48
	1000	17.96	17.70	98.54	168.07	0.26	1.46	2.49
BSR	**250**	17.10	16.61	97.13	157.69	0.49	2.87	4.67
	500	19.42	18.95	97.61	179.92	0.46	2.39	4.41
	750	19.72	19.25	97.65	182.79	0.46	2.35	4.40
	1000	19.72	19.25	97.65	182.79	0.46	2.35	4.40

This table 5.16 also depicts as to how increase in percentage of secondary loss in total loss affect percentage of profile loss and vice versa. In this section, effect of roughness on generation of secondary losses are discussed in detail.

The results tabulated in table 5.16 conclude that turbine cascades for the blade profile 6030 having both surfaces smooth, mass averaged total loss is 10.53%. Whereas this loss gets almost doubled and becomes 19.72% when a roughness of 1000 µm is applied on both the surfaces. When roughness of 1000 µm is applied separately on the suction and pressure surfaces of all the blades of turbine cascade, the mass averaged total loss is 17.96% and 12.33% respectively.

The components of total loss i.e. profile loss and secondary loss vary in such a way that increment in one type of component due to the effect of roughness would lead to decrement in another component and vice versa. The effect of roughness on profile and secondary loss are discussed separately.

5.2.14.1 Variation of secondary loss

In case of smooth blade cascade of the blade profile 6030, the secondary loss is 4.94%. Presence of roughness over the different part of blade affects the secondary loss differently. When 250 µm roughness is present on both surfaces together this loss was 4.65%. The secondary loss further reduces to 4.41% when roughness over both the surfaces is increased to 500 µm. However, the roughness of 250 µm applied separately over pressure surfaces results in secondary loss of 5.37 % which is higher than the secondary loss of smooth cascade (4.94%). The secondary losses reduce to 2.97, 2.75 and 2.48 % respectively when roughness of 250 µm, 500 µm and 750 µm applied over suction surface.

The magnitude of secondary loss decreases in case of BSR & SSR cascades with increase in roughness from 250 to 500 µm. Thus, it is clear that roughness over pressure surface strengthen the passage vortex, whereas suction side roughness weakens the passage vortex by stronger suction side counter vortex. When the

roughness over pressure and suction surface is applied together, the effect of counter vortex is more pronounced, thus causing secondary loss to decrease in this case. The decrement in secondary loss can be attributed to the formation of boundary layer. The PSR cascade makes, pressure side vortex and passage vortex strengthen due to which secondary loss is increased. As far as the effect of roughness is concerned, it can be concluded that presence of roughness over pressure surface increases secondary losses. This may be due to favorable effect of pressure side leg on the passage vortex. This is in line with the energy loss coefficient where roughness over pressure surface is least detrimental. The phenomenon of generation of secondary flow is affected by curvature and pressure difference between pressure side and suction side of adjacent blade of the corresponding flow passage also. If pressure difference is more, the Pressure side leg of horse shoe vortex would contribute more to the Secondary losses.

This may be due to strengthening of suction side counter vortex, which mixes with the passage vortex and reducing the effect of passage vortex. Therefore, the secondary losses are lower in this case. Increase in roughness further enhance counter vortex and hence secondary losses are further reduced. Profile loss due to roughness over suction surface also favors these results. The contribution of secondary loss in the total loss of same cascade is maximum for PSR cascades followed by smooth cascades, BSR cascades and SSR cascades. The percentage of secondary loss non-dimensionalising with the total loss in case of smooth blades is highest for PSR cascades followed by smooth cascades, BSR cascades and SSR cascades in order. The percentage of secondary loss in total loss for smooth cascade and BSR cascades are almost same. It may be so because the increment in the secondary losses with increase in roughness on pressure surfaces are offset by the decrement in the secondary losses due to

application of the same roughness on suction surfaces of the blades of the given cascade.

Magnitude of secondary loss at roughness value of 1000 µm was found to be approximately equal to that of 750 µm for all types of cascades i.e. PSR, SSR & BSR.

The trend of increase in secondary losses is insignificant with the increase in magnitude of roughness (beyond 750µm) for all types of cascades i.e. SSR PSR & BSR cascades for the turbine blade profile 6030 of roughness values 250, 500, 750 &1000 µm.

5.2.14.2 Variation of secondary loss

It can be observed from Table 5.16 that the profile loss is lowest for smooth blade and increases when roughness is applied over pressure, suction surface separately and together in the same order. Alternatively, profile loss for BSR cascade is maximum followed by SSR and PSR cascades in the same order. This is so because the magnitude of secondary loss decreases in case of BSR cascade with increase in roughness from 250 to 500 µm. On the other hand, the total loss increases in case of BSR cascade with increase in roughness from 250 to 500 µm. On the basis of this result it can be concluded that similar to the case of total loss, profile loss is also increased with increasing roughness. The percentage of profile loss in total loss of the smooth cascade is measured to be approximately 95%. The profile loss non-dimensionalising with this percentage of profile loss in total loss of the smooth cascade reaches to approximately 183 percent for BSR 1000 cascade. This percent is merely 106% for PSR 250 cascades. The profile loss follows trend of total loss with regard to changing of magnitudes of losses with the increasing roughness on the surface of the blades, for all cascades. The difference in values of profile losses for

increasing of roughness from smooth to 250 µm is maximum. This difference reduces for the increasing of roughness from 500 to 750 µm. This difference is least for the increasing of roughness from 750µm to 1000 µm, for all cascades.

The profile loss contribution in the total loss of same cascade is maximum for suction surface. The profile losses contributes maximum in the total losses. The magnitude of profile loss measured as a percentage of total loss of same cascade ranges between 95% to 98 % of total loss of same cascade. The profile loss contribution for smooth cascade is approximately 95% of total loss of same cascade whereas the same loss contribution reaches approximately 98 % for SSR cascades. This contribution is marginally lower for BSR cascade than that of the SSR cascades. The PSR cascades, on the other hand, do not change the profile losses appreciably. The PSR cascades even in the case of PSR 500 cascade reduces the contribution of profile loss in the total loss of the same cascade. This value is lowered in the case of PSR 500 cascade to 94.8% from 95.06% i.e. the contribution of profile loss of in the total loss of the same cascade for smooth cascade.

5.3 Measurement of magnitude of losses for Turbine Cascades employing blade profiles 5530

Computational study is also conducted for blade profiles 5530 focusing on analysis of the effect of roughness on the aerodynamic performance specially in terms of generation of losses for each cascade. The degree of reaction of the blade profile 5530 is about 65% which is highest among all the blade profiles. The same is about 55 % and 10 % for profiles 6030 & 3525 respectively. The convergence of inter blade channels formed by this profile is more as compared to that of other blade profiles of lesser degree of reactions. The curvilinear lengths of suction and pressure surfaces of

this profile are 55 mm & 64 mm [Samsher, 2002]. The thickness in the chord wise direction also differ for blade profile 5530 (comparing with blade profile 6030). The flow turning capacities of both of blades profiles i.e. 5530 and 6030 also differ largely from each other. The figure 5.21 may be referred which shows indicative shapes of all the three blade profiles i.e. 5530, 6030 and 3525 used for geometry creation of turbine cascades.

Measurement of total, profile & secondary loss was carried out by successively employing roughnesses on the surfaces of blades of the cascades simulated for profile 5530 using various combinations of surfaces and roughnesses. The computational methodology adopted for measurement of effect of roughness on the blades of cascades employing blade profile 5530 and 6030 is similar. The roughnesses of 250, 500, 750 &1000 μm are applied on suction and pressure surfaces individually as well as on both the surfaces together for the cascades employing blade profile 5530. It is observed that applying roughness on blade surface, increases the profile loss as well as total energy loss coefficient for all the cascades employing this blade profile also, similar to cascades employing blade profile 6030. The pattern of variation of parameters such as local loss coefficients, mass averaged loss coefficients for all such cascades are found similar in many respects to the blade profile 6030. However, the magnitudes of losses differ for both blade profiles. All the factors as described above such as degree of reaction, curvilinear lengths of suction and pressure surfaces and flow turning capacities for a given blade profile etc. largely impact the loss generation mechanism for a given cascade. The losses are measured to be more in case of blade profile 5530, comparing with blade profile 6030, attributing to the factors as mentioned in the preceding paragraphs.

The magnitudes of losses generated due to effect of roughness on the blades of the cascade depend on surface(s) for application of roughness and magnitude of roughness on the same surface. The local loss coefficients are, first of all, measured for all cascades employing blade profile 5530 for all pitch wise positions.Thereafter, the mass averaged loss coefficients are measured for all cascades including smooth cascade, employing same blade profile. The same coefficients are thereafter measured for each span position for all the similar cascades by applying various values of roughnesses, over the entire blade pressure surfaces and suction surfaces individually and on both the surfaces together, one by one. The local loss coefficients for cascades employing blade profile 5530 vary relative to pitchwise direction in the similar way to that of earlier discussed blade profile 6030. Similarly the variation of the mass averaged loss coefficients relative to span wise distance for the blade profile 5530 is also similar to that of blade profiles 6030. The graph showing variation of local loss coefficients and mass averaged loss coefficients for all cascades employing for blade profile 5530, reveals that the loss coefficient is high at hub and casing due to the endwall boundary layers for all roughness values. The mass averaged loss coefficients near the end walls at both ends, in case of cascades employing blade profiles 5530 are also higher than their values at mid span of the blade. Various graphs showing variation of the local loss coefficient and mass averaged loss coefficients relative to non dimensional pitchwise distance and span wise distance respectively for blade profile 6030 are included in previous sections of this chapter. The local loss coefficients and mass averaged loss coefficients thus obtained in case of cascades employing blade profiles 5530, as a result of CFD work, are used to find the magnitudes of total, profile and secondary losses. The same are presented in this section.

First of all, the results with regard to total, profile and secondary loss are measured for smooth cascade employing blade profile 5530 is presented. Thereafter the results for same blade profile are presented for effect of changing the location of application of roughness. The results for effect of changing the location of application of roughness choosing different magnitudes of roughnesses, one by one, are presented.

5.3.1 Measurements of magnitude of losses for Smooth cascades for blade profiles 5530

In order to make quantitative comparison of effect of changing the location of application of roughness or increasing of level of roughness, results for total, profile and secondary losses for cascades for turbine employing blade profile 5530 are tabulated. The table 5.17 shows results with regard to smooth and PSR250, SSR250 BSR 250 cascades employing blade profile 5530, similar surfaces of blades of which are applied a roughness of 250 μm. It is shown in the table 5.17 that the total and profile losses for smooth cascades are measured to be 19.61 and 19.35 % of the total energy of the air at the inlet. The secondary loss is measured to be 1.32% of total loss so measured (non-dimensionalising with total loss of same cascade)**.**

It is worthwhile to note that the total and profile losses for smooth cascades are measured to be 19.61 and 19.35 % of the total energy of the air at the inlet for the cascades employing blade profiles 5530 against total and profile losses of 10.53 and 10.01% for the cascades employing blade profiles 6030 respectively. It is concluded that magnitudes of losses are measured to be higher for the cascades employing blade profiles 5530 than the respective magnitudes of losses for cascades employing blade profile 6030. The difference of magnitudes of losses for two smooth cascades, employing blade profiles i.e. 5530 and 6030 separately, is significantly large. The

total and profile loss for smooth blade cascade for profiles 5530 is found to be 9.07 and 9.33 % higher than that for the 6030 blade profile. The large difference losses for two smooth cascades as above shows that shape or geometry of the blades of the cascades also affect the losses, significantly. In view of generation of more loss, as discussed above, blades of the cascades employing blade profile 5530 are aerodynamically lesser efficient than that of cascades employing blade profile 6030.

5.3.2 Measurements of magnitude of losses for PSR250, SSR250 BSR 250 cascades for blade profiles 5530

Similar to the case of blade profile 6030, a roughness of 250 μm is applied on surface(s) chosen for application of same on blades surfaces of various cascades employing blade profile 5530.

(i) on pressure surfaces only (PSR 250)

(ii) on suction surfaces only (SSR 250)

(iii) on pressure surfaces and suction surfaces together (BSR 250)

In order to make quantitative comparison of effect of changing the location for application of roughness of 250 μm, the table 5.17 shows results with regard to total, profile and secondary losses for turbine cascades i.e. PSR250, SSR250 BSR 250 cascades employing blade profile 5530 along with smooth turbine cascade for the same blade profile. The data in the table 5.17 may be used to make quantitative comparison of effect of changing of surface for application of roughness.

Table 5.14: Total, profile and secondary losses for turbine cascades i.e. PSR250, SSR250 BSR 250 employing blade profile 5530

Type of Cascade	Roughness levels	Total energy loss in total energy of the air (a)	Profile loss in total energy of the air (b)	Total loss in percentage of total energy	Profile loss n percentage of total energy	Percentage of profile loss in total loss of the same cascade	Non-dimensionalising profile loss with total loss in smooth blade cascade	Absolute value of percentage sec loss	Percentage of sec. Loss in total loss of the same cascade
smooth	0	0.196	0.194	19.610	19.350	98.673	98.673	0.260	1.327
PSR	250	0.197	0.194	19.687	19.425	98.673	99.056	0.261	1.327
SSR	250	0.199	0.196	19.883	19.591	98.527	99.900	0.293	1.473
BSR	250	0.200	0.197	19.958	19.665	98.528	100.277	0.294	1.472

It is clear from the table 5.17 that the total losses are maximum for BSR cascades followed by SSR and PSR Cascades in the same order. The total losses for PSR 250, SSR 250 & BSR 250 cascades for blade profiles 5530 are measured to be 19.68, 19.88 and 19.95 % of the total energy of the air at the inlet of the cascade respectively as against the total loss of 19.61 % for the smooth cascade.

Similarly, the trend for profile losses is also similar to that of total loss. The profile losses for PSR 250, SSR 250 & BSR 250 cascades for the same blade profile are measured to be 19.42, 19.59 and 19.66% respectively as against the profile loss of 19.35 % for the smooth cascade. Therefore, it can be concluded that the profile loss is found to be maximum for BSR Cascades followed by SSR and PSR cascades in the same order when same roughness is applied separately over various surfaces of the cascades, one by one. Similarly it can be mentioned that changing the location of application of roughness choosing different magnitudes of roughnesses, one by one, marginally affect the total as well as profile losses for the cascades employing blade profile 5530.

The secondary loss for PSR 250, SSR 250 & BSR 250 cascades for the same blade profile are measured to be 1.33, 1.49 and 1.49 (non-dimensionalising with total loss of

smooth cascade) respectively against the secondary loss of 1.32% for the smooth cascade**.** The results with regard to secondary loss show that this loss generated for PSR Cascades are least among all the three cascades i.e. PSR 250, SSR 250 & BSR 250. The roughness on pressure surfaces of the cascade are least detrimental as far as secondary loss is concerned and the same is found to be nearly equal to that of smooth cascade.

The combined graph showing the variation mass averaged loss coefficients for such as PSR 250, SSR 250 & BSR 250 and the smooth cascade, employing blade profile 5530, may be referred in figure 5.63. The combined plot in the figure 5.63 shows as to how mass averaged loss coefficients vary in the span wise direction for all PSR 250, SSR 250 & BSR 250 cascade. It is also clear that total and profile losses for PSR 250, SSR 250 and BSR 250 cascades are marginally higher than that of smooth cascade. The loss coefficient axis in the figure 5.63 has been formatted to exaggerate the variation so as the graphs for PSR 250, SSR 250 & BSR 250 and smooth cascade may be separately shown.

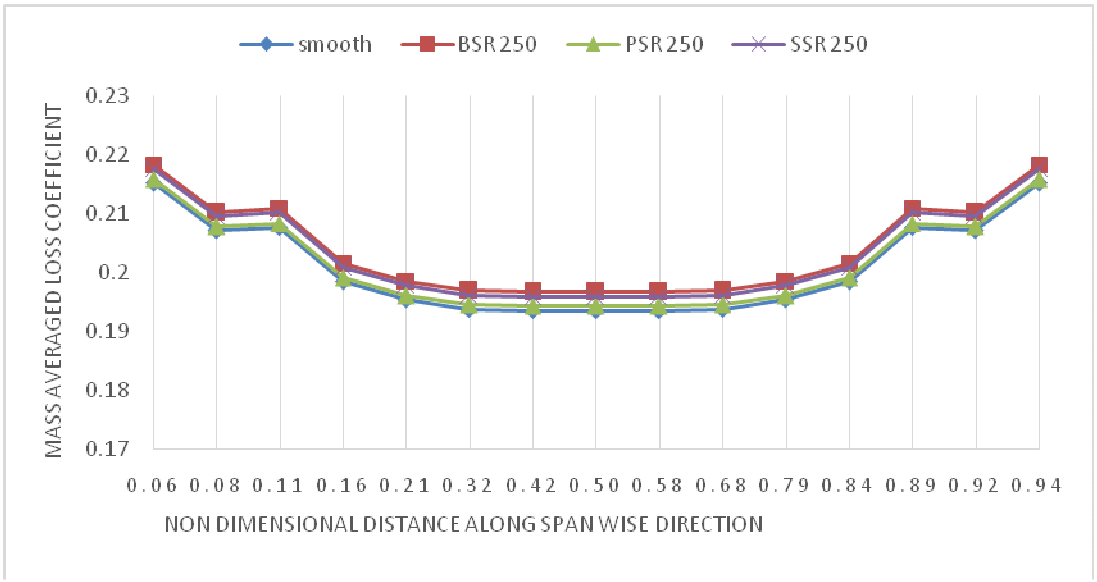

Figure 5.63: Variation of mass averaged loss coefficients with respect to Non-Dimensional Distance from bottom to top endwall for smooth, PSR 250, SSR 250 & BSR 250 cascades employing blade profile 5530(the loss coefficient axis has been formatted to exaggerate the variation)

5.3.3 Comparison of magnitude of losses for PSR250, SSR250 BSR 250 cascades employing two different blade profiles i.e. 5530 and 6030

It is evident from the results with regard to blade profile 6030 that magnitude of losses increase more rapidly when same roughness is applied separately over various surfaces of the cascades, one by one. The difference in magnitudes of total and profile losses between SSR 250 cascades and smooth blade cascade employing blade profile 6030 is more as compared to that of SSR 250 cascades and smooth blade cascade employing 5530 blade profile. It may therefore be concluded that total loss generated due to increasing the roughness is more for cascade employing blade profile 6030 comparing with the cascade employing blade profile 5530. The similar trend is observed for generation of profile losses also for cascades employing blade profile 6030, comparing with the cascade employing blade profile 5530. The profile losses for PSR 250, SSR 250 & BSR 250 cascades is measured to be 19.42, 19.59 and 19.66% respectively as against the profile loss of 19.35 % for the smooth cascade employing blade profile 5530. This goes to show that secondary loss, however has different trend when roughness of 250 µm was applied separately over entire suction surface and pressure surface. The blade profile 5530 showed opposite trend to that of blade profile 6030 and this loss increased marginally when roughness of 250 µm was applied separately over entire suction surface comparing with the losses so measured for PSR cascades. The results with regard to blade profile 6030 is reduced substantively when roughness of 250 µm was applied separately over entire suction surface than other case.

The difference of the magnitudes of losses when roughness of 250 µm is applied on pressure surfaces only for each of two cascades, (two different **PSR 250** cascades employing blade profiles i.e. 5530 and 6030) are also measured to be higher than

difference of the magnitudes of losses for other two similar cascades i.e. SSR 250 and BSR 250 cascades employing same blade profiles. However this difference is very less for two different **BSR 250** cascades employing blade profiles i.e. 5530 and 6030. The total and profile losses for **BSR 250** for cascades employing blade profiles i.e. 5530 are measured to be 19.61 and 19.35 % of the total energy of the air at the inlet respectively. The same losses are measured to be 17.10 and 16.61% of the total energy of the air at the inlet for the cascades employing blade profiles 6030 respectively. The results shown in table 5.17 reveal that the PSR 250 cascade results into highest losses followed by SSR 250 & BSR 250 cascades comparing with the similar cascades employing blade profile 6030 (table 5.16).

The results shown in columns representing total loss in the table 5.17 reveal that PSR 250, SSR 250 & BSR 250 cascades employing blade profile 5530 result 7.98, 3.91 and 2.85 percent more total loss than for similar cascades employing blade profile 6030 respectively. The result conclude that the difference in total and profile losses for two separate BSR cascades employing blade profiles i.e. 5530 and 6030 reduces up to a larger extent comparing with difference in total and profile losses for two separate smooth cascades, employing same blade profiles. Therefore it can alternatively be mentioned that both BSR cascades employing blade profiles 5530 and 6030 generate more losses as compared to smooth cascades employing same blade profiles. It can be stated on the basis of results for BSR cascades employing blade profiles 5530 and 6030 that losses generated are high irrespective of shape or geometry of the blades of the cascades when both surfaces of blades of turbine cascades are rough. Alternatively the effect of shape or geometry of the blades of the cascades do not affect the losses significantly when surfaces are not smooth.

It can also be stated on the basis of the results that the blade profile 5530 is more prone to generate the losses as compared to blade profile 6030. It is observed from the table 5.17 that the difference in magnitudes of total and profile losses between SSR cascades and smooth blade cascade employing blade profile 6030 is more as compared to the same for cascade employing 5530 blade profile. It may therefore be concluded that **the** trend of increasing of losses with increasing roughness is found to be stronger for cascade employing blade profile 6030 comparing with cascade employing blade profile 5530. The results as discussed above indicate that the same roughness on different surfaces of blades of the cascades employing blade profile 5530 is more detrimental than the cascades employing blade profile 6030 with regard to generation of magnitude of total losses.

5.3.4 Measurements of magnitude of losses for PSR, SSR & BSR 500 cascades for blade profile 5530

It is found that the results for roughness of 500 µm for PSR, SSR & BSR cascades employing blade profiles 5530 are similar to results for PSR, SSR & BSR cascades for roughness of 250 µm, employing same blade profile. However, the magnitudes of losses marginally differ for both blade profiles.

In order to make quantitative comparison of effect of changing of surface for application of roughness of 500 µm i.e. PSR, SSR & BSR 500 cascades employing blade profile 5530, results for total, profile and secondary losses are tabulated in table 5.18.

Table 5.15: Total, profile and secondary losses for turbine cascades i.e. PSR500, SSR500 BSR 500 employing blade profile 5530

Type of cascade	Rough-ness levels	Total energy loss in total energy of the air	Profile loss in total energy of the air	Total loss in percentage of total energy	Profile loss percentage of total energy	Percentage of profile loss in total loss of the same cascade	Non-dimensiona-lising profile loss with total loss in smooth blade cascade	Absolute value of percentage sec loss	Percentage of sec. loss in total loss of the same cascade	Non-dimensiona-lising sec. loss with total loss in smooth blade cascade
smooth	0	0.1961	0.1935	19.61	19.35	98.67	98.67	0.26	1.33	1.33
PSR	500	0.1985	0.1947	19.85	19.47	98.09	99.30	0.38	1.91	1.94
SSR	500	0.2000	0.1971	20.00	19.71	98.55	100.53	0.29	1.45	1.47
BSR	500	0.2015	0.1983	20.15	19.83	98.44	101.14	0.32	1.56	1.61

The percentage of total loss when roughness of 500 µm is applied separately over the entire pressure surface i.e. PSR 500 (roughness of 500 µm on blades of the cascade choosing all pressure surfaces for application of roughness) and suction surface i.e. SSR 500 are measured to be 19.85% and 20.00 % respectively for blade profile 5530. The total loss for BSR 500 cascade is also measured to be marginally higher than SSR 500 and PSR 500 cascades. The results of effect of roughness on profile loss for PSR, SSR & BSR cascades for roughness of 500 µm, employing blade profile 5530 are also similar to results for similar cascades for roughness of 250 µm, employing same blade profile.

Secondary loss for roughness value of 500 µm for cascades employing blade profile 5530, however, has different trend as compared to similar cascades for roughness value 250 µm, employing same blade profile. The secondary loss for PSR, SSR & BSR cascades for roughness value of 500 µm are measured to be 1.93, 1.47 and 1.60 percent of total loss of smooth cascade employing blade profile 5530 respectively. On the other hand, the secondary loss for same cascades for roughness value of 250µm are measured to be 1.32, 1.47 and 1.47 percent of total loss of smooth cascade employing blade profile 5530 respectively. It is concluded from the results that same roughness (500 µm), applied over pressure surface is marginally more detrimental

with regard to increasing the secondary losses than applying the same over suction surfaces or over both surfaces together. It increases marginally compared to the smooth blade value when roughness is applied over suction surface. The magnitude of secondary losses is of intermediate values when roughness of 500 µm is applied over both the surfaces together. Whereas the same losses measured for SSR cascades for roughness of 250 µm are found to be of intermediate values.

The combined graph showing the variation mass averaged loss coefficients for such as PSR 500, SSR 500 & BSR 500 and the smooth cascade, employing blade profile 5530, may be referred in figure 5. 64. The combined plot in the figure 5. 64 clarify as to how mass averaged loss coefficients vary in the span wise direction for all PSR 500, SSR 500 & BSR 500 cascade employing blade profile 5530. It is also clear that total and profile losses for PSR 500, SSR 500 and BSR 500 cascades are marginally higher than that of smooth cascade. The loss coefficient axis in the figure 5.64 has been formatted to exaggerate the variation so as the graphs for PSR 500, SSR 500 & BSR 500 and smooth cascade may be separately shown.

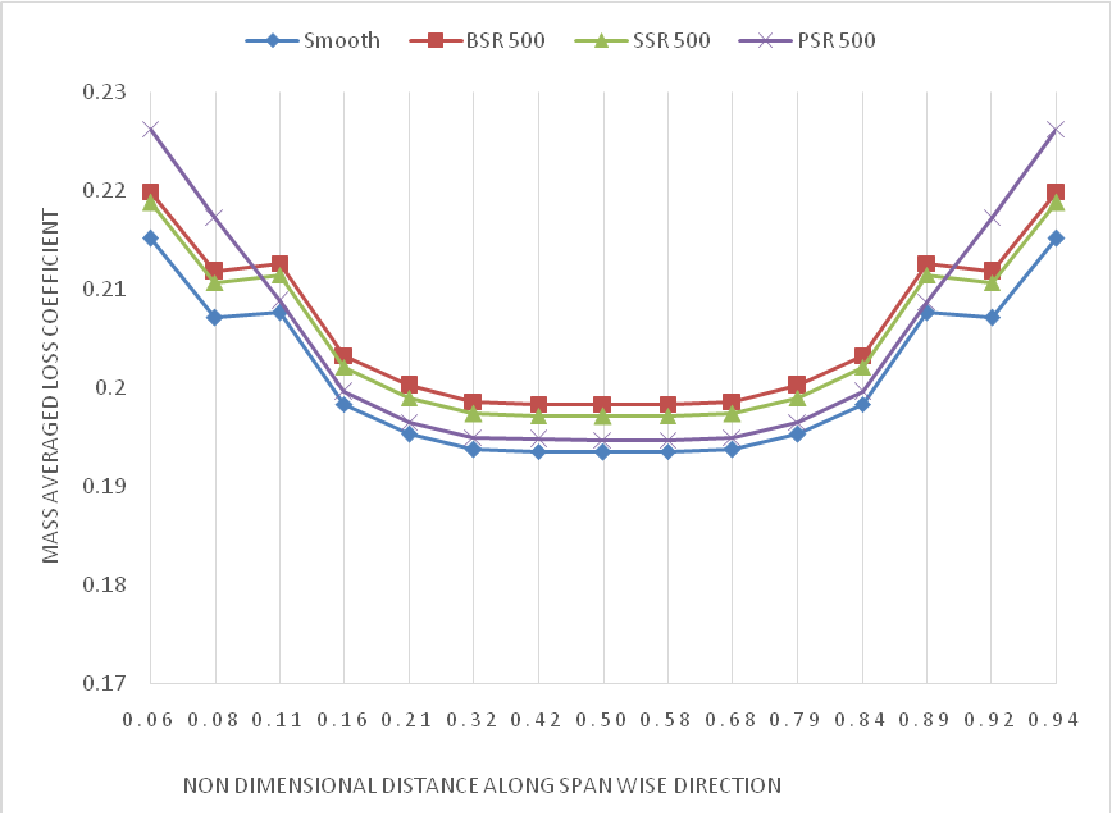

Figure 5.64: Variation of mass averaged loss coefficients with respect to Non-Dimensional Distance from bottom to top endwall for smooth, PSR 500, SSR 500 & BSR 500 cascades employing blade profile 5530

5.3.5 Comparison of magnitude of losses for PSR500, SSR500 BSR 500 cascades employing two different blade profiles i.e. 5530 and 6030

The magnitudes of losses for PSR500, SSR500 BSR 500 cascades employing two different blade profiles i.e. 5530 and 6030 are tabulated in table 5.19. The table 5.19 is specifically meant for comparison of effect of roughness of 500 µm on cascades employing two different blade profiles i.e. 5530 and 6030. The difference of corresponding losses for cascades employing blade profile 5530 and 6030 when surfaces chosen for application of roughness on the blades of the respective cascades are same are also tabulated in the table 5.19 along with magnitude of losses for each roughness of 500µm -location combination.

Table 5.16 : Difference between losses for cascades employing blade profile 5530 and 6030, for various surfaces chosen for application of roughness of 500 µm

The abbreviated name of the cascade losses measured for	blade profile for the cascade losses measured for	total loss measured	Profile loss measured	Secondary loss measured	Difference of losses between corresponding losses of 5530 and 6030		
					total loss measured	Profile loss measured	Secondary loss measured
PSR 500	5530	19.852	19.472	**1.94**	**7.612**	**7.862**	**-4.06**
	6030	12.24	11.61	6.00			
SSR 500	5530	20.003	19.714	**1.47**	**2.223**	**2.224**	**-1.28**
	6030	17.78	17.49	2.75			
BSR 500	5530	20.149	19.834	**1.61**	**0.729**	**0.884**	**-2.8**
	6030	19.42	18.95	4.41			

The results shown in the table 5.19 leads to the conclusion that roughness on suction surfaces only, on all the blades of the cascade, employing blade profile 6030 is more prone to generate losses comparing with other surfaces i.e. pressure surfaces of all the blades of the same cascade. This results shown in the table 5.19 clarify that changing the location of the applications of roughness affects the losses significantly in case of blade profile 6030 comparing to the cascades employing blade profile 5530.

The roughness of 500µm on suction surfaces only, on all the blades of the cascades employing blade profile 5530 lead to losses marginally higher than the case when same magnitude of roughness is applied on all pressure surfaces only of the same cascade employing blade profile 5530. The effect of changing the location of the applications of roughness is marginal in case of turbine cascade employing blade profile 5530 comparing with the corresponding effect of roughness for cascade employing blade profile 6030.

It is observed from the table 5.19 that the difference in magnitudes of total and profile losses between SSR cascades and smooth cascade employing blade profile 6030 is more as compared to the same for cascade employing 5530 blade profile. It may therefore be concluded that the trend of increasing of total losses with increasing roughness is found to be stronger for cascade employing blade profile 6030 comparing with cascade employing blade profile 5530. The magnitude of total loss for PSR 500 turbine cascade employing blade profile 5530 is 7.61 % more than corresponding losses for cascade employing blade profile 6030. It may be concluded that roughness on pressure surfaces are more detrimental for cascades employing blade profile 5530, in terms of resulted total loss. On the other hand, effect of the same, on cascades employing blade profile 6030 is lesser than cascades employing blade profile 5530.

The total and profile losses for SSR 500 for cascades employing blade profiles 5530 are measured to be 20.00 and 19.71 % against the respective values of 17.78 and 17.49% of the total energy of the air at the inlet for similar cascades with the roughness value of 500 μm, employing blade profiles 6030, respectively. The total and profile losses for BSR 500 for cascades employing blade profiles 5530 are measured to be 20.14 and 19.83 against the respective values of 19.42 and 18.95 % of the total energy of the air at the inlet for cascades employing blade profiles 6030 respectively. It is clear from the results with regard to SSR500 and BSR 500 for both of the blade profiles that the difference in magnitude of total loss between corresponding 2 PSR500 cascades, one each choosing blade profile 5530 and blade profile 6030, is higher than similar cascades i.e. SSR500 and BSR 500. The corresponding differences in magnitudes of total loss for SSR 500 and BSR 500

turbine cascade, employing blade profiles, one each from blade profile 5530 and blade profile 6030, are measured to be 2.22 % and 0.72% respectively.

This result concludes that the difference in total and profile losses for two separate BSR cascades, employing blade profiles i.e. 5530 and 6030, for roughness of 500 µm also (as in case of 250 µm roughness), reduces up to a larger extent comparing with similar smooth cascades. Therefore both BSR cascades employing blade profiles 5530 and 6030 generate more losses as compared to smooth cascades employing same blade profiles. It may be concluded that roughness on both surfaces of all the blades comparing to that on single side are more detrimental, for each of case of blade profiles 5530 and 6030.

The secondary loss for all the three cascades PSR 500, SSR 500 & BSR 500, employing blade profile 5530, when non- dimensionalised with total loss in respective smooth blade cascade shows similar trend that of cascades employing blade profile 6030. However the magnitude of the secondary loss (non-dimensionalising with total loss of smooth cascade) in case of PSR 500, SSR 500 & BSR 500 cascades is found to be 1.94, 1.47 and 1.61 against the 1.33, 1.49 and 1.49 respectively for PSR 250, SSR 250 & BSR 250 cascades employing same blade profile. Comparing the magnitudes of secondary loss for various cascades, it is found that the loss in case of PSR 500, SSR 500 & BSR 500 cascades is marginally higher than that for PSR 250, SSR 250 & BSR 250 cascades employing same blade profile. However this loss in case of PSR 500, SSR 500 & BSR 500 cascades employing blade profile 5530 is found to be less than the similar cascades employing blade profile 6030. This loss is measured to be 6.00, 2.75 and 4.41 for similar cascades employing blade profile 6030 respectively. The results with regard to secondary loss for roughness of 500 µm show that this loss generated for SSR cascades are least among all the three cascades i.e. PSR 500, SSR

500 & BSR 500. Whereas for the case of roughness of 250 µm, the secondary loss for PSR Cascades is least among all the three similar cascades. This loss, however, is found to be least for SSR Cascades among all the three similar cascades, for all roughness values i.e. 250, 500, 750 &1000 µm, employing blade profile 6030. Therefore the phenomenon of reduction in secondary losses due to formation of counter vortex, for the SSR cascades employing the blade profile 6030, seems not to be present for the case of roughness of 250 µm for cascades employing blade profile 5530. The same phenomena seems to be present for cascades for roughness value of 500 µm, employing blade profile 5530. The reason behind the absence of phenomenon of formation of counter vortex in case of roughness of 250 µm for cascades employing blade profile 5530, may be that the nondimensional equivalent roughness is not sufficiently high so as to protrude out from hydrodynamic layer formed closed to the rough surface i.e. suction surfaces of all blades.

The results presented in previous paragraphs concludes that similar trend is observed for total, profile and secondary loss generated due to increasing the roughness. The trend is observed to be similar for generation of losses on account of changing of location of roughness application for cascades employing blade profile 6030 and 5530. The results of secondary loss for 500 µm show that this loss generated for SSR cascades are least. So is in the case of blade profile 6030. Therefore it can also be concluded that behaviour of the two reaction type cascades employing different profiles i.e. 5530 & 6030, are qualitatively similar for total, profile and secondary loss. The increment or changes with the increase in roughness, in total, profile and secondary loss for blade profile 5530 are, however, different from the results compared with similar cases of blade profile 6030, choosing the respective losses of smooth cascade as base. The magnitude of secondary loss for the smooth cascades are

however found to be 1.3% higher for blade profile 6030 than that for blade profile 5530. This difference is maximum in the case of two PSR cascades employing blade profiles 6030 and 5530. It is found to be 1.5% higher for the roughness of 250 µm when applied over pressure surfaces of all blades of cascade employing blade profile 6030 comparing with the results for similar cascades employing blade profile 5530.

5.3.6 Measurements of magnitude of losses for PSR, SSR & BSR cascades for blade profile 5530 for roughnesses of 750 and 1000 µm

The above stated trend with regard to change in total, profile and secondary losses for other remaining roughnesses i.e. 750 and 1000 µm is found to be similar to that for the roughness magnitude of 250 and 500 µm. The total & profile losses are slightly increased when roughness is applied over pressure surface. The combined effect of roughness over pressure and suction surface is seen when the case of roughness over both the surfaces is applied together. It is observed from table 5.20 that the total & profile losses increased marginally when roughness of same magnitude is applied over suction surface comparing to losses for similar case of application of roughness on pressure surface. The trend for behaviour of the two reaction type cascades employing different profiles i.e. 5530 & 6030, are qualitatively similar for total, profile and secondary loss even for application of roughness of higher magnitudes such as 750 and 1000 µm. However, the increment or changes with the increase in roughness, in total, profile and secondary loss are very low, as compared with similar cases of blade profile 6030 comparing with respective smooth cascade. The results for total, profile and secondary loss for application of roughness of magnitudes such as 750 and 1000 µm are not discussed in detail in this dissertation to avoid repetitiveness. The losses so measured are tabulated and are shown in table 5.20.

5.3.7 Summary of the magnitudes of Total Energy Loss, Profile Loss and Secondary Loss for smooth, SSR, PSR & BSR cascades for different levels of roughness for turbine cascades employing blade profiles 5530

The table 5.20 shows a summary of the magnitudes of all types of losses for smooth, SSR, PSR & BSR cascades for different levels of roughness for turbine cascades employing blade profiles 5530.

Table 5.17 : Summary of the magnitudes of Total Energy Loss, Profile Loss and Secondary Loss for smooth, SSR, PSR & BSR cascades for different levels of roughness for turbine cascades employing blade profiles 5530

Type of cascade	Roughness levels	Percentage of Total energy loss in total energy of the air (A)	Percentage of Profile loss in total energy of the air (B)	Contribution of secondary loss (C=A-B)	percentage of Secondary loss relative to total loss in same cascade	percentage of Secondary loss as nondimensionalised with total loss of the smooth cascade	percentage of profile loss relative to total loss of the given cascade	Non-dimensionalising Profile loss with total loss in smooth Blade cascade
smooth	------	19.610	19.350	0.260	1.327	1.327	98.673	98.673
PSR	250	19.687	19.425	0.261	1.327	1.333	98.673	99.056
	500	19.852	19.472	0.380	1.914	1.937	98.086	99.297
	750	19.839	19.501	0.338	1.704	1.724	98.296	99.441
	1000	19.845	19.522	0.323	1.630	1.649	98.370	99.548
SSR	250	19.883	19.591	0.293	1.473	1.493	98.527	99.900
	500	20.003	19.714	0.289	1.446	1.475	98.554	100.526
	750	20.075	19.788	0.287	1.431	1.465	98.569	100.905
	1000	20.131	19.845	0.286	1.419	1.457	98.581	101.197
BSR	250	19.958	19.665	0.294	1.472	1.498	98.528	100.277
	500	20.149	19.834	0.315	1.564	1.607	98.436	101.141
	750	20.187	19.936	0.251	1.242	1.278	98.758	101.661
	1000	20.263	20.014	0.249	1.230	1.271	98.770	102.059

In order to present comparison of trends of change in losses with the increase in magnitude of roughness for SSR PSR & BSR cascades for blade profile 5530 and blade profile 6030, differences of magnitudes of various parameters i.e. Total Energy

Loss, Profile Loss and Secondary Loss for smooth, SSR, PSR & BSR cascades for different levels of roughness for the same blade profiles are presented in table 5.21. The magnitudes of losses presented in the table 5.21 may be analysed for finding quantitative differences and similarities for blade profile 5530, comparing with a blade profile 6030.

Table 5.18: Difference between magnitudes of various parameters i.e. Total Energy Loss, Profile Loss and Secondary Loss for smooth, SSR, PSR & BSR cascades for application of different levels of roughness

Type of cascade	Roughness levels	Difference in magnitudes of various parameters of cascades employing blade profile 5530 & 6030						
		Total loss in percentage of total energy	Profile loss in percentage of total energy	Percentage of profile loss in total loss of the same cascade	Non-dimensionalising profile loss with total loss in smooth blade cascade	Absolute value of percentage sec loss	Percentage of sec. Loss in total loss of the same cascade	Non-dimensionalising sec. Loss with total loss in smooth blade cascade
smooth	0	9.08	9.34	3.61	3.61	-0.26	-3.61	-1.33
PSR	250	7.98	8.29	3.51	-6.71	-0.30	-3.51	-1.55
	500	7.61	7.87	3.25	-10.89	-0.25	-3.25	-1.29
	750	7.51	7.77	3.21	-11.89	-0.27	-3.21	-1.36
	1000	7.51	7.80	3.28	-11.78	-0.28	-3.28	-1.44
SSR	250	3.91	3.93	0.49	-48.75	-0.02	-0.49	-0.10
	500	2.22	2.22	0.18	-65.56	0.00	-0.18	0.00
	750	2.11	2.09	0.02	-67.16	0.03	-0.02	0.13
	1000	2.17	2.14	0.04	-66.87	0.02	-0.04	0.12
BSR	250	2.86	3.06	1.40	-57.41	-0.20	-1.40	-1.01
	500	0.73	0.88	0.83	-78.78	-0.15	-0.83	-0.76
	750	0.47	0.68	1.11	-81.13	-0.21	-1.11	-1.08
	1000	0.55	0.76	1.12	-80.73	-0.21	-1.12	-1.09

The results shown in columns representing total and profile loss in the table 5.21 reveal that PSR cascades i.e. PSR 250, PSR 500, PSR 750 & PSR 1000 μm, employing blade profile 5530 result 7.98, 7.61, 7.50 and 7.51 percent more total loss than for similar

cascades employing blade profile 6030 respectively. This goes to show that same roughness is more detrimental on the pressure surface of blades of the cascades employing blade profile 5530 comparing with the cascades employing blade profile 6030. This difference in total loss reduces for higher value of roughnesses. However this difference in total loss for PSR 750 & PSR 1000 µm cascade is almost same.

The roughness on surfaces of blades of the cascades employing blade profile 5530 is lesser detrimental than the cascades employing blade profile 6030 with regard to generation of magnitude of secondary losses. Moreover, the same roughness of 750 & 1000 µm on the suction surfaces of the blade of cascades employing blade profile 5530 result into more secondary loss comparing that with the cascades employing blade profile 6030. In fact, the magnitude of secondary loss generated due to application of same roughness on pressure surfaces of blades of cascades employing blade profile 6030 are measured to be significantly higher than application of the same roughness on suction surfaces of the blades of the same cascades. However the same phenomena is not strong in the case of cascades employing blade profile 5530.

The profile loss contributes more into total loss for cascades employing blade profile 5530 than the cascades employing blade profile 6030. The magnitude of profile loss for all the cascades employing blade profile 5530, except PSR cascades even exceeded the magnitude of total loss for smooth cascades employing same blade profile. The percentage of profile loss when nondimensionalized with percentages of total loss for smooth cascades, for all the cascades employing blade profile 5530, except PSR cascades is shown to be exceeding value more than 100 in table 5.21.

It is also clear from figure 5. 65 and 5.66 that the total and profile losses for SSR and BSR cascades for both roughness values i.e. 750 and 1000µm are higher than that of

smooth cascade. The values of mass averaged loss coefficient for PSR and smooth cascade are almost same for both roughness values. Therefore the loss coefficient axis in both the figures 5.65 and 5.66 have been formatted to exaggerate the variation so as the graphs for PSR and smooth cascade may be separately shown in each figure.

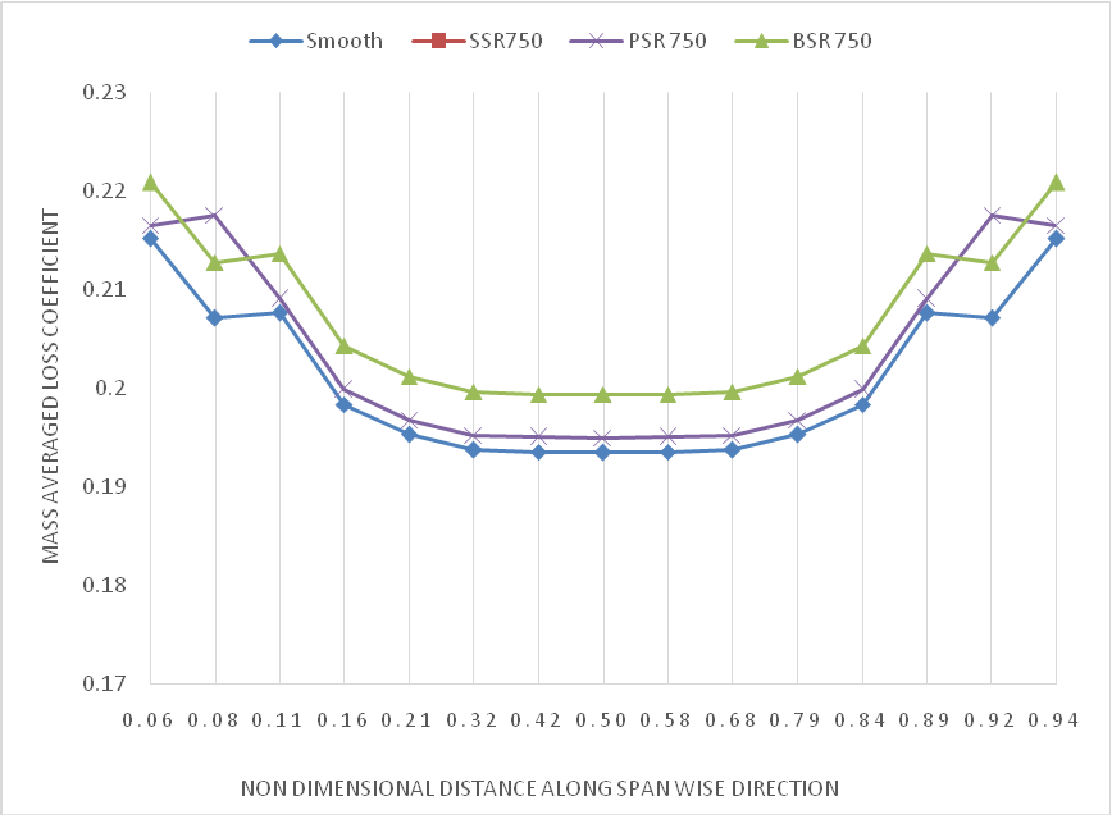

Figure 5.65 : Variation of mass averaged loss coefficients with respect to Non-Dimensional Distance from bottom to top endwall for smooth, PSR 750, SSR 750 & BSR 750 cascades employing blade profile 5530

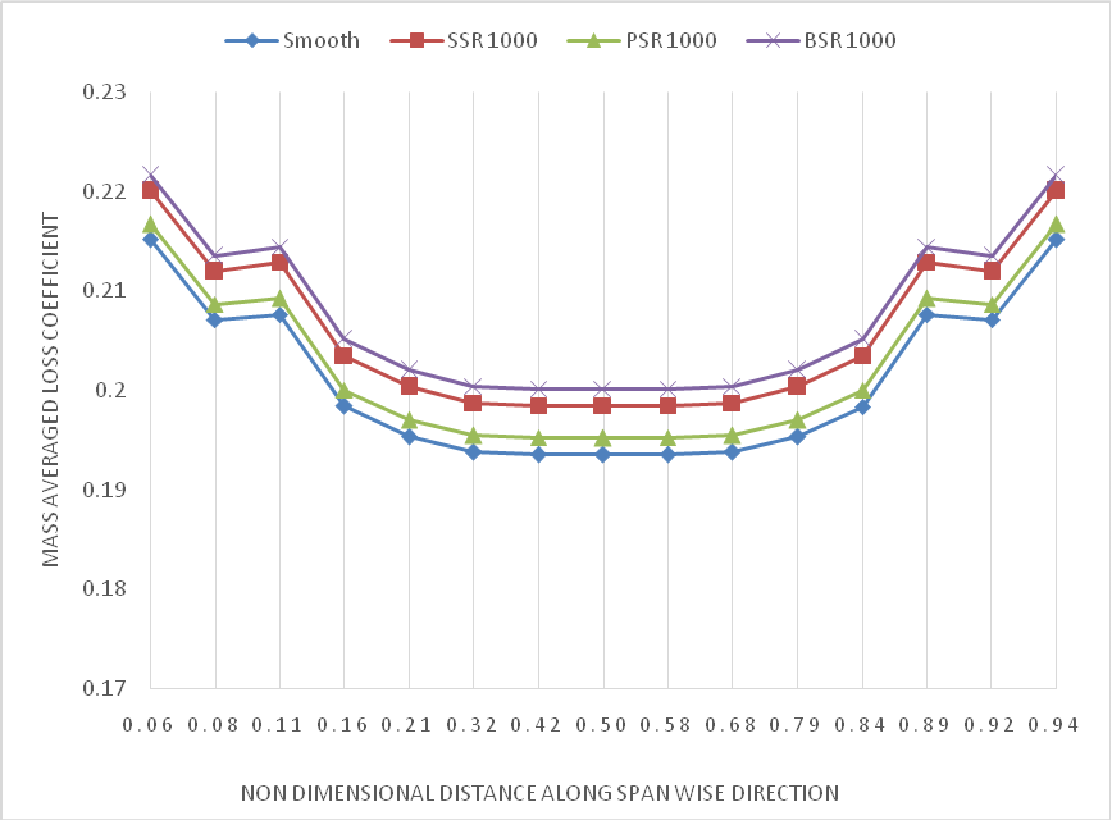

Figure 5.66: Variation of mass averaged loss coefficients with respect to Non-Dimensional Distance from bottom to top endwall for smooth, PSR 1000, SSR 1000 & BSR 1000 cascades employing blade profile 5530

5.4 Measurement of magnitude of losses for Turbine Cascades employing blade profiles 3525:

Computational study is conducted for blade profiles 3525 also, focusing mainly on analysis of the effect of roughness similar to other cascades employing blade profiles 6030 and 5530. Similarly, measurement of total, profile & secondary loss is carried out by successively employing roughnesses on the surfaces of blades of the cascades for profiles 3525 using various combinations of surfaces and roughnesses. The roughnesses of 250, 500, 750 &1000 µm are applied on suction and pressure surfaces individually as well as on both the surfaces together. It is observed that trend of increasing of total and profile loss coefficient on applying of roughness on blade

surfaces of cascade employing blade profile 3525 is also same that of cascades employing blade profiles 6030 and 5530. However the magnitudes of losses for this blade profile are different than previously discussed cascades employing blade profiles 6030 and 5530 for turbine.

The different magnitudes of losses are attributed to the difference in various parameters like shape, geometry etc. of blade profile 3525 with that of blade profiles 6030 and 5530, separately. The degree of reaction of blade profile 3525 is about 10 %, i.e., the convergence of inter blade channels formed by this profile is less than other blade profiles. The blade profile 3525 is comparatively more symmetric around the midspan position, due to its being nearly impulse type. The curvilinear lengths of suction and pressure surfaces of this profile are 59.5 mm & 82.5 mm, compared to 55 mm & 66 mm, and 55 mm & 64 mm for profiles 6030, 5530 respectively. The blade profiles discussed earlier i.e. 6030 and 5530 are not so different from each other. Therefore, losses generation mechanisms are similar in many respects for blade profiles 6030 and 5530. Whereas the losses generation mechanism for blade profile 3525 has less similarities with blade profile 6030. The pattern of variation of parameters such as local loss coefficients, mass averaged loss coefficients for all such cascades are found similar in shape to that of the blade profiles 6030 and 5530. Comparison of loss coefficients in all cascades employing for blade profile 3525, reveals that the loss coefficient is high at hub and casing due to the endwall boundary layers for both roughness values. It is clear that the mass averaged loss coefficients near the end walls at both ends are higher than their values at mid span of the blade, as in case of cascades employing blade profiles 6030 and 5530.

However, the magnitudes of losses for blade profile 3525, on account of various reasons as mentioned above, differ from that for both blade profiles 6030 and 5530.

The local loss coefficients vary relative to pitchwise direction in the similar way to that of earlier discussed blade profiles 6030 and 5530. Similarly the variation of the mass averaged loss coefficients relative to span wise distance is also same to that of blade profiles 6030 and 5530.

The details with regard to trend of change in magnitude of losses with the increase in magnitude of roughness for SSR PSR & BSR cascades for the blade profile 3525 are presented in this section.

5.4.1 Measurements of magnitude of losses for Smooth cascades for blade profiles 3525

The table 5.22 shows as to how total, profile and secondary losses vary for three different cascades employing smooth blade profiles 6030, 5530 and 3525 separately. The total and profile loss are expressed in percentage of total energy of the air at the inlet. The total and profile losses for smooth cascades employing smooth blade profile 3525 are measured to be 18.34 and **17.98**% of the total energy of the air at the inlet. The magnitude of total loss is measured to be 18.34 , 10.53 and 19.61 for cascades employing blade profiles 3525, 6030 and 5530 respectively.

The total loss for smooth blade cascade for employing blade profile 3525 is found to be higher than the total loss for cascade employing 6030 blade profile. This loss, for smooth blade cascade for employing blade profile 3525 is however found to be less than that of smooth blade cascade employing blade profile 5530. The profile loss also follows similar trend. The secondary loss however has different trend. This goes to show that the loss mechanism for two separate smooth cascades employing blade profile the 3525 and 5530 are different. The total loss for smooth cascade employing blade profile 6030 is found to be least among all smooth cascades for the three blade profiles.

The results also show that shape or geometry of the blades of the cascades significantly affect the losses. In view of generation of lesser loss in case of cascades employing blade profile 3525 than that of cascades employing blade profile 5530, it can be concluded that smooth blades of the cascades employing blade profile 3525 are aerodynamically more efficient. At the same time, it can also mentioned that smooth blades of the cascades employing blade profile 3525 lesser efficient than that of cascades employing blade profile 6030. The smooth blades of the cascades employing blade profile 6030 is most efficient followed by blade profiles 3525 and 5530 in the same order.

The secondary loss is found to be highest for 6030 followed by blade profiles 3525 and 5530. The magnitudes of secondary loss non-dimensionalising with total loss in smooth blade cascade employing the same blade profiles are found to be 1.97, 4.93 and 1.32 for cascades employing blade profiles 3525, 6030 and 5530 respectively.

In order to present comparison of trends of generation of losses for three different smooth cascades employing separately the blade profiles 3525, 6030 and 5530, magnitude of losses for such cascades are tabulated in table 5.22.

Table 5.19: Comparison of magnitudes of losses for smooth cascades employing blade profiles 3525, 6030 and 5530

Type of cascade	Blade type	Total energy Loss in total energy	Profile Loss in total energy	Total Loss in percentage of total energy	Profile Loss in percentage of total energy	Percentage of Profile Loss in Total Loss of the same cascade	Profile Loss non-dimensionalising with Total Loss in smooth Blade cascade	Absolute Value of percentage Sec. Loss	Percentage of Sec. Loss in Total Loss of the same cascade	Sec. Loss non-dimensionalising with Total Loss in smooth Blade cascade
smooth	3525	0.1834	0.1798	18.34	17.98	98.03	98.03	0.36	1.97	1.97
	6030	0.1053	0.1001	10.53	10.01	95.06	95.06	0.52	4.94	4.94
	5530	0.1961	0.1935	19.61	19.35	98.67	98.67	0.26	1.33	1.33

5.4.2 Measurements of magnitude of losses for PSR 250, SSR 250 & BSR 250 cascades for blade profiles 3525

The effect of changing the location of application of roughness is also measured for the cascades employing blade profile 3525, similar to the case of blade profile 6030 and 5530. This procedure is repeated for all roughnesses. First of all a roughness of 250 µm is applied on pressure surfaces only (PSR 250), suction surfaces only (SSR 250) and pressure surfaces and suction surfaces together (BSR 250) on blades of cascades employing blade profile 3525. The total, profile and secondary losses for turbine cascades i.e. PSR250, SSR250 BSR 250 employing blade profile 3525 are found using similar method as has been used for finding the losses in the case of blade profile 6030 and 5530.

The table 5.23 shows results with regard to total, profile and secondary losses for turbine cascades i.e. PSR250, SSR250 BSR 250 cascades employing blade profile 3525 along with smooth turbine cascade for the same blade profile. The results shown in table 5.23 may be used to compare effect of changing of surface for application of roughness quantitatively.

Table 5.20 : Total, profile and secondary losses for turbine cascades i.e. PSR250, SSR250 BSR 250 cascades employing blade profile 3525

Type of cascade	Roughness levels	Total Loss in total energy of the air	Profile Loss in total energy of the air	Total Loss in percentage of total energy of the air	Profile Loss in percentage of total energy of the air	percentage of Profile Loss in Total Loss of the same cascade	Profile Loss non-dimensionalising with Total Loss in smooth blade cascade	Absolute value of percentage Sec. Loss	percentage of Sec. Loss of the same cascade	Sec. Loss non-dimensionalising with Total Loss in smooth Blade cascade
smooth	–	**0.1834**	**0.1798**	**18.34**	**17.98**	**98.03**	**98.03**	**0.36**	**1.97**	**1.97**
PSR	250	0.1841	0.1803	18.41	18.03	97.92	98.30	0.38	2.08	2.08
SSR	250	0.1891	0.1853	18.91	18.53	97.98	101.03	0.38	2.02	2.08
BSR	250	0.1894	0.1858	18.94	18.58	98.08	101.30	0.36	1.92	1.98

The table 5.23 shows that the total losses are maximum for BSR cascades followed by SSR and PSR Cascades in the same order. The total losses for PSR 250, SSR 250 & BSR 250 cascades for blade profiles 3525 are measured to be 18.41, 18.91and 18.94 % of the total energy of the air at the inlet of the cascade respectively as against the total loss of 18.34 % for the smooth cascade employing same blade profile.

The trend for profile losses is also similar to that of total loss. The profile losses for PSR 250, SSR 250 & BSR 250 cascades for the same blade profile are measured to be 18.03, 18.53 and 18.58 % respectively as against the profile loss of 17.98 % for the smooth cascade. The profile loss is also found to be maximum for BSR Cascades followed by SSR and PSR cascades in the same order when same roughness of 250 μm is applied separately over various surfaces of the cascades, one by one. It is clarified from results that due to application of roughness of 250 μm, total and profile loss are increased for each of the PSR 250, SSR 250 & BSR 250 cascades. The effect on total and profile loss is however different for each of the PSR 250, SSR 250 & BSR 250 cascades. It can be mentioned that changing the location of application of roughness choosing different magnitudes of roughnesses, one by one, marginally affect the total as well as profile losses for the cascades employing blade profile 3525. The effect is marginal similar to case of blade profile 5530.

The secondary loss for PSR 250, SSR 250 & BSR 250 cascades for the same blade profile are measured to be 2.08, 2.08 and 1.98 (non-dimensionalising with total loss of smooth cascade) respectively against the secondary loss of 1.97 % for the smooth cascade**.** The results with regard to secondary loss show that this loss generated for PSR 250, SSR 250 Cascades are marginal higher than that for BSR 250 cascade. The roughness on pressure surfaces and suction surface of the cascade are equally detrimental as far as secondary loss is concerned. The magnitude of secondary loss for

both of the cascades are found to be nearly equal. The magnitude of secondary loss for BSR 250 cascade is found to be nearly equal to that of smooth cascade.

In view to make quantitative comparison of variation of mass averaged loss coefficients for cascades such as PSR 250, SSR 250 & BSR 250 cascades and the smooth cascade, employing blade profile 3525, the combined graph showing the variation mass averaged loss coefficients for all cascades may be referred in figure 5.67. The combined plot in the figure 5.67 clarify as to how total and profile losses for PSR 250 and smooth cascade are almost same. The total and profile losses for SSR 250 and BSR 250 cascades are higher than that of smooth cascade. The values of mass averaged loss coefficient for PSR 250 and smooth cascade. Therefore the loss coefficient axis in the figure 5.67 has been formatted to exaggerate the variation so as the graphs for PSR 250 and smooth cascade may be separately shown.

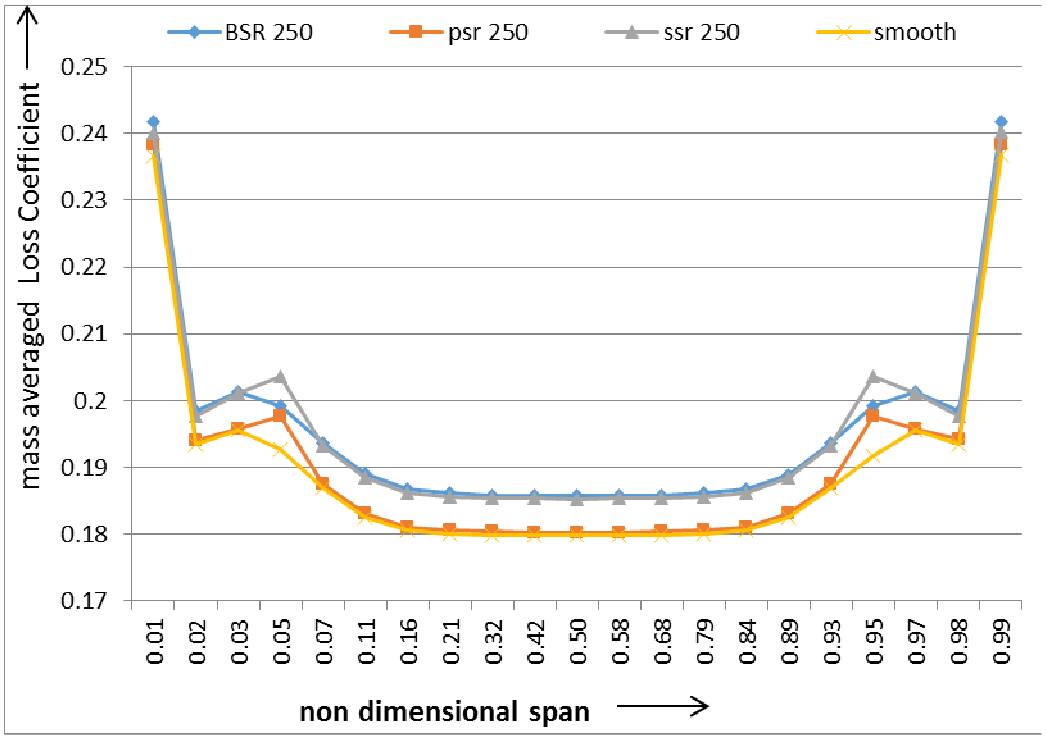

Figure 5.67: Variation of mass averaged loss coefficients with respect to Non-Dimensional Distance from bottom to top endwall for smooth, PSR 250, SSR 250 & BSR 250 cascades employing blade profile 3525

5.4.3 Measurements of magnitude of losses for PSR 500, SSR 500 & BSR 500 cascades for blade profiles 3525:

The total, profile and secondary losses for turbine cascades, employing blade profile 3525, are measured by applying roughness of 500 µm on pressure surfaces only (PSR 500), suction surfaces only (SSR 500) and pressure surfaces and suction surfaces together (BSR 500), one by one.

In order to compare effect of changing of surface for application of roughness of 500 µm, quantitatively, results with regard to total, profile and secondary losses for turbine cascades i.e. PSR500, SSR500 BSR 500 cascades employing blade profile 3525 along with smooth turbine cascade are tabulated in the table 5.24.

Table 5.21: Total, profile and secondary losses for turbine cascades i.e. PSR500, SSR500 BSR 500 cascades employing blade profile 3525

Type of cascade	Roughness levels	Total energy Loss in total energy	Profile Loss in total energy	Total Loss in percentage of total energy	Profile Loss in percentage of total energy	Percentage of Profile Loss in Total Loss of the same cascade	Profile Loss non-dimensionalising with Total Loss in smooth Blade cascade	Absolute Value of percentage Sec. Loss	Percentage of Sec. Loss in Total Loss of the same cascade	Sec. Loss non-dimensionalising with Total Loss in smooth Blade cascade
smooth	0	0.1834	0.1798	18.34	17.98	98.03	98.03	0.36	1.97	1.97
PSR	500	0.1894	0.1858	18.94	18.58	98.08	101.3	0.36	1.92	1.98
SSR	500	0.1841	0.1803	18.41	18.03	97.93	98.3	0.38	2.08	2.08
BSR	500	0.1891	0.1853	18.91	18.53	97.98	101.03	0.38	2.02	2.09

It is found that the percentage of total loss when roughness of 500 µm is applied separately over the entire pressure surface i.e. PSR 500 and suction surface i.e. SSR 500 are measured to be 18.94% and 18.41% respectively for blade profile 3525. This loss is measured to be 18.34 % when no roughness is applied. The total loss for BSR 500 cascade (18.91%) is measured to be marginally higher than SSR 500 cascades (18.41%).

The total loss for SSR 500 and BSR 500 cascades are measured to be less than that for SSR 250 and BSR 250 cascades. The total loss for SSR 500 and BSR 500 cascades are measured to be 18.41% 18.91% respectively. On the other hand, the total loss for SSR 250 and BSR 250 cascades are measured to be18.91% and 18.94% respectively. It concludes that total loss due to effect of higher roughness of 500 µm on suction surfaces individually and both surfaces together of the blades of a given cascades reduces comparing the same with the similar values of total loss measured for similar cascades for roughness of 250 µm. This trend is opposite to that of the blade profile 6030. It is observed that same roughness is significantly detrimental with regard to total & profile losses when applied over suction surface followed by pressure surface for the cascades employing blade profile 6030.

The secondary loss for roughness value of 500 µm for cascades employing blade profile 3525, however, has different trend as compared to similar cascades for roughness value 250 µm, employing same blade profile. The secondary loss for PSR, SSR & BSR cascades employing same blade profile 3525 for roughness value of 500 µm are measured to be 1.98, 2.08 and 2.09 percent of total loss of smooth cascade respectively against the secondary loss of 1.97 percent of total loss for smooth cascade employing same blade profile 3525. On the other hand, the secondary loss for same cascades for roughness value of 250µm are measured to be 2.08, 2.08 and 1.98 percent of total loss of smooth cascade employing blade profile 3525 respectively. The secondary loss for 500 µm roughness on the suction surfaces of the blades of the cascade is measured to be equal to the secondary loss measured for similar cascades for roughness of 250 µm. Effect of higher roughness as a result of increasing the roughness from 250 µm to 500 µm loss on suction surfaces individually of the blades of a given cascades is measured to be zero.

The combined graph showing the variation mass averaged loss coefficients for PSR 500, SSR 500 & BSR 500 and the smooth cascade, employing blade profile 3525, is shown in figure 5.68. The combined plot in the figure 5.68 clarify as to how mass averaged loss coefficients vary in the span wise direction for all PSR 500, SSR 500 & BSR 500 cascade. It is also clear that total and profile losses for SSR 500 and BSR 500 cascades are higher than that of smooth cascade. The values of mass averaged loss coefficient for PSR 500 and smooth cascade are almost same. Therefore the loss coefficient axis in the figure 5.68 has been formatted to exaggerate the variation so as the graphs for PSR 500 and smooth cascade may be separately shown.

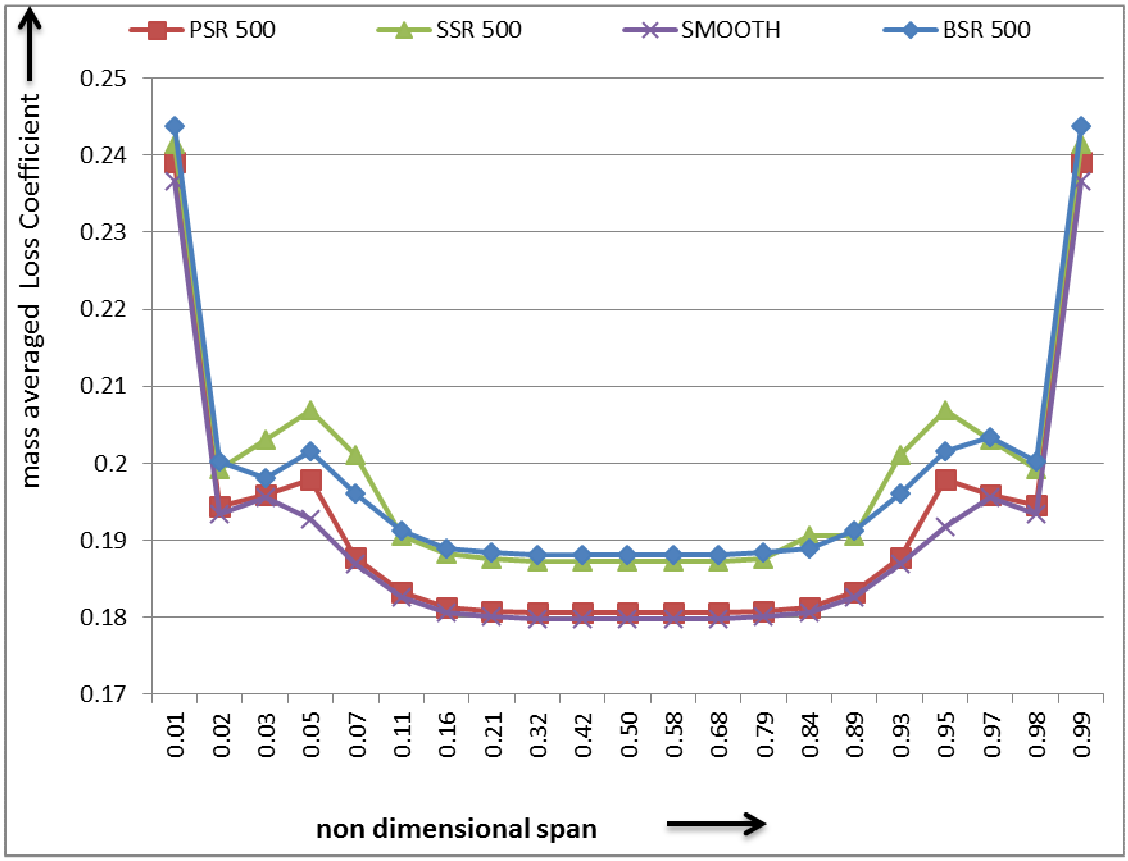

Figure 5.68: Variation of mass averaged loss coefficients with respect to Non-Dimensional Distance from bottom to top endwall for smooth, PSR 500, SSR 500 & BSR 500 cascades employing blade profile 3525

5.4.4 Measurements of magnitude of losses for PSR, SSR & BSR cascades for blade profile 3525 for roughnesses of 750 and 1000 µm

The magnitude of total and profile loss for the PSR, SSR and BSR cascades employing blade profile 3525, for other remaining roughnesses i.e. 750 and 1000 µm are found to be marginally high comparing with the losses measured for smooth cascade and cascades with roughness value of 250 and 500µm employing same blade profile ignoring few results with regard to cascades with roughness value of 500µm.

In order to find effect of same roughness on different locations (surfaces of blades), the results with regard to total, profile and secondary losses for turbine cascades i.e. PSR, SSR and BSR cascades, employing blade profile 3525 along with smooth turbine cascade are tabulated in the table 5.25 and 5.26 for roughness values of 750 and 1000 µm respectively.

Table 5.22: Total, profile and secondary losses for turbine cascades i.e. PSR750, SSR750 and BSR 750 cascades employing blade profile 3525

Type of cascade	Roughness levels	Total energy Loss in total energy	Profile Loss in total energy	Total Loss in percentage of total energy	Profile Loss in percentage of total energy	Percentage of Profile Loss in Total Loss of the same cascade	Profile Loss non-dimensionalising with Total Loss in smooth Blade cascade	Absolute Value of percentage Sec. Loss	Percentage of Sec. Loss in Total Loss of the same cascade	Sec. Loss non-dimensionalising with Total Loss in smooth Blade cascade
smooth	0	0.1834	0.1798	18.34	17.98	98.03	98.03	0.36	1.97	1.97
PSR	750	0.1846	0.1807	18.46	18.07	97.93	98.54	0.38	2.07	2.09
SSR	750	0.1927	0.1886	19.27	18.86	97.87	102.84	0.41	2.13	2.24
BSR	750	0.1930	0.1895	19.30	18.95	98.21	103.34	0.35	1.79	1.88

Table 5.23: Total, profile and secondary losses for turbine cascades i.e. PSR 1000, SSR 1000 and BSR 1000 cascades employing blade profile 3525

Type of cascade	Roughness levels	Total Loss in total energy of the air	Profile Loss in total energy of the air	Total Loss in percentage of total energy of the air	Profile Loss in percentage of total energy of the air	percentage of Profile Loss in Total Loss of the same cascade	Profile Loss non-dimensionalising with Total Loss in smooth blade cascade	Absolute value of percentage Sec. Loss	percentage of Sec. Loss of the same cascade	Sec. Loss non-dimensionalising with Total Loss in smooth Blade cascade
smooth	0	0.1834	0.1798	18.34	17.98	98.03	98.03	0.36	1.97	1.97
PSR	1000	0.1847	0.1809	18.47	18.09	97.93	98.62	0.38	2.07	2.09
SSR	1000	0.1938	0.1897	19.38	18.97	97.87	103.41	0.41	2.13	2.25
BSR	1000	0.1946	0.1907	19.46	19.07	98.00	103.98	0.39	2.00	2.12

The percentage of profile loss for PSR 750, SSR 750 and BSR750 cascades, non-dimensionalising with total loss of the smooth cascade, is measured to be 98.54, 102.84 and 103.34% respectively. The percentages of profile loss non-dimensionalising with total loss of the smooth cascade with regard to all BSR cascades and SSR cascades for roughness value of 750 and 1000 µm are obtained to be higher than 100. The percentages exceeding to 100 show that magnitude of profile loss for the given cascade is more than magnitude of total loss for smooth cascade, employing same blade profile.

The change in losses with the increase in roughness is highest when a respective total and profile losses for smooth cascade and another cascade with roughness of 250 µm are compared. Similarly the difference of respective losses for two cascades one each for roughness values 250 and 500 µm will be lower than the difference for smooth cascade and another cascade with roughness of 250 µm. This trend is continued for next two roughness values i.e. from 500 to 750 µm and 750 to 1000 µm. The difference in values of total and profile losses for increasing of roughness from 750µm to 1000 µm is least among all such intervals of roughness increments. Results with regard to total and profile losses show that the increment in the magnitude of total and profile losses from the magnitude of losses at lower values of roughnesses for BSR cascade, is very less. In fact, magnitudes of total and profile losses are almost equal for both roughness values i.e. 750µm and 1000 µm.

The results for total, profile and secondary loss for application of roughness of magnitudes such as 750 and 1000 µm are not discussed, in detail, in this dissertation to avoid repetitiveness. The losses so measured are tabulated and are shown in table 5.25 and 5.26.

The graphical representation of all PSR, SSR & BSR cascades for both roughness values i.e. 750 and 1000µm are shown in figure 5.69 and 5.70 respectively. The combined graph in the figure 5.69 shows the variation of mass averaged loss coefficients for all PSR 750, SSR 750 & BSR 750 and the smooth cascade. Another combined graph in the figure 5.70 shows the variation of mass averaged loss coefficients for all PSR 1000, SSR 1000 & BSR 1000 and the smooth cascade. The combined plots in both the figures 5.69 and 5.70 clarify as to how mass averaged loss coefficients vary in the span wise direction for all PSR SSR & BSR cascade for roughness values of 750 and 1000 µm respectively.

It is also clear from figure 5.69 and 5.70 that the total and profile losses for SSR and BSR cascades for both roughness values i.e. 750 and 1000µm are higher than that of smooth cascade. The values of mass averaged loss coefficient for PSR and smooth cascade are almost same for both roughness values. Therefore, the loss coefficient axis in both the figures 5.69 and 5.70 have been formatted to exaggerate the variation so as the graphs for PSR and smooth cascade may be separately shown in each figure.

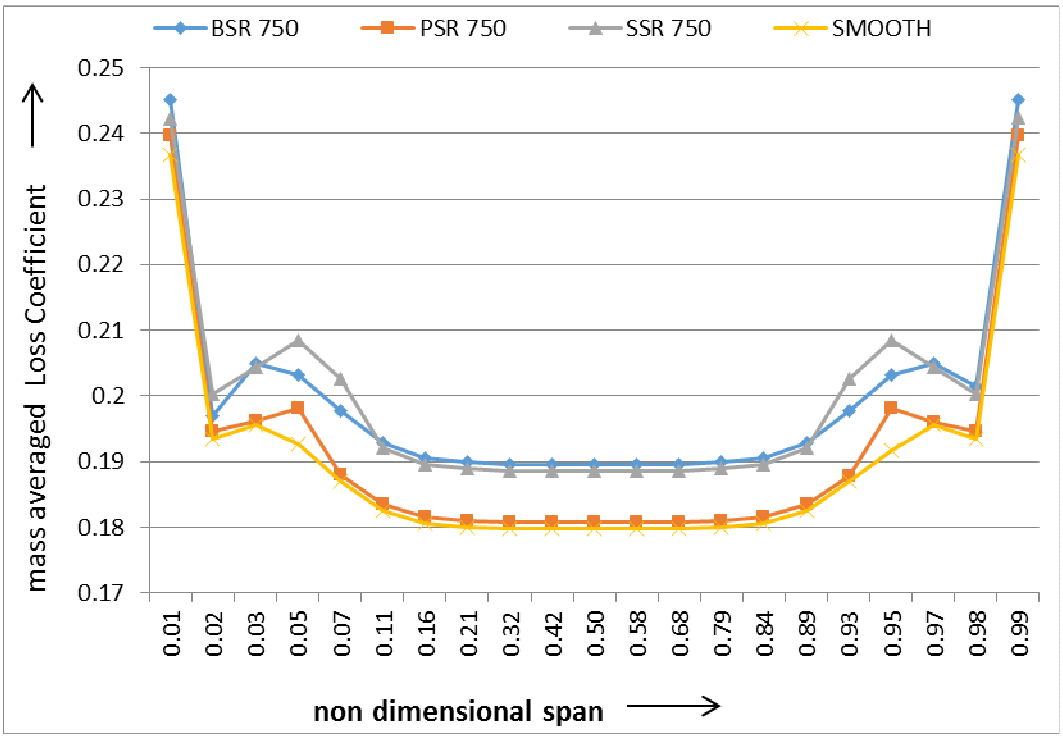

Figure 5.69: Variation of mass averaged loss coefficients with respect to Non-Dimensional Distance from bottom to top endwall for smooth, PSR 750, SSR 750 & BSR 750 cascades employing blade profile 3525

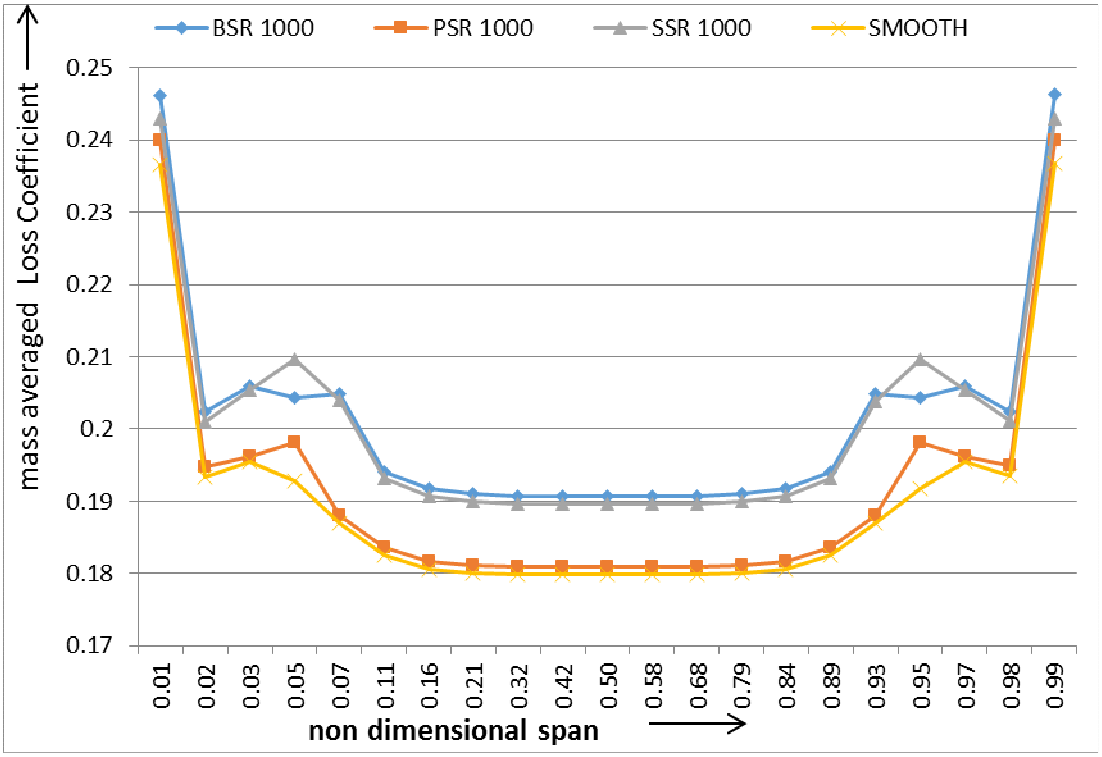

Figure 5.70: Variation of mass averaged loss coefficients with respect to Non-Dimensional Distance from bottom to top endwall for smooth, PSR 1000, SSR 1000 & BSR 1000 cascades employing blade profile 3525

The various figures related to variation of mass averaged loss coefficient reveal that the losses are higher at hub and casing than at mid span of the blade due to the endwall boundary layers for all roughness values.

5.4.5 Summary of Total Energy Loss, Profile Loss and Secondary Loss for smooth, SSR, PSR & BSR cascades for different levels of roughness for turbine cascades employing blade profile 3525

The table 5.27 shows a summary of the magnitudes of all types of losses for different levels of roughness for turbine cascades employing blade profile 3525.

Table 5.24 : Summary of the magnitudes of Total Energy Loss, Profile Loss and Secondary Loss for smooth, SSR, PSR & BSR cascades for different levels of roughness for turbine cascades employing blade profiles 3525

Type of cascade	Roughness levels	Total Loss in total energy of the air	Profile Loss in total energy of the air	Total Loss in percentage of total energy of the air	Profile Loss in percentage of total energy of the air	percentage of Profile Loss in Total Loss of the same cascade	Profile Loss non-dimensionalising with Total Loss in smooth blade cascade	Absolute value of percentage Sec. Loss	percentage of Sec. Loss of the same cascade	Sec. Loss non-dimensionalising with Total Loss in smooth Blade cascade
smooth	0	0.1834	0.1798	18.34	17.98	98.03	98.03	0.36	1.97	1.97
PSR	250	0.1841	0.1803	18.41	18.03	97.92	98.30	0.38	2.08	2.08
	500	0.1844	0.1806	18.44	18.06	97.93	98.45	0.38	2.07	2.09
	750	0.1846	0.1807	18.46	18.07	97.93	98.54	0.38	2.07	2.09
	1000	0.1847	0.1809	18.47	18.09	97.93	98.62	0.38	2.07	2.09
SSR	250	0.1891	0.1853	18.91	18.53	97.98	101.03	0.38	2.02	2.08
	500	0.1938	0.1897	19.38	18.97	97.87	103.41	0.41	2.13	2.25
	750	0.1927	0.1886	19.27	18.86	97.87	102.84	0.41	2.13	2.24
	1000	0.1938	0.1897	19.38	18.97	97.87	103.41	0.41	2.13	2.25
BSR	250	0.1894	0.1858	18.94	18.58	98.08	101.30	0.36	1.92	1.98
	500	0.1915	0.1880	19.15	18.80	98.22	102.52	0.34	1.78	1.86
	750	0.1930	0.1895	19.30	18.95	98.21	103.34	0.35	1.79	1.88
	1000	0.1946	0.1907	19.46	19.07	98.00	103.98	0.39	2.00	2.12

It is shown in the table 5.27 that the increment or changes in total, profile and secondary loss with the increase in roughness for the cascades employing blade

profile 3525, similar to the case of blade profile 5530, are very low comparing with respective smooth cascade. Therefore it is clear that increment or changes in the magnitude of losses with the increase in roughness is highest for blade profile 6030 followed by 5530 and 3525 in the same order. However the total and profile loss measured for SSR 500 (19.38 and 18.97%) cascade are exceptionally higher than that for SSR 750 cascade (19.27 and 18.86%) employing same blade profile. Therefore it can be concluded that trend of changing of magnitudes of losses i.e. profile loss and total loss with the increasing roughness on the surface of the blades of cascades employing blade profile 3525, ignoring few of magnitudes of total and profile losses for SSR 500 cascades (table 5.27), is similar to that of other blade profiles such as 6030 and 5530. On the basis of results it can be concluded that similar to the case of total loss, profile loss is also increased with increasing roughness. The percentages of profile loss non-dimensionalising with total loss of the smooth cascade are obtained to be higher than 100 for BSR cascades, for all roughness values. Similarly the roughness on suction surfaces of the blades of the cascades, employing blade profile 3525 are contributing more to generation of profile loss. The percentages of profile loss non-dimensionalising with total loss of the smooth cascade for all SSR cascades are also obtained to be higher than 100.

The secondary loss is measured to be high for high roughness values such as 750 and 1000 μm for cascades, employing blade profile 3525. The roughness on suction surfaces of the blades of the cascades, employing blade profile 3525, in general, contributes more to generation of secondary loss comparing with PSR and BSR cascades. The percentages of secondary loss non-dimensionalising with total loss of the smooth cascade for all SSR cascades are also measured to be higher than that obtained for PSR and BSR cascades (table 5.27).

In order to present comparison of trends of change in losses with the increase in magnitude of roughness, differences of magnitudes of various parameters i.e. Total Energy Loss, Profile Loss and Secondary Loss for smooth, SSR, PSR & BSR cascades for blade profile 3525 and blade profile 6030, for different levels of roughness are presented in table 5.28. The magnitudes of losses presented in the table 5.28 may be analysed for finding quantitative differences and similarities for blade profile 3525, comparing with a blade profile 6030.

Table 5.25: Difference between magnitudes of various parameters i.e. Total Energy Loss, Profile Loss and Secondary Loss for smooth, SSR, PSR & BSR cascades for application of different levels of roughness

Type of cascade	Roughness levels	Difference of values of various parameters for 3525 and 6030 blade profile						
		Total loss in percentage of total energy	Profile loss in percentage of total energy	Percentage of profile loss in total loss of the same cascade	Non-dimensionalising profile loss with total loss in smooth blade cascade	Absolute value of percentage sec loss	Percentage of sec. Loss in total loss of the same cascade	Non-dimensionalising sec. Loss with total loss in smooth blade cascade
smooth	0	7.81	7.97	2.97	2.97	-0.16	-2.97	-0.68
PSR	250	6.71	6.89	2.76	-7.47	-0.18	-2.76	-0.80
	500	6.20	6.45	3.09	-11.74	-0.25	-3.09	-1.14
	750	6.13	6.35	2.84	-12.79	-0.22	-2.84	-1.00
	1000	6.14	6.36	2.84	-12.72	-0.22	-2.84	-1.00
SSR	250	2.94	2.87	-0.06	-47.62	0.07	0.06	0.49
	500	1.60	1.47	-0.50	-62.67	0.12	0.50	0.77
	750	1.31	1.16	-0.68	-65.23	0.15	0.68	0.91
	1000	1.42	1.27	-0.67	-64.65	0.15	0.67	0.91
BSR	250	1.84	1.97	0.95	-56.39	-0.13	-0.95	-0.52
	500	-0.27	-0.15	0.61	-77.40	-0.12	-0.61	-0.51
	750	-0.42	-0.30	0.56	-79.44	-0.12	-0.56	-0.48
	1000	-0.26	-0.18	0.35	-78.80	-0.07	-0.35	-0.24

The results shown in columns representing total and profile loss in the table 5.28 reveal that PSR cascades i.e. PSR 250, PSR 500, PSR 750 & PSR 1000 µm, employing blade profile 3525 result 6.71, 6.20, 6.13 and 6.14 percent more total loss than for similar cascades employing blade profile 6030 respectively. This difference for two cascades employing smooth blade profile 3525 and 6030 is found to be 7.81 percent. The PSR cascades i.e. PSR 250, PSR 500, PSR 750 & PSR 1000 µm, employing blade profile 5530 result 7.98, 7.61, 7.51 and 7.51 percent more total loss than for similar cascades employing blade profile 6030 respectively. The difference for two cascades employing smooth blade profile 5530 and 6030 is found to be 7.81 percent. This goes to show that same roughness is more detrimental on the pressure surface of blades of the cascades employing blade profile 3525 comparing with the cascades employing blade profile 6030. However the total loss generated for smooth cascades employing blade profile 5530 is higher than other remaining profiles i.e. 3525 and 6030 in the same order. The total loss generated for cascades employing blade profile 3525, for all roughness values, is higher than that generated for cascades employing blade profile 6030 except for BSR500, BSR 750 and BSR 1000 cascades. The total loss generated for BSR500, BSR 750 and BSR 1000 cascades employing blade profile 3525 is measured to be lesser by 0.27, 0.42 and 0.26 percent than for similar cascades employing blade profile 6030 (table 5.16) respectively.

The roughness on surfaces of blades of the cascades employing blade profile 3525 is lesser detrimental than the cascades employing blade profile 6030 with regard to generation of magnitude of secondary losses. Moreover, the each roughness of 250, 500, 750 and 1000 µm on the suction surfaces of the blade of cascades employing blade profile 3525 result into more secondary loss comparing to secondary loss generated for the same cascades employing blade profile 6030 (table 5.16). However,

secondary loss generated for PSR 250, PSR 500, PSR 750 and PSR 1000 cascades employing blade profile 3525 are measured to be lesser than same cascades employing blade profile 6030. Similarly the secondary loss generated for BSR 250, BSR 500, BSR 750 and BSR 1000 cascades employing blade profile 3525 are measured to be lesser than same cascades employing blade profile 6030 (table 5.16).

5.5 Comparison of magnitude of losses for application of localized roughnesses for Turbine Cascades for blade profiles 6030, 5530 and 3525

In previous sections of chapter, the results of the study of a number of cascades for application of roughness on entire surface for all combinations of the profiles of blade, magnitudes of roughness and locations of roughness are presented. This number of cascades increases when additional locations for surface roughness application are added. There are total 13 numbers of cascades to be simulated separately for each of combinations of roughness magnitude, location of roughness and the given single blade profile for application of roughness on entire surface. In an actual turbine, roughness is not only found over entire surfaces of the blades but over a small portion of the surface of the blades also. The roughness is found, in the form of bands also on leading edge, middle chord and trailing edge of pressure and suction surfaces of turbine cascades.

Therefore, in order to study effect of localised roughness on the blades of cascades, numerous number of cascades are simulated in addition to earlier discussed cascades. In order to simulate such cascades, localised roughnesses of varying magnitudes are separately applied over three equal portions of pressure and suction surfaces of the cascade, one by one. There 6 number of locations over the suction and pressure surfaces of given cascade, in all, for application of roughnesses of 250, 500, 750 and

1000 µm. Each of the cascades is tested for six locations in addition to three locations used for application of roughness on entire surface. The abbreviated names of the cascades are mentioned along with a number out of number 1, 2 or 3 representing the location of application of roughness, as following:

(a) Suction surface leading edge region (SSR 1)

(b) Suction surface mid-chord region (SSR 2)

(c) Suction surface trailing edge end (SSR 3)

(d) Pressure surface leading edge (PSR 1)

(e) Pressure surface mid-chord region (PSR 2)

(f) Pressure surface trailing edge (PSR 3)

The number 1, 2 or 3 used as suffix to the abbreviated name of the cascade represent location as leading edge, middle chord and trailing edges respectively. Therefore a large number of cascades are required to represent all combinations of the blade profiles, magnitudes of roughness and locations of roughness for localised application of roughness.

The pattern of variation of parameters such as local loss coefficients, mass averaged loss coefficients for all such cascades are found similar in shape to that of the cascades with the entire surface roughness application for each of the blade profiles 3525, 6030 and 5530 separately. Comparison of loss coefficients in all cascades for localized roughness application, reveals that the mass averaged loss coefficients, similar to entire surface roughness application for each of the blade profiles 3525, 6030 and 5530, are high at hub and casing than their values at mid span of the blade due to the endwall boundary layers for all roughness values.

The pattern of variation of local loss coefficients and mass averaged loss coefficients are of similar shapes to that for cascades with entire surface roughness application. Therefore graphs showing the variation for localised roughness application are not included in this section to avoid repetitiveness. The results with regard to measurement of magnitude of losses are summarised as follows. However, the magnitudes of losses for localised application of roughness, on account of variety of reasons differ from those for application of roughness on entire surface. Moreover the difference between respective losses measured for localised roughness and the entire surface roughness application are marginally very low. In this section, the results will be discussed related to cascades with localised roughness comparing with entire surface roughness and cascades with smooth surfaces.

5.5.1 Results with regard to localised roughness of 250 µm on various locations of the blade surfaces of cascades employing different blade profiles

The total loss for localised roughness application on leading edge of pressure surface of cascades (PSR 1 250) for blade profiles 5530 are measured to be 19.65% of the total energy of the air at the inlet of the cascade against the total loss of 19.68% for the entire surface roughness application of 250 µm on the same surfaces of the cascade employing blade profile 5530. The difference in total loss is very less (0.03% only). The total loss for localised roughness application on leading edge of pressure surface of cascades for blade profiles 5530 is 0.04% higher than total loss measured for the smooth cascade employing same blade profile. The total loss for the smooth cascade employing same blade profile is measured to be 19.61%. The profile loss for localised roughness application on leading edge of pressure surface of cascades (PSR 1 250) for blade profiles 5530 are measured to be 19.35% of the total energy of the air at the inlet of the cascade against the profile loss of 19.42% for the entire surface

roughness application of 250 µm on the same surfaces of the cascade employing blade profile 5530.

Similarly the difference of 1% for each of total loss and profile loss is measured between similar cascades of entire surface roughness application (PSR 250) and localised roughness application on leading edge (PSR 1 250).

The total loss and profile loss for blade profiles 5530 for localised roughness application on suction side leading edge (SSR 1 250) are measured to be 19.73 and 19.43 % of the total energy of the air at the inlet of the cascade against the total loss of 19.65 and 19.35% for localised roughness application on pressure side leading edge (SSR 1 250) for the roughness application of 250 µm. The entire surface roughness application of on the same surfaces. The localised roughness of 250 µm on suction surfaces resulted in more total loss and profile loss than similar roughness on pressure surfaces. However the difference between respective losses measured for each of localised roughness applications is very less. The losses measured for blade profile 6030 also follows similar trend for the localized roughness application of 250 µm on leading edges of suction surfaces and on pressure surfaces separately.

Therefore it can be concluded that the total loss as well profile loss are less in the case of localized roughness as compared to entire surface roughness of 250 µm. For the same roughness application, the secondary loss measured for both type of application of roughness i.e. localized roughness and entire surface roughness application is very less and the difference may be ignored. It is also concluded that difference between respective losses measured for localised roughness and the entire surface roughness application are almost same. Therefore localised roughness may be supposed to be equally detrimental to entire surface roughness.

5.5.2 Results with regard to localised roughness of 500 µm on various locations of the blade surfaces of cascades employing different blade profiles

The total loss for localised roughness application on leading edge of pressure surface of cascades (PSR 1 500) for blade profiles 3525 are measured to be 18.57% of the total energy of the air at the inlet of the cascade against the total loss of 18.41% for the entire surface roughness application of 500 µm on the same surfaces of the cascade employing blade profile 3525. The total loss for the smooth cascade employing same blade profile is measured to be 18.34%. This blade profile shows different behavior for localised roughness application of 500 µm at leading edge of the cascade. The localised application at leading edge of the pressure surfaces of the case of localised roughness application at leading edge is higher than that for entire surface roughness application of the same roughness magnitude. The total loss in the similar case of other blade profiles i.e. 6030 and 5530 is found to be less in the case of localized roughness as compared to entire surface roughness.

In order to compare effect of an equal magnitude of roughness over various location, in a localised way, the total, profile and secondary loss for various cascades, for all the three blade profiles are tabulated in table 5.29. The table 5.29 shows effect of 500 µm roughness on each of six locations on leading edge, middle chord and trailing edge on pressure and suction surfaces separately. These data may be analysed along with results of same roughness on entire surface for all cascades and smooth cascade separately.

Table 5.26 : Comparison of Total, profile and secondary loss for various cascades employing blade profiles 3525, 6030 and 5530 for effect of 500 µm roughness on each of six locations on leading edge, middle chord and trailing edge

Type of Blade profile	Name of cascade (Location & roughness)	Total loss	profile loss	secondary loss absolute	secondary loss non-dimensionalised with total loss in smooth cascade
	PSR1 500	12.36	12.08	0.29	2.31
	PSR2 500	12.37	12.08	0.29	2.31
6030	PSR3 500	12.41	12.13	0.29	2.30
	SSR1 500	12.46	12.18	0.28	2.28
6030	SSR2 500	12.62	12.34	0.28	2.24
	SSR3 500	12.55	12.26	0.28	2.26
	PSR1 500	19.67	19.37	0.30	1.52
	PSR2 500	19.68	19.38	0.30	1.52
5530	PSR3 500	19.71	19.42	0.30	1.51
	SSR1 500	19.78	19.48	0.29	1.49
5530	SSR2 500	19.79	19.49	0.29	1.48
	SSR3 500	19.71	19.41	0.30	1.51
	PSR1 500	18.56	18.19	0.36	1.96
	PSR2 500	18.37	17.99	0.38	2.07
3525	PSR3 500	18.34	17.98	0.36	1.97
	SSR1 500	18.50	18.14	0.36	1.96
3525	SSR2 500	18.67	18.31	0.36	1.93
	SSR3 500	18.67	18.31	0.36	1.93

Some important observation with regard to comparison of effect of application of localized roughness of 500 µm individually on leading edge, middle chord and trailing edge on pressure & suction sides of blades are summarised in the following section. The profile wise effect of localized roughness is analysed comparing the

magnitudes of losses i.e. total, profile and secondary loss in each case of localised application of roughness with smooth cascade. The profile wise effect of localized roughness is analysed comparing the magnitudes of losses with the respective magnitudes of losses when the same roughness is applied on entire surface. The results are bifurcated broadly in two categories i.e. roughness application on pressure and suction sides of blades. The Profile wise comparison in each of cases is presented as under:

5.5.2.1 Blade Profile 6030: Pressure side application of roughness

The total and profile losses for localised roughness on trailing edge of the pressure side of all the blades of the cascade employing blade profile 6030 are measured to be higher than that for application of same roughness on middle chord and leading edge in the same order. The total and profile losses are highest for the entire surface rough (PSR 500) cascade than all localized roughness application on leading, middle & trailing edge. The losses in PSR 500 cascade are higher than smooth cascade.

The secondary losses are compared for each of localised application of same roughness with the losses generated for smooth cascade and cascades where respective entire pressure surfaces are applied with same roughness. The secondary loss is measured to be maximum in the case of smooth cascade. Whereas the middle chord roughness on pressure side is measured to be least detrimental in terms of generation of secondary loss.

The same loss is measured to be equal for leading edge and middle chord roughness on pressure side. In case localised roughness is applied on trailing edge of pressure side, the same loss is slightly reduced.

5.5.2.2 Blade Profile 6030: Suction side application of roughness

The localised roughness on middle chord on suction side is more detrimental in terms of generation of total and profile losses followed by localised roughness on trailing edge and leading edge in the same order. The SSR 500 (with entire surface application of roughness, on suction surfaces) cascade employing blade profile 6030 is higher than smooth cascade and all cascades with localised roughness.

The magnitudes of secondary loss measured for smooth cascade employing blade profile 6030 are compared with localised roughness applications for same roughness magnitude, and entire surface roughness application. The secondary loss measured for smooth cascade employing blade profile 6030 is observed to be maximum among all cascades. The secondary loss, in case of cascades with the same roughness on leading edge of suction side of the blades, is measured to be higher than that for cascades with the same localised roughness on trailing edge and middle chord separately, in the same order. The secondary loss is measured to be least in the case of entire surface roughness of 500μm on the same surfaces (SSR 500).

5.5.2.3 Blade Profile 5530: Pressure side application of roughness

The total and profile losses for localised roughness on trailing edge of the pressure side of all the blades of the cascade employing blade profile 5530 are measured to be higher than that for application of same roughness on middle chord and leading edge in the same order. However total and profile losses for localised roughness on trailing edge of the cascade is less than the respective losses for the cascade with roughness application on entire surfaces i.e. PSR 500 cascade. The total and profile losses for PSR 500 cascade employing blade profile 3525 are maximum among the cascades under reference.

The secondary losses for the for PSR 500 cascade employing blade profile 3525 are measured to be higher than smooth cascade and all other remaining cascades with localised roughness. The secondary losses for localised roughness on all the three locations on pressure surfaces of blades of the cascades are nearly equal. The secondary losses for localised roughness on middle chord and leading edge are equal in magnitude.

5.5.2.4 Blade Profile 5530: Suction side application of roughness

The total and profile losses for localised roughness on the middle chord of suction sides of blades are measured to be more than in the case of localised roughness on leading edge and trailing edge. The losses in the case of localised roughness on leading edge are higher than that in the case of localised roughness on trailing edge.

The respective losses for the cascade with roughness application on entire surfaces i.e. PSR 500 cascade are highest among all localised roughness cases and the smooth cascade.

Similar to case of blade profile 6030, magnitudes of secondary loss for cascade, employing blade profile 5530, with localised roughness applications are compared with similar results for smooth cascade and the PSR 500 cascade employing same blade profile. It is clear from the results shown in table 5.29 that the secondary loss measured for the localised application of roughness on middle chord and leading edge on pressure side are same. However this loss is measured to be maximum for PSR 500. The secondary loss due to localised roughness on trailing edges on pressure surfaces of the cascade is measured to be lesser than entire surfaces roughness and other remaining localised roughness applications.

Secondary loss, in case roughness is applied on trailing edge of suction side of the blades, is measured to be maximum followed by leading edge and middle chord in the same order. The secondary loss for SSR 500 cascade is measured to be lesser than each for localised roughness cases. The secondary loss is measured to be least in the case of smooth cascade.

5.5.2.5 Blade Profile 3525: Pressure side application of roughness

The leading edge localised roughness on pressure surfaces of the cascade employing blade profile 3525 is more detrimental in terms of generation of total and profile losses followed by localised roughness on middle chord and trailing edge. The total and profile losses are highest for the entire surface rough (PSR 500) cascade followed by leading edge localised roughness case. The secondary losses measured for smooth cascade and PSR3 500 cascade (i.e. the localized trailing edge roughness) are equal. The losses due to localized trailing edge roughness and losses measured for smooth cascade are lesser than all localized roughness application on leading and middle edge. The losses in PSR 500 cascade are higher than smooth cascade.

The secondary loss due to localized roughness on various locations on surfaces of blades of the cascades employing blade profile 3525 is maximum for middle chord roughness. The secondary loss due to middle chord roughness is higher than the losses measured in the case of entire surface roughness of 500μm on the same surface (PSR 500 cascade). The secondary loss due to localised roughness on middle chord is higher than that is in case of smooth cascade. The secondary loss due to localised roughness on leading edge is lesser than that in case of middle chord roughness. The secondary loss measured for the localised application of roughness on trading edge and that in case of smooth cascade are same. The secondary loss for PSR 500 cascade

is measured to be marginally higher than that for the localised application of roughness on trading edge and smooth cascade.

5.5.2.6 Blade Profile 3525: Suction side application of roughness

The localised roughness on the middle chord and trailing edge roughness on suction side is equally detrimental in terms of generation of total and profile losses. The localised roughness on the leading edge roughness on suction side is found to be least detrimental among all localised roughness cases. The total and profile losses in case of localised roughness are even higher than SSR 500 cascade. The same losses for the application of localised roughness in each case are higher than the losses for smooth cascade.

Secondary loss is maximum for Entire surface roughness of 500µm followed by smooth cascade in case roughness is applied on suction side of blades of the cascade employing blade profile 3525. The same loss is reduced for localised application of roughness on leading edge of suction side comparing with entire surface roughness of 500µm on the same surface. The secondary loss for localised application of roughness on leading edge of suction side is highest among all localised roughness application cases. The roughness on middle chord and trailing edge are equally detrimental if applied on suction side.

It is clear from the results (table 5.29) that the blade profile 6030 and 5530 behave in same way in terms of generation of total and profile losses.

5.6 Results and discussion for compressor cascade

A computational study is conducted for a low-speed linear axial flow compressor cascade also focusing mainly on analysis of the effect of roughness on the

aerodynamic performance of the cascade. Measurement of total, profile & secondary loss was carried out by successively employing different combinations of profiles and roughnesses on the surfaces of blades of the cascades. Magnitudes of various roughnesses i.e. 250, 500 and 750 μm are applied over blades of cascade. The results with regard to total, profile and secondary loss are discussed in the context of increase or decrease of loss with the increase in roughness from the reference level i.e. respective cascade with smooth blade.

5.6.1 Effect of roughness on Total losses for Compressor cascades

Similar to the turbine cascades, local loss coefficients for pitch wise position for compressor cascade are also found using relation proposed by Dejc and Trojanovskij (1973) and then these coefficients are used to evaluate mass averaged loss coefficient for various span position from bottom end wall till complete blade height for cascade of compressor. These coefficients are computed along the complete blade span.

In order to make a quantitative study with other cascades, a plot of mass averaged loss coefficients for PSR cascade with a roughness of 250 μm is shown in figure 5.71. The results for mass averaged loss coefficients for PSR cascades for roughnesses of 500 & 750 μm are also tabulated in table 5.30. It is needless to mention that all positions are not represented by graphs in order to avoid repetitiveness, in this section.

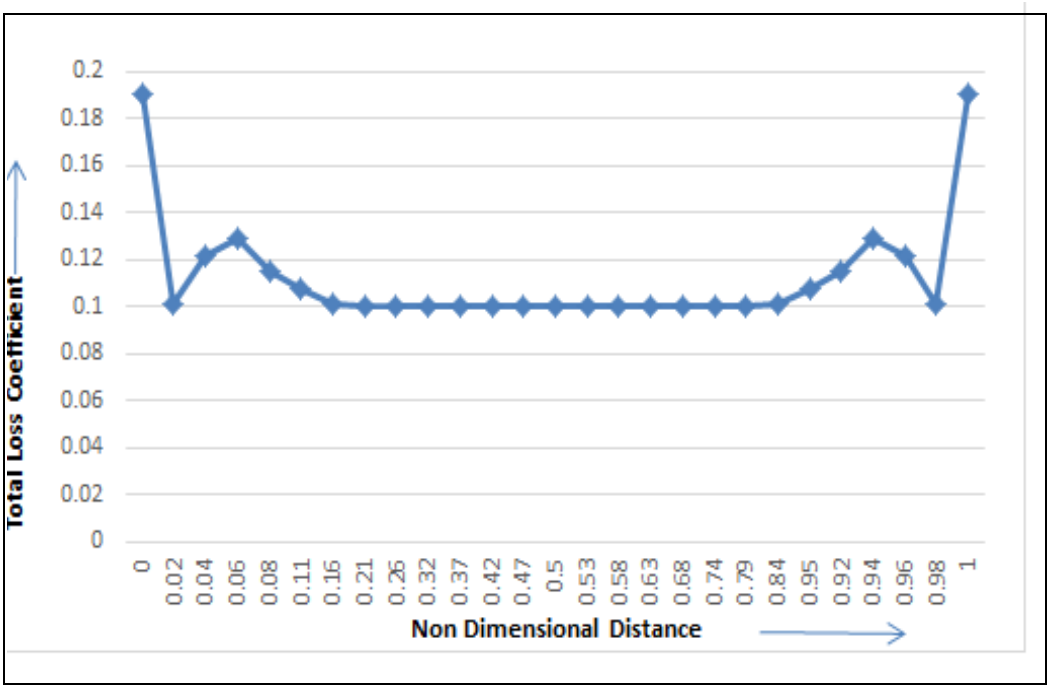

Figure 5.71: Variation of total energy loss coefficients with respect to non-dimensional distance from bottom to top endwall for roughness of 250 µm over pressure surface for compressor cascade

Table 5.27: Summary of Total Energy Loss, Profile Loss and Secondary Loss for smooth, SSR, PSR & BSR cascades for different levels of roughness of 250, 500 & 750 for compressor cascade

roughness	Roughness levels	Percentage of Total energy loss in total energy of the air (A)	Percentage of Profile loss in total energy of the air (B)	Contribution of secondary loss (C=A-B)	percentage of Secondary loss relative to total loss in same cascade	percentage of Secondary loss relative to total loss in smooth blades	percentage of profile loss relative to total loss of the given cascade
smooth		24.49	23.26	1.22	4.99	4.99	94.99
PSR	250	24.68	23.41	1.27	5.13	5.17	95.61
	500	24.73	23.47	1.27	5.12	5.17	95.83
	750	24.77	23.51	1.26	5.10	5.16	95.99
SSR	250	24.82	23.52	1.31	5.26	5.33	96.02
	500	24.88	23.61	1.26	5.08	5.16	96.42
	750	24.94	23.69	1.25	5.02	5.11	96.72
BSR	250	24.93	23.66	1.26	5.06	5.15	96.63
	500	25.07	23.82	1.26	5.01	5.13	97.25
	750	25.18	23.93	1.25	4.98	5.12	97.7

It is observed from the table 5.30 that the total loss increases as roughness increases on the same surfaces. The total losses as well, profile loss are minimum for smooth cascade. These losses increase marginally with the increase in roughness for compressor cascade. These losses are maximum when roughness of 750 µm was applied on both the surfaces of blades of Compressor cascade.

It is also observed from the table 5.30 that the mass averaged loss coefficients similar to that of the turbine cascades are found high at hub and casing due to the end-wall boundary layers. The trend of mass averaged loss coefficient for remaining cascades i.e. BSR & SSR cascades having roughnesses of 250, 500 and 750 µm is found same to that of PSR cascades**.** It can be concluded that roughness of a given magnitude is not much affecting the total loss contrary to the turbine cascade. The difference between data of total loss is minimal for the smooth surface and rough surface. This is so because roughness Reynolds Number k^+ is such that the roughness regime is fully rough for all type of location of roughness. Results of compressor cascade show that total losses amounting to very higher side because separation of boundary layer in case of compressor is more because of adverse pressure gradient in the direction of flow.

5.6.2 Effect of roughness on profile losses for compressor cascades

The profile loss contributes to very large extent in the total loss as the boundary layer formed is thicker and more prone to separate due to adverse pressure gradient during flow through compressor cascades. The profile loss contribution in the total loss ranges from 95% to 97% as shown in Table 5.30. The same table depicts that the percentage of profile loss in the total energy of the air at inlet of the cascade for smooth cascade is 23.26 % but when the roughness of 250µm was applied over pressure and suction surface separately and together, the profile loss increases to

23.41%, 23.52% and 23.66% respectively. Therefore the profile loss is lowest for smooth blade and increases when roughness is applied over pressure, suction surface separately and together in the same order. The difference between data of profile loss is also minimal for the smooth surface and rough surface due to reasons mentioned in preceding section pertaining to roughness Reynolds Number k^+.

5.6.3 Effect of roughness on Secondary loss for compressor cascades

It is evident from results for compressor cascade as shown in table 5.30 that difference in percentage values of total energy loss & Profile loss gives percentage of secondary loss in total energy. In case of smooth blade secondary loss is 4.99 %. The secondary loss is in a very small proportion in the total loss as the profile loss contributes to very large extent in it. Contribution of this loss in the total loss of same cascade ranges merely from 4.99% to 5.26 %.

In fact, results in table 5.30 show that the increase in roughness causes secondary loss to reduce for each of PSR, SSR and BSR cascades separately. This loss is also affected due to complexity of the fluid flow within the boundary layer and transition process of the boundary layer. There are various other factors such as Reynolds number and curvature of the blade surface, velocity of fluid flow over the blades of cascade etc. which largely affect the transition of boundary layer. Presence of roughness over the different part of blade also affects the secondary loss differently. The Pressure side leg of horse shoe vortex is affected by curvature and pressure difference between pressure side and suction side of adjacent blade of the corresponding flow passage thereby contribute more to the Secondary losses. The compressor blades have lesser curvature therefore presence of roughness over pressure surface would not contribute much in increasing of secondary losses contrary

to turbine cascades. The curvature over suction side of blades of cascade however affects secondary loss differently. The counter vortex which initiates from suction side of blades mixes with the passage vortex and reduces the effect of passage vortex. Therefore, the secondary losses are lowered in this case. Increase in roughness further enhance counter vortex and hence secondary losses are further reduced.

The results of computational study show that the total energy loss is increased with application of roughness for both of turbine and compressor cascades in spite of absolute change in secondary loss. Therefore, when the absolute change in secondary loss is non-dimensionalised with total loss with the same roughness the same is not truly reflected in the percentage change in secondary loss. Therefore, for the present study of compressor cascade percentage of secondary loss in total energy loss are non-dimensionalised with the total loss in case of smooth blades similar to that of cascades of turbine. The percentage of secondary loss in total energy loss, thus calculated, is shown in table 5.30.

The results of study of numerous numbers of cascades of different configurations representing roughness magnitude-location combination, for each profile, along with smooth blade profile both for turbine and compressor is presented in various sections of this chapter. The simulation of the flow through all such turbomachines cascades is used for measuring effect of roughness on the blades of the turbines and compressor blades on losses generation. In next chapter, conclusions with regard to this research work are presented. There is always a scope for future work for each research area. The same applies for this work also. Therefore scope for future work is also mentioned in the next chapter.

CHAPTER 6

CONCLUSIONS AND SCOPE FOR FURTHER WORK

This computational work is aimed to study the end wall effect on the total loss and predict the contribution of secondary loss and profile loss therein. The results of the computational study including simulation of flow through turbines and compressor cascades is summarised in this chapter.

The measurement of the total pressure and static pressure at measurement planes at inlet and exit of cascades has been done. The local loss coefficients are calculated using relation proposed by Dejc and Trojanovskij (1973) as shown in equation 4.2. The pattern of variation of total pressure measured at measurement plane at the exit of the cascade and local loss coefficients relative to nondimensional distance along pitch wise direction, for various span positions, are similar in many respects for same cascades. It is observed that the patterns of variation of local loss coefficients and magnitudes of total pressure are images of each other (in the upside-down direction only). The variation of local loss coefficient for typical blade passage for each of turbines and compressor cascades shows that the flow is highly viscous in the vicinity of blade surfaces. Due to formation of the boundary layer on the surface of the blades the fluid flows over blade surfaces in such a way that the fluid velocity changes from zero at the wall to its free stream value. The flow outside the boundary layer can be considered frictionless or potential flow. The total pressure reduces after entering the cascade section due to viscous drag over the cascade section and at the exit of the cascade the wakes are formed, where the total pressure drops significantly, however in the core flow region, the pressure drop is very less. The total pressure

further drops due to intermixing of the core flow and the wake. Width of the wake depends on the pressure drop in the cascade section, higher is the pressure drop and larger is the width of the wake. The non-uniformity at exit of the blade row is further enhanced by secondary flows.

The total pressure and local loss coefficients vary in such a way that their magnitudes changes alternatively from minimum to maximum for each flow channel formed between two consecutive blades of the cascade. The same phenomena is repeated for every such flow channels. The repetition of the variation of pattern for successive flow channels is because the blades are similar and accordingly the flow channels are almost same. The passage for the flow for given two blades is almost similar to the passage formed between next successive two blades. The properties of flowing fluid is almost constant for a particular span position for both the passages.

The magnitudes of losses coefficients for various span positions particularly in end wall regions are not equal. However, magnitude of losses for various span positions nearby to mid span position are almost same. The pattern of variation of total pressure and local loss coefficients comparing the same across various cascades, change a little, based on a magnitude of roughness on the blades of the cascade and selection of blade profile.

The mass averaged loss coefficients for selected span wise positions have been calculated using the pitch wise local loss coefficients. The total loss, secondary loss and profile loss, for a cascade, are calculated on the basis of mass averaged loss coefficients for all selected span wise positions.

The peak values of local loss coefficients over pitch wise distance for the smooth cascade are lower than corresponding peak values of other cascades such as PSR, SSR and BSR cascades. The pattern of local loss coefficients for all cascades vary from bottom to top end wall positions i.e. nondimensional span positions of zero to one, in such a way that the same are highest at end walls and minimum at mid span position. The local increase in loss coefficient is observed at end walls due to the secondary flow cores. The presence of humps at the end walls occur because of the formation of vortex cores that leads to high-value, mass averaged loss coefficient. The total (combined) losses in all blade cascade are estimated by the mass averaged loss coefficient, which is essentially the sum of profile loss coefficient & end loss coefficient.

The non-uniformity of flow in pitchwise direction at the exit of a row of blades undergoes a considerable increase with increase in roughness for each profile compared to the corresponding smooth blades. The results with regard the total, profile and secondary losses for BSR and PSR cascade based on mass averaged loss coefficients show that that the magnitudes of total loss these cascades for all roughness values are higher than that of the smooth cascade for all blade profiles i.e. 6030, 5530 and 3525.

It is evident from the summary of results that the total loss increases as roughness increases on the blade surfaces of each cascade for all blade profiles i.e. 6030, 5530 and 3525, ignoring few of magnitudes of total and profile losses for SSR 500 cascades employing blade profile 3525 (table 5.27). The losses increase in the same order when roughness was increased from lower roughness value to high roughness value for all type of cascades. The rate of increment of total and profile losses with the increase in magnitude of roughness over the blades of the cascade for each

profile reduces for high roughness values. The increase in total and profile loss in case of increasing roughness from smooth surface to 250 µm is higher than the same for increasing the roughness from 250 µm to 500 µm. For higher roughness applications the increase in losses is insignificant with the increase in magnitude of roughness.

The non-uniformity of the flow at the exit of blades cascades leads to losses for each of smooth, SSR, PSR & BSR cascades. There are two components of total loss i.e. profile loss and secondary loss. The losses mentioned in this dissertation are expressed in percentage loss. The total loss has been expressed as percentage of total energy of the air. Similarly profile loss is also expressed as percentage of total energy of the air. The secondary flow loss are expressed as percentage of total loss.The percentage of secondary loss is calculated by subtracting the profile loss percentage from the percentage of total loss. To avoid the effect of the increasing total loss with increase in roughness percentage of Secondary loss is nondimensionalised with total loss in smooth blades.

The work conducted for turbines and compressors is summarised in the following sections.

6.1 Turbine Cascade

Results of turbine cascades with smooth and roughnesses over entire surfaces are summarised below.

6.1.1 Smooth Turbine of profiles 3525, 6030 and 5530

The magnitude of total loss is measured to be 18.34 , 10.53 and 19.61 for cascades employing blade profiles 3525, 6030 and 5530 respectively. The different

magnitudes of losses are attributed to the difference in various parameters like shape, geometry etc.for all the blade profile 3525, 6030 and 5530.

In view of generation of lesser loss in case of cascades employing blade profile 3525 than that of cascades employing blade profile 5530, it can be concluded that smooth blades of the cascades employing blade profile 3525 are aerodynamically more efficient than blade profile 5530.

6.1.2 Turbine Cascade with roughness of different magnitudes over entire blade surfaces

The losses for cascades employing three different blade profiles i.e. 6030, 5530 and 3525, on account of application of roughness of different magnitudes, over pressure over suction and over both pressure and suction surfaces together, are measured and can broadly be concluded as under:

6.1.2.1 Roughness over pressure surfaces of each of cascades

The roughness of magnitude of 250 μm on pressure surfaces of cascade employing blade profile 5530 is more detrimental in terms of generation of total and profile loss than blade than same roughness on cascade employing blade profiles 3525 followed by 6030.

The total loss measured for cascade employing blade profile 6030 is 7.98 and 6.71% lesser than the same for blade profile 5530 and 3525 respectively. Whereas the profile loss for cascade employing blade profile 6030 is measured to be 8.29 and 6.89 % lesser comparing the same with that for blade profile 5530 and 3525 respectively.

The secondary loss is highest for blade profile 6030. The same is measured to be least for blade profile 5530. The secondary loss for blade profiles 5530 and 3525 are measured to be lesser by 1.55 and 0.08% than that for blade profile 6030.

Similarly, the roughness of magnitude of 500 µm on pressure surfaces of cascade employing blade profile 5530 is more detrimental in terms of generation of total and profile loss than same roughness on cascade employing blade profiles 3525 and 6030. The total loss measured for cascade employing blade profile 6030 is 7.61 and 6.2% lesser than the same for blade profile 5530 and 3525 respectively. Whereas the profile loss for cascade employing blade profile 6030 is measured to be 7.87 and 6.45 % lesser comparing the same with that for blade profile 5530 and 3525 respectively.

The secondary loss is highest for blade profile 6030. The secondary loss for blade profiles 5530 and 3525 are measured to be lesser by 1.29 and 1.14% than that for blade profile 6030.

Total and profile losses due to application of roughness of 750 and 1000 µm follows the same pattern as of 250 and 500 µm on the entire pressure surfaces. However, the quantity of losses has increased with the increase in magnitude of roughness.

6.1.2.2 Roughness over suction surfaces

The roughness of the magnitude of 250 µm on suction surfaces of cascade employing blade profile 5530 is more detrimental in terms of generation of total and profile loss than the same roughness on cascade employing blade profiles 3525 and 6030. The total loss measured for cascade employing blade profile 6030 is 3.91 and 2.94 % lesser than the same for blade profile 5530 and 3525 respectively. Whereas the profile loss for cascade employing blade profile 6030 is measured to be 3.93 and 2.87 % lesser comparing the same with that for blade profile 5530 and 3525 respectively.

The secondary loss is highest for blade profile 3525 followed by blade profiles 6030 and 5530 in the same order. The trend of generation of secondary loss for cascade employing blade profile 3525 is reversed when roughness of 250 µm is applied on suction surfaces. In case of application of roughness of 250 µm on pressure surfaces, the secondary loss generated for blade profile 3525 is lower than that for blade profile 6030.

The roughness of magnitude of 500 µm on suction surfaces of cascade employing blade profile 5530, similar to cases for pressure surfaces rough, is more detrimental than same roughness on blade profiles 3525 and 6030 in terms of generation of total and profile loss. The total loss measured for cascade employing blade profile 6030 is 2.22 and 1.6% lesser than the same for blade profile 5530 and 3525 respectively. Whereas the profile loss for cascade employing blade profile 6030 is measured to be 2.22 and 1.47% lesser comparing the same with that for blade profile 5530 and 3525 respectively.

The secondary loss is highest for blade profile 3525. This trend is again opposite to that for same roughness on pressure surfaces. The secondary loss is measured to be equal for blade profiles 6030 and 5530.

The total loss for blade profiles 5530 and 3525 are measured to be higher by 2.11 and 1.31% respectively than that for blade profile 6030 as a result of application of roughness of 750 µm on the suction surfaces. Also, the blade profile 5530 is more detrimental in terms of profile loss generation as a result of application of roughness of 750 µm, comparing with other blade profiles.

The secondary loss is highest for blade profile 3525. The secondary loss is measured to be least for blade profile 6030 among all the three blade profiles.

Similar to the case of 750 µm roughness, the total loss for blade profiles 5530 and 3525 are measured to be higher than that for blade profile 6030 as a result of application of roughness of 1000 µm on the suction surfaces. The trend of secondary loss is also similar that of 750 µm roughness.

6.1.2.3 Roughness applied over both the surfaces together

The roughness of the magnitudes of 250 µm on both surfaces of the blades of cascade employing blade profile 5530 is more detrimental in terms of generation of total and profile loss than the same roughness on blade profiles 3525 followed by 6030. The secondary loss is highest for blade profile 6030 followed by blade profiles 3525 and 5530 in the same order.

The application of roughness of 500, 750 and 1000µm separately on both surfaces of the blades of the cascade employing blade profile 5530 is more detrimental in terms of generation of total and profile loss followed by blade profiles 6030 and 3525 in the same order for all roughnesses.

Similarly, the secondary loss is highest for blade profile 6030 for 500, 750 and 1000 µm roughness separately.

It is found that the total and profile losses for cascades employing blade profile 5530 and 3525 are significantly higher than the respective losses for cascades employing blade profile 6030.

6.2 localised roughness effects

The magnitude of total and profile losses in the case of application of localised roughness on the blades of the cascadeemploying blade profiles 6030, 5530&3525,

separately on the pressure and suction surfaces, are higher than that of smooth cascade employing same blade profile.

The total and profile losses for localised roughness on trailing edge of the pressure surfaces of all the blades of the cascades employing blade profiles 6030 and 5530 are measured to be higher than that for application of same roughness separately on middle chord and leading edge, on the same surfaces of the cascade. Whereas application of localised roughness of same magnitude on middle chord on suction surfaces of cascades employing blade profile 6030and 5530 is more detrimental in terms of generation of total and profile losses followed by localised roughness on trailing edge and leading edge in the same order. Total and profile losses for localised roughness on trailing edge of suction side are higher than that in the case of localised roughness on leading edge on the same side of the same blade profile 6030. The behavior of trailing edge and leading edge in terms of magnitudes of total and profile losses for the cascade employing blade profile 5530 and 6030 is opposite. Total and profile losses in the case of localised roughness on leading edge are higher than that in the case of localised roughness on trailing edge of cascade employing blade profile 5530.

The secondary loss is measured to be higher in the case of smooth cascade comparing with the corresponding losses for each of localised roughness on various locations separately and in case of application of entire surface roughness for the cascades employing same blade profile . Whereas the middle chord roughness on pressure side is measured to be least detrimental in terms of generation of secondary loss for cascades employing blade profile 6030. The secondary loss is measured to be least in the case of entire surface roughness of same magnitude on the same surfaces.

The application of localised roughness on leading edge on pressure surfaces of the cascade employing blade profile 3525 leads to more generation of total and profile losses than localised roughness on middle chord and trailing edge of same surfaces for the same cascade. On the other hand, the localised roughness on trailing edge of the pressure surfaces for blade profile 6030 and 5530 leads to more generation of total and profile losses.

The application of localised roughness on middle chord and trailing edge of suction surfaces of the cascade employing blade profile 3525 leads to more losses than localised roughness on leading edge at the same surfaces for the same cascade.

The localised roughness on middle chord on pressure surfaces is more detrimental for generation of secondary loss than remaining localised roughness applications for the blade profile 3525. On the other hand, the same type of roughness application on leading edge of suction side ismore detrimental for generation of secondary loss than remaining localised roughness applications on the blades of cascade employing same blade profile. The application of entire surface (PSR 500) leads to more secondary losses as compared to application of localised roughness on various locations separately on suction side of blades of the cascade employing blade profile 3525. The smooth cascade has also resulted more secondary loss than localised roughnesson suction side of blades of the cascade employing blade profile 3525.

It can be concluded from the results (table 5.29) that the localised roughness on blade profile 6030 and 5530 effects the phenomena of losses generation in same way where as in case of profile 3525, it is different.

6.3 Compressor Cascades

The mass averaged total loss is found to be 24.49 % for smooth cascade of which profile loss and secondary loss contribute to 23.26% and 1.22% respectively. The total loss increase to 25.18% when roughness of 750 µm is applied on the both surfaces of the blades. The contribution of profile loss and secondary loss in the total loss for the BSR 750 cascade were found to be 23.93% and 1.25%. The mass averaged secondary loss is found to be 4.99% for smooth cascade. The same loss is found 5.17%, 5.17 % and 5.16% for PSR 250, PSR 500 and PSR 750 cascades. The percentage of secondary loss due to application of roughness on suction surfaces changed to 5.33 %, 5.16 % and 5.11% for SSR 250, SSR 500 and SSR 750 cascades.

The trend of increase in total loss with the increase of surface roughness on various surfaces is similar to that of turbine cascades. It is found that the percentage of secondary loss for SSR 250 cascade is more than PSR 250. The trend of change in percentage of secondary losses is different for SSR cascades than that of PSR cascades.

When roughness is increased from 250 µm to 500 µm and thereafter to 750 µm the percentage of secondary loss is not appreciably changed. The percentage of secondary loss for SSR 500 and SSR 750 is reduced to 5.16 % and 5.11% respectively from its percentage 5.17% for SSR 250 cascade.

It is noticeable that the profile loss contributes very significantly in the total loss for all type of compressor cascades and that the roughness magnitudes do not affect secondary loss very appreciably for all type of cascades.

6.4 Recommendations for future studies

The present research work is accomplished using commercial softwares used for computational fluid dynamics (CFD). The commercial softwares Gambit and Fluent has provided insights on the effects of roughness, applied over different profiles and at various locations, on profile and secondary loss. However, there is a need to generalize the study for actual operating conditions. The computational program need inputs for defining boundary conditions. Similarly the locations chosen for measurement of the parameters during computational study need more input from operating turbo machines in the power stations. The design of the cascade needs to ensure that simulated cascade nearing the roughness pattern, the losses at the walls and actual turbine conditions.

Further studies are required using cascades, which are more close to real-life turbomachines, a few are given below:

(i) The data needed for input for computational study, requires extensive field work for collecting roughness value, locations and their variation with time. A very voluminous data from various stages of operating turbines is needed prior to going for actual computational study. The simulation work after getting all required information would help in devising more realistic computational models.

(ii) The actual machine operate on different operating conditions including Reynolds numbers of the flow. The future study could include computational modeling using a wide range of Reynolds numbers

(iii) The roughness in the form of bands need more realistic data collection to devise more realistic computational models with regard to localised roughness applications i.e. in place of three parts of pressure and suction surface, more realistic locations need to be analysed.

(iv) The blade profiles chosen may have wider range in pursuit of nearing the actual turbine conditions. very definite profiles of wide range of blades of turbomachines including gas, steam, wind and hydraulic turbines need to be chosen.

(v) The future study may explore the phenomenon of vortex formation corelating with various parameters of shape and geometry of blades profiles.

REFERENCES

Abbott, I.H. and Von Doenhoff, A.E., 1949, Theory of Wing Sections, Navier-Stokes equations - section 5.4. Dover Publications, Inc., New York, USA

Ammar Bin Shaukat,2013, Master of Science Thesis, "Parametric Study of Operating Conditions in an Annular Turbine Sector Cascade" KTH School of Industrial Engineering and Management, Energy Technology, Division of Heat Power and Technology, SE-100 44, Stockholm.

Ansari, A. R., 1986, Blade erosion problem in steam turbine, J. Inst. Engrs., Mech. Engg Div., 67, 1-3.

Assim Hameed Yousif, 2011, Mixing losses investigation downstream of turbine blade cascade with coolant flow blowing, Journal of Engineering Science and Technology, Vol. 6, No. 2 (2011) 161-178 ©School of Engineering, Taylor's University

Bammert, K., and Sandstede, H., 1980, Measurements of the boundary layer development along a turbine blade with rough surfaces, ASME J. Engg. for Power, 102, 979-983.

Bassett M. D., Pearson R. J., et al., 2003, A Multi-Pipe Junction Model for One Dimensional Gas-Dynamic Simulations, SAE Paper 2003-01-0370.

Batcho, P. F., Moller, J. C., Padova, C., and Dunn, M. G., 1987, Interpretation of gas turbine response due to dust ingestion, ASME J. Engg. for Gas Turbine and Power, 109, 344-352.

Bolcs, A., and Sari, O., 1988, Influence of deposits on the flow in a turbine cascade, ASME J. Turbomachinery, 110, 512-519.

Bons, J. P, Taylor, R. P., McClain, S. T., and Rivir, R. B., 2001, The many faces of turbine surface roughness, ASME J. Turbomachinery, 123, 739-748.

Bons, Jared Crosby, James E. Wammack, Brook I. Bentley, 2007, High-Pressure Turbine

Coton, K. C., and Schofield, P., 1971, Analysis of changes in the performance characteristics of steam turbines, ASME J. Engg. for Power, 93, 225-237

Coton, T., Arts, T., and Lefebore, M., 2001, Effects of Reynolds and Mach numbers on the profile losses of a conventional low-pressure turbine rotor cascade with an increasing pitch-chord ratio, Proc. Instn. Mech. Engrs., 215 , 763-772.

Cotton, K. C., and Schofield, P., 1971, Analysis of changes in the performance characteristics of steam turbines, ASME J. Engg. for Power, 93, 225-237.

David D., 1999, Turbine deposits rob megawatts, but you can catch the thief, Power, March/April, 83-87.

Dejc, M. E., and Trojanovskij, B. M., 1973, Untersuchung und berechnung axialer turbinenstufen (Investigations and computations of the axial turbines stages), Veb Verlag Technik Berlin (in German).

Denton, J.D., 1993 "Loss Mechanisms in Turbomachines" ASME Journal of Turbomachinery, 115, pp. 621-656.

Denton, J.D., and Dawes, W.N., 1999, Computational fluid dynamics for turbomachinery design, Proc. Instn. Mech Engrs, 213, Part C.

Deposition in Land-Based Gas Turbines From Various Synfuels, Journal of Engineering for Gas Turbines and Power, ASME, vol. 129

Energy Statistics (Twentieth Issue), 2013, Central Statistics Office National Statistical Organisation, Ministry Of Statistics and Programme Implementation, Government of India

Friederike C. Mund et al., 2006, Gas Turbine Compressor Washing: Historical Developments, Trends and Main Design parameters for Online Systems, Downloaded 25 Jan 2008 to 202.164.60.2 344 / Transactions of the ASME, Vol. 128

Gostelow, J. P., 1984, Cascade aerodynamics, Pergamon, Oxford, U.K.

Hamed, A., 1984, Solid particle dynamic behavior through twisted blade rows, ASME J. Fluids Engg., 106, 251-256.

Hamed, A., and Fowler S., 1983, Erosion pattern of twisted blades by particle laden flows, ASME J. Engg. for Power, 105, 839-843.

Hesham M. El-Batsh, 2012, Effect of the Radial Pressure Gradient on the Secondary Flow Generated in an Annular Turbine Cascade, Hindawi Publishing Corporation International Journal of Rotating Machinery Volume, Article ID 509209

Horlock, J.H., 1966, "Axial Flow Turbines", Butterworth & Co. Ltd., London, Chap. 3, pp.85.

Japikse, D. and Baines, N.C., 1997, Introduction to Turbomachinery , Concepts ETI, Inc. and Oxford University Press

Kind, R. J.; Serjak, P. J., and Abbott, M. W. P., 1996, Measurements and prediction of the effects of surface roughness on profile losses and deviation in a turbine cascade, Proc. 1996 International Gas Turbine and Aeroengine Congress & Exhibition, Birmingham, U.K., June, 10-13.

Komarov, N. F., and Yurkov, E. V., 1991, Corrosion damage to the blading and discs of steam turbines, Thermal Engg., 38, 66-70.

Lakshminarayana, B., 1996, Fluid dynamics and heat transfer of turbomachinery, John Wiley, New York.

Langston, L. S., Nice, M. L., and Hooper, R. M., 1977, "Three-Dimensional Flow within a Turbine Cascade Passage," ASME Journal of Engineering for Power, 99, pp. 21–28.

Mann, B. S., 1999, Solid-particle erosion and protective layers for steam turbine blading, Wear, 224, 8-12.

Marchal, P., and Sieverding, C. H., 1977, "Secondary Flows Within Turbomachinery Bladings," Secondary Flows in Turbomachines, AGARD-CP-214, Paper No. 11, pp. 1–19.

Metwally, M., Tabakoff, W., and Hamed, A., 1995, Blade erosion in automotive gas turbine engine, ASME J. Engg. for Gas Turbines and Power, 117, 213-219.

Michael Moczala, Ernst, von, Lavante, Manuchehr, Parvizinia, 2002, Influence of axial stator-rotor gap on unsteady losses in a typical steam turbine stage, J. Turbomachinery, 122.

Murawaski, C. G., and Vafai, K., 2000, An experimental investigation of the effect of free stream turbulence on the wake of a separated low-pressure turbine blade at low reynolds numbers, ASME, J. Fluids Engg., 122, 431-433.

Pope, A. M. S., 1961, Wind tunnel testing, John Wiley, New York

Povarov, O. A., and Tomarov, G. V., 1985, Erosion-corrosion wear of the metal steam turbines, Thermal Engg., 32, 511-516.

Robert Svoboda and Maurice Bodme, 2004, Investigations into the Composition of the Water Phase in Steam Turbines, proceedings of 14th International Conference on the Properties of Water and Steam in Kyoto, 594-601

Rodrick, V., Chima, 1998, Calculation of multistage turbomachinery using steady characteristic boundary conditions, Proc. 36th Aerospace Sciences Meeting & Exhibit, Reno, NV.

Samsher, 2002, "Effect of Blade Surface Roughness on Profile Loss and Exit Angle in A Rectilinear Steam Turbine Cascade," Ph.D. Thesis, Mech. Engg. Dept. IIT Delhi.United Nations Framework Convention on Climate Change (UNFCCC), April 2012, Clean Development Mechanism (CDM), form for CDM project activities (F-CDM-PDD), Project Design Document (PDD) for Grid connected natural gas based power project in Raigad District, Maharastra, India, Version 04.1.

Samsher, 2002, "Effect of Blade Surface Roughness on Profile Loss and Exit Angle in a Rectilinear Steam Turbine Cascade," Ph.D. Thesis, Mech. Engg. Dept. IIT Delhi

Samsher, 2002, "Effect of blade surface roughness on profile loss and exit angle in a rectilinear steam turbine cascade", Ph.D. Thesis, Mech. Engg. Dept. IIT Delhi.

Schlichting, H., 1968, Boundary-layer theory, McGraw-Hill, New York.

Seung Chul Back et.al, JUNE 2010, Vol. 132 "Impact of Surface Roughness on Compressor Cascade Performance" Journal of Fluids Engineering

Shanov, V., and Tabakoff, W., 1996, Erosion resistance of coatings for metal protection at elevated temperatures, Surface & Coatings Technology, 86-87, 88-93

Sharma, O.P. and Butler, T.L., 1987, "Predictions of Endwall Losses and Secondary Flows in Axial Flow Turbine Cascades", ASME Journal of Turbo machinery, 109, pp. 229-236.

Shih T. I-P. and Lin Y.L, 2003, "Controlling Secondary-Flow Structure by Leading-Edge Airfoil Fillet and Inlet Swirl to Reduce Aerodynamic Loss and Surface Heat Transfer," Transactions of the ASME, 125, 48-56.

Shih.T.H., Liou,W.W., Shabbir,A.,and Zhu,J., 1995, "A new κ-ε eddy viscosity model for high Reynolds number turbulent flows –models development & validation", Computer Fluids 24, 3, pp, 227-238

Sieverding, C.H. and Van den Bosch, P., 1983, "The Use of Coloured Smoke to Visualise Secondary Flows in a Turbine-Blade Cascade", Journal of Fluid Mechanics, 134, pp. 85-89

Stamatis, A., Mathioudakis, K., and Papailiou, K., 1999, Assessing the effect of deposits on turbine blading in a twin shaft gas turbine, Proc. International Gas Turbine & Aero-engine Conference and Exhibition, Indianapolis, Indiana.

Tabakoff, W., 1984, Review-Turbomachinery performance deterioration exposed to solid particulates environment, ASME J. Fluids Engg., 106, 125-134

Tabakoff, W., and Metwally, M., 1992, Coating effect on particle trajectories and turbine blade erosion, ASME J. Engg. for Gas Turbine and Power, 114, 250-257.

Tabakoff, W., Hosny, W., and Hamed, A., 1976, Effect of solid particles on turbine performance, ASME J. Engg. for Power, 98, 47-52.

Tabakoff, W., Hosny, W., and Hamed, A., 1976, Effect of solid particles on turbine performance, ASME J. Engg. for Power, 98, 47-52.

Taylor, R. P., 1990, Surface roughness measurements on gas turbine blades, ASME J. Turbomachinery, 112, No. 2, 175-180

V. Ganapathy, ABCO Industries, Abilene, Chemical Engineering Progress, pp 32-44, August 1996

Vasilenko, G. V., 1991, Water-chemistry factors in corrosion damage to the moving blades and discs of turbines, Thermal Engg., 38, 609-611.

Walsh, P. N., Quets, J. M., and Tucker, R. C. Jr., 1995, Coatings for the protection of turbine blades from erosion, ASME J. Engg. for Power, 117, 152-155.

Wang H.P., Olson S.J., Goldstein R.J., Eckert E.R.G., 1997, "Flow visualization in a linear turbine cascade of high performance turbine blades", ASME Journal of Turbomachinery, 119, pp1-8.

Winterbone D. E. and Pearson R. J., Theory of Engine Manifold Design—Wave Action Methods for IC engines, Professional Engineering Publications, London, UK, 2000.

Winterbone D. E. and Pearson R. J.,1999, Design Techniques for Engine Manifolds—Wave Action Methods for IC Engines, Professional Engineering Publications, London, UK.

Yaras, M.I., and Sjolander, S.A., (1992b), "Effects of Simulated Rotation on Tip Leakage in a Planer Cascade of Turbine Blades: Part II-Downstream Flow Field and Blade Loading", ASME Journal of Turbomachinery, 114, pp. 660-667

Yahya, S.,M., "Turbines, compressors and fans", Tata McGraw-Hill, New Delhi (2002)

Web site 1 "http://www.powermin.nic.in/JSP_SERVLETS/internal.jsp" visited on 11-10-08

Web site 2 "http://agneyablog.wordpress.com/2011/10/25/coal-and-power" visited on 25-10-11

Web site 3 "www.iapws.jp/Proceedings/Symposium11/594Svoboda.pdf" visited on 10-12-12

Web site 4 "https://www.google.co.in/search?q=lift+drag+flow4 +pdf&ie=utf-8&oe=utf-8&aq=t&rls=org.mozilla:en-US:official&client=firefox

a&channel=np&source=hp&gfe_rd=cr&ei=EJtWU8rVCOiJ8QeZ5IHYDg#"visited on10-01-13

Web site 5 "http://en.wikipedia.org/wiki/Flow_separation" visited on 01-01-13

Web site 6 "https://www.google.co.in/iopscience.iop.org/0031-9120/38/6/001/pdf/pe3_6_001.pdf" visited on 21-01-13

Web site 7 "http://www.physicsforums.com" visited on 31-03-14

Web site 8 "http://adg.stanford.edu/aa241/ airfoils /airfoilpressures.html" visited on 01-04-14